

Copyright Undertaking

This thesis is protected by copyright, with all rights reserved.

By reading and using the thesis, the reader understands and agrees to the following terms:

- 1. The reader will abide by the rules and legal ordinances governing copyright regarding the use of the thesis.
- 2. The reader will use the thesis for the purpose of research or private study only and not for distribution or further reproduction or any other purpose.
- 3. The reader agrees to indemnify and hold the University harmless from and against any loss, damage, cost, liability or expenses arising from copyright infringement or unauthorized usage.

IMPORTANT

If you have reasons to believe that any materials in this thesis are deemed not suitable to be distributed in this form, or a copyright owner having difficulty with the material being included in our database, please contact lbsys@polyu.edu.hk providing details. The Library will look into your claim and consider taking remedial action upon receipt of the written requests.

A SMART INTERACTIVE RETRO-REFLECTIVE CLOTHING FOR PEDESTRIAN SAFETY AT NIGHT-TIME

SEIDU RAPHAEL KANYIRE

PhD

The Hong Kong Polytechnic University

The	Hong	Kong	Poly	vtechi	nic I	Iniv	ersity
1110	HUILE	170115	T OI		\mathbf{u}		

School of Fashion and Textiles

A Smart Interactive Retro-reflective Clothing for Pedestrian Safety at Night-time

SEIDU Raphael Kanyire

A thesis submitted in partial fulfilment of the requirements for the degree of Doctor of Philosophy

CERTIFICATE OF ORIGINALITY

I hereby declar- it reproduces n			-			_	_
accepted for	_	_	_				
acknowledgem	ent has been	made in	the tex	t.			
			(5	Signed)			

Raphael Kanyire Seidu (Name of Student)

DEDICATION

In Memory of my Beloved Grandmother – Mrs Martha Dabuo Pageema Seidu

ABSTRACT

Addressing pedestrian safety at night is important to help limit the accidents recorded. Reports have revealed that pedestrian accidents are higher at night-time as compared to daytime. These accidents are among other factors due to the clothes worn and the conditions of darkness which places difficulty for pedestrian visibility and drivers' vision at night-time to recognise the pedestrian on the road. This situation has exposed pedestrians to a lot of dangers, thus the need to innovate pedestrian clothing to improve their visibility and visual detection by drivers. Recent research has reported on the use of retro-reflective materials to improve the visibility of road users and driver's response rate on the road. These retro-reflective materials have the unique property of redirecting light rays back to their source of origin in an equal distribution across different angles of observation and incidence. This property exposes the wearer by making them visible to the approaching vehicle for a quick response by the driver. These retro-reflective materials are configured to the various joints of the human body in biomotion configurations for easy recognition and visibility. Further studies have reported on the use of light-emitting diodes operated manually to produce lights to enhance the visibility of pedestrians on the road. These are by far how recent studies have sought to provide solutions for the critical issue of improving pedestrian safety at night. However, there are limited research studies on pedestrian safety using material innovation and sensory technology to produce a smart clothing for enhanced safety features of vibration, lighting effects, and sounds. The creation of this smart clothing is still yet to be explored after careful analysis of the literature.

The emergence of smart and intelligent technologies for textiles has advanced the production of smart clothing for improved safety and protection. Harnessing these potentials combined with retro-reflective materials would further enhance the visibility and safety of pedestrians on the road. This design project investigates the integration of the unique concepts of design and technology to create a smart interactive clothing to respond to light stimuli to produce safety features. The aim of this project focuses on developing and combining retro-reflective materials and an integrated wearable detection or interactive system to provide and improve the visibility and alert ability for pedestrians most esp. blind and deaf individuals who use the road at night time. A smart interactive retro-reflective clothing (SIRC) design model, which combined design and technology for a smart clothing to enhance the alert level, visibility, and recognition of pedestrian on

the road was developed. Based on this SIRC design model, three (3) experiments are conducted for the effective integration of materials and technologies for the creation of smart interactive clothing. In the first experiment, retro-reflective textiles were developed with design elements drawn from African design patterns specifically the Sirigu wall paintings of Ghana. This design process adopted weaving on a jacquard loom to produce three different textiles with different weave combinations. Relevant testing procedures conducted revealed that fabric RF 3 with ¼ satin, move 2, and ½ twill, has an overall good total hand value (THV) with an average values of 2.605. Subsequently, three (3) different retro-reflective textiles with different basic weave structures (plain, twill, and diamond) were conducted on a dobby loom in the second experiment. Results revealed that the eventual THV of RF2 was higher than RF1, and the unique retro-reflective property of RF1 was higher than RF2 (based on the qualitative approach used to test the retro-reflective property of the textiles). Further design treatments of the 40 dpi-120 μs parameter on the textile surface showed some clarity of design patterns without affecting the retro-reflective abilities of the textiles.

In the final experiment, braided electronic-yarns and an interactive unit was developed. Herein, 0603 light-emitting diodes (LEDs) were embedded and encapsulated (using a heat shrinkable tube (HST)) in two stainless steel conductive threads (SS-CTs). This heat-shrinkable tube was further used to insulate one part of the stainless-steel conductive thread to ensure the flow of current and prevent any short circuit when the eyarns are braided. Results on the washing test of the braided electronic-yarns showed the robustness of the braided electronic-yarns even after 20 mechanical washing and drying cycles. These e-yarns were able to produce the necessary lighting effects needed to improve the visibility of the pedestrian at night. Subsequently, the interactive unit which comprised of a micro-controller, rechargeable battery, transistor, and sensors (vibration motor and light detector) was developed and coordinated with a written code. These were integrated into two prototype smart interactive retro-reflective clothing with design patterns inspired by the Sirigu wall paintings of Ghana. Different vibration patterns and sounds (ringtones) were characterised for the selection of the best option. Results revealed that, vibration patterns with a delay time of 100ms provided the needed acceleration critical to alert the pedestrian via the human skin. Additionally, ringtone High B has a higher sound effect of 161Hz after characterising three different sound patterns or ringtones. A test of the range of detection showed the ability of the smart interactive retro-reflective clothing to detect lights from a 25-metre distance with average light levels of 10.35. With different numbers of braided electronic yarns (containing LEDs) integrated to produce the smart clothing, the battery discharge was however different as presented in this work. It was shown that the developed output proved a success for further research geared towards enhancing night-time safety for pedestrians. This proposed system will significantly help pedestrians most especially the elderly and disabled (deaf and blind) pedestrians for improved visibility, alert levels, and recognition on the road.

PUBLICATIONS ARISING FROM THE THESIS

Journal Publications

- 1. Seidu, R. K, Jiang, S.X. (2024). Functional performance of Low-Cost Electronic-yarn for E-textiles, *MRS Bulletin*, https://doi.org/10.1557/s43577-024-00736-3
- 2. Seidu, R. K, Jiang, S.X. (2023). Analysis of performance properties of retroreflective woven fabrics made with retro-reflective yarns and natural yarns, *Textile Research Journal*, https://doi.org/10.1177/00405175231202786
- 3. Seidu, R. K, Sun, L. and Jiang, S.X. (2023). A Systematic Review on Retroreflective Clothing for Night-time Visibility and Safety, *The Journal of the Textile Institute*, https://doi.org/10.1080/00405000.2023.2212194
- 4. Seidu, R. K, and Jiang, S.X. (2023). Functional performance of thin Ag, SS, and Ti films on retro-reflective fabrics, *The Journal of the Textile Institute*, https://doi.org/10.1080/00405000.2023.2201981
- 5. Seidu, R.K., Choi, S.Y. and Jiang, S. (2023). Development and performance of jacquard woven retro-reflective textiles with African design patterns. *Fashion and Textiles*. 10, 2. https://doi.org/10.1186/s40691-022-00322-8
- 6. Seidu, R. K, Jiang, S.X. A Review of High-Visibility Clothing for Accident Prevention and Safety, *The Journal of the Textile Institute* (under review)

Conference Publications & Presentations

- Seidu, R. and Jiang, S.X. (2023). Performance quality of braided e-yarns for pedestrian interactive textiles. E-Textiles 2023: 5th International Conference on the Challenges, Opportunities, Innovations and Applications in Electronic Textiles, Ghent, Belgium. 14 and 16 November 2023. https://doi.org/10.3390/engproc2023052004
- 2. Seidu, R. and Jiang, S.X. (2023). Visibility aids for pedestrian safety at night: Review and recommendations for future studies. International Conference Smart Textiles and Emerging Technologies Conference (STET-2023): New Zealand, pp. 65-72. August 22-23. https://doi.org/10.61135/stet2023
- 3. Seidu, R. K, and Jiang, S.X. (2023). Interactive clothing for enhancing pedestrian safety at night Autex 2023 Conference, RMIT University, Melbourne, Australia. 26 -28 June 2023.

Patent

1. Jiang, S.X., Seidu, R. K. Jing, L. 一种带有互动装置的夜间行人安全服, *China Patent*, 202322678021.6, 2024/03/22

Award

 SFT's RPg Outstanding Research Achievement Award 2024 – Fashion design category

ACKNOWLEDGEMENTS

It is of great importance I give thanks to the ALMIGHTY GOD for integrating in me wisdom and knowledge to push through successfully my PhD studies. My deepest gratitude to my mentor and Chief Supervisor, Professor Shou-xiang Kinor Jiang in the School of Fashion and Textiles for his great interest, support, encouragement, and guidance in seeing me through this research study. Professor Jiang has a remarkable understanding, attention to detail, and in-depth knowledge in the field of textile design and metallic textiles. These critical attributes coupled with his ability to originate ideas that translate into core experiments for effective solutions, hence scientific papers are written to share the knowledge. A special thanks to Mr Ng Shui-wing, the technical officer at the weaving workshop for his great support, teaching and guidance during the development of my materials for my study.

Furthermore, I express my deep gratitude to my Big Brother Mr Stephen Donniri, and his family for their great contributions towards my PhD studies at PolyU. His support and inspiration have greatly motivated me to reach greater heights in this academic journey. I also want to acknowledge the support, prayers, and encouragement from my parents, Frederick Y. K. Seidu and Theresa Suglo, and my Big Sisters, Flavia Naa and Lucy Ziebanye, and Mr Prince Koveh for his immense contribution to my academic journey. Special thanks to my former mentors at KNUST-Ghana, Prof Ebenezer Kofi Howard, Prof Charles Frimpong, Prof Benjamin Kwablah Asinyo, and also Prof Richard Acquaye at TTU-Ghana. My gratuity further goes to Miss Mavis Amo-Affo, Mr Reindolf Monnie Amponsah, and Mr Alex Osei Afriyie for their contribution and prayers which have helped me in my PhD studies.

It is however important I acknowledge and extend my gratitude to The Hong Kong Polytechnic University for the unique academic funding support for my PhD studies at SFT. This support has exposed me greatly and has shaped me within the academic world where I have contributed with academic publications and a patent. I am truly honoured to have undertaken my PhD studies here at PolyU.

Finally, to my friends back home in Ghana and here in Hong Kong, most especially the Association of Ghanaian Scholars in Hong Kong (AGSK), my extreme appreciation to them all.

TABLE OF CONTENTS

	Page
CERTIFICATE OF ORIGINALITY	i
DEDICATION	ii
ABSTRACT	iii
PUBLICATIONS ARISING FROM THE THESIS	vi
ACKNOWLEDGEMENTS	vii
LIST OF FIGURES	xi
LIST OF TABLES	xviii
LIST OF ABBREVIATIONS	xix
CHAPTER 1: Introduction	1
1.1 Research background	1
1.2 Research objectives	4
1.3 Methodology	5
1.4 Originality, Significance and Value	6
1.5 Research scope	8
1.6 Thesis outline	8
CHAPTER 2: Review of related literature	11
2.1 Introduction	11
2.2 Pedestrian accidents and significant approaches	11
2.3 Global market of retro-reflective materials	19
2.4 Retro-Reflective (RR) materials	21
2.5 Technologies for retro-reflection	24
2.6 High-visibility clothing	27
2.7 Experimental studies on retro-reflective textiles	46
2.8 Functional applications of RR materials	50
2.9 Summary and research gap	56
CHAPTER 3: Methodology	57
3.1 Introduction	57
3.2 Practice-based research methodology	57
3.3 Design models for interactive and smart textiles or clothing	58

	Page
3.4 Smart interactive retro-reflective clothing (SIRC) design model	59
3.5 Concept of the research	62
3.4 Mechanism of methods/techniques	63
3.5 Materials	67
3.6 Characterisation	67
3.7 Design inspiration for the study: <i>African patterns</i>	71
CHAPTER 4: Material Development and Finishing Treatment	74
4.1 Introduction	74
4.2 Jacquard woven retro-reflective fabric samples with African design pat	terns74
4.2.1 Methodology	76
4.2.2 Experimental and Characterisation	81
4.2.3 Results and Discussion	81
4.2.4 Summary	90
4.3 Development of retro-reflective textiles via dobby loom	91
4.3.1 Methodology	91
4.3.2 Experimental and Characterisation	93
4.3.3 Results and Discussion	94
4.3.4 Summary	104
4.4 Retro-reflective textiles treated with laser engraving	105
4.4.1 Methodology	105
4.4.2 Laser treatments on the samples	106
4.4.3 Experimental and Characterisation	107
4.4.4 Results and Discussion	108
4.4.5 Summary	114
4.5 General summary	115
CHAPTER 5: Development and Integration of materials and systems	116
5.1 Introduction	116
5.2 Design and development of the interactive unit or system	116
5.2.1 Methodology	117
5.2.2 Design Concept	117
5.2.3 Preliminary procedure for the design of e-yarns	122
5.2.4 Evaluating direct current voltage (V _{DC})	

	Page
5.2.5 Summary	130
5.3 Design and development of functional electronic yarn	130
5.3.1 Methodology	133
5.3.2 Characterisation	139
5.3.3 Results and Discussion	142
5.3.4 Proof of concept	148
5.3.5 Summary	149
5.4 Smart interactive clothing for pedestrian safety	150
5.4.1 Methodology	153
5.4.2 Characterisation	156
5.4.3 Evaluation	159
5.5 Prototypes	161
5.6 Performance of the prototype smart interactive retro-reflective clothing	169
5.7 Summary	170
CHAPTER 6: Conclusions and Suggestions for future research	172
6.1 Conclusions	172
6.2 Suggestions for Future Research	175
6.3 Limitations of the study	176
References	178

LIST OF FIGURES

	Page
Figure 1.1. Procedures for research activities	5
Figure 1.2. Theoretical framework for the study	
Figure 2.1. Road user type death distribution in the world	
Figure 2.3. Projected global market of retro-reflective materials for 2021 - 202	
Figure 2.4. Retro-reflective sheeting. (a) prismatic sheet, (b) glass beads sheet;	
layer on the base substrate and glass bead embedded in the layer	
Figure 2.5. Orientation of retro-reflective materials; (a) glass beads (b) cube co	
prisms	
Figure 2.6. Principle of retro-reflection	
Figure 2.7. Retro-reflection of glass beads	
Figure 2.8. Indirect manufacturing process of glass beads	
Figure 2.9. Direct manufacturing process of glass beads	
Figure 2.10. Coating technology for producing high-performance fabric	
Figure 2.11. Cube corner/prismatic retro-reflection	
Figure 2.12. High visibility clothing: fluorescent colours and placement of retre	
reflective markers or strips	29
Figure 2.13. Garment combinations for pedestrians	30
Figure 2.14. (a) Experimental laboratory setup with the participants sitting 5 m	away
from the samples, (b) participants observing samples in a sunset cond	lition at
the laboratory and (c) images that show the appearance of evaluated s	samples.
	33
Figure 2.15. Stages of vision tracking system to detect workers with high-visib	ility or
reflective safety clothing in an industrial working environment	35
Figure 2.16. Different biomotion configuration diagrams on road worker clothic	ing38
Figure 2.17. (a) Pedestrians with biomotion configurations at night: (b) different	nt
configurations of retro-reflectors	38
Figure 2.18. Innovative Thai silk fabrics with retroreflective yarns	
Figure 2.19. Retro-reflective semi-transparent fabrics, (a, b) appearance under	a light
source; (c, d) transparent appearance of the fabrics	47
Figure 2.20. (a) Woven fabrics with RR yarns; (b) garment from RR woven fabrics with RR yarns;	orics48
Figure 2.21. (a-1) 25% pattern covering area; (a-2) appearance after abrasion to	
screen printed fabrics with 25% pattern covering area; (b-1) 85% pattern	tern
covering area; (b-2) appearance after abrasion test on transfer film pr	inted
fabrics with 85% pattern covering area	49
Figure 2.22. Design patterns printed on garments with RR inks	50
Figure 2.23. RR materials used in road construction. (a) road traffic control; (b) high-
visibility (high-vis) clothing; (c) protective clothing for firefighters	
Figure 2.24. Three optical technologies	
Figure 2.25. Illustration of urban thermal environment influenced by the mater	
in the buildings	
Figure 2.26. (a) Windows with reflective films set-up; (b) temperatures from in	ıfrared
imagery	52

Figure 2.27. Application of RR tapes in the automobile industry. (a, b) visuals at
daytime; (c, d) retro-reflective effects at night-time; (e) patterns and colour
combination of RR tapes on heavy trucks to test their visibility or recognition
53
Figure 2.28. Marine life-saving floating devices fitted with RR materials in stripes54
Figure 2.29. (a) Fashion Clothing and accessories; (b) sneakers by Adidas; (c) anti-
paparazzi scarf55
Figure 2.30. Representation of previous research studies with an identified gap that the
present study seeks to explore and fill56
Figure 3.1. Design model for smart fashion with visible light communication ability58
Figure 3.2. Design model for smart garments in rehabilitation59
Figure 3.3. Smart interactive retro-reflective clothing (SIRC) design model for the
current research60
Figure 3.4. Concept of SIRC62
Figure 3.5. (a) Appearance of the jacquard weaving loom, (b) detailed information of
the Dornier / PTV 8J jacquard weaving loom64
Figure 3.6. (a) Appearance of the rapier sample loom with dobby shedding, (b) detailed
information of the rapier sample loom65
Figure 3.7. (a) Laser engraving machine. (b) alignment of the laser beam. (c) beam
reflecting the path of the laser engraving machine and (d) parameters of the
laser engraving machine66
Figure 3.8. Appearance of the retro-reflective yarns67
Figure 3.9. Experimental set-up to capture the reflective nature of the woven fabrics68
Figure 3.10. Low-stress mechanical property. (a) shear properties, (b) surface
properties, (c) compression properties, and (d) bending properties69
Figure 3.11. African geometric patterns. (a) ndebele wall paintings in South Africa; (b)
sirigu wall paintings in Ghana; (c) geometric motifs on asante kente cloth in
Ghana72
Figure 3.12. African Figurative Patterns: (a) motifs commonly found in Fon Applique
cloth in Benin, and (b) motifs used for Adire cloth produced in Nigeria73
Figure 4.1. Activities in the research methodology: RQ – research question77
Figure 4.2. Stages for jacquard weaving of reflective woven textiles inspired by African
art forms
Figure 4.3. (a-c) African design patterns in Sirigu wall paintings, and (d-f) graphic
patterns for designs 1-379
Figure 4.4. Weave structure: the design on the front face and reversed design at the
back face80
Figure 4.5. Images taken during the day: (a) RF 1, (b) RF 2, and (c) RF 3. Images taken
in a dark room: (d) RF 1, (e) RF 2 and (f) RF 382
Figure 4.6. Microscopic images of sample surfaces at 500 µm: (a) RF1 with silver
reflective yarns as weft, (b) RF2 with black reflective yarns as weft, and (c)
RF3 with black reflective yarns as weft, all in the horizontal plane82
Figure 4.7. Bending property (a) bending rigidity, and (b) bending hysteresis83
Figure 4.8. (a) Linearity of compression and compressional energy (gf.cm/cm2), and
(b) compressional resilience (%)

Page
Figure 4.9. (a) Coefficient of friction, (b) fabric mean deviation, and (c) fabric
roughness85
Figure 4.10. (a) Shearing rigidity (G), (b) hysteresis of shear force at 0.5° (2HG), and (c) hysteresis of shear force at 5° (2HG5)86
Figure 4.11. Air resistance of the woven textiles with different weave structures87
Figure 4.12. Thermal conductivity of samples88
Figure 4.13. Tensile strength of samples
Figure 4.14. Microscopic images of the yarn structures under 500 µm magnification, (a)
100% 40s/2 Cotton; and (b)120D/2 Reflective yarns
Figure 4.15. Plan for weave design, (a) plain weave (RF1), (b) twill weave (RF2), and
(c) diamond weave (RF3), for one yarn picking pattern92
Figure 4.16. (a) Original appearance of the woven textiles with plain weave (A-1), twill
weave (A-2), and diamond weave (A-3); (b) reflective effects of woven
textiles with plain weave (B-1), twill weave (B-2), and diamond weave (B-3)
94
Figure 4.17. Microscopic images of the structural appearance of woven fabric samples
(a) RF1 - plain weave, (b) RF2 - twill weave, (c) RF3 - diamond weave95
Figure 4.18. (a) Bending rigidity and (b) bending hysteresis of the fabric samples96
Figure 4.19. (a) Compressional linearity and compressional energy of the fabric
samples, (b) compressional resilience of the fabric samples and (c) thickness
values of the fabric samples at pressures 0.5 gf/cm2 (To) and 50 gf/cm2 (Tm)
98
Figure 4.20. (a) MIU of the fabric samples, (b) MMD of the fabric samples, and (c)
SMD of the fabric samples99
Figure 4.21. (a) Shear rigidity of the fabric samples and (b) shear hysteresis of the
fabric samples100
Figure 4.22. Air permeability of the fabric samples
Figure 4.23. Thermal conductivity of the fabric samples
Figure 4.24. Original appearance of (a-1) plain woven fabric (b-1) twill woven fabric
and (c-1) diamond woven fabric; Retro-reflective effects or appearance of the
laser parameters on (a-2) plain woven fabric (b-2) twill woven fabric and (c-
2) diamond woven fabric
Figure 4.25. The appearance of (a-1) LA-RF1 (with plain weave), (b-1) LA-RF2 (with
twill weave) and (c-1) LA-RF3 (with diamond weave) engraved with 30 dpi-
110 µs parameters; appearance of (a-2) LA-RF3 (with plain weave), (b-2)
LA-RF2 (with twill weave) and (c-2) LA-RF3 (with diamond weave)
engraved with 40 dpi-120 µs parameters109
Figure 4.26. (a) Structure of the reflective thread captured under a magnification scale
of 200 µm, (b) burning effect of the laser engraving on the woven structure
under a magnification scale of 500 μm110
Figure 4.27. Microscopic images of laser-treated fabrics under 500 µm magnification,
(a) $-$ (c) engraved with 30 dpi/120 μ s and (d) $-$ (f) engraved with 40 dpi/120
ue 111

Figure 4.28. SEM images of the laser-treated fabrics under x180 magnification, (a) –
(c) engraved with 30 dpi/120 μ s and (d) – (f) engraved with 40 dpi/120 μ s.
Figure 4.20. SEM images showing malten polyector on the surface of the class heads at
Figure 4.29. SEM images showing molten polyester on the surface of the glass beads at
40 dpi/120 μs laser engraving under x180 magnification,
Figure 5.1. Methodological approach used in the experimental work
Figure 5.2. Design principle of the electronic interactive system
Figure 5.3. Open-sourced system (Micro:bit V2) by BBC in UK
Figure 5.4. Testing procedure to light up the LEDs using the power supplied from the PCB120
Figure 5.5. (a) Modelling case housing the interactive unit and (b) case housing the
micro-controller with its related components. (c) controller switch unit (case
housing the battery for easy supply of power to the micro-controller) 122
Figure 5.6. Stainless Steel conductive yarns. (a) 91*3 thread with THK of 0.36mm (b)
100*3 thread with THK of 0.25mm, (c) 275*3 thread with THK of 0.42mm, and (d) 1000*3 thread with THK of 0.65mm. (THK means thickness) 123
Figure 5.7. Two LEDs were used in the experiments. (a) front and back image of 0603
diodes (red), (b) front and back image of 2835 diode (red)
Figure 5.8. (a) Appearance of the solder pads of the LEDs after using the soldering
process (b) appearance after using a heat-shrinkable tube to encapsulate the
LEDs to the stainless-steel conductive threads
Figure 5.9. Appearance of responsive action (lights turned on/off) of the 2835 LEDs
(red) embedded in different yarn types. (a,e,i) – yarn A with 1, 3, and 5
diodes, (b,f,j) – yarn B with 1, 3, and 5 diodes, (c,g,k) – yarn C with 1, 3, and
5 diodes, and (d,h,l) – yarn D with 1, 3 and 5 diodes
Figure 5.10. Effect of the number of 2835 LED lights embedded in different yarn types
on the direct current voltage (VDC). (a) VDC against the number of LEDs,
(b) magnified diagram of VDC against the number of LEDs showing values
for all yarn types embedded with 1, 3, and 5 diodes above 1.5V.
Measurements were taken using a digital multimeter
Figure 5.11. Appearance of responsive action (lights turned on/off) of the 0603 LED
lights (red) embedded in different yarn types. (a,e,i) – yarn A with 1, 3, and 5
diodes, (b,f,j) – yarn B with 1, 3, and 5 diodes, (c,g,k) – yarn C with 1, 3, and
5 diodes, and (d,h,l) – yarn D with 1, 3 and 5 diodes
Figure 5.12. Effect of the number of 0603 LED lights embedded in different yarn types
on the direct current voltage (VDC). (a) VDC against the number of LEDs,
(b) magnified diagram of VDC against the number of LEDs showing values
for all yarn types embedded with 1, 3, and 5 diodes above 1.8V.
Measurements were taken using a digital multimeter
Figure 5.13. (a-1) Front of SMD 0603 LED and (a-2) Back of SMD 0603 LED, (b)
stainless steel conductive yarns, (c) different types of HSTs, (d) scotch®
transparent tape, (e) Ø1.5 mm HST before and after shrinkage, and (f) Ø0.6
mm HST before and after shrinkage
Figure 5.14. Initial design of the e-yarns without insulting the stainless-steel conductive
threads 134

Figure 5.15. Design one fabrication process of e-yarn. (a) schematic of the cross-
sectional view of embedding SMD 0603 LEDs on stainless-steel (SS)
conductive yarns and encapsulating with HST, (b) attaching two parallel
yarns to the solder pads using conductive adhesive, (c) placing AT on one
side of the parallel yarn to prevent short-circuiting when the surface of the
yarns come into contact, and (d) encapsulating the light-emitting diode (LED)
to the yarns with a heat-shrinkable tube (HST)
Figure 5.16. Design two fabrication processes of e-yarn. (a) schematic of cross-
sectional view of embedding SMD 0603 LEDs on stainless-steel (SS)
conductive yarns and encapsulating with heat-shrinkable tube (HST), (b)
cross-sectional view of SMD 0603 light-emitting diode (LED), (c) placing
side of LED on AT, (d) placing two SS conductive threads on both sides of
LED, (e) concealing using adhesive tape (AT) to ensure yarns come into
contact with LED, (f) placing HST over the concealed region, and (g)
encapsulating the LED with the threads in an HST136
Figure 5.17. (a-c) E-yarn development process with Ø1.5 mm heat-shrinkable tube
(HST), (d-f) e-yarn development process with Ø0.6 mm heat-shrinkable tube
(HST), (g-h) shape of the ends of the encapsulated light-emitting diodes
(LEDs) for Samples 1 and 2 respectively, (i) insertion and braiding technique
of the e-yarns. Eight core RR threads are used to braid around two conductive
threads with light-emitting diodes (LEDs) in series
Figure 5.18. Design plan to produce the e-textiles on a loom
Figure 5.19. Temperature colour indicators for captured infrared (IR) images140
Figure 5.20. Experimental set-up to measure the light intensity values with lux meter
141
Figure 5.21. (a) Front view of a white t-shirt with Sample 1 in both fabric and braided
e-yarn forms and, (b) back view of a white t-shirt with Sample 2 in both
fabric and braided e-yarn forms
·
Figure 5.22. Surface morphology of: (a) sample 1 with Ø1.5 mm HST, (b) Sample 2
with Ø0.6 mm HST, (c) thickness of the insulated conductive thread with Ø0.6
mm HST (top) and Ø1.5 mm HST (bottom), and (d) thickness of braided e-
yarns at CT insulated regions with Ø0.6 mm HST (top) and Ø1.5 mm HST
(bottom) (Note: CT denotes conductive thread)142
Figure 5.23. Tensile strength of e-yarns and braided for Samples 1 and 2. (a) breaking
load and breaking extension for samples 1 and 2, (b) tenacity for samples 1
and 2, (c-1 and c-2) nature of the fabricated e-yarn and braided e-yarn after
tensile strength test for sample 1 and (d-1 and d-2) nature of the fabricated e-
yarn and braided e-yarn after tensile strength test for Sample 2143
Figure 5.24. (a) Thickness of fabric samples, (b) weight of fabric samples. (Note: Area
of CT means the area where the HST is used to cover the side of the SS-CT,
and the LEDs portion means the encapsulated region that joins the LED to
two SS conductive threads for positive and negative terminals)144
Figure 5.25. Shearing property values of e-textiles in the weft direction. (Note: G
means shear rigidity, 2HG means hysteresis of the shear force and 2HG5
means hysteresis of the shear force at 5°) 145

Page
Figure 5.26. (a-1) and (b-1) Sample 1 electronic textiles powered with the use of a 3 V battery. (a-2) IR images of Sample 1 electronic textiles at 0 min and (b-2) IR images of sample 1 electronic textiles after 5 mins; (c-1) and (d-1) sample 2 electronic textiles powered with the use of a 3 V battery. (c-2) IR images of Sample 2 electronic textiles at 0 min and (d-2) IR images of Sample 2 electronic textiles after 5 mins.
Figure 5.27. Effects of encapsulation on the light intensity values of the LEDs147
Figure 5.28. Washing durability results of braided e-yarns: various washing and drying cycles
Figure 5.29. (a) Detachment of braid at end of the encapsulated area of sample 1 braided e-yarns, (b) non-functioning LED in Sample 1 braided e-yarns, and (c) non-functioning LED in sample 2 braided e-yarns
Figure 5.30. (a) Braided e-yarns with 1.6 mm HST, used for (b) and (c) woven e-textiles, (d) flexible nature of the e-textiles; (e) braided e-yarns with 0.5 mm HST, used for (f) and (g) woven e-textiles, (h) flexible nature of the e-textiles.
Figure 5.31. Application of light-emitting materials for safety and aesthetic clothing.
(a) interactive smart fashion with visible light communication ability (Kim et al., 2017), (b) illuminative smart fashion for women (Demerdash and Mostafa, 2018), (c) design concept of LED clothing for cyclists (Wei et al., 2015), and (d) transformable warning clothing for children (Studzińska et al., 2022)152
Figure 5.32. Initial prototype plan of the various components of a garment to be constructed using jacquard retro-reflective woven fabrics
Figure 5.33. Assembled components on the jacquard retro-reflective woven fabrics. (a) the appearance of the assembled components on the front and back bodice, (b) reflective effects in the darkroom setting taken by a digital camera, (c) and (d) positioning of the light detector sensor and vibration motor, (e) positioning of the controlling unit at the upper side of the back bodice, (f) pocket for housing the batter pack to power the microcontroller
Figure 5.34. (a) Front appearance of the assembled clothing, (b) no lighting effects in the darkroom setting taken by a digital camera, (c) lighting effects of the red LEDs when light is detected in the darkroom conditions at the laboratory taken by a digital camera
Figure 5.35. Experimental set-up to measure the vibration patterns of the vibration
motor. (a) no retro-reflective textile material is placed in between the vibration motor and the accelerometer. (b) retro-reflective textile material is placed in between the vibration motor and the accelerometer
Figure 5.36. Experimental set-up to test the range of detection of the smart interactive clothing. (a) image of the laboratory experimental set-up (b) image of the developed simulated car headlights (c) 12V LED projector lens with 8000 lumens and 6000K white light for automotive headlight (d) image of the

rechargeable battery (e) image of the switch button to turn on/off the

Page
Figure 5.38. (a) No retro-reflective textile material is placed in between the vibration
motor and the accelerometer (b) retro-reflective textile material is placed in
between the vibration motor and the accelerometer
Figure 5.39. Sound levels (Hz) of (a) ringtone - low b. (b) ringtone - middle b. (c)
ringtone - high b. and (d) sound levels of all ringtones from the micro-
controller
Figure 5.40. The range of detection of the presence of lights from (a) simulated car
headlight; under (b) 5 metre, (c) 10 metre (d) 15 metre, (e) 20 metre and (f)
25 metre
Figure 5.41. (a) Technical drawing of the sleeve men's shirt showing the positions of
the various components. (b) light detector sensor. (c) location of the braided
e-yarns. (d) appearance of the smart interactive clothing showing the front
and back side. (e) location of the pocket for the micro-controller unit and (f)
location of the pocket for the battery unit to power the micro-controller unit.
Eigen 5.42 (a) A management of the accomplished plathing with no lighting official in the
Figure 5.42. (a) Appearance of the assembled clothing with no lighting effects in the
darkroom setting. (b) retro-reflective effects in the darkroom setting. (c)
lighting effects of the green LEDs when light is detected in the darkroom
conditions at the laboratory
Figure 5.43. Terminal voltage change of battery A (500mAh) and battery B (300mAh)
when charged and discharged.
Figure 5.43. (a) Technical drawing of the sleeve men's shirt showing the positions of
the various components. (b) light detector sensor. (c) location of the braided
e-yarns. (d) appearance of the smart interactive clothing showing the front
and back side. (e) location of the pocket for the micro-controller unit and (f)
location of the pocket for the battery unit to power the micro-controller unit.
166
Figure 5.44. (a) Appearance of the assembled clothing with no lighting effects in the
darkroom setting. (b) retro-reflective effects in the darkroom setting. (c)
lighting effects of the red LEDs when light is detected in the darkroom
conditions at the laboratory
Figure 5.45. Terminal voltage change of battery A (500mAh) and battery B (300mAh)
when charged and discharged
Figure 5.46. Performance indicators of the smart interactive retro-reflective clothing 170

LIST OF TABLES

	Page
Table 2.1. Influential causes of pedestrian accidents	14
Table 2.2. Modelling techniques to analyse crash data	
Table 2.3. Various classes of high-vis clothing according to (AS/NZS 1906.4)	31
Table 2.4. Studies on performance conditions of high-visibility clothing	33
Table 2.5. Studies on the influence of clothing with biomotion configurations	39
Table 3.1. Description values and units for the three KES-F tests	69
Table 4.1. Specifications of the woven reflective textiles	81
Table 4.2. Tensile properties of samples in this study	87
Table 4.3. Primary and total hand values of samples	89
Table 4.4. Specification of the woven fabrics	93
Table 4.5. Fabric weight and thickness of the woven fabrics	95
Table 4.6. Tensile properties of samples	
Table 4.7. Primary and total hand values of samples	104
Table 4.8. Specification of fabrics	105
Table 4.9. Properties of the original and treated or engraved fabrics	110
Table 4.10. Colour appearance of the untreated and laser-treated fabric samples	113
Table 5.1. Parameters of the electronic components used for the interactive unit	119
Table 5.2. Resistance measurement of stainless-steel conductive yarns	124
Table 5.3. Different approaches were adopted to insulate the stainless-steel condi-	uctive
threads	126
Table 5.4. Specification of the woven e-textiles	139

LIST OF ABBREVIATIONS

E-yarns - Electronic yarns
E-textiles - Electronic textiles
HCT - Heat Contraction Tube

SS - Stainless Steel

SS-CT - Stainless Steel Conductive Threads

RR - Retro-reflective

KES-F - Kawabata Evaluation System of Fabric

LED - Light emitting diodes
SMD - Surface Mount Device
CT - Conductive Threads
GSM - Grams per Square meter

SIRC - Smart interactive retro-reflective clothing

HVM - High visibility materials

HVSA - High visibility safety apparel

CHAPTER 1: Introduction

1.1 Research background

Pedestrian safety has been a major concern in road traffic management in the World. Studies by Hu and Cicchino (2018); Chong et al. (2018) has revealed pedestrian fatalities at night are higher than at day which has accounted for about 20 per cent of deaths on the road (World Health Organization, 2013). This hike in fatalities according to a report from WHO accounted for about 40% (an increase from previous statistics) of road clash deaths in Africa meaning 26.6 per 100,000 estimated residents (WHO, 2015). Attributable factors are driver-cause i.e., fatigue, visual impairment, alcohol consumption and over speeding, and most importantly pedestrian-cause i.e., not wearing reflective protective clothing at night (Ackaah and Adonteng, 2011, Cho et al., 2017). The latter coupled with low lighting conditions at night, leads to poor visibility of road users or pedestrians hence increasing night vehicle-pedestrian collisions (Sullivan and Flannagan, 2002).

A rise in fatalities numbers may broadly be attributed to the pedestrians' failure to wear reflective protective clothing that tends to improve their visibility to the approaching motorists at night. This is because some of the roads in both urban and rural areas lack the needed lighting system and road makings. This is a major road safety concern or problem since pedestrians walk along or across the road at night. In fact Tyrrell et al. (2016) reported that pedestrians tend not to appreciate the problem of nighttime conspicuity since a large number of them see the approaching vehicle via the headlights of the vehicles. This is however different in the case of the drivers where the visibility of the pedestrian is not clear enough from that distance to help detect them on time. Such lack of visibility at night by the pedestrians is largely due to the choice of clothing they wear. Green (2021) revealed that pedestrian clothing makes it difficult for visual detection by the drivers to avoid possible collisions. A resultant factor from the low reflectance rate or level of the clothing at night making its detectability very difficult. Additionally, in most cases, motorists just simply find it difficult to see pedestrian at night (Fylan et al., 2020a) hence an increase in the risk of an accident. Green further stated that the use of biological motion i.e., retroreflectors which are placed at specific joints of the human body improves their visibility.

Developments in the field of textile materials have occurred to imperatively produce a product that ensures the safety of the wearer most especially at night-time. With such a challenge, retro-reflective materials were developed to be applied in different areas most especially in clothing to produce products that improve the visibility of individuals at night thus limiting fatalities. They are made by first coating adhesives on the fabric surface and then glass beads are applied and held together with the substrate by the adhesive. These reflective materials are inherent with a surface property i.e., retroreflectivity or retro-reflection that enhances its ability to reflect light back to its source without scattering the light. Retro-reflection is a surface property of any material (Bible and Johnson, 2002, Mary, 2021) where incident light is reflected back to its source. Lloyd (2008) further added that retro-reflection adopts three key principles; specular reflection, refraction and total internal reflection, to bounce light back to origin without absorbing it. The refractive index of glass beads is an imperative property (Taek et al., 1999) that dictates the visibility and reflection distribution of light back to its source without scattering the reflected light in different directions. This retro-reflective effects of a surface are accomplished by two system technologies; glass beads and cube or prismatic corners (3M, 2014, Önlü and Halaçeli, 2012a), which are different in structural composition. With such reflective properties, different material types such as film, sheet, tape and trim, sheeting, paint, coating and inks are produced for different applications in the building, road, construction, clothing and fashion industries.

Researchers have explored these materials for some design and aesthetic performance. This approach has given numerous research studies to apply them as strips to improve the visibility of the pedestrian on the road. In most cases, these retro-reflective strips are applied onto clothing in biomotion configuration for easy recognition by the approaching vehicle. This study therefore acknowledges studies conducted to use reflective films as strips on clothing to investigate their performance (Babić et al., 2021, Black et al., 2021, Wood et al., 2011). These films are attached in biomotion configurations (BC) on the clothing to help drivers recognise the silhouette of the human body. BC are motion configurations that are structured to fit several human joints. These motion patterns enhance effective detection, identification and conspicuity of the pedestrian's body (Mian and Caird, 2018) for effective response judgement by the driver. Further studies by Fylan et al. (2021) and Fylan et al. (2020a) revealed that pedestrians

prioritised their style and comfortability to improve their visibility because these biomotion garments are poor in nature and design.

In a more design approach, Kharenkova (2018) screen printed retro-reflective inks on varying types of fabrics. Results proved an improved retro-reflection of the fabrics suitable for fashion garments. Nualdaisri (2022), Önlü and Yaşar (2011) and Önlü and Halaçeli (2012a) further reported on using reflective yarns for the aesthetic appeal of Thai silk fabrics and fashion fabrics respectively. The latter was revealed to have, puffy and voluminous effects coupled with shimmering and brighter effects that reflect light.

It is thus imperative to state that, previous studies have dealt with the usage of retro-reflective materials like films as strips or biomotion patterns on clothing, and inks or threads for producing fabrics. The efficiency of such approaches to improve the retroreflective performance of textiles depends on the properties of the combined materials. Limited attempts have therefore been advanced to provide alternative approaches that collectively aim at improving the safety and visibility of pedestrians. The area of smart clothing provides an effective alternative to improving conspicuity and safety at night. This clothing according to Ahsan et al. (2022), are next-generation advanced clothing with embedded wearable systems that monitor, interact and produce responses in the environment. Even though the growth of the smart clothing industry for varying applications has been on a progressive trajectory, research studies for the use of wearable systems to improve the visibility of pedestrians on the road at night-time are still lacking. The study however acknowledges studies by Tsuji et al. (2002) and Goodall (2016) on detection and night vision technologies developed to improve the driver's response and recognition at night-time for fewer vehicle-pedestrian collisions. There is therefore little knowledge and research into detection or interactive systems for pedestrian clothing for night-time safety.

Considering the great potential of wearable technologies for smart clothing, this study seeks to develop a smart interactive retro-reflective clothing to improve the safety of pedestrians at night-time. Different retro-reflective materials can be fashioned to produce the needed retro-reflective properties to improve the visibility of pedestrians. The study therefore used retro-reflective yarns to create textile designs on the woven fabrics. Aside from this, detection or interactive systems are further necessary to provide

quick and additional responses to help improve the visibility and recognition of pedestrians by approaching vehicles on the road. The focus therefore is to combine reflective materials and an integrated wearable detection or interactive system to improve and provide more visibility for pedestrians at night-time. The study adopts an integrated smart interactive retro-reflective clothing (SIRC) model that combines design and technology to produce innovative designs for pedestrian safety.

1.2 Research objectives

The aim of this project focuses on developing and combining reflective materials and an integrated wearable detection or interactive system to improve and provide more visibility for pedestrians at night time. This textile design system seeks to enhance the visibility and conspicuity of wearers on the road to help limit collisions with approaching vehicles. To achieve the set focus, the following stipulated objectives were outlined:

- To identify research studies on retro-reflective materials and to design an
 integrated smart interactive retro-reflective clothing (SIRC) model that combines
 both design approach and technology for an interactive system to improve the
 visibility of and alert pedestrians.
- To evaluate and study the characteristics and performance of woven retroreflective materials for their physical and functional properties and to investigate the properties of creating designs using laser engraving on woven retro-reflective materials.
- 3. To design the coordination and integration of sensors and LEDs for an interactive system that can produce three interactive outputs i.e., lights, vibration, and sound as additional features to alert pedestrians at night time.
- 4. To fabricate prototyping clothing with retro-reflective materials and interactive system and test the performance of conspicuity or visibility that opens commercial applications for safety of the pedestrians on the road at night.

1.3 Methodology

A systematic flowchart outlined in five (5) critical stages (Figure 1.1) indicates the relevant procedures undertaken for the activities in the research project. These effectively guided and aided in accomplishing the set goal and focus of the research that draws on producing retro-reflective fabrics and an interactive system for clothing applications to help improve the recognition and visibility of wearers or pedestrians at night.

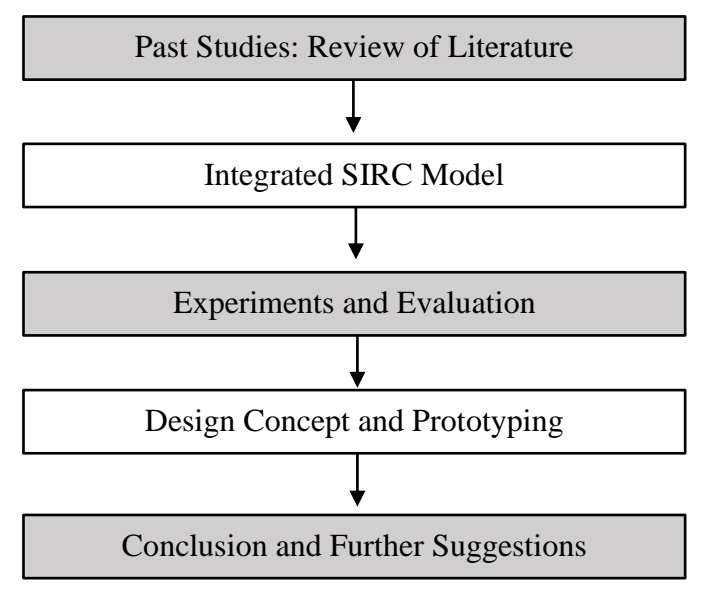


Figure 1.1. Procedures for research activities

To clearly understand the approaches, concept and context of the study, a systematic review of related literature was conducted on retro-reflective materials and high visibility (high-vis) clothing coupled with their applications in textile and fashion. These past studies provided great insights on the aspects experimented on so far and hence the behaviour of users that has influenced its usage and application. Knowledge gained from the analysis of past studies influenced the development of a SIRC model that seeks to produce an interactive system coupled with retro-reflective fabrics for smart interactive visibility clothing. Subsequently, textile design technologies such as weaving, and printing helped in the experimental works to produce retro-reflective fabrics. These materials were then tested, and results were evaluated based on their physical, mechanical, and functional/performance properties. The successful outcomes influenced the creation of designs on the fabrics for clothing application. Furthermore, a wearable interactive system was developed to interact and enhance the visibility of the pedestrian. This finally led to conducting remarks and future research suggestions.

Figure 1.2. Theoretical framework for the study

This systematic flow of research activities was guided by a theoretical framework (Figure 1.2) to produce smart interactive retro-reflective clothing for night-time safety. Here, materials (such as retro-reflective yarns) and technologies (weaving, embroidery, and wearable sensors) were adopted in the production process. This approach means the retro-reflective yarns were used to produce woven fabrics (jacquard fabrics and weave fabrics) while the weave fabrics were then laser engraved to create design patterns on their surfaces, still using the retro-reflective yarns. Additionally, technologies in the use of sensors and LEDs were adopted and coordinated via codes to produce lighting, sound, and vibration effects to further improve visibility and interact with the pedestrians on the road at night time.

1.4 Originality, Significance and Value

In this project research, three major sections are formulated; the first section highlights fabric synthesis through weaving (via jacquard and rapier sample loom) using appropriate retro-reflective, and cotton yarns, where fabric samples from the rapier sample loom are treated with laser engraving for design creation; the second section entailed the development of a braided electronic yarn (for lighting effects) and an interactive system (using micro-controller and sensor devices) that can be embedded into clothing to enhance the recognition or visibility; and finally the third section highlights the working procedure of the developed interactive clothing for pedestrian use at night-time. It is imperative that in all sections, the required characterisation and testing procedures are conducted and established.

Pedestrian accidents remain a recurring phenomenon on the road at night time that has claimed many lifes. Such high accidents recorded at night are largely due to the insufficient use of warning clothing that reduces the visibility of the road users for the approaching vehicles. Importantly, the manufacturers of retro-reflective textiles form part of the warning clothing that plays a role in improving their visibility. This is due to

its inherent retro-reflectivity properties that are made of either micro-prism or glass bead sheets. However, these retro-reflective and high-visibility clothing are specifically designed that are widely used by road users, construction workers, and security agents amongst others.

To further provide innovative solutions to help alert users, improve user visibility and recognition, hence limit the rate of accidents, this study proposes to investigate and develop a smart interactive retro-reflective clothing (SIRC) that combines textile design and sensory technology through the SIRC model. In this alternative approach, an interactive system was developed using wearable sensors and materials coordinated by a working code. This produces an output of lighting effects via LEDs, sound, and vibration to effectively interact with the pedestrian and approaching driver when light falls on a sensor embedded in the clothing, based on this design concept for the study, the main contribution of this project is highlighted here:

A smart interactive retro-reflective clothing with a two-way communication system for the pedestrian and the driver is successfully developed. Herein, the braided electronic yarns (embedded with LEDs and stainless-steel conductive yarns) which produce sufficient lighting effects of red or green are used to communicate with the driver as a warning signal of the presence of road user. The developed interactive system coupled with its sensors is used to communicate with the road user about the presence of an approaching vehicle. This creates an alert system through vibration and sound.

Secondly, in this study, the developed smart interactive retro-reflective clothing will significantly help pedestrians most especially the elderly and disabled (deaf and blind) road users to be cautious on the road. Through the two safety alert features of vibration and sound, the elderly and disabled (deaf and blind) road users would be effectively alerted to the presence of an approaching vehicle.

A design model developed from the study serves as a valuable and significant reference material for further research to improve the alert level, visibility, and recognition of road users at night. This model details how material development and electronic components can be effectively integrated (combining textile and technology) for a proposed approach to enhance the safety of road users. This study further contributes to the use of electronic and sensing devices for smart clothing applications to

improve the visibility of pedestrians hence ensuring their safety at night-time, a situation that opens future advances in this research area.

1.5 Research scope

The purpose of this current research is to combine design and technology to produce smart interactive retro-reflective clothing to ensure the safety of pedestrians at night. This research aims at employing retro-reflective yarns (made of glass beads), sensory devices, light-emitting diodes (LEDs), micro-controller, and stainless-steel conductive yarns. These materials would be combined effectively using weaving, braiding and laser techniques to efficiently produce retro-reflective textiles, braided electronic yarns (with embedded LEDs and stainless-steel conductive yarns) and create design patterns on the woven textiles respectively. Herein, the LEDs would be embedded into the stainless-steel conductive yarns to produce electronic yarns so-called e-yarns, which are further braided to aid in easy integration into a woven fabric. These braided e-yarns would contribute to producing the needed lighting effects in the clothing. Subsequently, the sensory devices and the microcontroller would be effectively coordinated to produce additional safety features in the form of sound, lighting effects, and vibration. Further evaluation of the assembled system on the retro-reflective clothing would be conducted to ascertain its workability.

It is worthy to note that, the design aspect of the study would be created based on inspiration drawn from African symbolic patterns most especially for the Sirigu wall paintings in Ghana. These are indigenous hand-painted motifs on the walls of traditional mud houses created by women in the community to communicate symbolic meanings to their viewers. Selected motifs would be used for producing woven fabrics and modified as design patterns to be laser engraved on the surfaces of plain-woven retro-reflective fabrics, the eventual assembled interactive clothing would fit both men and women.

1.6 Thesis outline

This thesis is a complete and broad compilation of experimental works which are published in leading journals and subsequently presented in international conferences on retro-reflective materials. These materials are widely used as strips to produce safety clothing to improve the visibility of pedestrians at night largely due to their ability to reflect light rays incident on their surface. Based on this property, they are utilized in the

study's creative process combined with a developed interactive system to produce three safety outputs of lights, sound, and vibration for a two-way communication approach for the pedestrians and the driver. An approach that is the first in its kind to be reported in the academic and research space for pedestrian safety clothing. This study is structured in six (6) chapters as carefully outlined.

Chapter 1 which is Introduction, lays the firm foundation by providing the background information on the need to provide safety clothing for pedestrians on the road and help limit accidents at night. This section of the thesis further highlights the objectives set for the study, the significance, originality, and value, and the research scope of the research study.

Chapter 2 which is the literature review, provides a comprehensive overview of retro-reflective (RR) materials, their application for use as high-visibility clothing, functional applications of RR materials, and related approaches used by studies to improve the visibility of wearers. The chapter concludes by providing the research gap from which this study seeks to cover or contribute to the research space. Subsequently, the details contained in this chapter are published.

Chapter 3 which is the methodology, highlights on practice-based research methodology, provides details about the study's developed design model, general materials, techniques, and equipment adopted in the study. The smart interactive retroreflective clothing (SIRC) design model is developed to effectively integrate electronic components into retro-reflective textiles for an interactive clothing for pedestrian use at night. This developed design model fills the research need for a specialised model for a smart interactive retro-reflective clothing for pedestrian safety. Furthermore, the different characterization information generally used in the study are described.

Chapter 4 highlights material development and finishing or embellishing treatments adopted in the study. This chapter details on three key experimental procedures conducted using jacquard weaving loom, dobby weaving loom and laser engraving. Firstly, retro-reflective textiles are produced via the jacquard weaving loom with patterns inspired by African design patterns, where the mechanical and reflective properties of the resultant fabrics are tested and presented. Secondly, retro-reflective textiles with basic weaves (plain, twill and diamond) are produced via the dobby weaving loom, where the mechanical and reflective properties of the resultant fabrics are tested

and presented. These retro-reflective textiles are further subjected to an embellishing technique i.e. laser engraving, for design creation on its surfaces. It is important to note that, relevant studies on laser engraving have established the reduction in size and weight of the treated fabrics. Based on this, the study adopts the best possible laser parameters for design creation. The respective findings from these experimental procedures contained in this chapter are published in leading journals.

The design, development and integration of the retro-reflective materials, braided electronic yarns, and the interactive system are described in Chapter 5. Herein, the interactive system or unit was developed using microcontroller, electronic components, and sensing devices, to effectively detect and trigger the production of safety outputs i.e. lights, vibration, and sound. The development of the braided e-yarns forms a firm foundation for easy integration into clothing and the production of lighting effects. By using a small 0603 LEDs and stainless-steel conductive yarns, the e-yarns are produced, which are further braided. In the last section of the chapter, the retro-reflective textiles braided e-yarns and the developed interactive system are combined effectively to form a smart interactive retro-reflective clothing for pedestrian use a night-time. An initial prototype was produced to provide great insights into the working procedures of the clothing, based on the success of the initial prototype, two final prototypes were created. It is worth noting that, the respective findings from these experimental procedures contained in this chapter are published in leading journals.

Chapter 6 details the concluding parts of the current study which developed a prototype smart interactive retro-reflective clothing with a two-way communication system for pedestrian use a night-time. The main findings of the study are summarized, with the study's limitations provided and critical points recommended for future research projects on interactive clothing for pedestrian safety at night.

CHAPTER 2: Review of related literature¹

2.1 Introduction

This review of related literature was deemed necessary to give a clear understanding and detailed information to the reasons that triggered the introduction of RR materials, the principles and sheeting technologies of retro-reflection, the application of RR materials via aesthetic and functional research approaches for RR fabrics and high-vis clothing, their functional applications in different sectors and finally the concept of African patterns. It is imperative that the rise in pedestrian and vehicular fatalities at night are the pushing factors that led to the introduction of sheeting technologies inherent with the properties of returning incident lights to their source hence improving the visibility and recognition of the object to limit collisions. As such, design and research studies have been conducted to utilise RR materials like inks, yarns, fabric, and films amongst others, to identify its visual effects and performance to retro-reflect lights. This has influenced its application in different sectors like fashion, marine, automobiles, building, and road construction. A review of these critical aspects provided an in-depth knowledge into past and current research studies undertaken which aided in identifying the clear research gap to which this current research project seeks to cover.

2.2 Pedestrian accidents and significant approaches

Transportation modes such as walking remain an effective means for most pedestrians to commute from one location to another aside from the use of vehicles, bicycles, and motorcycles as used by other road users. This makes them very vulnerable road users and hence prone to accidents and injuries (Hosseinian et al., 2021). Accidents, collisions, and injuries on our roads continue to be a global health challenge (Chang et

Seidu, R. K, Sun, L., Jiang, S. X. (2023). A systematic review on retro-reflective clothing for night-time visibility and safety. *The Journal of The Textile Institute*, 1-13. https://doi.org/10.1080/00405000.2023.2212194

Seidu, R. K, Jiang, S. X. (2023). Visibility aids for pedestrian safety at night: Review and recommendations for future studies. *International Conference – Smart Textiles and Emerging Technologies*: New Zealand, pp. 65-72. https://doi.org/10.61135/stet2023

Seidu, R. K, Jiang, S. X. A Review of High-Visibility Clothing for Accident Prevention and Safety, *The Journal of The Textile Institute*, (under review)

¹ Parts of this chapter are *published with details*.

al., 2020) that has claimed more lifes. The increase in deaths is predominantly associated with cyclists, motorcyclists, and pedestrians making road accidents the eighth leading cause of death globally (World Health Organization, 2018). This as opined by Movahhed et al. (2020) makes it very imperative for the provision of safety measures for pedestrians as they use the road either at day or night time. The latter according to Uttley and Fotios (2017) accounts for higher pedestrian accidents which have recorded fatalities much higher at intersections with no lighting systems and even at streets with lighting systems (Siddiqui et al., 2006). In fact, according to the World Health Organization (2018) report of Global status on road safety, pedestrian accidents account for the majority of road crashes in the World (Figure 2.1). These high numbers are caused by intoxicated pedestrians or drivers, high vehicular speeds (Sullivan and Flannagan, 2001), poor street lighting systems and road infrastructure, and the poor visibility or conspicuity of pedestrians on the road (Mphela et al., 2021).

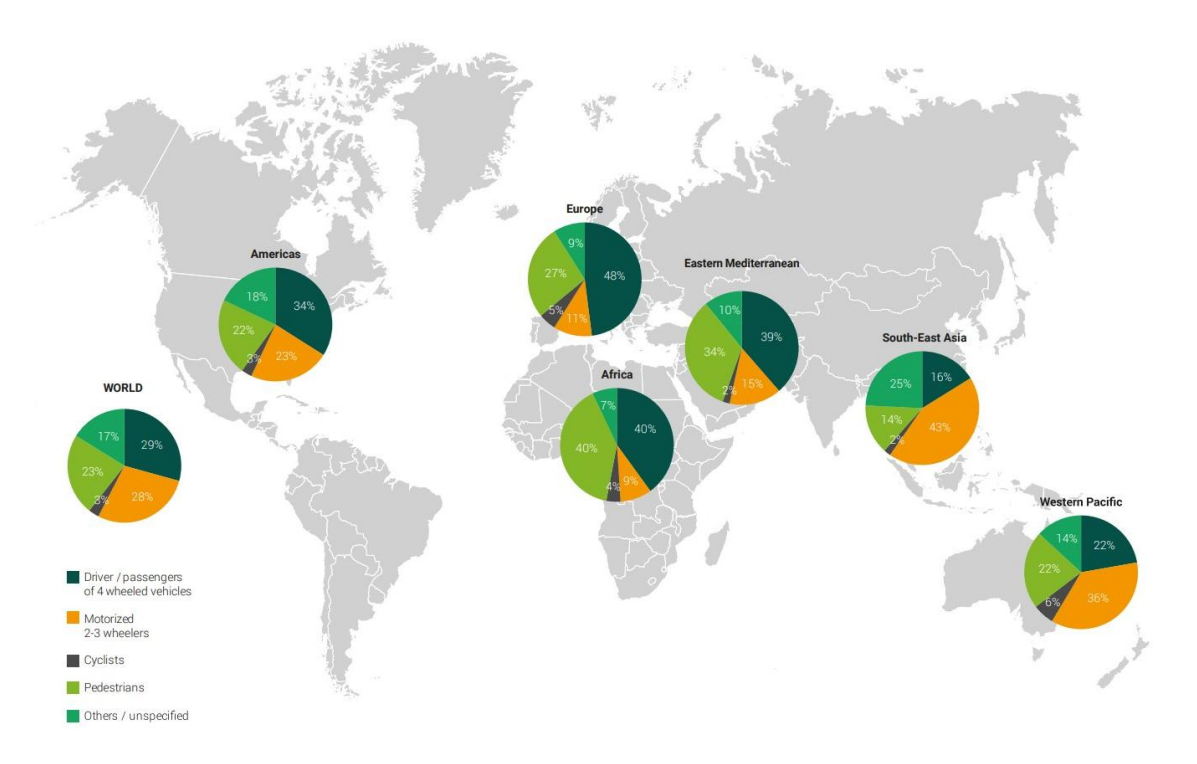


Figure 2.1. Road user type death distribution in the world (World Health Organization, 2018)

2.2.1 Influential causes of pedestrian accidents

In this section, the key influential factors that cause pedestrian accidents are identified to anlayse the ten most cited publications in the field. The issue of enhancing and improving vehicular headlighting systems has received adequate attention from

manufacturers (Sullivan and Flannagan, 2002). A clear technological advancement has led to intelligent lighting or adaptive headlighting with effective relevel beams to neutralize acceleration forces, help to improve lighting conditions in either urban or rural settings, foreground luminance adjustment, and effective control of veiling luminance due to adjustable illumination (Manassero and Dalmasso, 1998, Hogrefe and Neumann, 1997). These lighting systems were put to test in previous studies to understand their effects at low ambient conditions and dark conditions (Whittaker, 1996, Ferguson et al., 1995). The results from these studies revealed that pedestrians are vulnerable in the darkness. This means that the effects of headlighting of vehicles could influence the collision of vehicles with pedestrians. Further to these result reports and findings, Sullivan and Flannagan (2002) investigated the influence of ambient light levels on fatal crashes and established three scenarios. Findings in Scenario One (pedestrian crashes at intersections) showed that because of the illumination of light levels fixed at intersections, pedestrian crashes show smaller effects at night. These numbers were however higher in dark conditions as compared to conditions with lighting systems as is the case in Scenario Two (pedestrian crashes on rural roads). The results of these scenarios are relatively different from those of the third scenario (single-vehicle run-off road crashes) where there are minimal effects from the level of light on crashes even though these pedestrian crashes are predominantly found at night. Irrespective of the scenario, the issue of darkness plays an important role in helping drivers in their response and recognition time for ease of detection of pedestrians on the road to prevent collisions. Sullivan and Flannagan (2002) suggested that this should influence the introduction of alternative measures such as additional vehicle light sources, fixed illumination at runways, and improvements in road makings to help reduce crashes at night.

Subsequently, the research findings of Haque et al. (2009) to identify factors that influence motorcycle crashes on the road, revealed that the time period especially at night is a major contributor to crashes. This phenomenon which has increased crashes at expressways and intersections to 26.4 percent and 43.3 percent respectively is largely due to the poor conspicuity of road users. Haque et al. (2009) indicated that this significant problem could be remedied by wearing bright clothing and using illuminated headlights when using the road at night. Table 2.1 identifies the influential factors or causes outlined by previous studies that contribute to vehicular pedestrian accidents. Further work by Ulfarsson et al. (2010) on pedestrian-motor vehicle crashes in North

Carolina in the United States revealed that the majority of the pedestrian crashes on the road are the fault of the pedestrians followed by the drivers. This implies that pedestrians are not cautious enough when walking along the road, or waiting to cross or crossing the road, especially at night when dark conditions could affect their visibility to the drivers. Falling asleep while driving is also a recurring cause of accidents on the road. Filtness et al. (2012), showed young drivers were vulnerable to sleep loss under prolonged driving in the afternoon. Not wearing contrasting clothing, dark conditions, drunk drivers, older drivers, and night-time and older pedestrians are identified as the major causes that affect the injury severity of pedestrians on the roads in Illinois, in a study by Pour-Rouholamin and Zhou (2016). They suggested effective educational training programs for pedestrians especially the elderly on wearing contrasting clothing and ensuring safety at night-time. Strengthening road offender penalties, effective training sessions and road safety campaigns are other effective measures that could limit pedestrian motor vehicle accidents in China as identified by Zhang et al. (2014).

Table 2.1. Influential causes of pedestrian accidents

Cause	References
driving experience and exposure	Savolainen and Mannering (2007b);
	Lin et al. (2003)
sleeping	Maycock (1996);
	Åkerstedt and Kecklund (2001)
alcohol impairment	Turner and Georggi (2001);
	Kim et al. (2000)
over speeding	Kim et al. (2008);
	Damsere-Derry et al. (2010);
	Öström and Eriksson (2001)
human, environment and roadway factors	Pai and Saleh (2007);
	Quddus et al. (2002)
ineffective training programs	Savolainen and Mannering (2007a);
	Mortimer (1988)
pedestrian conspicuity problems at night	Yuan (2000);
	Langham and Moberly (2003)
use of low beam lights or headlights in dark	Sullivan et al. (2004); Sullivan and
conditions or decrease in illumination	Flannagan (2002);
	Andre and Owens (2001);
ambient and focal vision	Owens (2003)
age-related vision problems at night	Evans (2004); Owens and Tyrrell
	(1999); Owens and Brooks (1995)

The importance of bright, retroreflective, or highly visible clothing for enhanced conspicuity of pedestrians can not be underestimated, as evidenced by Owens et al. (2007) who demonstrated the importance of the behaviour of drivers based on age and reduced illumination. Their findings revealed that pedestrians who wear clothing with retroreflective stripes arranged diagonally on the torso region are not as recognisable as retroreflective markings on the limb joints both older and middle age. There is a clear indication that the use of retroreflective materials as markings in biomotion configurations on clothing improves pedestrian safety and recognition, and reduces the response time of drivers to prevent collisions at night. These findings validate previous studies including Balk et al. (2005), Wood et al. (2005) and Owens et al. (1994) on the effective recognition of pedestrians when they are wearing retroreflective materials in a full joint configuration, most especially they are when standing on the road. Further onroad testing measures conducted by Tyrrell et al. (2004b) revealed underestimated conspicuity benefits of treated materials hence overestimating their visibility to drivers at night-time, which validates the previous findings of Tyrrell et al. (2004a) and Shinar (1984).

Fontaine and Gourlet (1997) reported in their study on pedestrian accidents in France that factors such as intoxicated pedestrians who walk on the road, children who are running or playing on the streets, and elderly pedestrians who cross the road are among the leading causes of increases in accidents either in the daytime or night from 1990 March to 1991 February. Further results showed that the blood alcohol concentrations (BACs) of pedestrians involved in accidents at night-time was high or in excess, hence an indication that the pedestrians are also at fault. These results validate findings in Holubowycz (1995) and Everest (1992) on the associated risks of alcohol impairment on pedestrians when walking on the road which would increase their risk. These increases according to Fontaine and Gourlet (1997) could be reduced by adopting effective educational and informative campaigns or programs on road safety, especially at night for pedestrians. In an earlier study, Owens and Sivak (1996), indicated that alcohol and poor visibility of pedestrians and drivers who have consumed alcohol are the major factors that contribute to highly fatal accidents at night-time. These make it difficult for drivers to see pedestrians to take prompt actions that would prevent collision. It is not only the pedestrian but also the driver as intoxication negatively affects mood, motor coordination, attention, perception and vision (Evans, 1991). Along with poor

weather conditions, it would be difficult to prevent accidents for both pedestrians and drivers. The results further revealed that vehicular lighting and reflective markings do not influence the visibility of pedestrians on the road at night. However, Evans (1991) recommended effective lighting conditions on the roads, reflective markings and public education on traffic hazards at night.

2.2.2 Model systems or techniques for analysing crash data

Detection and computational model systems are important means of effectively identifying, predicting, and describing accident scenarios by creating and calibrating accident events which are used to determine effective responses and policies that enhance road safety (Mussone et al., 1999). One such modelling system is the use of artificial neural networks (ANNs) that effectively collects and manipulates accident-based data based on different variables. ANN models provide significant results. For instance, Mussone et al. (1999), used an ANN model to predict the occurrence of accidents at intersections in Milan, Italy by using variables including road geometry. Their findings revealed an increase in the degree of risk for accidents or collisions and running over pedestrians at night-time for signalised versus non-signalised intersections. That is, pedestrians are more likely to be hit by a vehicle at non-signalised intersections during the night.

For effective countermeasures, the literature has identified factors including crash severity and frequency, that influence crash occurrence. Therefore, prediction analyses are essential for understanding the correlation of these variables for effective road safety policies. In a different modelling approach, Huang et al. (2008) predicted and identified influential factors that contribute to the severity of vehicle damage and injury of drivers at signalised intersection traffic crashes. They developed a Bayesian hierarchical binomial logistic model, and sourced crash data from Singapore in their calibration and analysis work. The development of this novel model preceded other identified models used in previous studies (see Table 2.2) for analyses of crash severity. Relevant influential factors identified as the major causes include whether a pedestrian is involved, the presence of red light cameras, lighting on the streets, location of the lane, type of intersection and most importantly, the time of the day. For example, there are increased accidents that involve vehicles and pedestrians at night-time on T/Y types of intersections. Their findings revealed that the age of the driver and type of vehicle used influence the crash severity, damage to vehicle and injury to driver and pedestrian.

Table 2.2. Modelling techniques to analyse crash data

Modelling technique	Object of calibration analysis	Reference
Ordered logit or probit models	Crash severity at signalised intersections	Abdel-Aty and Keller (2005)
	Severity of vehicle damage and injury in motorcycle accidents	Quddus et al. (2002)
	Severity of injuries in pedestrian crashes on two-lane rural highways	Zajac and Ivan (2003)
Mixed logit model	Determinants of the severity of pedestrian injuries	Kim et al. (2010)
Binomial or multinomial logistic model	Factors or variables that contribute to accident severity	Al-Ghamdi (2002)
	Influence of gender and age on injury severity	Mercier et al. (1997)
	Influence of single-vehicle collision on accident severity	Shankar and Mannering (1996)
	Use of restraint for children who are involved in road crashes	James and Kim (1996)
Multilevel model	Hierarchical structure of road crashes	Lenguerrand et al. (2006)
	Prediction of influential factors for road accidents	Jones and Jørgensen (2003)
Binomial multilevel model	Road crashes at rural intersections	Kim et al. (2007)
Logistic regression	Pedestrians involved in accidents	Kim et al. (2008)
Log-linear model	Correlation between pedestrian crashes and other factors	Lee and Abdel-Aty (2005)

With traffic collisions becoming a major safety concern because they lead to countless deaths, Geurts et al. (2005) utilised data mining to understand accidents that occur at the "black" zones (i.e., hot spots or hazardous locations) in a Belgian periurban region. Key findings from the results showed increased collisions with pedestrians within the black zone and intoxicated pedestrians outside the black zone. Their findings validate previous findings that there are increased pedestrian collisions with vehicles on roadway systems that have a large pedestrian usage (Julien and Carré, 2002, LaScala et al., 2000, Braddock et al., 1994). Other causes identified from their study include poor weather conditions, road infrastructure, and loss of steering wheel control by drivers who drive at high speeds.

2.2.3 Detection mechanisms to reduce accidents

Mechanisms have been developed to help detect the speed of vehicles for traffic discipline purposes to reduce traffic accidents on the road. Reinforcing that is the responsibility of the driver to abide by the assured clear distance ahead (ACDA) rule has been difficult since speed limits are still very high, especially for night-time driving (Leibowitz et al., 1998). The ACDA rule requires a motorist to maintain or reduce his/her speed limit under low illumination most especially at night to ensure a quick response if there are hazards. However, most drivers find it difficult to abide by the ACDA rule which has increased collisions with pedestrians. Thus, Leibowitz et al. (1998) called for a review of this rule so that it becomes a large-scale responsibility of road users since visibility at night is limited. In response, different testing mechanisms were examined. One is the use of static speed and mobile speed cameras. These cameras are reported to have reduced injury crashes closer to the site of the cameras on the road (Hooke et al., 1996). Christie et al. (2003) indicated that these cameras are widely used in South Wales - UK to help identify overspeeding vehicles on the road which results are fine. Thus, the cameras effectively reduce crashes and injury to pedestrians and other road users.

For ease of detection and notification to drivers about potential road hazards, Tsuji et al. (2002) developed a night vision system that processes images from an infrared stereo camera. This system uses an algorithm that recognises a pedestrian via high body temperature to enable the driver to effectively detect and quickly respond which would reduce collisions at a vehicular speed of 40-80m/h. The system which is displayed on the windshield can detect a pedestrian crossing or walking on the road. Even though the issues of quick response and recognition with the use of automated self-driving vehicles remain problematic, Goodall (2016) suggested that a defensible and thoughtful ethical solution can be coded into the related programs based on information from other accidents, to help with quick recognition and responses which would prevent accidents and injury to pedestrians. These associated injuries according to Kong et al. (1996) include femur fractures (common in children) and the most common of all is pedestrian motor vehicle trauma, which can be recorded at night-time. Further injuries to the head, pelvis, and chest are common with the majority (more than half of their 273 samples) of the victims being adults, less than half being children and a small percentage being the elderly in Kong et al. (1996). Thus, pedestrian injuries vary with age group and their related behaviours on the road (DiMaggio and Durkin, 2002).

The visibility of pedestrians on the road is important to reduce their increasing rate of collision with vehicles, thus ensuring effective response and detection by other road users. In a review study by Kwan and Mapstone (2004) on the visibility aids for cyclists and pedestrians on the road, they showed that fluorescent materials with orange, red, and yellow colours improve daytime recognition and detection by other road users. Additionally, retroreflective materials, tires, and biomotion makings or configurations with retroreflective materials at night-time improve the response, reaction, recognition and detection of drivers. They called for the acceptance of retroreflective materials and high visibility garments to improve conspicuity even though they conclude that doing so can be difficult and the garments can be uncomfortable to wear in humid and hot climates. Thus, improvements to these materials and products would help pedestrians and other road users accept their use to ensure their safety on the road.

An analysis of the literature showed that pedestrian accidents mainly range from poor road infrastructure to low conspicuity of the pedestrians on the road. As such, effective policy initiatives should be offered and existing ones strengthened to improve road and lighting infrastructures, safety training programs for all road users should be rolled out, and funding for innovations in detection mechanisms and pedestrian visibility materials for night-time should be provided. The production of textile materials with retro-reflective elements for regular clothing which lend visibility to pedestrians at night for ease of recognition by drivers is highly recommended to reduce the number of pedestrian-vehicle-related collisions on the road.

2.3 Global market of retro-reflective materials

Retro-reflective (RR) materials have gained progressive growth in usage and sale on the global market. This is largely due to its wide application for protective and visible clothing in construction and other sectors. With such growth, a report on the Global retro-reflection market as cited by Research and Markets (2021) revealed that the market of retro-reflective materials in the world would increase from the current \$3.6 billion to \$8.6 billion for a five-year period (2021-2026). Figure 2.3 illustrates the projected value of the global market for retro-reflective materials. With increasing concerns for vehicular safety on the road and safety of construction activities, a report by (Grand View Research, 2019) revealed that the demand for RR materials has been or would be on the increase most especially for the automotive industries. These high demands coupled with

strict rules by the government to ensure the safety of vehicles and workers on the road have influenced the production of the RR materials and clothing that are used to limit and avoid the high rate of accidents.

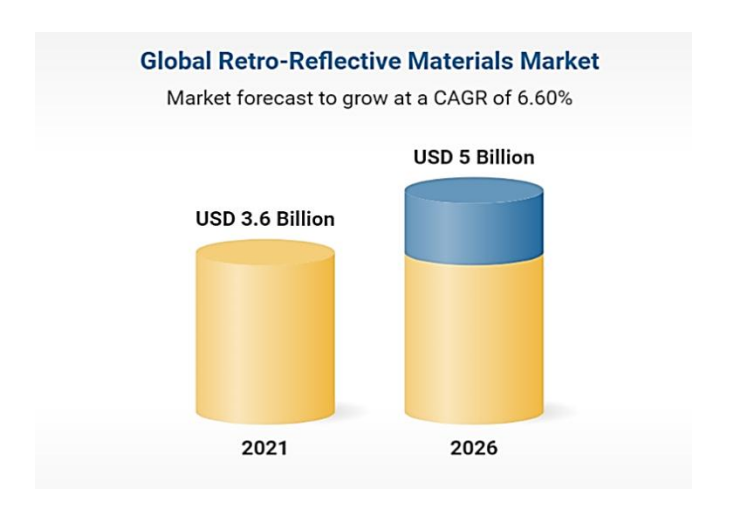


Figure 2.3. Projected global market of retro-reflective materials for 2021 - 2026 (Research and Markets, 2021)

Subsequent findings from a report from InsightSLICE (2021) projected that the market sale of retro-reflective materials is expected to accumulate \$ 29.5 billion by 2031. RR materials are incorporated for shoes, bags, and clothing and in the form of tapes or films used for bicycles, motorcycles, and vehicles to improve their visibility most especially in dark conditions to reduce the rates of accidents. The report by Grand View Research (2019) further affirms that the market application of RR materials is categorised into industrial, automotive, safety apparel, traffic control and work zone, and others, where the automotive, safety apparel, traffic control, and work zone applications have propelled the market growth for RR materials.

These high projections indicate the high demand for the materials for different applications. Retro-reflective materials are categorized into various items such as coatings or inks, paints, tapes, sheets, and films, which according to Research and Markets (2021) cover all end users for oil and gas safety, mining, road, and construction safety. Furthermore, these materials ensure safety of workers and asserts at site to limit fatalities and accidents that may occur, most especially firefighting clothing used in rescue missions (Mäkinen, 2008). It is worth noting that, advancements in technology such as cube corner or prismatic technology, ceramic technology, and glass technology have produced highly sensitive and highly visible materials. These performance benefits

have influenced brands such as 3M, DM Reflective India, Aura Optical Systems amongst others to produce quality products for different applications.

2.4 Retro-Reflective (RR) materials

Material developments have been made to improve the properties of a base fabric with inherent performance to ensure pedestrian or road user visibility at night. This is imperative since night visibility is poor in environments with low lighting conditions, poor markings, and road infrastructure. As such, retro-reflective materials were developed to fill such an important gap in ensuring night-time visibility for road users. These materials have an inherent retro-reflection property that redirects incident light rays in a maintained distribution that leads to even observation and incidence angles (Glombikova et al., 2021). Such a phenomenon reflects the illumination of headlights from a vehicle toward the drivers (Black et al., 2021) which improves the driver's response and pedestrian visibility at night. This is to say, pedestrians or road users are easily recognised by an approaching vehicle at night time hence increasing the conspicuity of the vulnerable road users (Fylan et al., 2021).

With such benefits, retro-reflective (RR) materials are categorised into two groups (Figure 2.4) which may either come in plain or pattern surfaces; prismatic and glass bead sheeting (Park, 2019). This categorization is largely based on the nature of light reflection back to its source and the sheet design (Dinakar et al., 2021). This further influences the eventual weight and surface nature of the retro-reflective materials. In given distinguishing features between the two groups, Dinakar et al. (2021) further stated that, for prismatic sheeting, the surface of a base fabric is printed directly with microscopic layers of prisms and for glass beads, the surface of the base fabric is first filled with a layer of the adhesive before the supply of glass beads. The adhesives hold a portion of the glass beads with the remainder visible for reflecting lights. With such a design, a total internal reflection is adopted by the small glass beads to reflect lights back to its source. The design of the prismatic sheet makes it easier for the prisms to reflect eventually all the light's incidence on its surface. This according to Dinakar et al. (2021) produces better reflection, brightness, and visibility with the same amount of incidence lights as compared to the glass beads structure. For prismatic sheets, the incident and penetrated light is refracted via an internal slope before being reflected back to its source (Cho and Song, 2021).

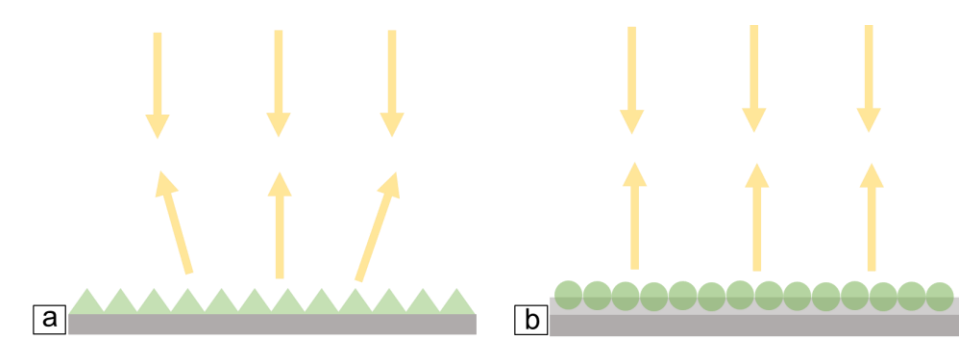


Figure 2.4. Retro-reflective sheeting. (a) prismatic sheet, (b) glass beads sheet; adhesive layer on the base substrate, and glass bead embedded in the layer

Retro-reflective (RR) materials are no exception, as they increase the visibility of an individual by employing a retroreflection technology made of either glass beads, cube corners, or prisms (shown in Figure 2.5). These materials effectively reflect the incident light in the same direction as its source while maintaining an even distribution of observation and incidence angles (Kang and Lee, 2017, Park, 2019). With such retro-reflectivity provided, RR materials with prisms/micro prisms produce a small loss of reflectivity as a result of precipitation and are highly visible or produce high retroreflection from a far distance when the incident light is perpendicular to the reflector surfaces (Pościk et al., 2019). Furthermore, other RR materials with microlens or glass beads provide good retroreflection and visibility at angles that are not perpendicular to the incident light.

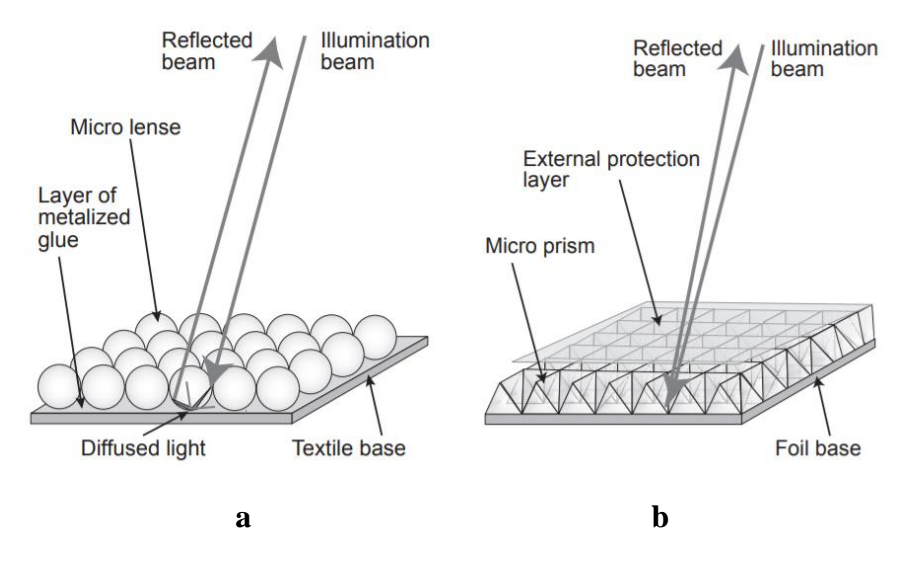


Figure 2.5. Orientation of retro-reflective materials; (a) glass beads (b) cube corners or prisms (Pościk et al., 2019)

RR materials such as fabrics or tapes or films or sheets, paints, or inks are produced using either glass beads or micro-lenses and cube prisms or micro prisms. For example, glass beads are integrated onto the surface of a base fabric using silver-plated adhesives. The retro-reflectivity of such materials depends primarily on the embedding depth, arrangement, and geometry of the glass beads or micro-lenses. Aside from this, cube corners or prisms are applied on a foil base or a thick polymer film and further protected from external conditions with a thin polymeric layer. The effectiveness and durability of the glass beads rely mostly on the base fabric strength, properties, and flexibility of the adhesives.

2.4.1 Principles of retro-reflection

This is a surface property of any material (Mary, 2021, Bible and Johnson, 2002) where incident light is reflected back to its source (Figure 2.6). This property eliminates the situation where incident light rays are scattered back in different directions. As such, this property improves the visibility of materials for easy detection and recognition from afar or close distance. A clear example is the reflective nature of the eyes of a cat which reflects light directly to the source in a respective colour shade. Supporting this, Lloyd (2008) states that the light source receives its incident light in a reflected manner. In other words, the light incident to a surface with retro-reflection property is reflected in the same path to its source.



Figure 2.6. Principle of retro-reflection

Lloyd (2008) further added that retro-reflection adopts three key principles; specular reflection, refraction, and total internal reflection, to bounce light back to its origin without absorbing it. For specular reflection to occur, the incident light is reflected directly opposite, resulting in an equal angle of incidence and angle of reflection (Gangakhedkar, 2010, Baek et al., 2018). The directional change or deviation or bending of light rays from one medium with different velocities into another results in the refraction of light (Greenspon, 2003, Arfken et al., 1984, Martínez-Borreguero et al.,

2018). A total internal reflection occurs when light is completely reflected i.e. when a light ray with a high refractive index from a medium is greater than another medium with a low refractive index, the ray is reflected totally to the initial medium (Jahani and Jacob, 2015).

2.5 Technologies for retro-reflection

Technologies have been developed to produce reflectors with quality performance and visibility to ensure safety at night. The principle governing these reflectors is reflecting of light incident on its surface back to the source in the same direction or path with less scattering. These retro-reflective effects of a surface are accomplished by two system technologies; glass beads and cube or prismatic corners (Önlü and Halaçeli, 2012a, 3M, 2014), which are different in structural composition. Aside from such structural differences, they guarantee night or dark visibility that provides certain safety or security cover to wearers to limit accident fatalities.

2.5.1 Glass beads retro-reflection

These are made of oxide and silica compounds that collectively create an insulating medium which is inorganic and non-metallic, durable, temperature resistant and retro-reflective (Rua Seguridad, 2020). Regarded as the simplest retro-reflector (Lloyd, 2008), glass beads or spheres are made from colourless glass with low thermal expansion, chemical stability, good flowability and high strength (Yuan, 2018). The retro-reflective property is possible when its spherical shape reflects its source (Figure 2.7). The spherical shape provides the possibility of refracting or bending lights on its rear surface for reflection back to the light source through its front surface (Lloyd, 2008) in a parallel direction to its light source. With such surface shape and property, glass beads used in clothing can reflect incident light from multiple angles (Flagger Force, 2017). Rua Seguridad (2020) and 3M (2014) further outlined certain unique glass bead properties, which include; durability, lower density, bonding well with paint and other materials, and having a good refractive index. The latter is influenced when the glass beads have a lower density that effectively determines the retro-reflectivity when light falls on them. The refractive index of glass beads is an imperative property (Taek et al., 1999) that dictates the visibility and reflection distribution of light back to its source without scattering the reflected light in different directions (as compared to reflection).

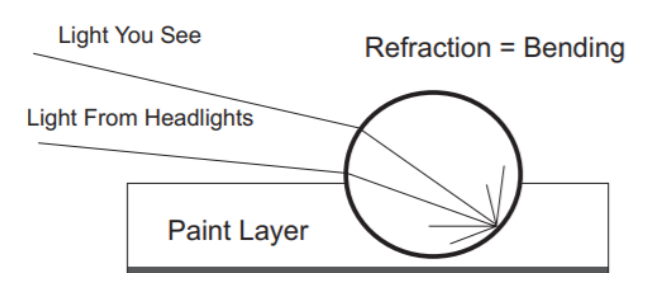


Figure 2.7. Retro-reflection of glass beads (Sandhu, 2012)

The spherical shape of the glass beads coupled with its refractive index is derived from the nature of the manufacturing process. In a report by Virginia Department of Transportation (2016), two methods are commonly used in the manufacturing process; indirect and direct methods of production. In the indirect method (Figure 2.8), the basic material needed to make the glass beads is glass powder (fine particles) which are produced from pulverized waste, recycled or new glass materials (cullet). These fine powdery particles are introduced into a story furnace, air aids to blow the particles through the heat exchange system (which houses several flames), and the glass particles are refined to take a spherical shape with the aid of heat. The softened spherical-shaped glass beads are then cooled to maintain their shape and graduated at the collection point.

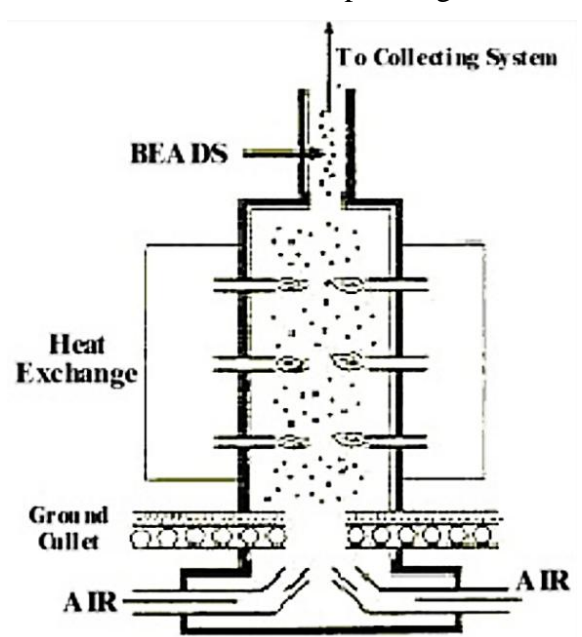


Figure 2.8. Indirect manufacturing process of glass beads (Virginia Department of Transportation, 2016)

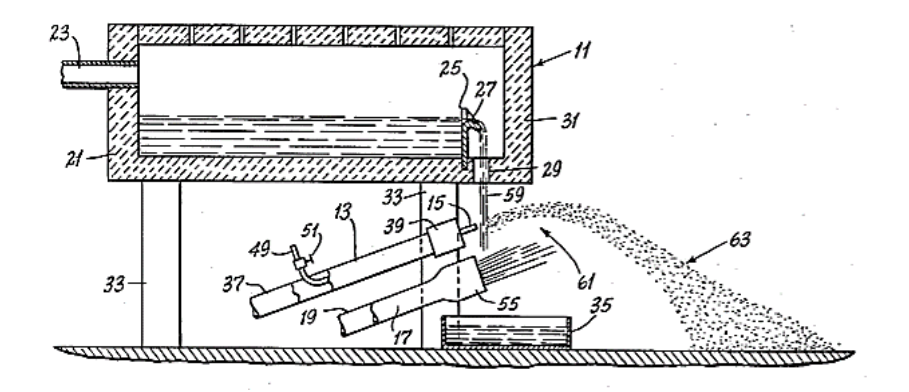


Figure 2.9. Direct manufacturing process of glass beads (Bland, 1964)

In a different approach, the direct method (Figure 2.9) produces spherical-shaped glass beads by melting the cullet, and dispersing the molten glass as droplets through nozzles into a cooling system that solidifies the glass beads. This approach is similar to the process described by Bland (1964) in his patent *method for the production of glass beads by dispersion of molten glass*. The glass is heated at high temperatures into a molten state (with low viscosity), extruded through a spout in a falling stream manner, dispersed by force of air into smaller spherical shape droplets (soft in nature) and finally solidified by cooling using water introduced from the conduit (water distributing nozzles). These reflective glass beads are then collected, graduated, and packed. Unprocessed and undispersed molten glass from the spout is collected in a quench tank with water and added back to the furnace for melting.

The integration of the glass beads onto the surface of the base fabric adopts a coating technology (clearly illustrated in Figure 2.10). This patent filed by Vandenberg et al. (2002), a base fabric either woven or non-woven is first coated with a binder or adhesive material and further applied with large quantities of aluminium-coated glass beads. Portions of these aluminium coating exposed to the atmosphere are removed using an alkali solution i.e., an etching agent like potassium hydroxide. The etched surface of the glass beads makes it an effective reflector when light is incident on it. The fabric is further neutralized using water to prevent any reactions.

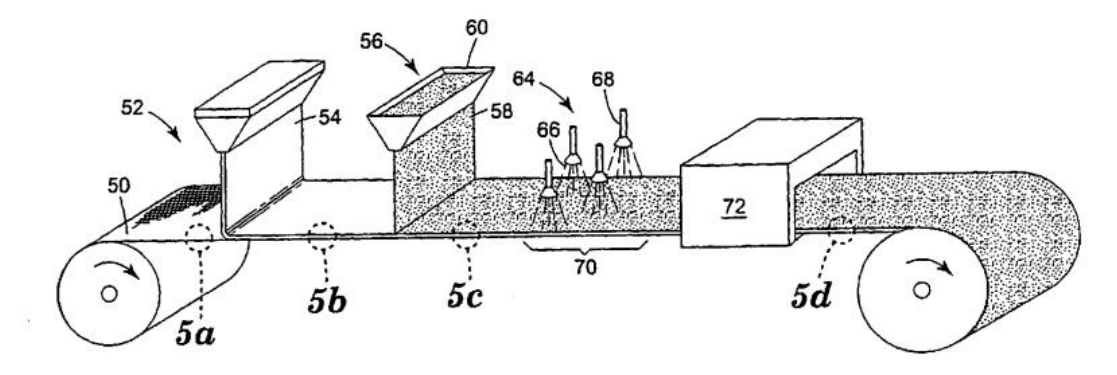


Figure 2.10. Coating technology for producing high-performance fabric (Vandenberg et al., 2002)

2.5.2 Cube-corner / Prismatic retroreflection

Described as a more retro-reflective surface to the glass beads, the cube corner or prismatic reflectors reflect incident light off its three surfaces (3M Safety, 2021). Additionally, due to the angles of the three cube corners, light in the prism is reflected internally to all faces before being reflected back or out to its source in a parallel direction (Lloyd, 2008). The reflection of light is made possible by the total internal reflection between the three reflective faces (Figure 2.11) of the cube reflector or prism (Chegg, 2021). Cube corner technology according to Lloyd and 3M Safety (2021) are difficult to produce but achieve the desired accuracy of returning light to their source than simple spherical glass beads.

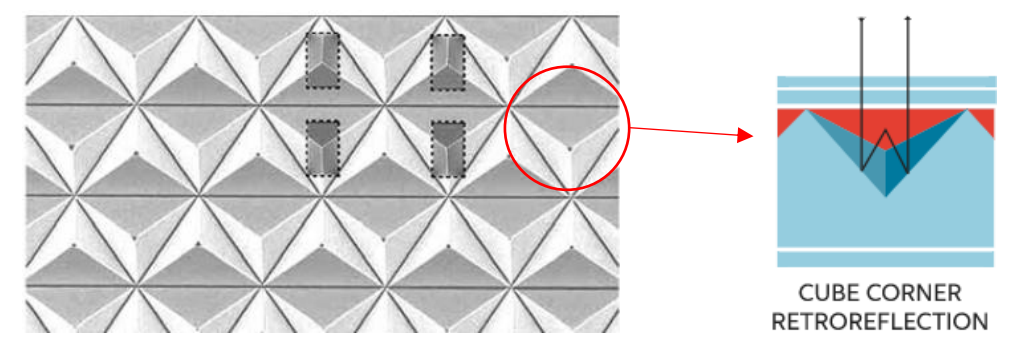


Figure 2.11. Cube corner/prismatic retro-reflection (Lloyd, 2008, Chegg, 2021)

2.6 High-visibility clothing

High visibility or High vis or High visibility safety apparel are garments that are used to ensure visual conspicuity of the wearer during the day and night to reduce injury or accidents (Kim and Song, 2021, Høye et al., 2020). Other studies like Park (2019) identified these are warning clothing that improves the wearer's visibility. These are

characterised by fluorescent colours dyed into different shades that are influenced by the fibre type (Vijayan et al., 2016). The choice of colours as opined by (Kim and Song, 2021) helps drivers to easily respond and recognise the wearer on the road. These colours function in the natural sunlight where they appear brighter to the viewer on the road even under low lighting conditions in a natural setting like dawn, and dusk amongst others. These RR materials are classified with other materials such as phosphorescent, fluorescent and chemiluminescence as high visibility materials (3M Safety, 2021). High visibility materials (HVM) are effective materials that ensure and enhance the visual visibility of anything be it a living or non-living thing, a movable and immovable object in a space. As such different HVM produces varying visual visibility effects to ensure the ultimate safety of the individual or object.

A high vis clothing features two elements, a fluorescent vest either in yellow or orange and retro-reflective strips placed at specific portions i.e., either horizontally, vertically or diagonally (Vijayan et al., 2016). Fluorescent colour vests improve daytime visibility while retro-reflective strips with inherent retro-reflectivity reflect light for improved night visibility. Testing standards usually stipulate colours such as fluorescent red, yellow, orange-red (ISO 20471:2013), fluorescent orange-red, yellow-green, red, bright orange-red or bright yellow-green (CSA Z96-15 (R2020)) for the vests or strips. Figure 2.12 shows high-visibility clothing for both day and night. The different shades of fluorescent colours are influenced by the type of fibre used (Vijayan et al., 2016). Kim and Song (2021) stated that the choice of colour is a contributing factor that influences whether drivers can easily respond and recognise the wearer on the road. These colours also function in natural sunlight where they appear brighter to the viewer on the road even under low lighting conditions in a natural setting like dawn and dusk amongst others. Due to the unique properties of high-visibility clothing, GlobeNewswire (2022) conducted a survey which found that the compound annual growth rate of this type of clothing is expected to hit 6.1% with a market value slightly above USD 2 million in the forecast year of 2028. The report further outlined that with increased awareness of highvisibility clothing, its use has increased for protection and safety purposes amongst industrial workers. This rise in the usage of high-visibility clothing has influenced its market growth. The report further highlighted that key regulation activities by governments on the safety of workers have pushed for more protective clothing for them in hazardous conditions. For example, workers in the construction industry are required

to wear high-visibility clothing when working on the road, to help improve their safety and visibility to approaching traffic.

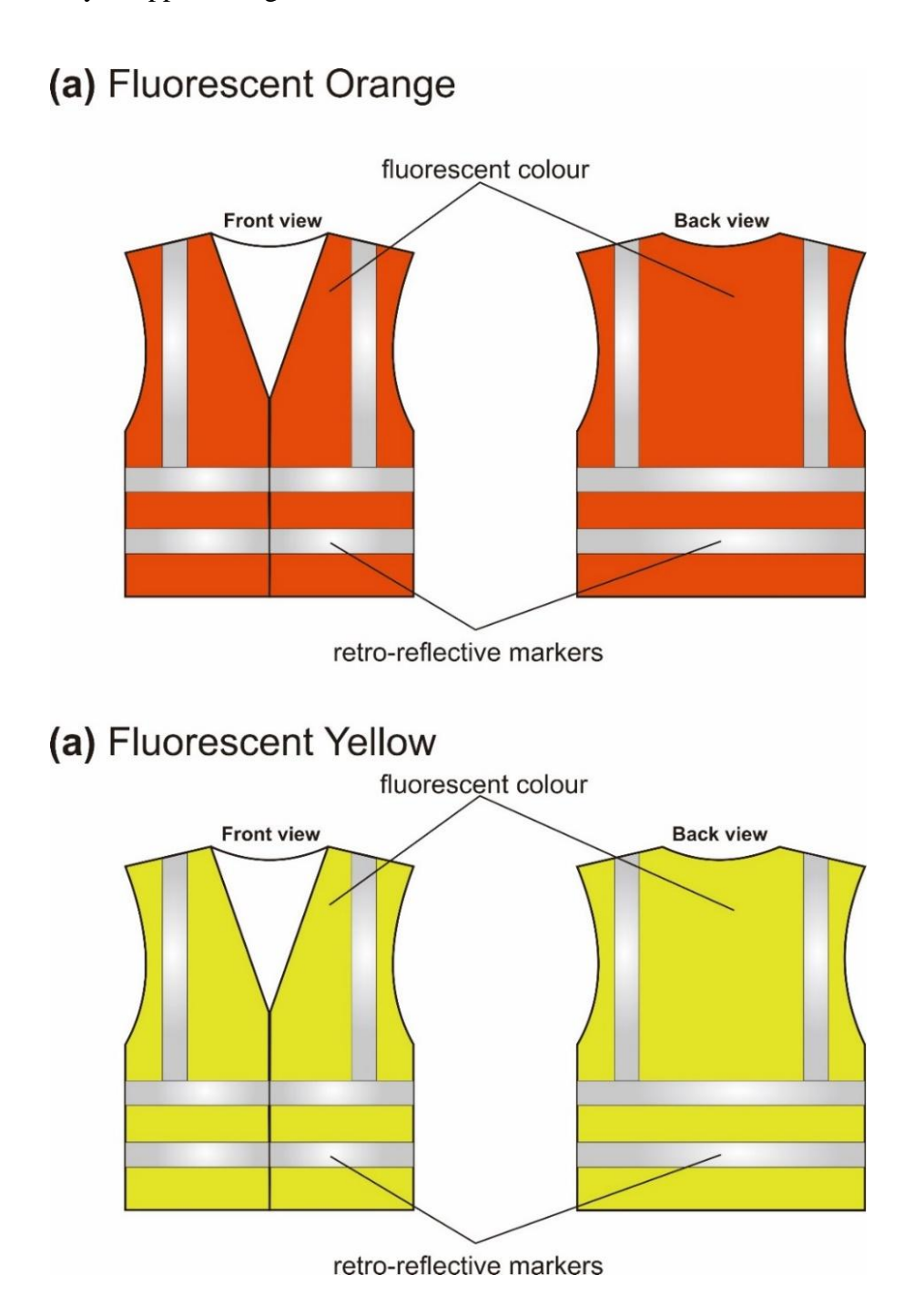


Figure 2.12. High visibility clothing: fluorescent colours and placement of retroreflective markers or strips (Authors' own drawing, 2023).

As mentioned early on, the fluorescent colours in the vests improve daytime visibility and the retro-reflective strips with inherent retro-reflectivity return lights incidence for improved night visibility. Findings from an eye tracing approach in a study by Babić et al. (2021) show that pedestrians wearing reflective vests with orange or yellow colours (Figure 2.13) were noticed at distances exceeding 200m as compared to a much shorter distance of 17-50m for pedestrians wearing black or grey and white clothing.



Figure 2.13. Garment combinations for pedestrians (Babić et al., 2021)

This implies the type of clothing used by a pedestrian at night influences or determines one's conspicuity at night. Furthermore, this clothing should meet the requirements set by either individual countries or the committee of the International Organisation for Standardization (ISO). For example, in a study by Kim and Song (2021), they stated that high visibility safety apparel (HVSA) referred to as personal protective clothing and reflective vests for use in the United States must meet the requirements of the American National Standard. The ANSI/ISEA 107-2020 visibility standard provides requirements and categorisation of HVSA in class and type for specific industry use. Vijayan et al. (2016) in their study further stated that this clothing adheres to the Australian safety standard *retroreflective materials and devices for road traffic control purposes* (AS/NZS 1906.4). This standardises the clothing into various categories (Table 2.3) that define its usage at a particular time period.

Table 2.3. Various classes of high-vis clothing according to (AS/NZS 1906.4)

Class	Description	
F	High fluorescent material for daytime visibility	
F(W)	Meets Class F requirements and subsequently fit for use in wet	
	weather	
R	Night-time retro-reflective materials	
RF	Combine the performance of retro-reflective materials and	
	fluorescent materials suitable for conditions in the day and night	
NF	Non-fluorescent materials with daytime visibility	
	· · · · · · · · · · · · · · · · · · ·	

In their study (Vijayan et al., 2016) to test the compliance of high visibility garments with fluorescent orange (FI-orange) against international standards like AS/NZS 1906.2.2010, ANSI Z535.2011 and BS EN ISO 20471.2013, it was revealed that three of the four sampled garments (either made of cotton or polyester) complied with AS/NZS 1906.2 standard in terms of FI-orange after 20 washing cycle. Subsequent chromaticity coordinates showed the colour was yellower and wider in Australian standard AS/NZS 1906.2 as compared to the Britain standard BS EN ISO 20471.2013 and American standard ANSI Z535.2011. This implies that the dyestuff and material types (either cotton or polyester) may influence the suitability of the fluorescent colours to meet safety standards and ensure colour brightness during the daytime. In a subsequent study by Lahrmann et al. (2018) to identify the rate of cyclist accidents influenced by yellow bicycle jackets in Denmark, findings revealed that the test group with 3402 cyclists wearing yellow jackets showed a 47% reduction in personal injury accidents on the road as compared to the control group with 3391 cyclists without any yellow jackets. This showed cyclists are more protected with the wearing of cycling jackets (yellow colour) that come with reflective strips to ensure their visibility on the road. Subsequent studies by Park (2019) to test RR and fluorescent materials for ISO 20471 compliance to be used for warning clothing to show that the luminance and retro-reflective properties of the sampled RR materials meet ISO standards even after 5 post-conditions treatments. The fluorescent materials however are less ISO complaint after subsequent testing methods.

2.6.1 Performance conditions

The performance of high-visibility clothing to address external conditions is important to ensure its functionality. This type of clothing is widely used by people who are exposed to ultraviolet (UV) radiation during the day. However, such exposure degrades high-visibility clothing, hence reducing the visibility values set by international standards (EN 471:2003+A1:2007). Based on this, Pościk (2013) reported on the UV degradation of high-visibility clothing (made of different polymers) with photochromic indicators. The findings revealed that polystyrene films with photochromic dyes can be used as a degradation indicator of the background materials of high-visibility clothing. The study drew on the need to discard any personal protective equipment when they are degraded over time under sunlight exposure. This is to improve the safety of workers or users on the road. Similarly, Vijayan et al. (2016) reported on the degradation of fluorescent colours used for high-visibility clothing in the Australian railway industry. Here, four orange fluorescent coloured high-visibility clothing items were used to investigate their compliance with AS/NZS 1906.2.2010. The findings revealed that these sample fabrics degrade and do not meet the AS/NZS test standard but however, comply with the ISO standard after exposure to UV and washing cycles. They concluded that the selection of appropriate colours for high-visibility clothing to be used by railway workers must be based on durability, reproducibility, commercial viability and conspicuity. The study further stated the need to ensure the implementation of regular inspections and maintenance of these high-visibility clothing to ensure that their performance properties still meet EN471 Standards (Holmes, 1997).

Subsequently, the performance ability of high-visibility clothing to illumination conditions (light and dark) is imperative because this influences their design for consumer dress or other applications. These are necessary to ensure that they still improve the conspicuity and recognition of users in both dark and light conditions. As such, a recent study conducted by Iizuka et al. (2021) examined the influence of sunset conditions on the performance of high-visibility clothing. The study adopted a dark room experimental setup where participants observed two sample fabrics with yellow and black colours from a distance of 5 metres as shown in Figures 2.14a and 2.14b. The findings showed that the sample fabrics of both black and yellow colours arranged with a 5.0 spatial frequency and 165° stripe patterns (Figure 2.14c) are more visible and could improve the conspicuity of the wearer due to the contrast provided by the black colour

when combined with a brighter yellow colour. Table 2.4 further provides details of the performance of high-visibility clothing under different conditions which could be used as a reference source in the design of suitable high-visibility clothing.

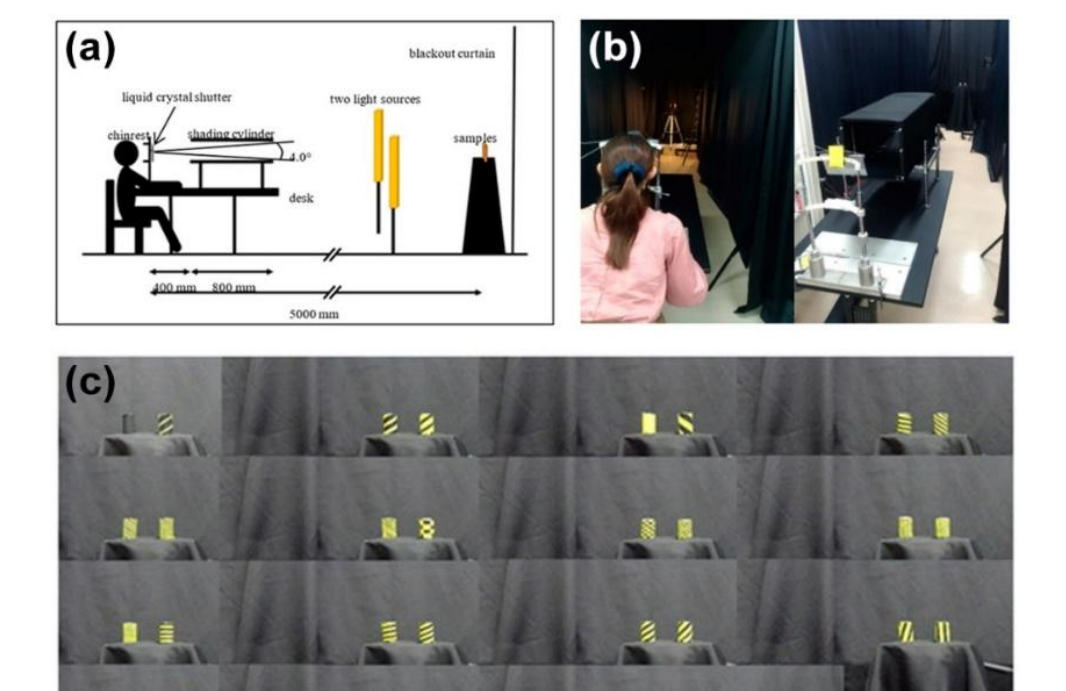


Figure 2.14. (a) Experimental laboratory setup with the participants sitting 5 m away from the samples, (b) participants observing samples in a sunset condition at the laboratory and (c) images that show the appearance of evaluated samples (Iizuka et al., 2021) (This article is an open-access article distributed under the terms and conditions of the Creative Commons Attribution (CC BY) license - https://creativecommons.org/licenses/by/4.0/).

Table 2.4. Studies on performance conditions of high-visibility clothing

Methodology	Findings	Reference
Participants have 6/9 visual acuity	• Fluorescent vests worn by cyclists do not	Wood et
or better, which includes 12 older	provide the needed visibility in night	al. (2010b)
and 12 younger drivers.	conditions because the vests are	
	activated through UV radiation which is	
Two cyclists wore clothing with	not available at night. This creates a	
different configurations and were	situation where cyclists who wear these	
positioned in two locations on a	fluorescent vests overestimate their	
1.8km closed-road circuit.	conspicuity and hence risk their safety at	
	night.	

The study adopted a dark room experimental setup where participants with >20/20 corrected visual acuity observed 16 different sample fabrics with different colour combinations from a distance of 5 meter.	• Colour combinations of white/red-purple stripes, black/yellow-red, black/white, black/yellow and black/fluorescent yellow are highly conspicuous.	Iizuka et al. (2022)
Data retrieved from 1460 drivers and cyclists in Australia	 Use of fluorescent vests and clothes, and other reflective strips by both cyclists and drivers improve their visibility. Some confusion on the visibility properties of certain visibility aids was revealed. For example, fluorescent vests and clothes are ideal for daytime use due to their response to UV light. 	Wood et al. (2009)
Data from the National Road Safety Strategy (NRSS)	• Fluorescent colorants (like yellow-green) combined with high-visibility markings, enhance the detection, visibility and conspicuity of workers and vehicles at dusk and dawn, night and day.	Berces (2010)
Two groups of 16 licensed drivers (both young and old) were recruited for field tests.	 Wearing either fluorescent red-orange or fluorescent yellow-green high-visibility clothing improves the detection of pedestrians on the road during day. Pedestrians are easily detected further away on the road in less complex scenes. 	Sayer and Buonarosa (2008)

Adopting a more technology-based approach, Mosberger et al. (2014) developed a vision-tracking system to identify workers who wear high-visibility or reflective safety clothing in an industrial work environment. This is largely due to the challenging and complex nature of reliably tracking and detecting workers within such an environment. Their study was influenced by a previous study that detected the movement of workers who wore high-visibility clothing in a video frame (Park and Brilakis, 2012), where the fluorescent colours of the clothing contributed to the effective detection of the construction workers. In Mosberger et al. (2014), their customised algorithm of a vision tracking system detects the retro-reflective markers placed on high-visibility clothing worn by industrial workers, as illustrated in Figure 8. In this experiment, a setup of stereo cameras was used to observe and acquire the necessary images of reflectors that are shown in "high-intensity regions in front of the non-reflective scene background".

Subsequently, images were captured by using an infrared flash camera whereas the stereo camera was used for video streaming. The findings revealed that the system is able to track, detect and segment reflective patterns on the safety clothing of workers from other reflective objects in the industrial environment. The system further showed a robust ability and accurate tracking performance for different illumination conditions, body pose variations and partial occlusions. This system can help to monitor and identify workers in different work postures at the workplace for enhanced safety.

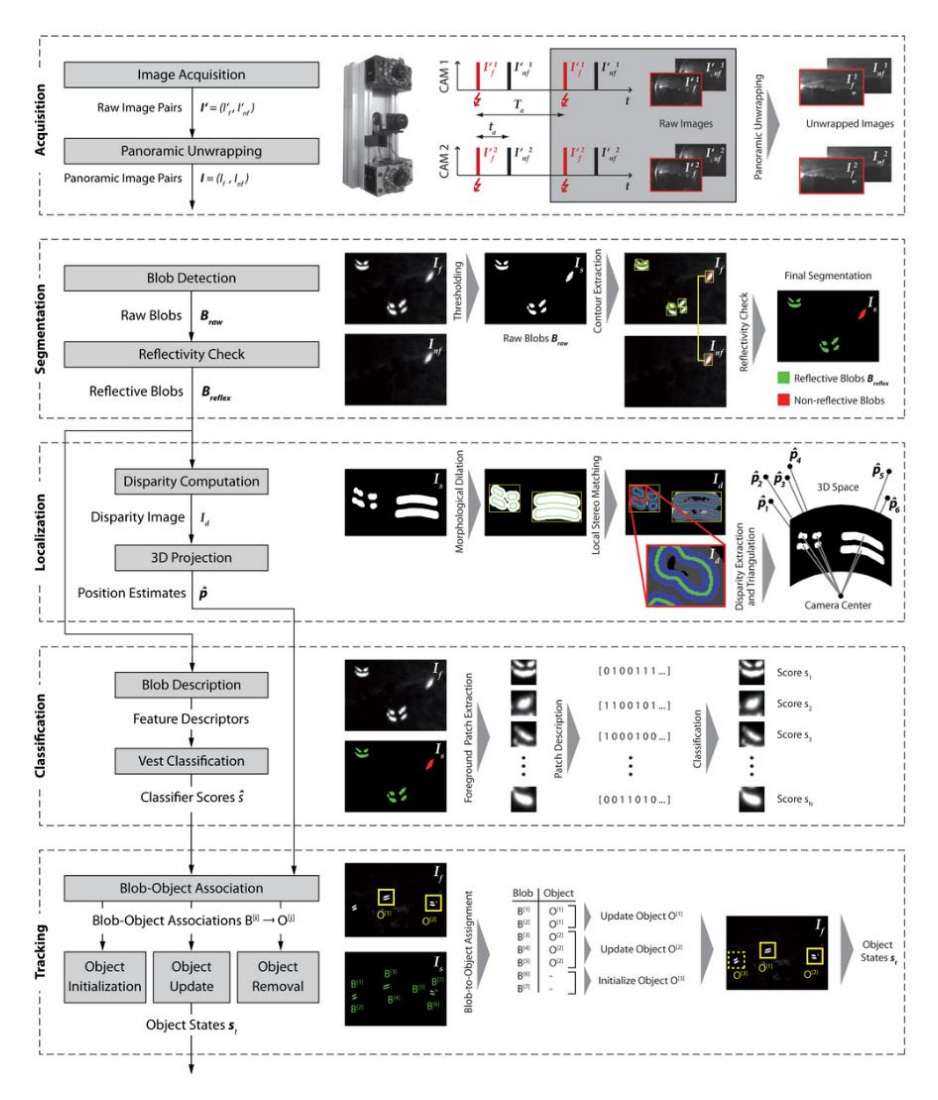


Figure 2.15. Stages of vision tracking system to detect workers with high-visibility or reflective safety clothing in an industrial working environment (Mosberger et al., 2014) (This article is an open access article distributed under the terms and conditions of the Creative Commons Attribution license - http://creativecommons.org/licenses/by/4.0/).

Laing et al. (2006) designed workplace clothing with integrated passive cooling and high-visibility abilities to evaluate UV protection and thermal acceptability of workers who work on public roads. The creative design process used an outer high-

visibility fabric which complies with AS/NZS 1906.4 and an inner weft knit polyamide fabric. Here, the design of the passive cooling ability followed the model in Webster et al. (2005), where each vest contained seven (7) coolant packs. The vests were tested in workplace settings at temperatures that ranged from 25-35°C for 10 days. The findings indicated that the workers feel cool when they wear the vest during work hours. This shows the possibility of ensuring both enhanced safety and wear comfort amongst workers in workplaces where workers are exposed to solar radiation and outdoor elements.

Aside from worker safety in the industrial workplace, bicyclist safety on the road also continues to be very important since bicyclists share the road with other motorists, and hence are vulnerable to collisions. The proximity of overtaking vehicles is relevant due to the risk of injury to bicyclists (Stone and Broughton, 2003, Parkin et al., 2007). Accordingly, a study was conducted by Walker et al. (2014) to investigate the proximity of overtaking drivers based on the appearance of bicyclists on the road in the UK. A field experimental test used seven (7) different garments to give the following appearances: commute, casual, HIVIZ (high-visibility), racer, novice, police, and polite. A total of 5690 overtaking events were recorded from an Arduino Uno microcontroller which was connected to a temperature-compensated ultrasonic distance sensor (MaxBotix MB1200 XL-MaxSonar-EZ0). The findings suggested that even though the mean space left by the moving vehicles or motorists is not influenced by the different signalling apparel worn, the high-visibility vest with police inscription resulted in more space left by the moving motorist on the road. As a result, the authors concluded that "there is little riders can do, by altering their appearance, to prevent the closest overtakes". The study findings suggest that moving motorists are more likely to give more space when passing bicyclists with a "Police" inscription on their high-visibility apparel due to their fear of getting arrested.

2.6.2 Biomotion configuration / biological motion

It is imperative that the conspicuity of road users is enhanced to limit collisions and improve recognition on the road at night. Suggestions have been made that applying RR trimmings at the respective joints of the human body would help drivers to recognise the full silhouette of the individual for prompt response and action. As such, the term biological or biomotion configuration was established. These are motion patterns that are configured with the various joints of the human body. The placement of RR materials in

strip form at these areas (movable joints) improves the conspicuity of the body of the wearer on the road at night (Wood et al., 2011, Fylan et al., 2021, Fylan et al., 2020a, Glombikova et al., 2021). This enhances the orientation of the body of the wearer for easy identification and detection (Mian and Caird, 2018). These configurations further help drivers to make judgements on the walking direction of the pedestrian on the road to avoid collisions or accidents (Black et al., 2021). Additionally, Valentin et al. (2010) reiterated the importance of visibility clothing to workers on road maintenance for enhanced safety. Studies have been conducted with the use of different configurations to investigate their influence, significance, and accuracy to improve the visibility of road users (pedestrians or cyclists).

In a recent study by Babić et al. (2021), a field-based eye-tracking method was used to investigate the influence of different clothing on the recognition ability of drivers at varying distances. Using 115 drivers, the results showed that recognition of pedestrians wearing a reflective vest is achieved at a greater distance of 200 m as compared to 17-50 m for a pedestrian wearing black or grey and white clothes. Other influential factors such as driving experience, age and gender do not significantly affect recognition. Babić et al. (2021) further concluded that pedestrian safety is largely dependent on the conspicuity of pedestrians at night on the road. In a related study, 21 young participant drivers in Black et al. (2021) evaluated the conspicuity of pedestrians who wore clothing with four different biomotion configurations (RR strips placed at the legs only, torso only, torso and legs and a full biomotion) and regular black clothing. The results revealed an 83% response accuracy by drivers to pedestrians with full biomotion configurations followed by 64% for RR strips on the legs and torso, 53% for the torso only, 50% for legs only and significantly low response accuracy for black clothing with no RR strips. The results are supported by previous studies Wood et al. (2011), which showed that the conspicuity of road workers with full biomotion configurations on their high visibility clothing is improved significantly along with recognition regardless of their orientation (Figure 2.16). This implies that, the use of RR strips in multiple to full biomotion configurations not only would improve the identification or orientation of the wearer but further influences the response accuracy, recognition, and conspicuity.

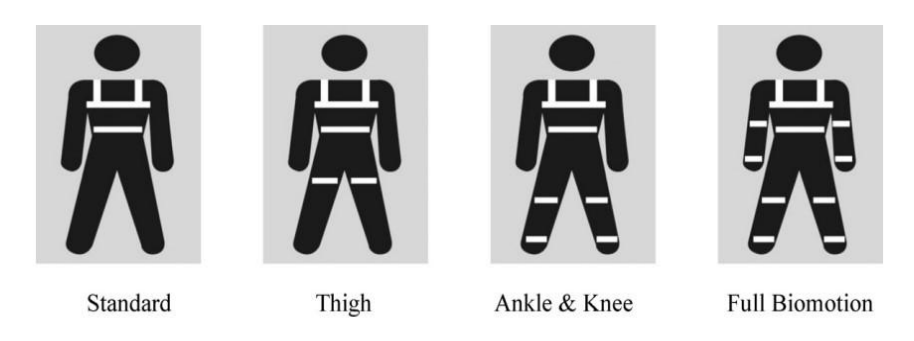


Figure 2.16. Different biomotion configuration diagrams on road worker clothing (Wood et al., 2011)

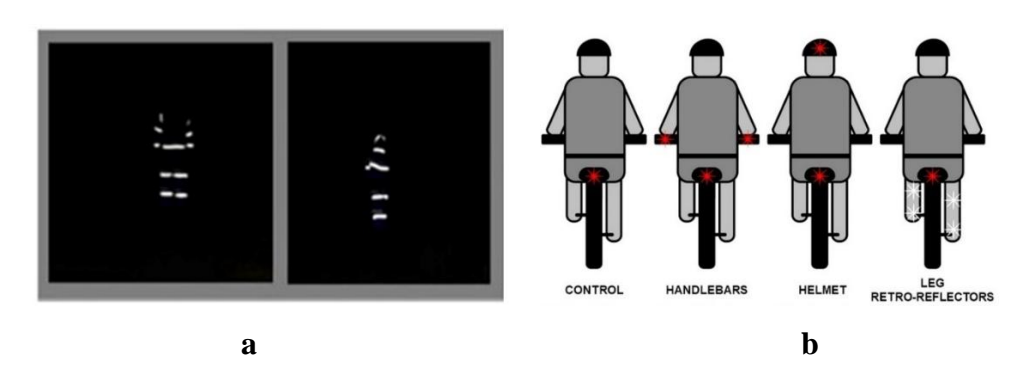


Figure 2.17. (a) Pedestrians with biomotion configurations at night (Mian and Caird, 2018): (b) different configurations of retro-reflectors (Black et al., 2020)

Mian and Caird (2018) found that the speed of the human body with biomotion configurations affects their conspicuity at night, where observers identified pedestrian running with biomotion configurations are more recognisable than those walking and standing (Figure 2.17). This further affirms that the application of RR materials in strips on clothing with full biomotion configurations gives a structural silhouette of the human body for ease of recognition and the ability of approaching vehicles to quickly respond. In Black et al. (2020), the inclusion of additional visibility aids like retro-reflectors positioned on the ankles, knees, handlebars, and helmets amongst others improves conspicuity and helps drivers to give a safe passing distance to bicyclists to prevent collisions at night. This confirms findings from a review study done by Kwan and Mapstone (2006) that showed RR materials applied in biomotion configurations improve the recognition of pedestrians and the prompt detection of drivers on the road at night.

It is evident from these studies that, the inclusion of RR markings on clothing improves the visibility of road users for effective response and action by drivers at night. Table 2.5 further gives details of additional studies conducted on the influence of RR markings in biomotion configurations.

Table 2.5. Studies on the influence of clothing with biomotion configurations

Subject	Experimental design se	t-up	Results	Reference
50 participants	 Nine focus groups (3 and 6 in Brisbane (A) participants from Lee Brisbane. Semi-structured intergather information. 	ustralia)) with 16 eds and 34 from	It was evident from the discussion that, design, function or comfort of the running or cycling garments with RR trimmings in biomotion configurations are factors that influence their use on the road. The participants revealed that the garments should have a goodfit and high visual appeal but not "looking like road worker garment". Most of the participants revealed that they reject such garments because they are uncomfortable to wear. These garments generate heat as they use them on the road hence new innovations should ensure such garments are convenient and comfortable to wear.	(Fylan et al., 2021)
50 participants	 Nine focus groups (3 and 6 in Brisbane (A) participants from Lee Brisbane. Semi-structured interused to gather inform 	ustralia)) with 16 eds and 34 from	The participants identified that, colour (fluorescent and bright clothing) and lights (both static and flashing) help to increase their conspicuity at night for drivers. They however have no knowledge of the effective role that RR materials have to improve their conspicuity. As such, they use roads with good lighting systems to help improve their visibility at night.	(Fylan et al., 2020b)
			Participants thus prioritise their comfort or style over improving their conspicuity. They lacked effective strategies to help them in low light conditions on the road at night.	

14 licensed young drivers	0	ASL Mobile Eye was used to record the eye movement of drivers. Field test was conducted in a closed-road circuit at night.	Pedestrians who wore clothing with biomotion configurations are recognised by drivers at a greater distance of 319.1 m as compared to 184.5 m for pedestrians without biomotion markings on their clothing.	(Wood et al., 2017)
			The eye movement of the drivers showed that their attention quickly turns to pedestrians with biomotion configurations. These configurations the driver's fast recognition and identification for such pedestrians on the road at night.	
50 participants	0	Lab study design 3D eye-tracking technology e.g. Participants used Pupil Pro 3D eye-tracking glasses to watch a 15-minute video of cyclists who wore clothing with four different biomotion configurations.	Cyclists who wear clothing with biomotion or pseudo-biomotion markings have significantly high visibility. The study participants further revealed that aesthetics and the use of visibility aids influence why they purchase these garments.	(Stapleton and Koo, 2017)
	0	A questionnaire was given to participants to obtain qualitative data after the experiment.		
190 student participants	0	Field experiment conducted at night in an open-road course.	The response distance is greater for pedestrians who wear clothing with both RR markings and electroluminescent materials, even when pedestrians are out of the range of the vehicular headlight.	(Fekety et al., 2016)
24 participants comprising 12 young and 12 elderly drivers	0	A vehicle with low-beam headlamps was used in an experiment conducted on a closed road circuit.	The response distance is greater for pedestrians wearing clothing with RR markings in a biomotion configuration. The response distance was however reduced for elderly drivers as compared to the younger drivers.	(Wood et al., 2015)

25 participants	0	Field experiment conducted at night on	RR vest with RR tape on the legs improves the visibility of the	(Wood et al.,
		a closed-road circuit.	participants as compared to wearing black clothing.	2013)
	0	The participants wore different clothing configurations like fluorescent RR vests with knee and ankle reflectors, fluorescent RR clothing with RR tape, and black clothing	The participants however misjudged the fluorescent vest with RR markings which did not improve their conspicuity at night. They further underestimated their conspicuity when using RR markings at the knees and ankles.	
120 participants	0	Experiments were conducted at night	The response distance of the participants is greater for those who wore clothing with RR markings in a biomotion configuration.	(Balk et al., 2008)
	0	on an open-road route. The participants pressed a button after they noticed the presence of a pedestrian on the road.	wore crouning with KK markings in a diomotion configuration.	2008)
65 participants	0	Recordings of a car journey were played to participants in a laboratory setting.	There is no significant increase in detection for stationary or moving pedestrians who wore either a standard visibility vest or clothing with a biomotion configuration.	(Moberly and Langham, 2002)
	0	Participants were instructed to press a button should they see a pedestrian.	Aside from this, pedestrians in motion were seen further away than stationary pedestrians.	

With more recorded cases of pedestrian fatalities at night, Borzendowski et al. (2014) opined that "pedestrians overestimate their conspicuity at night and underestimate the impact of clothing on their conspicuity", hence there is a need for effective public education. In their study to improve pedestrian safety and understanding, their findings showed that educational intervention should improve understanding of how wearing clothing with RR materials enhances conspicuity at night. This would further influence the desire of pedestrians to purchase and use athletic garments enhanced with RR markings. Borzendowski et al. (2014) concluded that developing and implementing educational programs would help pedestrians to appreciate and ensure personal safety. This is in agreement with previous studies that public education is an effective way to convince pedestrians about the night-time dangers on the road and the need to use visible materials to enhance conspicuity (Tyrrell et al., 2004a, Tyrrell and Patton, 1998).

It is imperative that even though RR materials improve the visibility of pedestrians who wear them, how they are attached to clothing further influences visibility. With this, findings from other studies have revealed that putting these RR materials in biomotion configurations not only enhances their visibility but further helps other road users to recognise them for quick response action. This would undoubtedly reduce collisions with pedestrians.

2.6.3 Conditions that influence conspicuity at night

Understanding the conditions that affect the ability of drivers to recognise road users for a prompt response and, the visibility of pedestrians or road users at night is imperative for effective strategies to reduce fatalities. One such condition includes the vision of drivers. Wood et al. (2021) examined the effects of refractive blur on driver judgement at night and found that refractive blur significantly influences the accuracy of drivers in determining the walking direction of pedestrians. Refractive blur or uncorrected refractive error which increases with age is the major cause of reversible visual impairment which affects driving safety and ability on the road, especially at night (Foreman et al., 2018, Flaxman et al., 2017). The type of clothing worn by the pedestrians coupled with the refractive blur of drivers further affects the recognition and response of drivers at night. In the testing procedure, however, pedestrians who are wearing biomotion clothing with RR materials can be more easily recognised which increases the response accuracy of drivers (Wood et al., 2021). These findings validate those in Wood et al. (2010a) that the

appropriate positioning of RR materials in biomotion improves the conspicuity of pedestrians which ultimately enhances the response accuracy of drivers hence improving their performance. Wood et al. (2010a) experimentally investigated the influence of simulated visual impairment on driving performance and recognition ability at night by modifying goggles with normal vision to simulate refractive blur and cataract effects. The results showed that refractive blur and cataracts affect the ability to detect and recognise road signs and pedestrians who wore black clothing. The recognition ability of the participants however increased to around 80% when the garments of the pedestrians had RR materials which greatly enhanced their visibility.

Driving on the road can mean adjusting to varying conditions that collectively influence the performance of drivers, especially at night, including the headlights of the car or moonlight or streetlights installed on the streets (Wood, 2020). Wood (2020) found that mesopic lighting conditions reduce the visual function of drivers during night-time driving. Indeed, these low lighting levels affect contrast sensitivity and visual acuity which deteriorate visual performance. It is imperative to understand that the recurring flickering of lights from incoming vehicular headlights coupled with low-level street lighting affects the visual functionality of drivers at night hence influencing their performance. Aside from the benefits of vehicular headlights, variations in lighting from oncoming vehicles negatively affect recognition abilities and increase visual difficulties (Kimlin et al., 2017). Wood (2020) further acknowledged that recent technology in headlights, most importantly adaptive headlights, can reduce glare problems and improve visual functionality at night. These adaptive headlights according to Fleming (2012) can effectively adapt and change their lighting output to meet the changing conditions on the road.

In a field experiment study, Whetsel Borzendowski et al. (2015) investigated the accuracy of drivers in evaluating the conspicuity of pedestrians when faced with different levels of oncoming headlight glare. The test in their study is imperative since pedestrians overestimate their conspicuity to vehicles approaching them at night. Pedestrians are further limited in understanding the issues of night vision of drivers that could contribute to collision and driver performance. The results from Whetsel Borzendowski et al. (2015) showed that drivers inaccurately gauge that their vision is not affected by the glare effects of headlights. These findings confirm Whetsel et al. (2012) on how pedestrian clothing and glare from headlights in the opposite direction can affect the ability of the driver to recognise a pedestrian on the road at night. Whetsel Borzendowski et al. (2015) hence

proposed effective education for drivers to understand their vision at night and how to appropriately improve their night driving performance. It was however evident that drivers can recognise pedestrians who are wearing an RR vest even with different levels of oncoming headlights. This affirms the ability of RR materials to improve conspicuity. Tyrrell et al. (2016) also concluded the misunderstanding and lack of awareness of drivers to recognise the limitations of their vision during night-time. Driving under low luminance typically affects hue perception and colour vision, hence limiting the visual abilities of drivers at night for improved recognition and performance. They further found that contrast sensitivity and visual acuity are negatively affected at low luminance levels, a situation that affects visual performance and the ability of drivers to recognise objects with low contrast.

Wood et al. (2005) and Tyrrell et al. (2003) found that factors like glare, black clothing and low beam affect the ability of drivers to recognise pedestrians on the road at night. This ability can be improved with RR materials attached to biomotion configurations on clothing, which reduce the fatalities of pedestrians (Sayer and Mefford, 2004). In a related study, Shinar (1985) found that the use of RR tags for pedestrian clothing helps drivers at night to recognise the presence of pedestrians. These tags improve the visibility of pedestrians at greater distances as compared to pedestrians who are wearing dark clothing on the road. Not only is pedestrian conspicuity very important, but the conspicuity of motorists or bicyclists also remains a concern for road safety. Olson et al. (1981) reiterated the need for motorists to use running lights and wear RR garments to improve their visibility. They suggested that motorists could apply glass beads on their clothing and motorcycle for more conspicuity at night.

In a different approach, Tyrrell et al. (2009) investigated the influence of visual clutter on the visibility of pedestrians on the road at night. After conducting a closed experiment, the findings showed that the age of the driver, the motion of pedestrians and clothing configurations influence the ability of the driver to recognise pedestrians. In particular, the recognition ability of elderly drivers is low largely due to age-related visual changes. However, visual clutter does not influence the conspicuity and visibility of pedestrians who wear RR materials in biomotion configurations. These pedestrians were seen at greater distances as compared to pedestrians who only wore a reflective vest. Islam and Hossain (2015) identified weather conditions as variables that increase bicyclist and pedestrian motor accidents on roadways in Alabama, USA. Foggy weather for example

has a significant effect on the vision performance of both road users hence increasing crashes on the road and injury severity. This coupled with dark roadway conditions and a temporal variable "time" from midnight to 7 am contributes to the inability of drivers to see other road users.

2.6.4 Behavioural changes of road users towards retro-reflective materials/high-vis clothing

The behaviour exhibited by road users and the law enforcers (police) plays a critical role in influencing road safety during the day or night. To understand such behavioural changes to the use of high visibility clothing or retro-reflective materials, relevant studies have reported on that for improved mindset. In Kim and Song (2021) study to identify the wearing behaviour or compliance to wearing high visibility safety apparel (HVSA) amongst police officers in four cities in the Yarapai county of Arizona, revealed that occupation risk, professional appearance, perceived levels, safety education, HVSA functionalities, safety attitudes and ethics were the key indicators that influence the officers use of HVSA. For instance, high safety ethics influence safety education amongst officers where safety becomes more imperative than comfort hence the wearing of HVSA. Aside from this, officers with perceived attitudes of non-functionality of HVSA, tend not to use this clothing hence affecting their conspicuity at night. Ferraro et al. (2020) survey study on the behaviour of bicycle users in Italy regarding the use of bike safety measures revealed that the males but older population of the sampled cyclists who are from the south adopts the use of conspicuous clothing and bike safety devices to improve their safety at night. Furthermore, sport bike riders used less of these safety clothing and devices than their counterparts, city cyclists. In an observational study on safety measures for children by Tosi et al. (2021), findings showed reduced use of safety measures such as highvisibility clothing, and helmet for children and in most cases adults. This practice puts the safety of the children at greater risks in the event of an accident.

Using a combine analysis approach for qualitative interviews, Aldred and Woodcock (2015) in their study in England revealed that because of cycling less and discomfort, cyclists used less of safety clothing and devices. However, with cyclists perceived risk associated with injuries, there is increase in safety clothing. Previous misconceptions on the use of high-vis clothing or RR materials in a study by Wood et al. (2013) revealed bicyclists underestimated the benefits and use of RR markings on the knees and ankles to improve their visibility, and that fluorescent vests without RR strips

enhance their conspicuity at night. To clearly understand pedestrian or road users receptibility and attractiveness to the use of WAKE (waist, ankle, knee, elbow) garments with biomotion configurations developed by Fylan et al. (2021) their findings revealed that the vulnerable road users were uncomfortable and less likely to use biomotion garments due to their poor design and nature even though these garments would ensure their conspicuity at night. In a related study by Fylan et al. (2020a), they revealed that participants prioritised comfort and style to their own conspicuity at night. Hence a recommendation for manufacturers to include informative labels for education on the benefits of biomotion configurations on the safety of wearers.

Legislation on the use of these safety visibility aids may attribute to behaviour changes for road users. To understand such influences, Prati (2018) study findings showed legislation on mandatory use by cyclists did not influence the reduction of pedestrian road accidents for the years 2001-2015. Prati further stated that behavioural changes of the pedestrian to the law, police enforcement, and implementation problems of the law need effective investigation for campaigns and education to improve cyclist usage and safety.

2.7 Experimental studies on retro-reflective textiles

With the promising market share for retro-reflective materials for different applications, manufacturers have expanded their production to include retro-reflective inks and yarns for wider users. The retro-reflective technology - glass beads, are used to produce yarns or yarns (having an additional polyester thread wrapped around) and are added to printing paste for colouring effects. These two materials have been applied in some design aesthetic and research approaches for products that could fit a wider application. In a most recent design practice, Nualdaisri (2022) added some aesthetic values to traditional Thai Silk fabrics. In this process, retro-reflective yarns together with silk yarns were utilised via weaving techniques to add both functional and aesthetic values to the Thai silk fabrics. This design practice expanded innovative approaches for weavers in the communities to make the fabrics more attractive, and aesthetically pleasing with some functional values for interactive art forms or installations (Figure 2.18). These as opined by Nualdaisri (2022) seeks to highlight and provide knowledge on the origins or rich heritage of Thai silk.

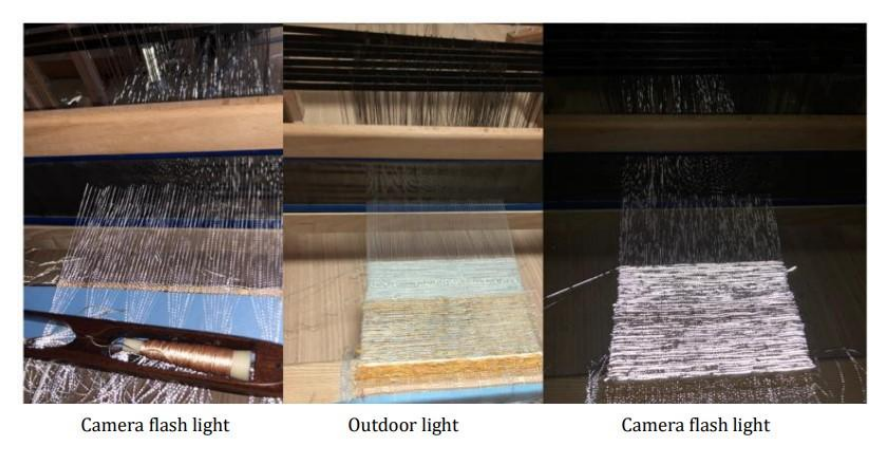


Figure 2.18. Innovative Thai silk fabrics with retroreflective yarns (Nualdaisri, 2022)

Still on a more aesthetic approach, a previous study by Önlü and Yaşar (2011) produced woven transparent fabrics (Figure 2.19) for fashion design garments. In this method, varying yarn types like retro-reflective, bamboo, metallic and silk, were used to produce woven fabrics where the eventual visual effects influenced by certain factors like yarn density, weave structures and type are studied. Subsequent findings on the visual effects reveal that the use of the retro-reflective yarns produced shimmering and bright effects when introduced to lights at night due to the retro-reflective nature of the glass beads inherent in the RR yarns. Additionally, the weave and fabric structures coupled with the light source further influence the degree of transparency of the woven fabrics which produces shimmer and brighter effects at night.

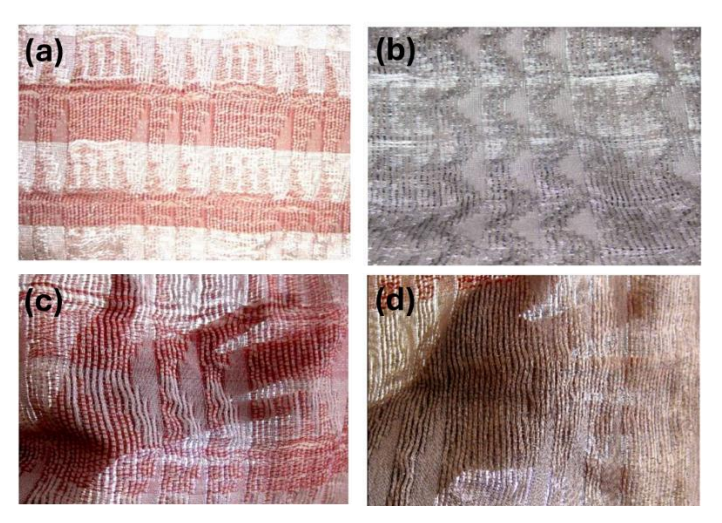


Figure 2.19. Retro-reflective semi-transparent fabrics, (a, b) appearance under a light source; (c, d) transparent appearance of the fabrics (Önlü and Yaşar, 2011)

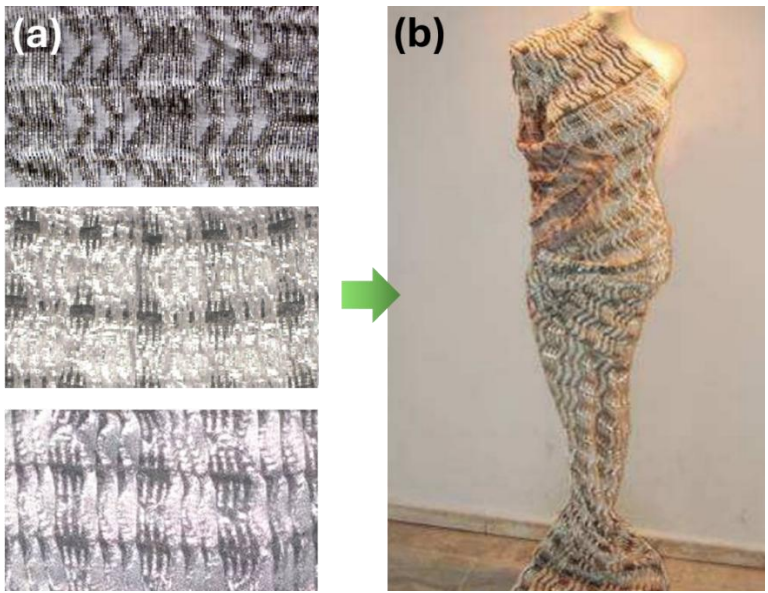


Figure 2.20. (a) Woven fabrics with RR yarns; (b) garment from RR woven fabrics (Önlü and Halaçeli, 2012a)

In a related study, Önlü and Halaçeli (2012a) utilize stainless-steel and retroreflective yarns to produce woven fabrics with different structural patterns (double, patterned and single) for attractive garments (Figure 2.20). Results on the visual effects produced by the woven fabrics reveal puffy and voluminous effects coupled with shimmering and brighter effects that reflects light back to its source at night. This property depending on the light source could influence the body cover, attractiveness, and thinner looks of the wearer. The study further revealed that differences in the structures of woven fabrics and the weft densities influence the visual effects with regards to its shimmering, brightness, puffy and voluminous effects that intend impact on the fabric's ability to retroreflect light.

Aside from the yarns, retro-reflective inks have also been applied. In a research work by Glombikova et al. (2021) as shown in Figure 2.21, reflective transfer films and retro-reflective inks were experimented on Coolmax® athletic fabrics. The screen printing and transfer film process utilised a pattern covering area or sizes of 25% and 85%.

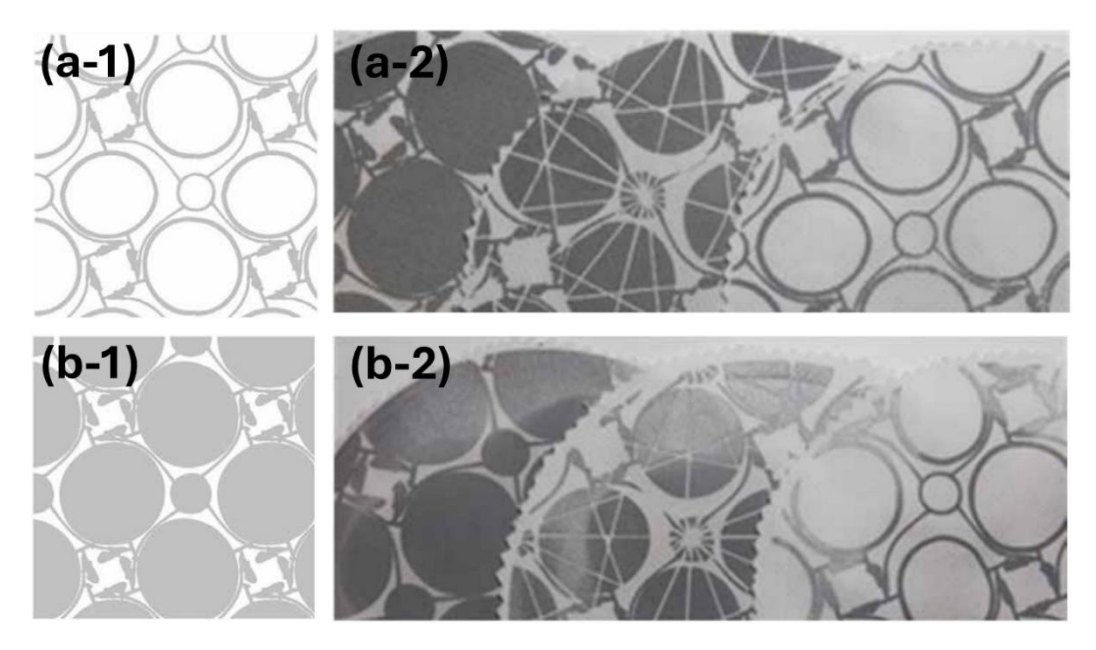


Figure 2.21. (a-1) 25% pattern covering area; (a-2) appearance after abrasion test on screen printed fabrics with 25% pattern covering area; (b-1) 85% pattern covering area; (b-2) appearance after abrasion test on transfer film printed fabrics with 85% pattern covering area (Glombikova et al., 2021)

The retro-reflectivity properties of the eventual fabrics produced showed design patterns made with transfer printing exhibited good retro-reflection as compared to screen-printed designs. Further test on the abrasion resistance reveals that the visibility quality of the screen-printed fabrics showed good values as compared to transfer-printed fabrics. With the difference in thermo-physiological and physical-mechanical performance between the fabrics, it was encouraged that the two printing approaches i.e., transfer film printing and screen printing should be used together on the same fabrics to achieve their full benefits.

In design practice, the screen printing technique was used to transfer retroreflective inks onto the surfaces of different fabric types by Kharenkova (2018) for fashion garments (Figure 2.22). This practice not only enhanced the aesthetic values of the garments but also improved the performance to retro-reflect lights to their source. The eventual fabrics produced met the minimum standard requirements of EN ISO 20471 on the retro-reflectivity properties. Further findings revealed that the nature of printing the inks onto the fabric surfaces and cover of the design area could influence its reflectivity hence the property of retro-reflecting lights to its source.





Figure 2.22. Design patterns printed on garments with RR inks (Kharenkova, 2018)

It was evident from the studies on the design and research approach of using RR inks and yarns or yarns for products inherent with aesthetic and performance properties. This would aid in enhancing the visibility of the users at night.

2.8 Functional applications of RR materials

With the inherent properties of retro-reflecting light to its source, RR materials have found applications in different areas like construction and building, automobiles, and fashion design. The application of these materials seeks to enhance the visibility and cognition of the materials from approaching objects without causing any damages or accidents that could lead to loss of properties and lifes.

2.8.1 Applications in road construction

Enhancing safety on the road is paramount especially at night-time since the dark conditions impede the visibility and recognition of materials or objects and humans. As such retro-reflective materials with its prime property of returning lights back to its source, are applied for road markings e.g., on pavements or road signs. These applications employed as visual elements according to Obeng et al. (2021), enhance the visibility of the roadway, provide road information to road users and further helps drivers stay within their lane on the road hence preventing lane diversion crashes at night. In fact, construction workers apply these RR materials for road traffic control (Figure 2.23a) to prevent collisions from approaching vehicles. For example, high-vis clothing coupled with RR materials in stripes form (Figure 2.23b) either vertically or horizontally are worn by workers at construction sites to make known their exact location even in an event of a blockage from working equipment (Kerbow, 2020, Wood and Chaparro, 2011, Tyrrell et al., 2016) to prevent collision or accidents. Furthermore, RR materials are applied in

firefighting clothing (Figure 2.23c) to help victims identify the search team due to the retro-reflective nature of the RR materials for immediate rescue to safety.



Figure 2.23. RR materials used in road construction. (a) road traffic control (Dennison, 2022); (b) high-visibility (high-vis) clothing (Kerbow, 2020); (c) protective clothing for firefighters (HighViz, 2022)

2.8.2 Applications in buildings

The increasing growth of the human population in the urban areas has resulted to the construction of more low to high-rise buildings to house the dense population (Wang et al., 2020). Such growth has made it difficult for an improved green environment but has encouraged for more construction using asphalt, reflective materials and concrete which has led to increase solar energy absorption (Gustavsson et al., 2021, Kubota et al., 2017). This has influenced the urban thermal conditions where temperatures in the environments are very high than in the rural areas hence affects three key aspects; urban surface temperature, indoor temperature and urban thermal environment (Wang et al., 2021). As such retro-reflective materials with different optical technologies (Figure 2.24) were introduced in buildings to retro-reflect lights and solar energy back to its source thereby having a significant influence in the three key aspects. Figure 2.25 illustrates the thermal conditions in urban environments influenced by reflective materials (left) and retro-reflective materials (right) for buildings.

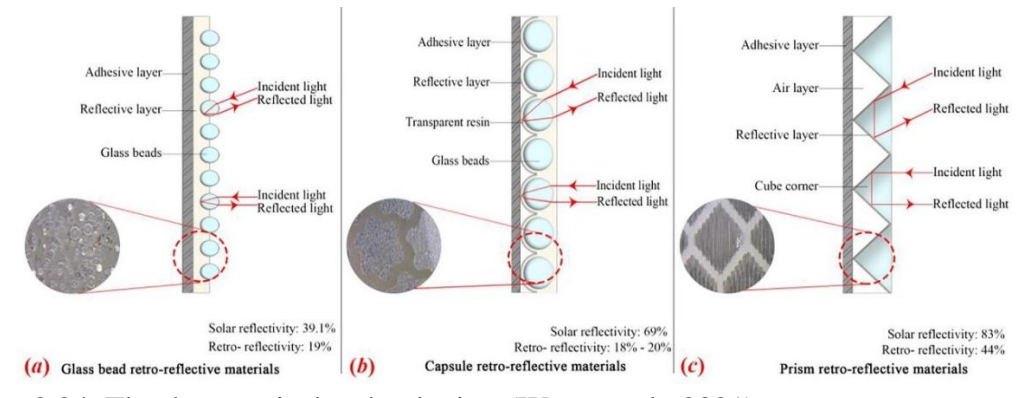


Figure 2.24. The three optical technologies (Wang et al., 2021)

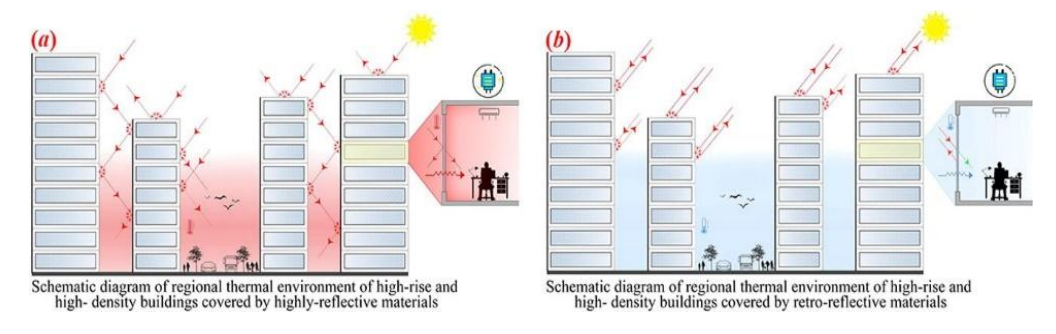


Figure 2.25. Illustration of urban thermal environment influenced by the materials used in the buildings (Wang et al., 2021)

On the issue of urban surface temperature, the use of retro-reflective materials with window glass helped to upwardly reflect the solar radiation back to the sun as shown in an experiment by Inoue et al. (2017) (see Figure 2.26). This prevents the further reflection of solar radiation on the urban environment, however, this approach reduces the temperature of the immediate environment (Rahman et al., 2019). e.g. the pavement surface in a study by (Martin et al., 2019) or a surrounding close to a wall with RR materials (Castellani et al., 2020).

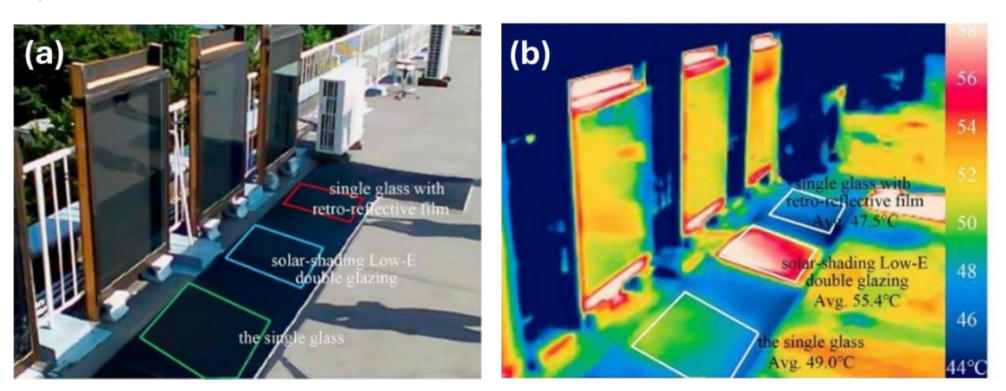


Figure 2.26. (a) Windows with reflective films set-up; (b) temperatures from infrared imagery (Inoue et al., 2017)

The further application of these RR materials reduces the temperature indoors hence the reduction in the transfer of heat from the outside environment through the walls. This subsequently influences the urban thermal environment hence a reduction in the consumption rate of cooling systems in the buildings. Aside from this, in a more winter condition, the RR materials prevent the absorbance of heat from the sun rays via the wall of the building thereby resulting in a reflection of the solar radiation, increasing the consumption of heat in the buildings (Zhou et al., 2020, Wang et al., 2019).

2.8.3 Applications in automobiles

The issue of conspicuity of vehicles, cyclists and motorcycle users continue to be a major concern most especially at night where dark conditions and other related factors impede their recognition and visibility. This has greatly resulted to increase in road traffic fatalities in the World (Oxley et al., 2018, Lee and Sheppard, 2018, Che-Him et al., 2018) and a growing contributor to deaths and premature deaths in a WHO report (Shah and Ahmad, 2019, Ptak, 2019, Hashempour et al., 2019). A critical problem that has led to an increase in RR material application in automobiles to improve their visibility to prevent them from being unnoticed by others (Samuel, 2015) which could result in crashes or collisions on the road. The cube-corner or prismatic sheeting technology is commonly used on the bodies of these moving vehicles or motorcycles or bicycles to retro-reflect lights back to their source. This aids in easy recognition of the objects in front for quick response to prevent accidents on the road. Figure 2.27 shows the application of RR tapes on security vehicles.

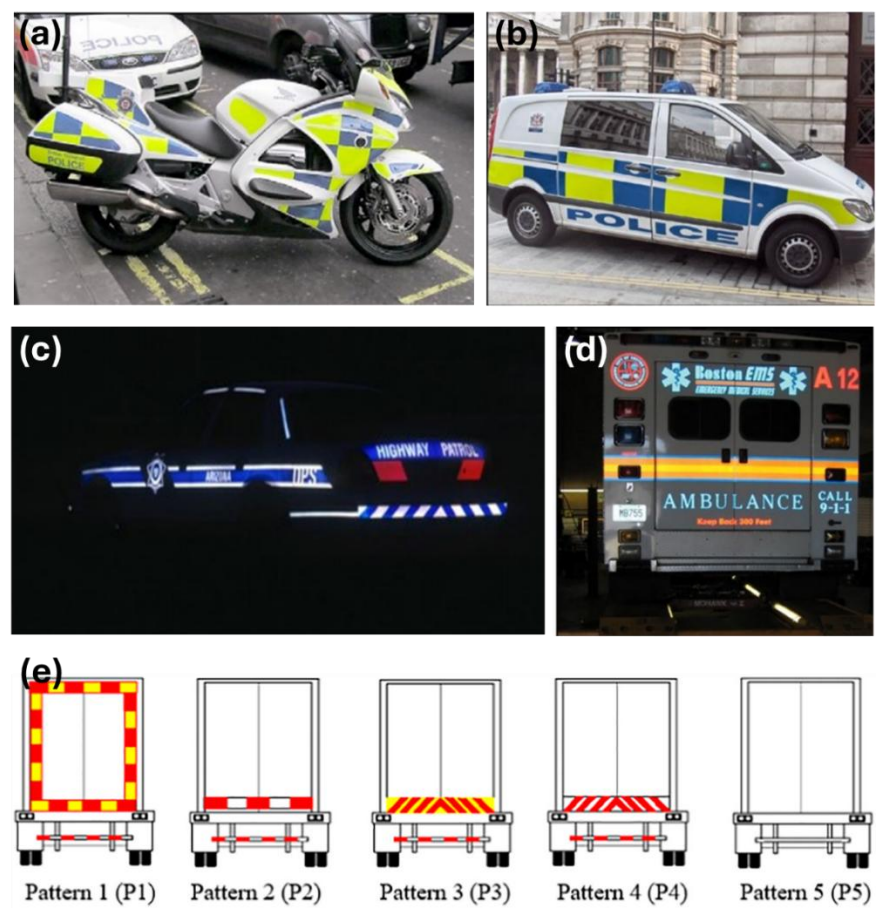


Figure 2.27. Application of RR tapes in the automobile industry. (a, b) visuals at daytime; (c, d) retro-reflective effects at night-time (Hughes–ifsta); (e) patterns and colour combination of RR tapes on heavy trucks to test their visibility or recognition (Lan et al., 2019)

Most importantly, enhancing the visibility of heavy trucks on the road is paramount since the size of these trucks without any RR materials obstruct the road signals and makes the approaching driver recognise its shape (limited truck visibility) leading to increased rear end truck crashes or collision on the road at night (Sullivan and Flannagan, 2012, Radwan et al., 2006, Abdel-Aty and Abdelwahab, 2004). As such RR tape with cubecorner sheeting technologies recognised as a cost-effective approach, improves the visibility of heavy trucks in dark or low-lighting conditions (Berces, 2011, Green et al., 1979) hence has reduced rear-end crashes or collisions of other road users with heavy trucks on the road according to a study by (Morgan, 2001). Supporting this, a study by Lan et al. (2019) on the effectiveness of RR tapes for heavy trucks (Figure 2.23e) revealed that, RR tapes with alternating yellow and red coloured patterns are ideal for effective detection at long to short distances, visibility, and reduction of rear-end collisions with heavy trucks on the road at low light or dark conditions. These RR tapes should meet the standard requirements and policy recommendation of Regulation 48 by the United Nations Economic Commission for Europe (UNECE) which mandates all R104 heavy trucks to be fitted at their rear sides with RR tapes (Babic, 2014).

2.8.4 Applications in marine life and fashion design

Transportation at sea remains an imperative mode to transfer goods and humans from one destination to another. With the harsh and unpredictable weather climates at sea, ensuring the safety of the vessel and humans is critical. As such, RR materials plays an important role in producing or fitting on rescue boats, life jackets, immersion suits, lifebuoys, life rafts and buoyant apparatus which constitutes marine life-saving accessories or appliances. These help in the rescue and life-saving missions of individuals by security agents or the marine at sea due to the retro-reflective properties of the RR sheeting technology fitted on the accessories (Figure 2.28).







Figure 2.28. Marine life-saving floating devices fitted with RR materials in stripes (OSHAcademy Occupational Safety and Health Training, 2022)

In the fashion industry, the incorporation and application of RR materials have grown progressively for popular sportswear that are used in cycling and night running developed by big brands like Nike, Adidas Puma amongst others (WYSE, 2020). Furthermore, fashion designers have applied these RR materials in stripes on fashion clothing and accessories (Figure 2.29) to help in the good optical function of making the wearer visible at night most especially in remote areas hence limiting the scattering of lights. In a more fashionable approach, Adidas developed footwear (sneakers) as shown in Figure 2.29(b) with inherent RR materials that return light incidence on its surface producing an iridescent effect with varying colour changes (Dunne, 2015). This introduced not only an aesthetic value to the product but also a functional performance to the wearer to draw the attention of approaching road users. In a simple protective concept, an anti-paparazzi scarf made of RR materials is used by individuals most especially celebrities to evade the picture shots taken by photographers at night. With the property of the RR material returning lights to its source, images captured at night are without the wearer's face as shown in Figure 2.29(c).



Figure 2.29. (a) Fashion Clothing and accessories (WYSE, 2020); (b) sneakers by Adidas (Dunne, 2015); (c) anti-paparazzi scarf (Aldred, 2016)

2.9 Summary and research gap

It is evident that, due to the poor visibility and high vehicular-pedestrian collisions at night, retro-reflective materials were produced. These materials have the inherent ability to reflect light back to its source in the right path without scattering. Such property has aided in improving the recognition and visibility of pedestrians when lights from an approaching vehicle fall on its surface. In the literature review, varying studies have employed retro-reflective materials (in the form of sheets or films) as strips on certain portions of the clothing. These arrangements form a biomotion configuration that aids in exposing the full body silhouette of the wearer. Other studies also experimented and reported separately with retro-reflective yarns and inks to improve the visibility of plain materials. It is worth noting that, this is by far the approach adopted by various studies to improve pedestrian visibility at night-time. However, further study on the integration of sensors and LEDs into woven or printed retro-reflective materials is still lacking or hasn't been explored yet. Recent advances in smart technology for clothing which produces interactive and responsive actions in the environment have been a driving force or inspiration in this study. This research acknowledges the research gap (Figure 2.30) of limited studies on the integration of sensors and LEDs to produce additional responsive actions for improved visibility and interaction of pedestrians. To help fill this research gap and expand the application of smart technologies for pedestrian safety, this research aims at developing and combining retro-reflective materials into an integrated interactive system. The latter will produce sound and vibration, and the LEDs will produce lights to ensure the visibility of the pedestrian at night-time.

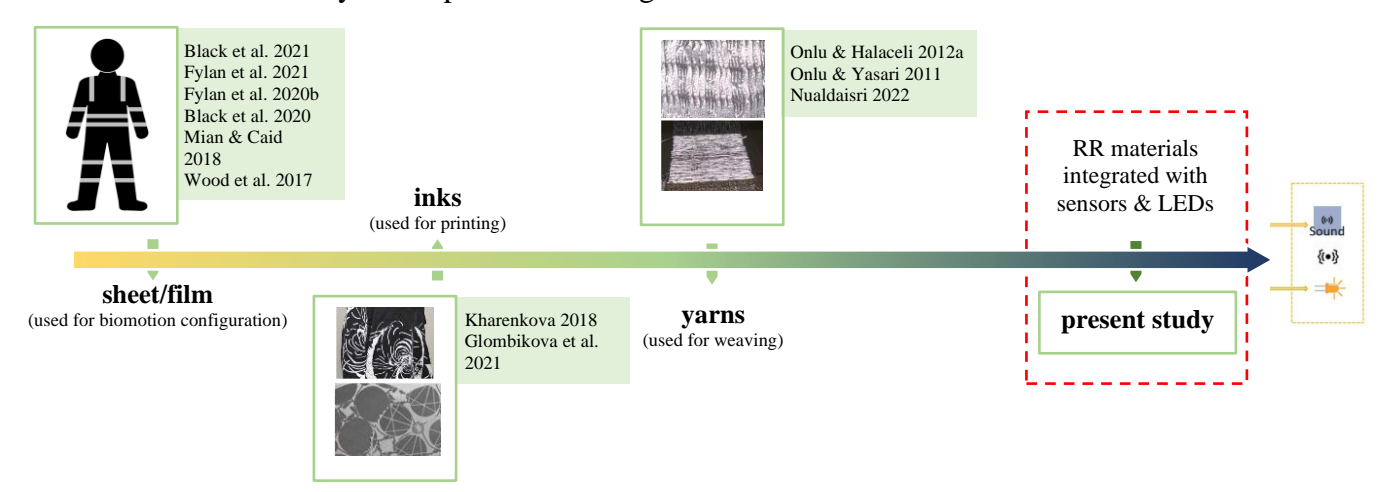


Figure 2.30. Representation of previous research studies with an identified gap that the present study seeks to explore and fill.

CHAPTER 3: Methodology

3.1 Introduction

This chapter introduces the concept of the research, the development of a conceptual model, materials, and methods adopted in the research. The concept of the research was identified which illustrates the integration of RR materials and sensory devices for smart interactive retro-reflective clothing. To carefully achieve the set focus, a conceptual model identifying five critical stages was developed to aid in the exploration and evaluation, testing and characterization of materials, and the application of the finished prototypes. These were carefully utilised in the study based on the adopted practice-based research methodology.

3.2 Practice-based research methodology

The rigorous nature of an inquiry in a study is dependent on the research methodology adopted. As such the credibility, quality, and reliability of the research outcomes are enhanced by the choice of the research methodology. In principle, creative methods are adopted to generate new outcomes based on the approaches (practice-led or practice-based) utilised in a practice-related research. Practice-based research (PBR) as opined by Candy (2006) highlights the generation of new knowledge that is obtained when undertaking an original investigation in the field of practice. Herein, creative outcomes are deemed as a contribution to knowledge, where experimental procedures are conducted to directly answer key research questions (Skains, 2018). Thus, the contribution of knowledge is based on the creative work produced. In this study, the unique qualities of practice-based research are adopted for an investigation and development of a new knowledge imperative for the practice. This implies that the experiences and research results coupled with the creative process all contribute effectively to the practice. Based on this, the design and development of retro-reflective textiles using jacquard and dobby loom (of which textiles from dobby loom are further laser engraving for design creation), fabrication of braided e-yarns and the eventual smart interactive clothing for pedestrian safety at night-time. In this study, the unique understanding of the processes leading to the production and integration of the various key components i.e. retro-reflective textiles and electronic devices to form the interactive clothing. In this practice, a novel design model was proposed and utilised in the creative process.

3.3 Design models for interactive and smart textiles or clothing

Several design models have been developed to create smart and interactive clothing or textiles for different applications. These models are unique in their creative process to effectively produce a creative work with significant importance. Two critical design models proposed by key researchers; Kim et al. (2017) and Wang (2018) were reviewed. Design models by Kim et al. (2017) proposed a design model for an interactive smart fashion with visible light communication ability; and Wang (2018) proposed a design process model for designing smart garments that find applications in rehabilitation.

With regards to the process design model (Figure 3.1) proposed by Kim et al. (2017), it consists of six (6) key stages which highlight the various steps contained in the model. These stages entail the planning and development of the killer application stage, brainstorming, and roadmap stage, the design and technology concept stage, the designing stage, and the eventual prototype stage was outlined to produce the visible light communication-based smart fashion design. This model significantly created a smart fashion designed specifically to fit the needs of the users by incorporating design and technology in the creative process. The issues of safety, satisfaction, usability, and wearability, were taken into consideration by the authors in the design process to ensure the product met user demands.

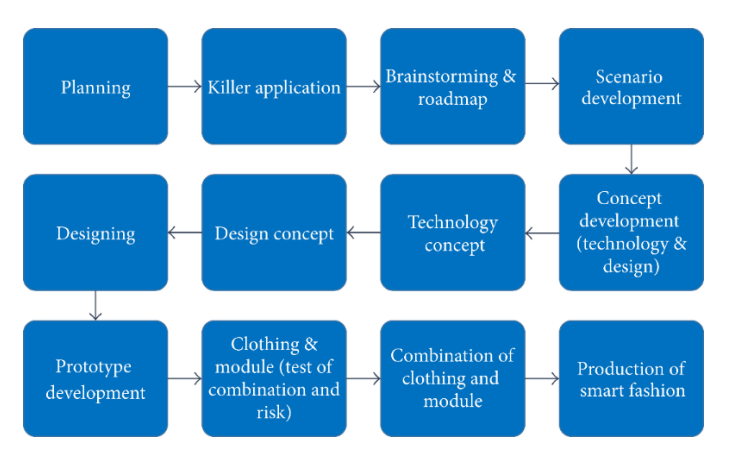


Figure 3.1. Design model for smart fashion with visible light communication ability (Kim et al., 2017). (This is an open-access article distributed under the Creative Commons Attribution License)

In the proposed design process model by Wang (2018) for designing smart garments for rehabilitation, it effectively combines materials and technology for the product's intended applications. This design model was inspired by research-through-design approaches (Zimmerman et al., 2007), key aspects of aesthetics, technology, and

functions influenced the design practice. In the model (Figure 3.2) by Wang (2018), five (5) circular stages; design requirement, concept development, prototype making, evaluation and reflection for disseminating the lessons acquired during the process. The success of the laboratory testing procedures and feedback would influence further development for the market.

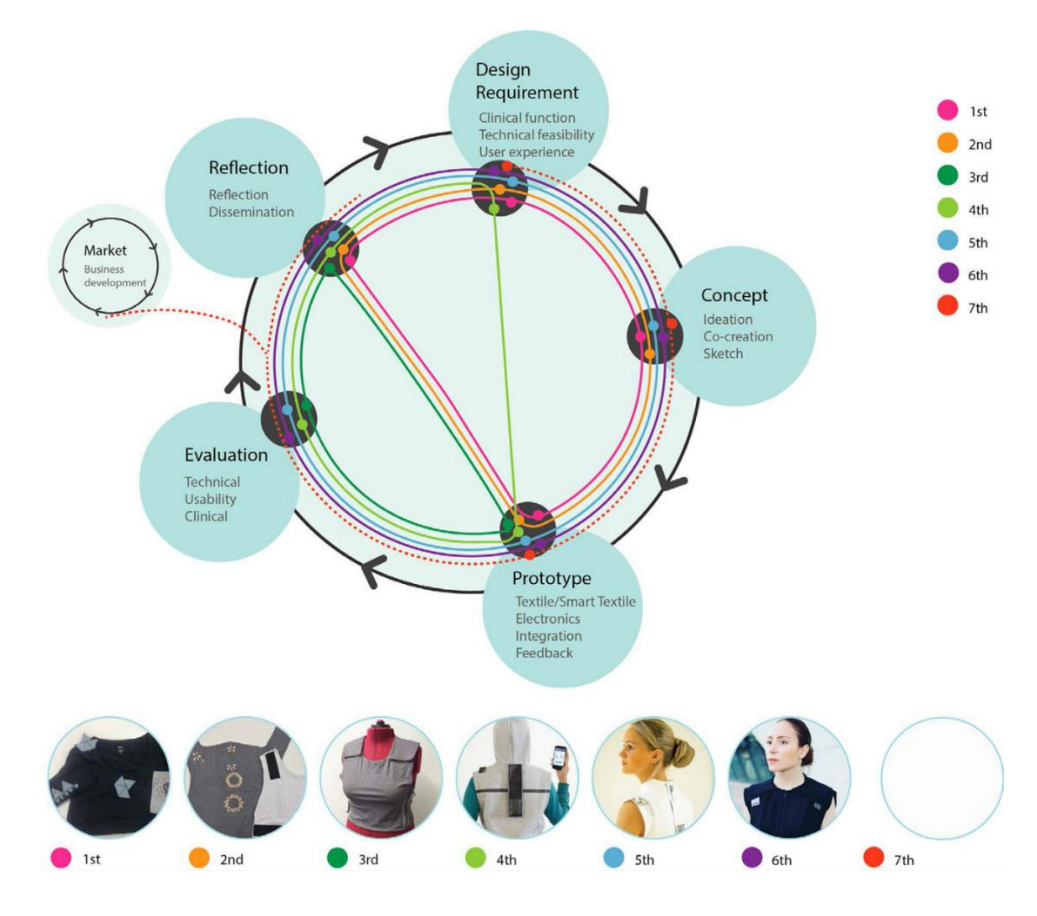


Figure 3.2. Design model for smart garments in rehabilitation (Wang, 2018)

Herein, the above two design models proposed by key researchers aided in the development of the smart interactive retro-reflective clothing (SIRC) design model for the current research, which combined design and technology for a smart clothing to enhance the alert level, visibility, and recognition of the pedestrian on the road.

3.4 Smart interactive retro-reflective clothing (SIRC) design model

Guided by key areas of planning, design and material development, prototyping, and user feedback as examined from the design models of Kim et al. (2017) and Wang (2018), Figure 3.3 illustrates the process design model for the SIRC research. As shown in the figure, there are three (3) distinct parts that constitute the design model for the research project; concept, exploration and evaluation, and application. Inherent in these

core stages are identifying and designing an action plan (concept), development material, electronic yarns, and the interactive system (exploration and evaluation) and the development of prototypes (application) after combining key components.

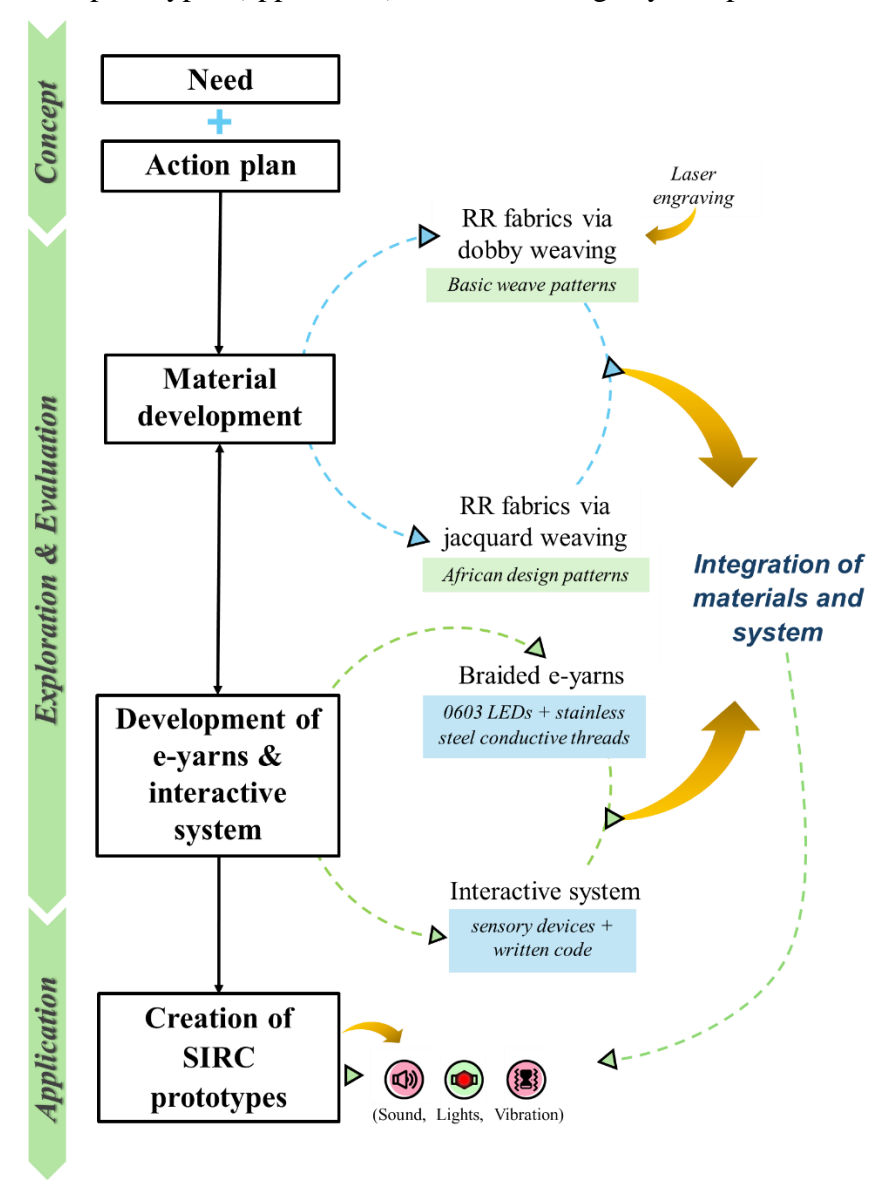


Figure 3.3. Smart interactive retro-reflective clothing (SIRC) design model for the current research

Concept: A rise in pedestrian accidents on the road at night time has exposed advances in innovative materials and concepts aimed at protecting road users, hence limiting accidents. Recent applications highlight the use of retro-reflective materials as strips on clothing to improve the pedestrian's conspicuity. The nature of these clothing designs coupled with their discomfort as revealed by Aldred and Woodcock (2015) and Fylan et al. (2021), have influenced pedestrians' use of safety devices at night. This has exposed the *need* to produce materials and clothing through design innovation embedded

with modern technology to enhance safety. For an *action plan*, advancements in smart textiles using sensory devices provide a critical platform for this study to adopt in producing additional safety features to enhance the alert level, visibility/conspicuity, and recognition of pedestrians. Here, the approach of combining design and technology is utilised in this study to come out with smart interactive retro-reflective clothing.

Exploration & Evaluation: This stage clearly details the systematic development of key components; retro-reflective textiles, braided electronic yarns, and the interactive system. Herein, materials like retro-reflective (RR) yarns (as weft yarns) play a critical role in producing the fabric samples using the jacquard and dobby looms. These RR fabrics which come with design patterns are produced via the jacquard weaving technology with design inspiration drawn from African design patterns. Additionally, the dobby loom aided in the production of RR fabrics with basic weave structures which are further laser engraved for design creation on their surfaces. With the interaction of laser engraving on fabric's weight and size, the appropriate set parameters were used in the design creation process so as not to damage the functional property of the retro-reflective fabrics i.e. limiting their ability to retro-reflect lights back to their source. The relevant laboratory testing procedures were conducted to investigate their retro-reflective effects using a qualitative approach, air permeability, and the low-stress mechanical properties of the fabrics. Conducting the latter properties is imperative due to the application of the materials for clothing, hence the needed comfort and hand of the fabrics are required. Subsequently, using a small LED and stainless steel conductive yarns, electronic yarns are developed which are further braided for effective use on clothing.

Again, the appropriate test methods are conducted to understand the durability, flexibility, and performance of the braided e-yarns in producing lighting effects. These are then linked with a developed interactive system (combining sensors and micro-controllers) to produce the safety features conceptualised for the study i.e. sound, lights, and vibration. The *exploration and evaluation* stage concludes with the integration of the braided e-yarns, interactive system, and the materials developed. Subsequently, the two important parts; material development and, the development of braided e-yarns and interactive systems, are critical in creating an effective smart interactive retro-reflective clothing for the research. These parts are critically discussed in Chapter 5 which provides a comprehensive guide to the design and development procedures.

Application: This stage details the creation of smart interactive retro-reflective clothing (SIRC) prototypes based on the successful integration of the interactive system with the braided e-yarns, on the retro-reflective textiles. These prototypes provide the first workable products for their intended application.

3.5 Concept of the research

Textile design has moved beyond just providing aesthetic appeal to the wearer through the choice of colours and weave patterns. Advancements in combining textile design and digital technology have added functional abilities that provide solutions to problems in the environment. In a more specific case, interactive textiles or smart textiles and clothing embedded with the appropriate technology have provided problem-driven solutions for monitoring human vitals to produce interactive responses to the wearer. As such, Kim et al. (2019) have encouraged textile designers to experiment using varying technologies and materials, together with modern technology for problem-solving. This draws the fact that, at every design creation stage, technology can be combined to re-invent materials for functional performance aside from the recurring aesthetic values of the textile materials.

Premise on this, the study on SIRC dovetails in combining the positives of technology with textile designing processes for innovative and interactive retro-reflective (RR) clothing. This approach intends to produce smart interactive clothing with good comfort, form, appeal, and functional performance to provide safety to the wearer or pedestrian. It is revealed from the literature that, combining technology and design for smart clothing according to Ahsan et al. (2022) are next-generation advanced clothing with embedded wearable systems that monitor, interact, and produce responses in the environment. Thus, it is practically imperative that the combination of technology and textile design would aid in creating a smart interactive RR clothing with good responses as identified in Figure 3.4.

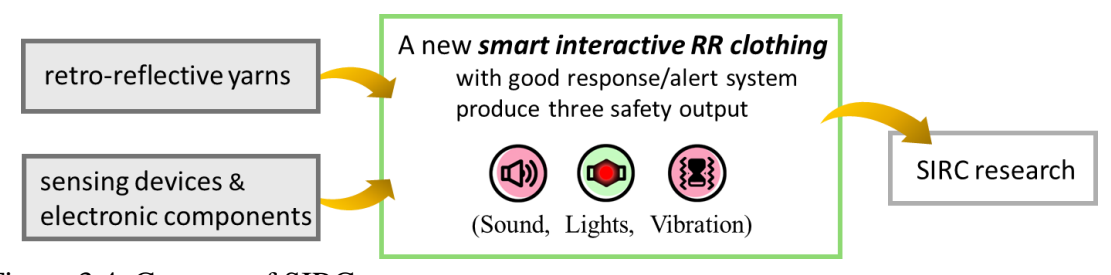


Figure 3.4. Concept of SIRC

3.4 Mechanism of methods/techniques

3.4.1 Weaving

Weaving is a fabric construction method that utilise two sets of yarns; weft and warp yarns interlaced at right angles. This technique of producing fabrics is undertaken on a constructed loom either manual or automated loom, to insert weft yarns or fillings across the width of the tensioned warp yarns. the uniform packing of these fillings interlaced depends on the yarn tension, the read beat-up, and the selected picks-per-inch (related to automated looms). Premise on this, set parameters were selected for weaving on the jacquard loom (as shown in Figure 3.5) and rapier sample looms to produce figurative woven fabrics and normal fabric weave designs (plain, twill, and diamond) respectively.

In the jacquard weaving process, the design graphic patterns are first converted into a picture with the respective colours set using Arahpaints software. The saved png files are easily read by ArahWeave software, where different weave designs are selected for both the front and back sides of each highlighted colour in the picture. The finished jacquard design pattern is saved for card production and woven on the jacquard loom. Here, the appropriate parameters i.e. warp tension and weft densities are carefully set.



Jacquard weaving loom				
Details	Description			
Manufacturer	Dornier / PTV 8J			
Shedding motion	Jacquard			
Loom speed	300 rpm			
Weaving width max	190 cm 74.8 inch			
Drawing-in width	173.4 cm	68.27 inch		
Total warp ends	8167 ends			
Warp density	47.1 ends/cm	119.6 ends/inch		
Warp count	100 den (denier)			
Weft density	17.7 picks/cm	45.0 picks/inch		
Weft count	75 den (colour 1)	8 colours at will		
	75 den (colour 2)			
Reed count	15.7 dents/cm 39.9 dent			
Denting plan	3 ends/dent			

Figure 3.5. (a) Appearance of the jacquard weaving loom, (b) detailed information of the Dornier / PTV 8J jacquard weaving loom

Weaving on the rapier sample loom (Figure 3.6) involved the creation of the desired weave pattern (i.e. plain, twill and diamond) to be woven. These weave patterns are opened in the appropriate CCI sample loom software where weft density per inch, number of beat-ups and picks woven are set. These parameters aside from the yarn properties influence the eventual fabric handle of the woven fabrics (Begum and Milašius, 2022).

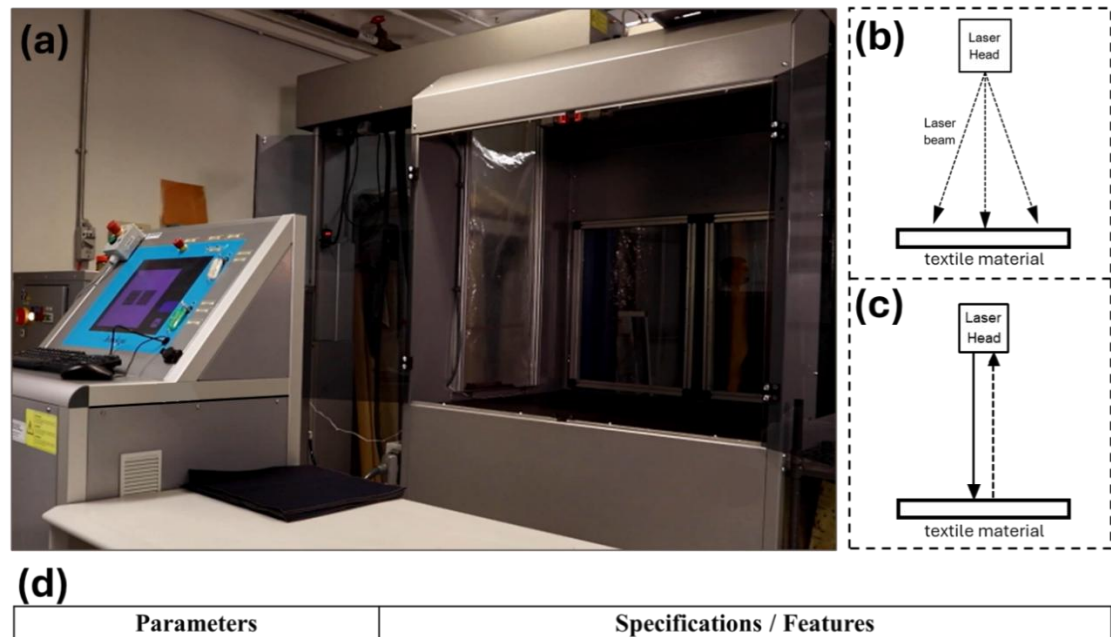


b) CCI/SL7900 Rapier Sample loom				
Details	Description			
Manufacturer	CCI / SL7900			
Shedding motion	Dobby			
Loom speed	25 rpm			
Weaving width max	56 cm	22.0 inch		
Drawing-in width	51 cm	20.08 inch		
Total warp ends	723 ends			
Warp density	14.2 ends/cm	36.0 ends/inch		
Warp count	40/2 s			
Weft density	13.8 picks/cm	35.0 picks/inch		
Weft count	20/2 s (colour 1)	8 colours at will		
Reed count	7.1 dents/cm	18.0 dents/inch		
Denting plan	2 ends/dent			

Figure 3.6. (a) Appearance of the rapier sample loom with dobby shedding, (b) detailed information of the rapier sample loom

3.4.2 Laser engraving

The laser engraving process (Figure 3.7) is a form of embellishing technique that largely uses a laser beam to remove or engrave away (Yuan et al., 2018) some portions from a textile surface. As a subtractive process, the laser beam evaporates or burns the surface of the textile material guided by the design on the computer. This process enhances sustainability and reduces wastewater, energy, and chemicals during textile design finishing processes (Ortiz-Morales et al., 2003, Nourbakhsh et al., 2011, Dascalu et al., 2000b). This cost-effective process expands the possibilities for designers to create interesting design patterns on the surface of textile materials hence ensuring ease and flexibility of the design process (Štěpánková et al., 2010). This has influenced studies by Yuan et al. (2013a), Yuan et al. (2012a), Kan (2014), Yuan et al. (2012b) to adopt the laser engraving technique for patterning and embellishing designs on a textile surface.



(u)			
Parameters	Specifications / Features		
Manufacturer / Model	Jeanologia, Flexi-e V2		
Laser medium	Carbon Dioxide (CO ₂) [Pointer: Laser Diode]		
Laser class	Class 4 [Pointer: Class 3R]		
Wavelength	10600 nm [Pointer: 670 nm]		
Wave mode	Pulsed		
Output Power & Energy	Raw beam: 10 – 175 W		
	Pulse energy: $5 - 230 \text{mJ}$; with pulse activation time $< 45 \mu\text{s}$		
	[Pointer: < 10 mW]		
Beam Excitation	Radio Frequency (RF)		
Beam Diameter	Raw: $6.8 \pm 0.5 \text{ mm} (1/e^2)$ [Focused: ~ 2.0 mm]		
Beam Characteristic & Polarization	K > 0.8; Linear Polarization (Horizontal)		
Pulse Width & Frequency	< 60μs; 0-130 kHz		

Figure 3.7. (a) Laser engraving machine. (b) alignment of the laser beam. (c) beam reflecting the path of the laser engraving machine and (d) parameters of the laser engraving machine.

Based on the benefits of the laser engraving technology, this study adopted the CO₂ laser to engrave design patterns on the retro-reflective textiles developed from the dobby loom. Herein, this CO₂ laser as opined by Nourbakhsh et al. (2011) emits hundreds of kilowatt radiation at 9.6 µm and 10.6 µm hence are suitable for use in the textile industry due to its high efficiency (Kan, 2014). As such the Jeanologia CO₂ laser was used for the surface finishing or embellishing process to transfer African design patterns from the computer to the surface of the textile material. Figure 3.7 provides the image and detail parameters of the laser engraving machine used in the experimental process for the surface embellishment.

3.5 Materials

Herein, different materials categorised as yarns, and electronic components were used in the experimental process. 150D/2 retro-reflective (RR) threads (Figure 3.8) with thickness of 0.12 mm and 22.348 NE (in different colours) were purchased from Dongguan Cheng Wei RR yarns Material Co., Ltd, China. This thread comprises of a polyester thread wrapped around the retro-reflective core thread which contains glass beads structures. These structures are spherical in shape which provides the possibility of refracting or bending lights on their rear surface for reflection back to the light source through its front surface (Lloyd, 2008) in a parallel direction to its light source.

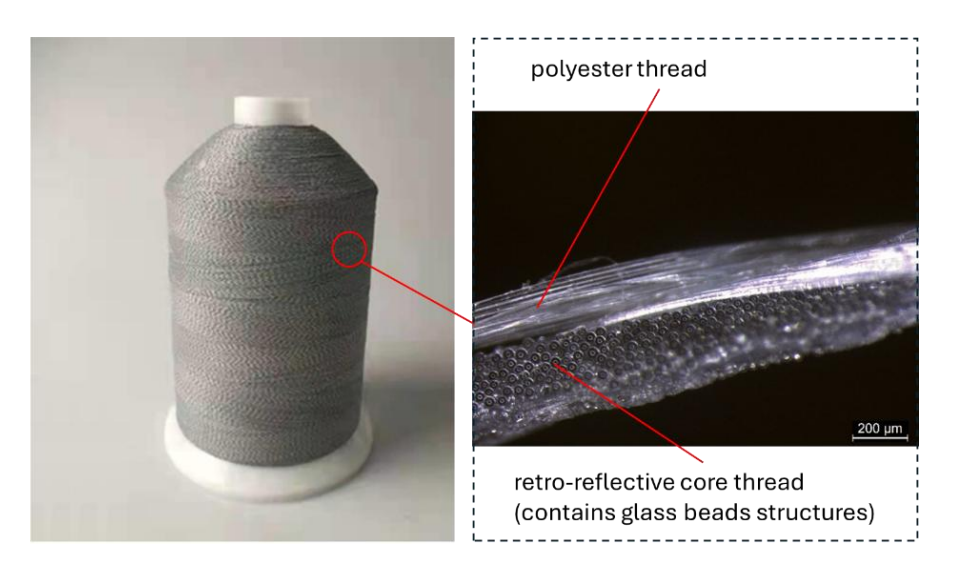


Figure 3.8. Appearance of the retro-reflective yarns

Additionally, electronic components and accessories like stainless steel conductive threads were purchased from Fujian QL Metal Fiber Co. Ltd, China, micro-controller and sensor modules such as a light detector sensor and vibration motor were purchased from Shenzhen KEYES DIY Robot Co. Ltd, China, red and green light-emitting diodes (LEDs) were purchased from Shenzhen Lianxinrui Technology Co. Ltd, China, and sensory devices were used in developing e-yarns and the control system that produces three appropriate outputs (sound, light, and vibration).

3.6 Characterisation

The physical and mechanical properties of the retro-reflective woven textiles and the treated textiles (printed) are tested and evaluated with the following. Aside from the qualitative reflective test on the woven and printed samples, other tests conducted are significant to understand the properties of the samples due to their end use in clothing construction.

Reflective effects

An experimental qualitative approach was used in this study to observe the retroreflection ability of the materials when lights fall on their surface. To test the reflective effects, images of the samples were taken with a digital camera to capture them in the daylight and then in the dark at a distance of 1.5 meters (Figure 3.9).

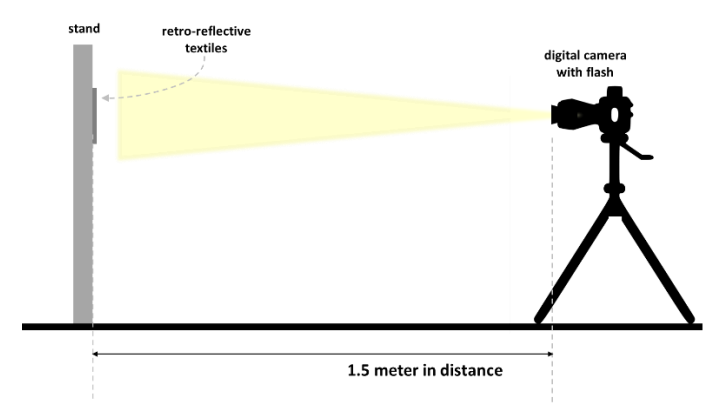


Figure 3.9. Experimental set-up to capture the reflective nature of the woven fabrics.

Fabric weight

The weight of the pristine and treated five fabric samples with dimensions of 200mm by 200mm square was measured using the electronic balance (BX300, Shimadzu Corp., Hong Kong) in accordance with the testing method ASTM D3776. The averages of the five specimens for each weave structure were calculated and recorded.

Thickness

The digital thickness gauge with a fixed pressure of 4 g/cm² was used to determine the thickness of the pristine and treated five fabric samples in accordance with ASTM D1777-96. The averages of the five specimens for each weave structure were calculated and recorded.

Structure morphology

The structure of the original and treated fabric samples was observed under an amplified size with an optical microscope (Leica M165 C).

Low-stress mechanical property

The bending, compression, surface, shear, and tensile properties of the fabric samples were tested by using the Kawabata Evaluation System of Fabric (KES-F) testing instruments

(Kato Giken Co., Ltd. Japan), i.e., tensile and shear tester (KES-FB1), pure bending tester (KES-FB2), compression tester (KES-FB3) and surface tester (KES-FB4). The testing of samples was measured and cut into standard dimensions 20 x 20 cm, and then conditioned under standard atmospheric air and humidity. Table 3.1 shows the characteristic values by Kawabata (2005) for the three tests conducted. Subsequently, an illustration of the testing procedure for the various properties is shown in Figure 3.10.

Table 3.1. Description values and units for the three KES-F tests

Properties		Description	Unit
Tensile (KES-FB1)	WT	Tensile energy	gf.cm/ cm ²
	RT	Tensile resilience	%
Shear (KES-FB1)	G	Shear modulus	gf/cm. °
	2HG	Shear hysteresis at 0.5°	gf/cm
Bending (KES-FB2)	В	Bending rigidity	gf.cm ² /cm
	2HB	Bending Hysteresis	gf.cm ² /cm
Compression (KES-FB3)	LC	Compressional linearity	-
	WC	Compressional energy	gf.cm/ cm ²
	RC	Compressional resilience	%
Surface (KES-FB4)	MIU	Coefficient of friction	-
	MMD	Mean deviation of MIU	-
	SMD	Geometrical roughness	μm

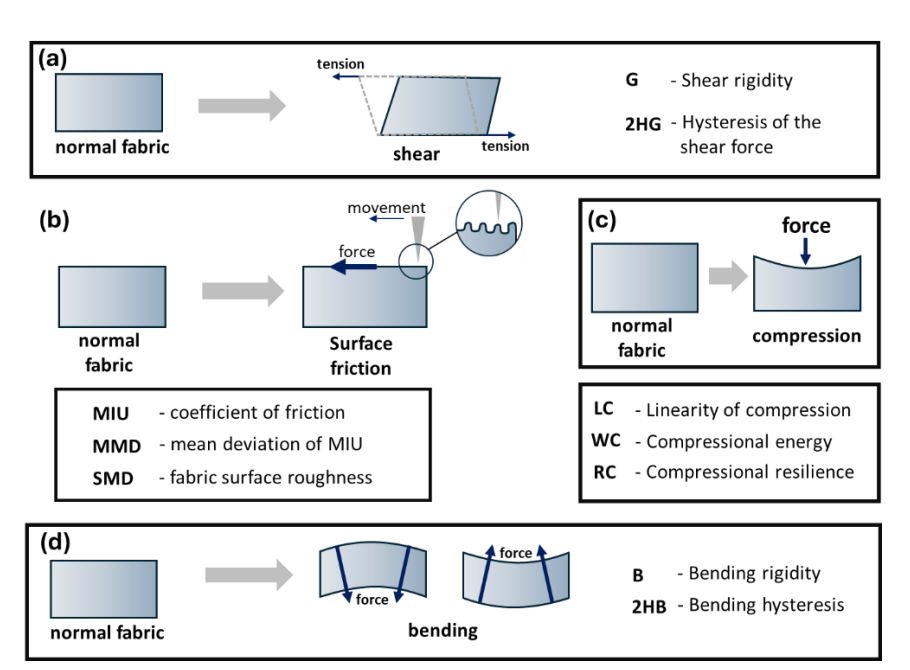


Figure 3.10. Low-stress mechanical property. (a) shear properties, (b) surface properties, (c) compression properties, and (d) bending properties.

Air permeability

The permeability and breathability of the samples in air were measured by using an air permeability tester (KES F8 AP1; Kato Giken Co., Ltd. Japan), to record the resistance R

in kPa•s/m following ASTM D737-04. The test was conducted by using 5 specimens of each of the three textiles of which their average was calculated and recorded.

Thermal conductivity

The thermal conductivity was evaluated by using the KES FB7 Thermo Labo Tester (Kato Giken Co., Ltd. Japan) with the dry contact method. The specimens were placed on the water box with a circulating temperature of 25°C and the BT-box (area of 25 cm² and preset at 30.3°C) was then placed onto the fabric specimen. This transferred the heat from the BT-box through the fabric to the water box. The heat loss (watt) was displayed on the digital panel of the tester. The thermal conductivity k was calculated in (W/cm·°C) by using Equation:

$$k = W \cdot D/A \cdot \Delta T_o$$
 (2)

where W denotes the – heat loss and is the unit of the readings on the digital panel, D is the – thickness of the specimens, A is the – area of the BT-box and ΔT_o is the temperature difference). After obtaining the values in (W/cm·°C), they were converted to the SI unit of W/mk.

Tensile strength

The tensile strength of the specimens was measured by using an Instron 411 tester in both the warp and weft directions following the grab test methods in ASTM D5034. Five specimens were cut from the woven textiles with 10 by 20 cm dimensions. The top and bottom jaws of the tester were firmly centered on the specimens. The gauge length for testing was 75 mm at a speed rate of 300 mm/min. Alternatively, the Instron 5566 Universal Testing Machine was used to measure the tensile strength of both e-yarns and braided e-yarns samples following ISO 2062:2009. Herein, the clamping distance or gauge length was set at 100 mm. Five samples were tested for each sample and the average results were calculated and recorded.

Primary hand and total hand value

The primary hand value (PHV) and total hand value (THV) of the three samples were measured in koshi (stiffness), fukurami (fullness and softness), shari (crispness), hari (antidrape) and numeri (smoothness) hand values in accordance with the Kawabata Evaluation System for Fabrics (KES FB). The low mechanical stress properties of the samples were calculated to obtain tactile comfort which is the total hand value (Kawabata and Niwa, 1975).

3.7 Design inspiration for the study: *African patterns*

The African art forms produced by skilled craftsmen in the second-largest continent in the world incorporate indigenous symbols in their patterns. These art forms are found on different items like textiles, sculptures, pottery, architecture, baskets, and jewellery amongst others. They carry significant messages or have meanings that tell a unique cultural history of events or happenings. The wealth of patterns in Africa is generally grouped into two types; geometric and figurative patterns. They are a visual expression of the history, beliefs, and philosophy of the culture (Evans, 2017). Depending on the cultures, their patterns may vary in terms of style, shapes, and colours. These African patterns are used by craftsmen to produce simple to complex visual forms through different techniques like weaving, carving, dyeing, sewing, painting, and hand printing.

African geometric patterns are composed of rectangles, triangles, squares, and circles which are incorporated into textiles, and painted on walls of buildings amongst others. These geometric patterns carry significant cultural value. Notable examples are the Ndebele wall paintings in South Africa, and Kente cloth and Sirigu wall paintings in Ghana. Figures 3.11(a) – 3.11(c) show these geometric patterns which are either painted on walls or woven into traditional types of fabric. The patterns of the Ndebele wall paintings in Figure 3.11(a) are created by women who use earth colours to paint the walls of buildings. Patterns are grouped together based on the five main colour choices (pink, green, sky blue, yellow to gold, red to dark red) from interesting design structures that reinforce their message to viewers (Jcroman, 2015, Rose, 2013). In the Sirigu wall paintings,

Agurinuuse motif in Figure 3.11(b)(i) means linked hands, Zaalin daa motif in Figure 3.7(b)(ii) symbolizes male essence, and Zaalin nyanga motif in Figure 3.11(b)(iii) symbolizes female essence. These last two symbols are collectively called Zaalinga or net, which draws on the importance of netted containers or fish or calabash nets to safeguard their calabashes from breaking (Wemegah, 2013). Finally, there are the geometric motifs on Asante Kente cloth in Figure 3.11(c). The Nkyemfre motif in Figure 3.7(c)(i) means a pot shed, and symbolises service, knowledge, healing power, recyclability, and history. The Fa hia kətwere Agyeman motif in Figure 3.11(c)(ii) means lean your poverty on or carry your poverty to Agyeman (a noble individual who was known to be generous when this pattern emerged) symbolises faith and hope (Essel, 2019). Apremo motif in Figure 3.11(c)(iii) means canon and symbolises resistance against foreign domination, and the

Achimota *Nsafoa* motif in Figure 3.11(c)(iv) means Achimota keys, symbolises harmony, unity in diversity, knowledge (Asibey et al., 2017).



Figure 3.11. African geometric patterns. (a) ndebele wall paintings in South Africa (Rose, 2013); (b) sirigu wall paintings in Ghana (Asmah et al., 2013); (c) geometric motifs on asante kente cloth in Ghana (Essel, 2019, Asibey et al., 2017)

Figurative patterns are composed of images of animals and humans that depict the historical significance of the culture. These types of patterns are found commonly on the Fon Applique cloth of Benin (West Africa) which is produced by men who cut out images that depict animals, humans, plants, and objects which are then sewn onto a traditional woven fabric (Kimani, 2018) and the Adire cloth of Nigeria which resists starching and dyed indigo colour. In terms of textile forms, simple to complex figurative patterns are either woven, sewn, embroidered, dyed, or painted directly on the surface of the fabric. Figures 3.12(a) and 3.12(b) show some of the African figurative patterns that are used in textile applications.

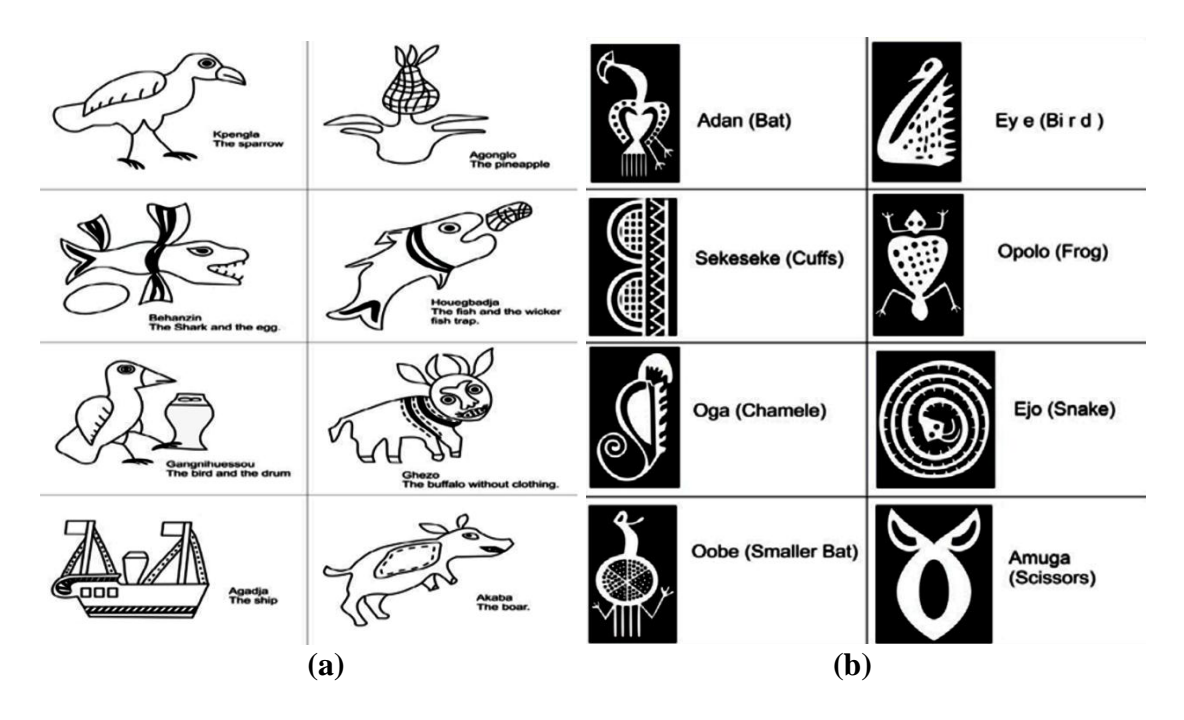


Figure 3.12. African Figurative Patterns: (a) motifs commonly found in Fon Applique cloth in Benin (Kent, 1971), and (b) motifs used for Adire cloth produced in Nigeria (Areo and Kalilu, 2013).

CHAPTER 4: Material Development and Finishing Treatment ²

4.1 Introduction

This chapter details an experimental work conducted to produce retro-reflective fabrics using jacquard and dobby weaving looms for design and basic weave structures respectively. Herein, the retro-reflective textiles were developed with designs inspired by African design patterns. This practical weaving process utilised the jacquard weaving loom to create shapes or figurative design patterns within the structure of the fabrics. A polyester yarn was used for the warp and the retro-reflective yarn for the weft during weaving. Furthermore, retro-reflective textiles from the dobby sample loom are developed with plain, twill, and diamond weave structures with retro-reflective yarns as weft and cotton yarns as warp. The eventual textile samples produced from the jacquard and dobby weaving looms are characterized by international test standards and experimental approaches developed for this study. Finally, the retro-reflective textiles produced by the dobby sample loom are further experimented with a finishing treatment i.e. laser engraving. This technique is used to produce designs inspired by African design patterns on the textile samples. The best results from the experiments are used to produce the final prototypes in the study.

4.2 Jacquard woven retro-reflective fabric samples with African design patterns

Pedestrian fatalities comprise a larger percentage of all deaths and injuries on the road (Damsere-Derry et al., 2010; Schlottmann et al., 2017). In Africa, cases are particularly high with 35% of all deaths attributed to pedestrian accidents in South Africa in 2021 (Stoltz, 2021) and 35% in Kenya in 2020 (Kimuyu, 2021). These high percentages of pedestrian fatalities according to the World Health Organization (2013) report accounted for about 38% of the total road traffic accidents in Africa in 2010. The average rate of road death in Africa increased to 40% or 26.6 per 100,000 individuals in 2013 (World Health Organization, 2018).

Seidu, R. K, Choi, S. Y. and Jiang, S. X. (2023). Development and Performance of Jacquard Woven Retro-reflective Textiles with African Design Patterns, *Fashion and Textiles*, 10 (2). https://doi.org/10.1186/s40691-022-00322-8

Seidu, R. K, Jiang, S.X. (2023). Analysis of performance properties of retro-reflective woven fabrics made with retro-reflective yarns and natural yarns, *Textile Research Journal*, https://doi.org/10.1177/00405175231202786

² Parts of this chapter is *published with details*:

A study by Ackaah et al. (2020) to examine road traffic crashes at night in Ghana during 2013-2017 revealed the severity of pedestrian fatalities with 44% of the accidents happening at night. This is because some of the roads in both the urban and rural areas lack the needed lighting systems and road markings. These are major road safety concerns or problems since pedestrians walk along the roads or cross them at night. Other attributable factors for pedestrian accidents in Africa especially in Ghana includes illegal road crossing, driver fatigue (Tulu et al., 2013), speeding, drunk drivers or drunk pedestrians (Ackaah & Adonteng, 2011; Cho et al., 2017), visual impairment, low or no lighting system at night (poor street lighting), poor road infrastructure, use of electronic gadgets while driving or walking and low visibility of the pedestrian (Ackaah et al., 2020; Kouabenan & Guyot, 2004; Mphela et al., 2021; Schwebel et al., 2012). The latter coupled with low lighting conditions at night, leads to poor visibility for road users or pedestrians hence an increase in night vehicle-pedestrian collisions after dark (Sullivan & Flannagan, 2002). A key reason has been the type of clothing that pedestrians normally wear, which is not reflective and according to Green (2021) makes it difficult for drivers to visually detect pedestrians to avoid possible collisions. Additionally, poor visual perception in most cases makes it difficult for drivers to see pedestrians at night (Fylan et al., 2020), hence increasing the risk of an accident.

In fact, a recent article by the Ghana News Agency (GNA, 2021) stated that Sgt Timinka Richard of the Motor Transport and Traffic Department (MTTD) in Ghana urges pedestrians to wear reflective clothing to ensure safety and curb road knockdowns at night. Even though many pedestrians in developed economies can afford to purchase these reflective clothing, the unavailability, low aesthetic appeal, and increased cost of such clothing have made it difficult for pedestrians in developing countries in Africa to afford them (Wood et al., 2012). Nevertheless, considering the increase in pedestrian accidents in Africa especially in Ghana, recommendations have been made for road users to wear reflective clothing (Ackaah et al., 2020; Green, 2021; Tyrrell et al., 2004) to enhance their visibility. This is imperative since most of the streets are dark and there is a lack of lighting infrastructures so that they can be seen by approaching vehicles.

Although there are benefits from wearing clothing with reflective properties to ensure safety at night, there needs to be incentive and motivation to wear them. African patterns are cherished by the indigenes and are applied creatively to enhance the aesthetics, and their interest and the use of reflective fabrics. This experimental work therefore aims

to use modern jacquard weaving technology to produce African-inspired reflective textiles with cultural patterns to reignite local interest and reinforce the need for reflective clothing to ensure safety at night. A new approach of using reflective threads in materials that can be used in everyday wear during the day and night is proposed. This jacquard weaving technology is environmentally friendly, fast, and efficient as compared to the more time-consuming and labour-intensive traditional weaving production methods widely practiced by craftsmen to produce textiles. The production process from jacquard weaving produces no effluent or toxic waste that is potentially hazardous when released into the environment. These however do not come with functional performance to ensure the safety of the wearer, especially at night.

As such, this experiment poses the following research questions: i) how can the performance of African-inspired textiles be improved for night use? ii) which eco-friendly approach or technique can be used in the creative process that can incorporate African elements and retro-reflective threads in textiles? and iii) what are the performance properties of these retro-reflective textiles using African cultural motifs as their design elements?. The significance of the experimental work is the use of a design approach to expand the availability of reflective materials with cultural elements or patterns that not only reduce the high pedestrian fatalities at night but further showcase the rich heritage of the African culture to the World. These textiles would improve the interest of the people to provide materials that ensure personal safety at night-time due to their retro-reflection properties.

4.2.1 Methodology

Design models or frameworks are widely used by designers to produce a sequence of events or activities within a creative process especially when utilising technology with cultural elements to produce innovative products. As such, Arslan et al. (2020) developed a design process for culturally inspired jacquard fabrics from the stories of the Ottoman Sultans in the community. The design process maps out the chain of activities from adopting relevant sketches in the initial stages to importing them into digital software (Nedgraphics) for effective colour selection for jacquard weaving. Alternative models were proposed by Mathur (2018) on the design sequence for transferring artworks through a computer-aided design (CAD) system for colour and weave selections for jacquard weaving. All of these frameworks provided the necessary reference materials for this study

to create an ideal design process for the weaving of retro-reflective fabrics inspired by African cultural patterns. This is vital because a special type of yarn is used and the cultural patterns require different weave structures and parameters.

The aim of the study was accomplished after completing multiple activities captured in the research methodology (Figure 4.1). This features four (4) vital activities that connect well to provide appropriate solutions for the stated research questions (RQ).

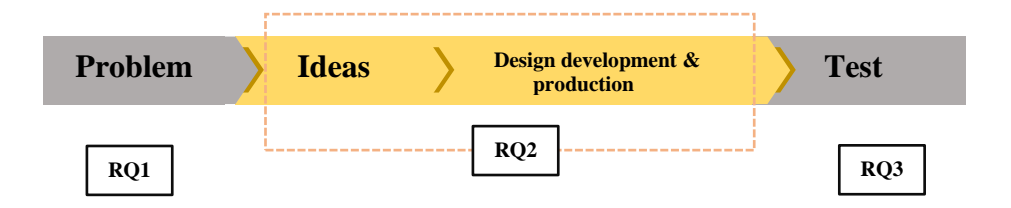


Figure 4.1. Activities in the research methodology: RQ – research question

Activity 1: Problem (RQ1)

Textiles inspired by African culture are made using different techniques such as batik, printing, and knitting amongst others that provide materials with aesthetic values for the consumers. These textiles are undoubtedly colourful and used for different occasions. Aside from the aesthetic values, they are limited to providing the necessary functional property that can ensure personal safety especially at night. Studies captured in the Introduction section clearly highlight the increase in road traffic accidents at night in Africa and the need to wear functional textiles to ensure safety. Therefore, in identifying the problem, this study clearly stated in RQ1 "how can the performance of African-inspired textiles be improved for night use?" for a possible solution. One possible adopted in this study is the use of retro-reflective yarns (inherent with the ability to retro-reflect lights back to their source) to produce textiles with African cultural elements.

Activity 2: Ideas (RQ2)

The jacquard weaving technology was brainstormed as an eco-friendly approach capable of producing figurative textiles to solve RQ2 "which eco-friendly approach or technique can be used in the creative process that can incorporate African elements and retroreflective yarns in textiles?".

Activity 3: Design development and production (RQ2)

Figure 4.2 involves a synchronisation of the stages in design development and production with the use of materials and design parameters to produce the final woven reflective

textiles. The design process begins with a selection of yarns and cultural elements as the CAD patterns (Adobe Photoshop 2022). The created design patterns which have a resolution of 200 dpi ensure an effective weaving process and reduce image distortions. Subsequent parameters were selected for the jacquard weaving and on ArahWeave software (for different weave structures of the fabric face and back). These efforts have led to the production of reflective woven textiles with different weave combinations.

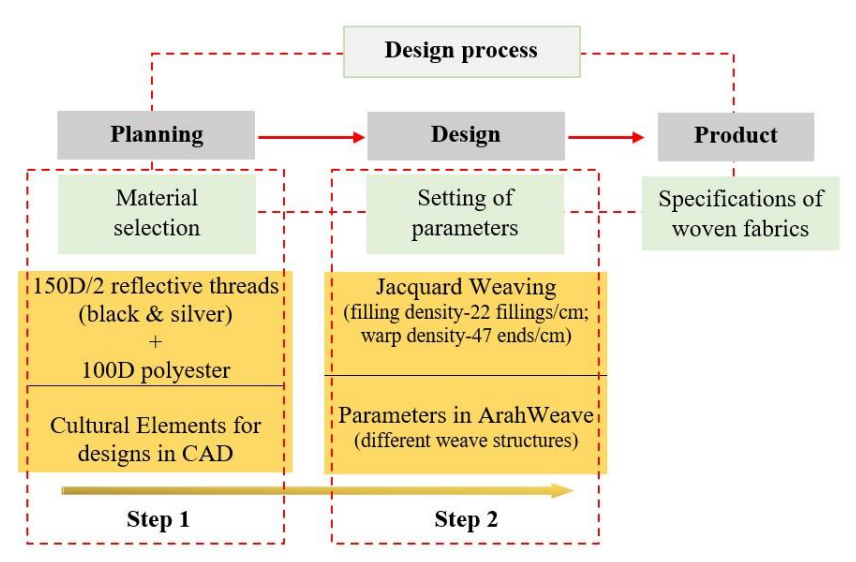


Figure 4.2. Stages for jacquard weaving of reflective woven textiles inspired by African art forms

Stage 1: This details the careful selection of the materials and African cultural elements for use in the design concepts.

Materials. In this experiment, a 150D/2 reflective yarn (either silver or black) was used with a filling density of 22 picks/cm for the weft yarns and 100 denier polyester yarns (white colour) with a density of 47 ends/cm for the warp yarns. The 100 denier polyester yarns, aside from its strength, durability and ristance to certain cehmicals amongst others, this yarn was used since it was already pre-set on the jacquard loom (could not be changed). The 150 D/2 reflective yarns were purchased from Dongguan Cheng Wei Reflective Material Co., Ltd in China.

Using African design patterns. Three graphic images from the Sirigu wall paintings were used in the design process. These have symbolic values that highlight certain activities or events or individuals in the communities. Figure 4.3(a), shows the *Ligipela* motif which means cowry or shells (symbolise the role of cowries during trading or used to seek the hand of a woman in marriage). Figure 4.3(b) is the *Wanzagsi* motif which means broken calabash which is the shell of a gourd (their value is highlighted in use as pottery). Figure

4.3(c) is the *Zaalinga* motif which means fiber net (used to secure and prevent the calabashes or cooking utensils from damage). The images were processed into graphic patterns by using Adobe Photoshop CC as shown in Figures 4.3(d) to 4.3(f).

Sirigu wall paintings are traditional murals created on the walls of indigenous mud houses built in the Sirigu community located in the Kassena Nankana West District in the Upper West Region of Ghana. These paintings are created by grinding earth and rocks which are mixed with water, and cow dung "nambeto" (in the local Nankam language) is used as a binder. Sometimes these wall paintings are called mural paintings. They have existed through centuries and the technique is passed on through apprenticeship from the women to their daughters in the community. Geometric and figurative patterns with symbolic connotations are drawn on the walls by the indigenous women to send coded messages (Wemegah, 2013). This artistic female art form predominantly utilises white, red, black, and ochre as the hues of the art patterns on the walls. These patterns were chosen for the design creation due to their great historical insights on how cowry, broken calabash, and fiber net played an important role in the lives of the indigenous people.

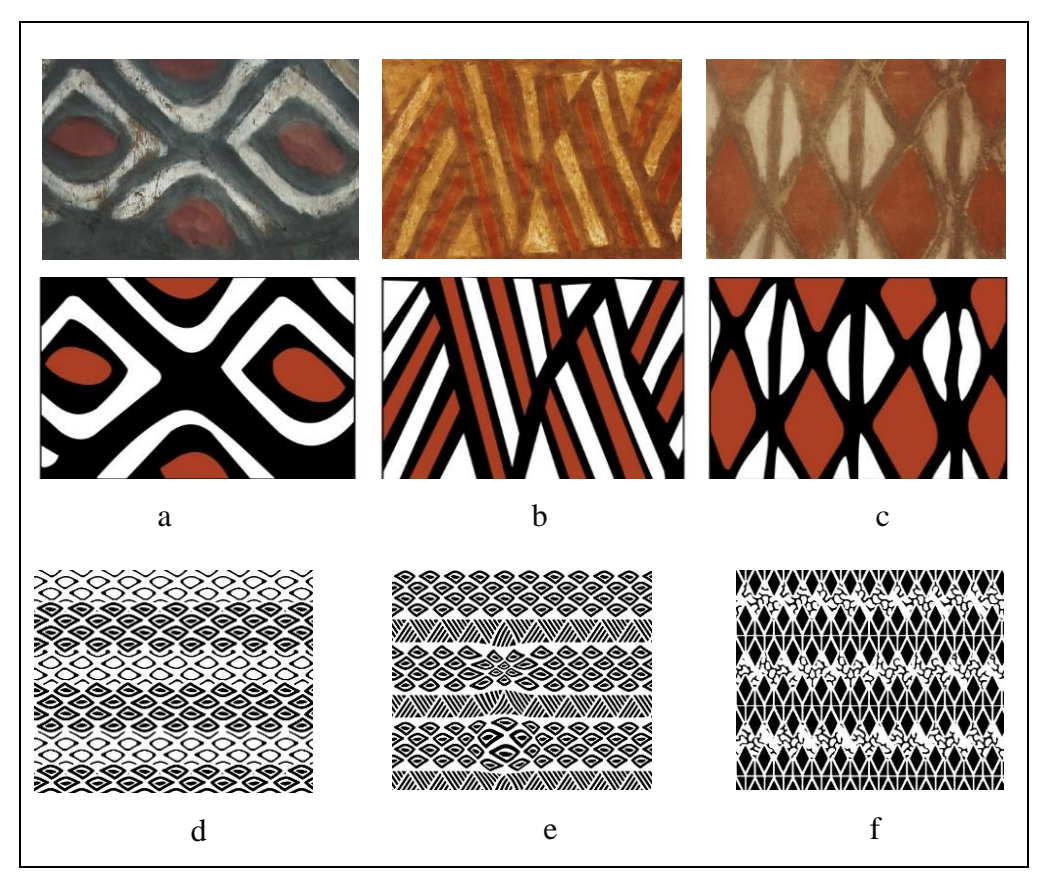


Figure 4.3. (a-c) African design patterns in Sirigu wall paintings, and (d-f) graphic patterns for designs 1-3

Stage 2: The parameters are set for the various weave structures for the selected cultural element and parameters for the Jacquard weaving of the fabric samples. The resultant graphic patterns were uploaded to ArahWeave to isolate the design into weave structures for ease of recognition by the jacquard loom. The experiment utilised two colour schemes, i.e., black and white, with the former representing the design patterns or weft yarns and the latter the warp yarns. This format typically creates a reversed design pattern on the back of the textile, which makes it possible to use either side of the textile. The weave structures are one weft face to a one warp face and one weft back to a one warp back (Figure 4.4).

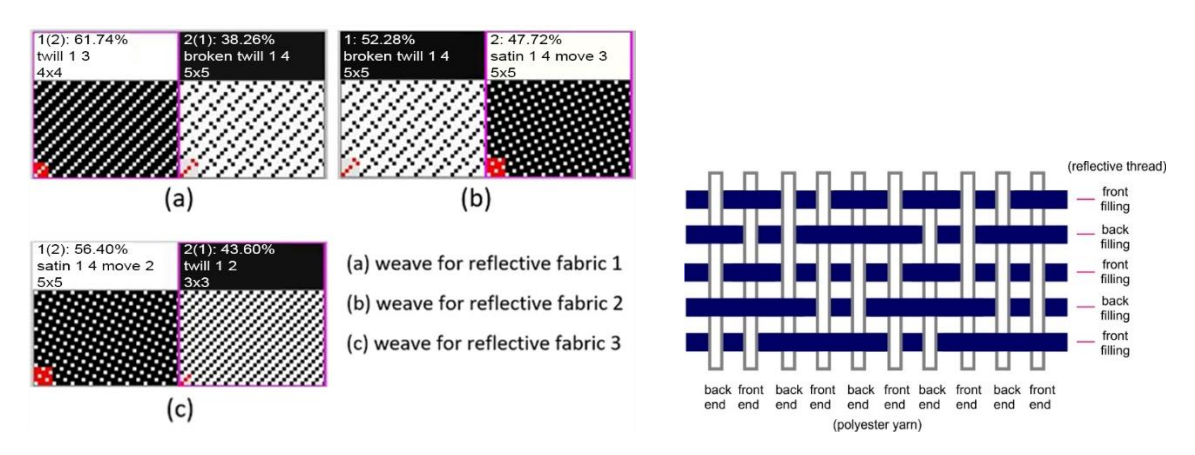


Figure 4.4. Weave structure: the design on the front face and the reversed design at the back face

Reflective yarns and polyester yarns were used to weave three reflective textile samples with African-themed patterns on a Dornier/PTV 8J Jacquard weaving loom at a loom speed of 300 rpm, warp density of 47.1 ends/cm and 8167 warp ends. All of the woven fabrics have assumed dimensions of 160 cm (width) by 90 cm (length). Table 4.1 shows the specifications of the woven textiles. The sample labeled as RF 1 has a weave structure of 1/3 twill and ½ broken twill; RF 2 has ¼ broken twill and ¼ satin, move 3; and RF 3 has ¼ satin, move 2 and ½ twill.

Table 4.1. Specifications of the woven reflective textiles

Sample	Composition	Weave	Yarn colour	Ends/inch	Picks/inch
RF 1	100 denier	1/3 twill 1/4 broken twill	white (warp) silver (weft)	120	54
RF 2	polyester yarn (warp yarns)	1/4 broken twill 1/4 satin, move 3	white (warp) black (weft)	120	54
RF 3	150 D/2 reflective thread (weft yarns)	1/4 satin, move 2 1/2 twill	white (warp) black (weft)	120	54

Note: RF means reflective fabric

4.2.2 Experimental and Characterisation

The three woven samples with different weave structures and design patterns were subjected to physical and mechanical tests, and their retro-reflective effects were also tested. The testing methods are; reflective effects, fabric thickness and weight, surface morphology, low-stress mechanical properties, air permeability, thermal conductivity tensile strength, primary hand value (PHV), and total hand value (THV). The low mechanical stress properties of the samples were calculated to obtain tactile comfort which is the total hand value (Kawabata and Niwa, 1975).

4.2.3 Results and Discussion

This section provides the test results of the woven fabric samples to answer the third research question of the study.

Reflective effects

The woven samples produced with reflective yarns were examined in daylight and a dark room. Images were taken from a distance of 1.5 meters using a digital camera to identify the retro-reflectivity of the woven samples, which are shown in Figure 4.5. Figures 4.5(a), 4.5(b), and 4.5(c) show visible patterns on the three woven samples with the reflective yarns in silver colour in Figure 4.5(a) and black colour for Figures 4.5(b) and 4.5(c). Subsequently, after capturing the reflective effects of the woven samples with the digital camera and using a flash (Figures 4.5(d), 4.5(e), and 4.5(f)) the retro-reflective ability of the textiles is evident even though the visibility of the patterns in the RF 1 (Figure 4.5(d)) is less blurred as compared to RF 2 and RF 3 in Figures 4.5(e) and 4.5(f) respectively.

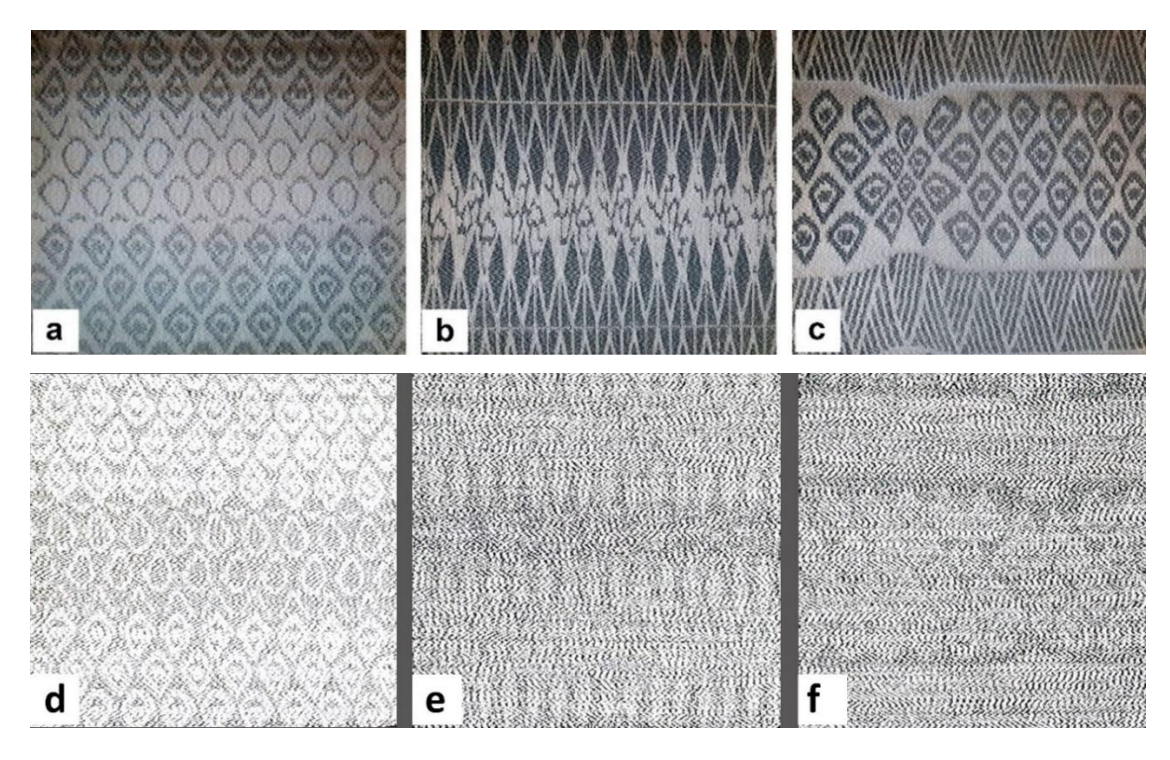


Figure 4.5. Images taken during the day: (a) RF 1, (b) RF 2, and (c) RF 3. Images taken in a dark room: (d) RF 1, (e) RF 2 and (f) RF 3

Fabric weight and thickness

The results from the testing showed that the fabric weight of RF 1 is 272.08 g/m², RF 2 is 276.28 g/m², and RF 3 is 272.5 g/m². Their fabric thickness (mm) is as follows: RF 1 is 0.75, RF 2 is 0.67 and RF 3 is 0.62 hence RF 1 is thicker than RF 2 and RF 3.

Structure morphology

All of the woven textiles were observed under a magnification of $500 \mu m$ (Figure 4.6). The images in Figure 8 show that, the reflective yarns are imbedded with small glass beads that have retro-reflective ability to bounce light back in the same path without scattering.

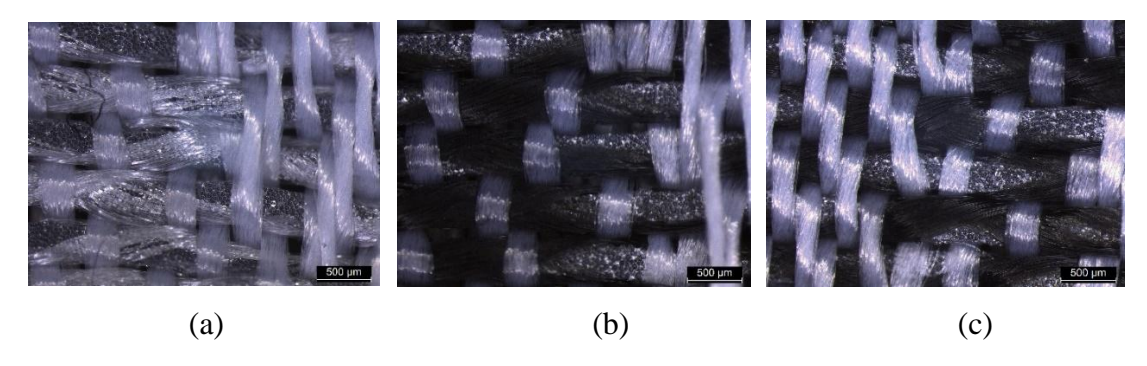


Figure 4.6. Microscopic images of sample surfaces at $500 \, \mu m$: (a) RF1 with silver reflective yarns as weft, (b) RF2 with black reflective yarns as weft, and (c) RF3 with black reflective yarns as weft, all in the horizontal plane

Low-stress mechanical property

Bending property

The bending rigidity (B) and bending hysteresis (2HB) values of the woven samples were recorded. They are shown in Figures 4.7(a) and 4.7(b) respectively. The results of B in Figure 4.7(a) in both the warp-wise and weft-wise directions show that RF 1 has the lowest values as compared to RF 3 and then RF 2. This indicates the inability of RF 1 to resist bending during handling as compared to RF 2 which has the highest resistance to bending. The weave combination of RF 2 (¼ broken twill, ¼ satin, move 3) contributed to its resistance to bending. The results of 2HB in Figure 4.7(b) show that, RF 1 has the lowest value in the warp-wise direction as compared to RF 2 and RF 3. Therefore, RF 1 has a better recovery after bending. RF 2 has a different design pattern and weave combination (¼ broken twill, ¼ satin, move 3) and has the lowest 2HB value in the weft-wise direction, and hence can better recover after bending.

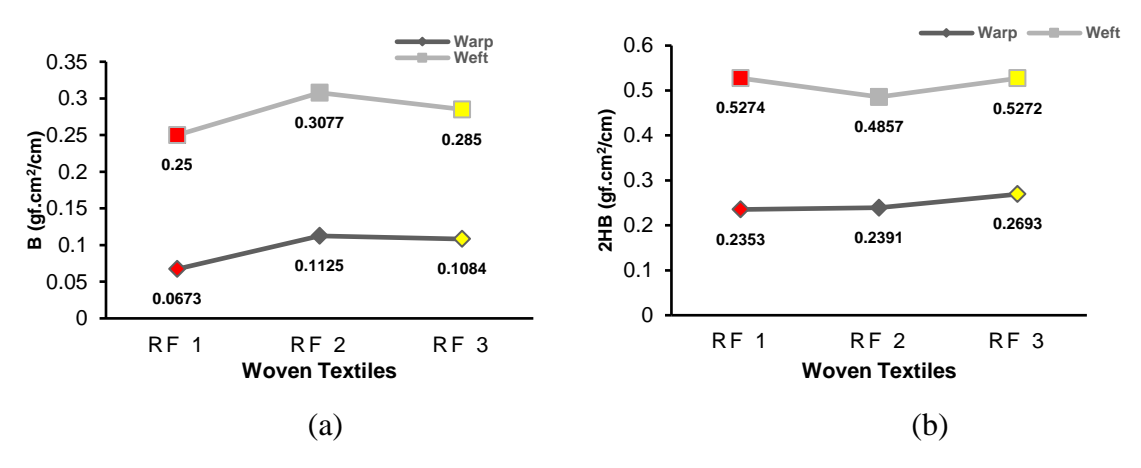


Figure 4.7. Bending property (a) bending rigidity, and (b) bending hysteresis

Compression property

The plots in Figure 4.8(a) show the linearity of compressional (LC) and compressional energy (WC) values where RF 3 has a slightly higher LC value as compared to RF 1, thus indicating higher compressional behaviour, which is influenced by the compressional properties of the weft and warp yarns of the textiles (Mukhopadyhay et al., 2002). On average, LC values have a similar range which denotes the relative hardness of the samples with the different weave structures and design patterns. As such, the high WC values of RF 2 mean that this sample requires slightly higher compressibility or higher energy for compression as compared to RF 3. This may be attributed to the weave combination of ½ broken twill and ½ satin (move 3) of RF 2 versus the ½ satin (move 2) and ½ twill for RF 3. However, RF 1 is constructed with a similar weave combination as

that of RF 2 with 1/3 twill and 1/4 broken twill, so lower compression energy is necessary. In terms of compressional resilience (RC), RF 1 has better recoverability as compared to RF 2 and RF 3 which have fairly similar value ranges. Özgüney et al. (2009) indicated that variations in the weft float, significantly affect the fabric properties like compression and bending rigidity. The recoverability of RF 1 may be attributed to the similar twill weave structure used to produce the sample.

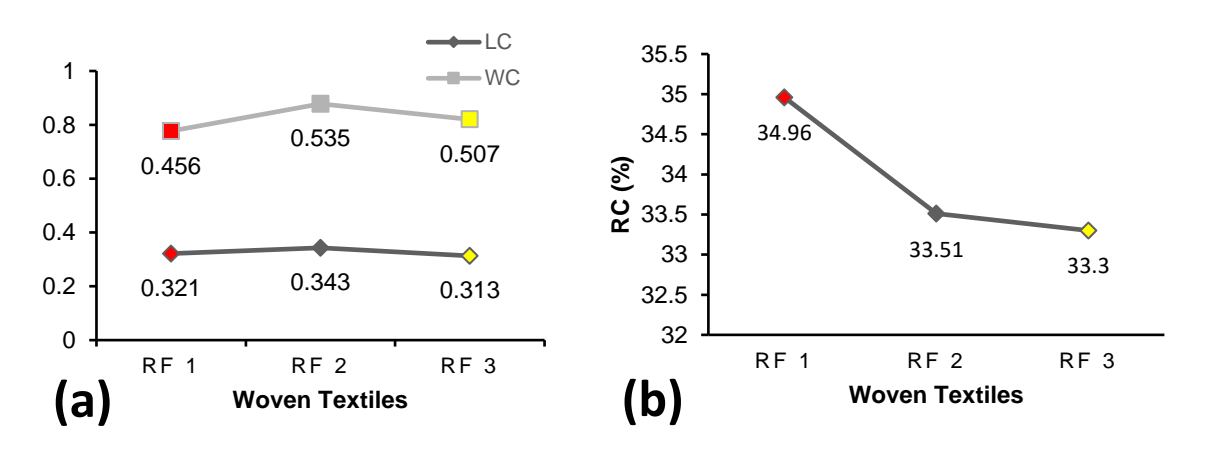


Figure 4.8. (a) Linearity of compression and compressional energy (gf.cm/cm²), and (b) compressional resilience (%)

Surface properties

The coefficient of friction (MIU), fabric mean deviation (MMD), and fabric roughness (SMD) were measured to determine the surface properties of the samples, and the results are shown in Figure 4.9(a) and 4.9(b). In terms of the MIU values in the warpwise direction, the higher MIU values of RF 2 show that this sample is not as slippery or has more friction force compared to RF 1 and RF 3 even though the values are within similar ranges. In the weft-wise direction, RF 3 has higher MIU values as compared to RF 1 and RF 2. This shows the resistance of RF 3 to movement when rubbed against an object or between the fingers. Atalie et al. (2021) indicated that resistance to movement is determined when the surfaces of fabrics come into contact. Such resistance may be attributed to the type of yarn used. In this study, polyester is used for the warp and reflective thread for the weft, and the yarns are interlaced to form the weave structures.

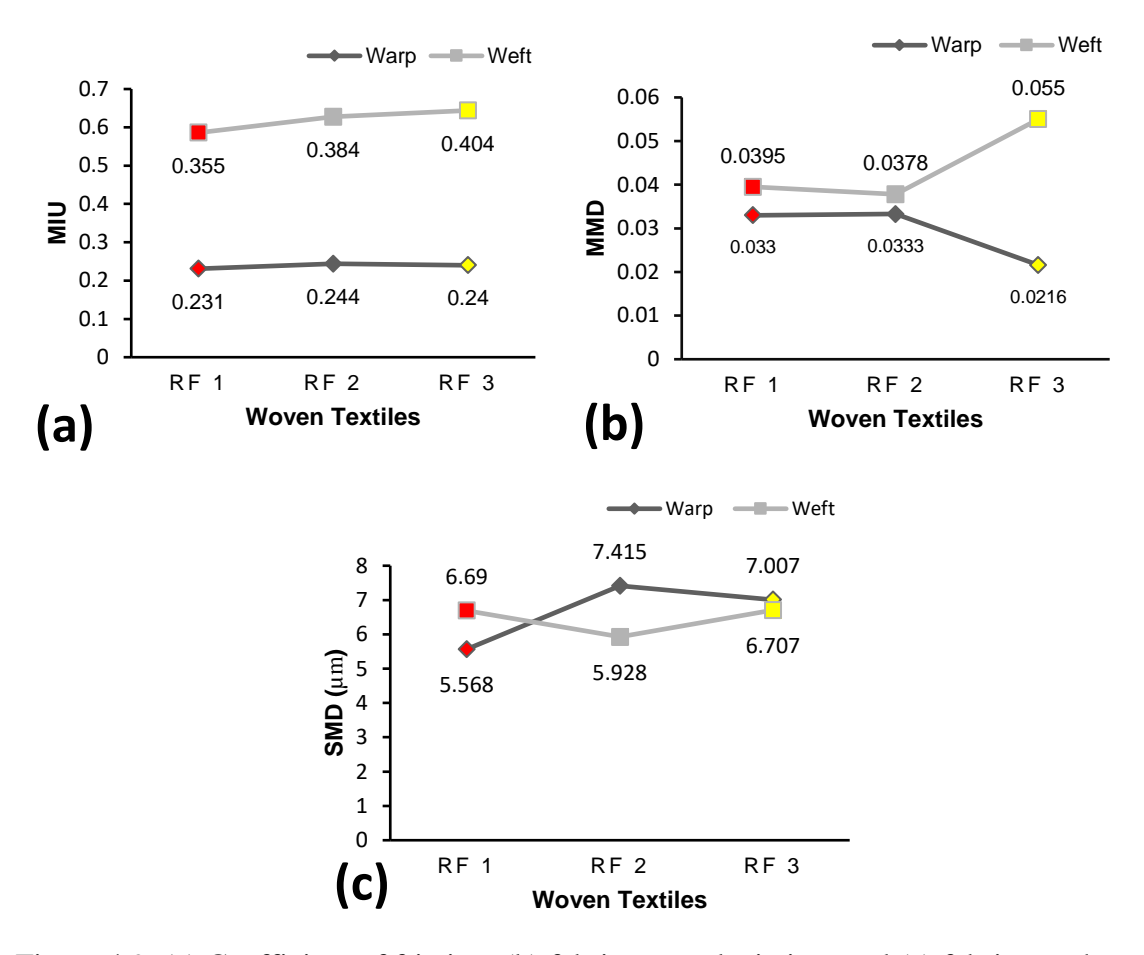


Figure 4.9. (a) Coefficient of friction, (b) fabric mean deviation, and (c) fabric roughness

The MMD values reflect the roughness of the fabric surfaces, where a higher value denotes a higher surface roughness. RF 2 has a higher MMD value followed by RF 1 and RF 3 in the warp-wise direction as shown in Figure 4.9(b). In the weft-wise direction, however, RF 3 has the highest MMD values followed by RF 1 and RF 2. The SMD values were measured to determine the evenness of the fabric surface. RF 2 has the highest SMD value as opposed to RF 1 and RF 3 as shown in Figure 4.9(c) which indicates the uneven surface of RF 2 in the warp-wise direction. In the weft-wise direction, RF 3 has a higher SMD value than RF 1 and RF 2. The surfaces of RF 2 and RF 3 in the warp-wise and weft-wise directions have a higher MIU value, which indicates that they are less slippery. The latter factors may also be attributed to the weave combinations (i.e., ½ broken twill and ½ satin, move 3 for RF 2; ¼ satin, move 2 and ½ twill for RF 3) and the design patterns of these two woven textiles.

Shearing properties

The samples were measured to determine their shearing properties (recovery after shear) by using the shear rigidity (G) values, hysteresis of shear force at 0.5° (2HG), and hysteresis of shear force at 5° (2HG5). The G, 2HG, and 2HG5 values of the woven textiles are reduced in RF 3, RF 1, and RF 2 in both warp-wise and weft-wise directions respectively, see Figures 4.10(a), 4.10(b), and 4.10(c). the higher G values of RF 3 show that this sample is less deformable as compared to the lower G values of RF 2 which can easily deform. The lower 2HG and 2HG5 values of RF 2 in both directions show that this sample has better recoverability or resilience, to a poor recoverability of RF 3 which has a higher 2HG value after shearing.

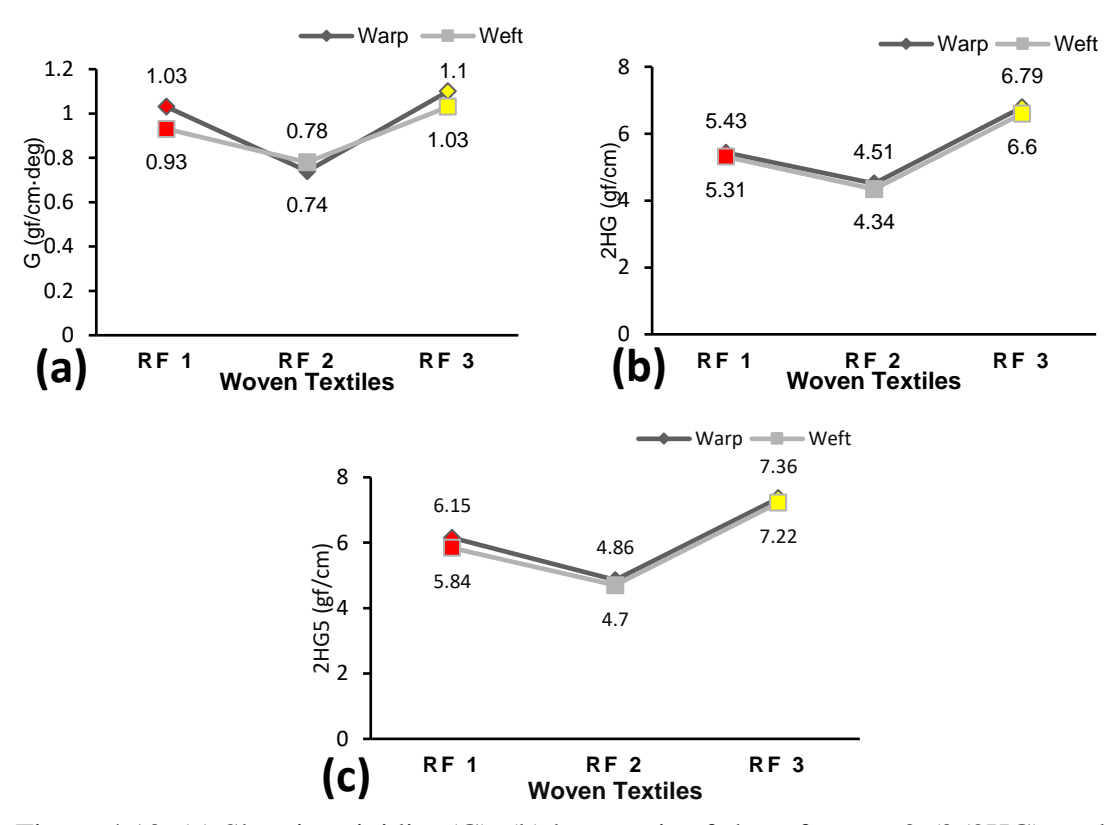


Figure 4.10. (a) Shearing rigidity (G), (b) hysteresis of shear force at 0.5° (2HG), and (c) hysteresis of shear force at 5° (2HG5)

Tensile properties

The tensile resilience (RT), tensile energy (WT), tensile linearity (LT), and extensibility (EMT) were measured to determine the tensile properties of the woven textiles. As seen in Table 4.2, RF 1 has the highest LT and WT in both the weft-wise and warp-wise directions. The higher LT means that RF 1 is more robust and harder than RF 2 and RF 3. For the WT, the higher WT of RF 1 shows that this sample can easily stretch and can withstand external stress during extension as compared to the two other samples.

Table 4.2. Tensile properties of samples in this study

Samples	Direction	Tensile Properties			
		LT	WT	RT	EMT
			(gf.cm/cm ²)	%	(%)
RF 1	warp	0.135*	1.6*	55.67	0.96
	weft	0.128^{*}	0.08^{*}	130.00	0.25
RF 2	warp	0.131	0.38	55.71*	1.16
	weft	0.096	0.05	140.00^*	0.21
RF 3	warp	0.11	0.39	52.22	1.42*
	weft	0.123	0.05	100.00	0.82^{*}

^(*) denotes higher values in warp-wise and weft-wise directions

In contrast to the LT and WT values, RF 2 and RF 3 have the highest RT and EMT in the warp-wise and weft-wise directions respectively. The higher RT of RF 2 shows that the sample has good recoverability after being subjected to tensile stress. RF 3 however has the greatest EMT thus indicating good extensibility or elongation.

Air permeability

The recorded results as plotted in Figure 4.11 show the air resistance (kPa•s/m) values of the three samples with different weave structures. Lower values indicate good breathability or permeability of the textile. As such, RF 1 has the lowest R-value as compared to RF 2 and RF 3 and is hence more permeable to atmospheric air which would ensure wear comfort. The different weave structures of the samples could affect the air permeability which would eventually impact wear comfort. The results show that the weave structure of RF 3 causes lower fabric porosity.

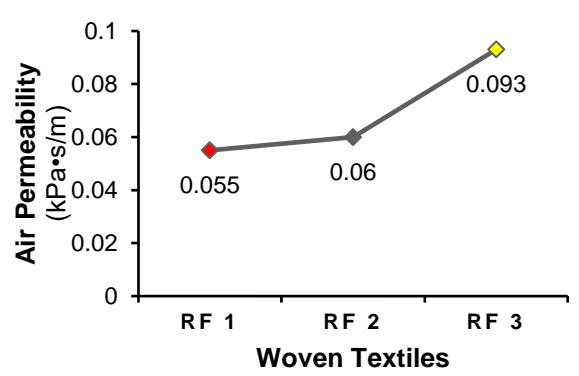


Figure 4.11. Air resistance of the woven textiles with different weave structures

Thermal conductivity

The k values for the thermal conductivity of the samples in Figure 4.12 indicate that RF 2 has the lowest k value followed by RF 3. This reveals that the structure of RF 2 cannot readily release heat from the body to the atmosphere. Fabrics like RF 2 can be used in cold weather since body heat is trapped longer before being released into the atmosphere. RF 1

has the highest k values which shows that this sample readily releases more heat into the atmosphere. This clearly indicates that the fabric structure can influence the thermal conductivity and hence the eventual wear comfort (Musa et al., 2021).

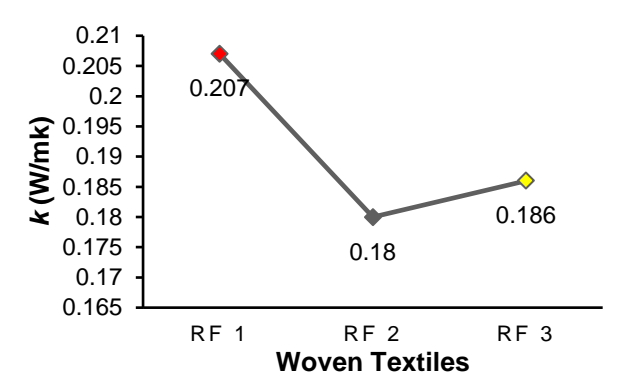


Figure 4.12. Thermal conductivity of samples

Tensile strength

The tensile strength is an imperative property of woven textiles that determines how much extension or elongation a fabric can bear under maximum force. This factor further influences according to Ko and Lee (2003) human movement either easing or restraining movement when wearing a garment constructed from this sample. With this, the results plotted in Figure 4.13 shows a reduction in force required to break the woven textiles, with RF 1 having the highest force followed by RF 2 and RF 3 in the warp-wise direction. This translates into greater extension at break for RF 1 followed by RF 2 and RF 3. In the weft-wise direction, however, the force and extension at break are reduced in RF 1 followed by RF 3 and RF 2. A greater force is required for the extension of RF 1 which may be attributed to its weave combination which implies that a twill weave combination gives woven textiles good tensile strength.

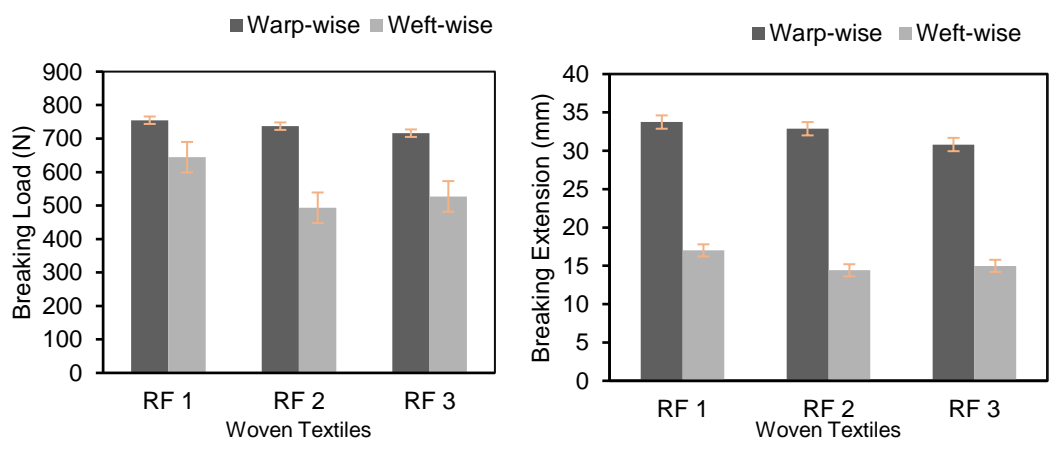


Figure 4.13. Tensile strength of samples

Primary hand and total hand value

The PHV and THV of the three samples were measured by using koshi, fukurami, shari, hari and numeri as listed in Table 4.3. The samples were evaluated for both winter and summer men's dress shirts. The results showed that RF 1 has the highest stiffness followed by RF 3 and RF 2. This may be attributed to the high shearing, bending and compression properties. These largely influence the springiness and stiffness of any given fabric (Sun and Stylios, 2006). Overall, the samples have adequate stiffness for men's winter dress shirts even though the PHV and THV of RF 2 were less than average. The values of all three samples for crispness are negative hence there is no crisp feeling. The subsequent results are positive for fullness, softness and anti-drape stiffness all of the samples. RF 3 has the highest fullness and softness value and RF 1 with the highest crispness, hence there is a crisp feeling. Thus, THV showed all three samples are good for men's winter dress shirts, with RF 3 showing the highest THV, followed closely by RF 1 and RF2. These textiles are however not suitable for men's summer dress shirts since the THV values are all negatives.

Table 4.3. Primary and total hand values of samples

Properties	Primary 1	hand value	
-	RF 1	RF 2	RF 3
Men's dress shirt (winter)			
Koshi	7.68	4.98	6.33
Shari	-0.37	-2.05	-0.83
Fukurami	13.40	13.39	13.99
Hari	5.07	3.85	4.81
Total hand value (THV)	7.76	7.15	7.98
Men's dress shirt (summer)			
Koshi	7.68	4.98	6.33
Shari	-0.37	-2.05	-0.83
Fukurami	13.40	13.39	13.99
Hari	5.07	3.85	4.81
Total hand value (THV)	-1.70	-1.38	-1.76
Women's thin dress fabric (winter)			
Koshi	8.00	6.65	6.56
Numeri	6.09	4.62	5.80
Fukurami	9.83	8.57	9.19
Total hand value (THV)	3.17	3.47	4.00
Women's thin dress fabric (summer)			
Koshi	8.00	6.65	6.56
Numeri	6.09	4.62	5.80
Fukurami	9.83	8.57	9.19

Total hand value (THV) -1.53 0.46 0.20

Hand value (HV); 1 - weak to 10 - strong

Total hand value (THV); 1 – poor to 5 – excellent

The three samples were also evaluated for thin dresses for both the winter and summer, with the results showing that RF 1 has the highest stiffness, smoothness and fullness and softness followed by RF 3 and RF 2. Thus, all three samples have a positive THV for all of the samples with RF 3 having the highest value. Hence, RF 3 is suitable for thin winter dresses. For the summer, however, the THV values show negative values for RF 1 and positive values for RF 2 and RF 3 even though they are given a poor rating for use. From the THV values, RF 1, RF 2 and RF 3 fabrics are suitable for both men's winter dress shirts and women's winter thin dresses. Subsequent results show that RF 2 and RF 3 are suitable for women's thin dress for summer.

4.2.4 Summary

Reflective textiles in this study are prepared using reflective yarns and polyester yarns via jacquard weaving where patterns are sourced from Africa (specifically from the Sirigu wall paintings). Three reflective woven textile samples are evaluated based on standard testing procedures. The design process utilises different weave combinations and colours on the reflective woven textiles, influencing the physical and mechanical properties. Subsequent testing procedures show variations in the fabrics' low-stress mechanical properties, air permeability, thermal conductivity, tensile strength, and THV. Results of the total hand value using the KES-FB system show that on average, the woven textiles with positive values are suitable for men's dress shirts and women's thin dresses for the winter. Overall, RF 2 and RF 3 showed good total hand value (THV) with average values of 2.425 and 2.605 respectively.

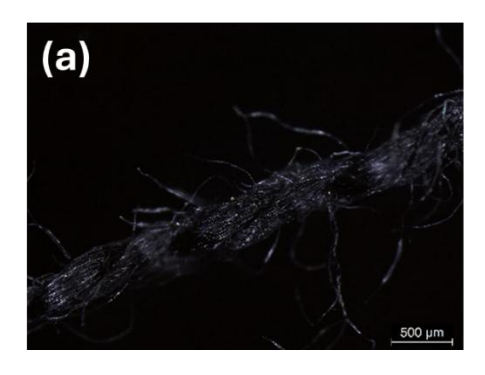
4.3 Development of retro-reflective textiles via dobby loom

This section presents the manufacturing and properties of retro-reflective woven fabrics produced using natural and retro-reflective yarns. Retro-reflective materials have gained progressive growth in usage and sale on the global market from the current \$3.6b to \$8.6b for five years (2021 - 2026) (Research and Markets, 2021). This is largely due to its wide application for protective and visible clothing in construction and other sectors. Retro-reflective materials come in different forms like paints, reflective yarns and transfer reflective tapes. Research studies have explored these materials in a design approach to produce textiles with aesthetic values. For example, Nualdaisri (2022) adopted reflective yarns to improve the aesthetic values of the traditional Thai Silk fabrics, Önlü and Yaşar (2011) and Önlü and Halaçeli (2012b) previously used reflective yarns for woven fabrics with shimmering and brighter effects reflecting light back to its source at night. Despite research in producing retro-reflective textiles for aesthetic values, further evaluation of their performance has not been done to give their functional ability for clothing.

As such, this section aims to produce RR fabrics combined with natural yarns. Additionally, with the application of these fabrics aimed at clothing, further evaluation to understand their reflective effects, low-stress mechanical properties, air permeability, thermal comfort, and total hand value (THV) were investigated.

4.3.1 Methodology

Materials: All the woven fabric samples used in the experimental works were produced using a combination of two types of yarns; 100% 40s/2 Cotton, and 150D/2 Reflective yarns with 0.12mm thickness and 22.348NE (Dongguan Cheng Wei Reflective Material Co., Ltd). The choice of these yarns is due to their inherent properties that makes it suitable to produce the fabric samples. The 100% 40s/2 black Cotton yarns used for the warp was already processed from the factory, hence no need for any pre-treatments. The strength of the yarns was sufficient for the weaving on the dobby loom. As shown in Figure 4.141, the surface structure of the yarns was observed using the Leica M165C microscope under different magnifications. The cotton yarn in Figure 4.14(a) is made of two single yarns twisted in opposite directions with an S-twist. The reflective thread however in Figure 4.14(b) consists of three items; two single polyester yarns and the reflective core containing the glass beads. The polyester yarns (either in black or white) are wrapped around in opposite directions on the reflective core.



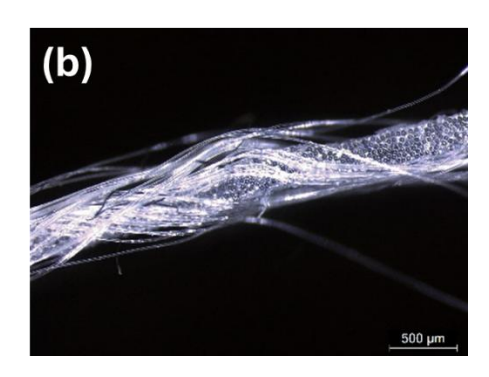


Figure 4.14. Microscopic images of the yarn structures under 500 µm magnification, (a) 100% 40s/2 Cotton; and (b)120D/2 Reflective yarns.

Reflective yarns are special types of yarns made of different thicknesses from polyester which have glass beads on its surface to retro-reflect any light incident on it, making it visible at night. Cotton is a natural fibre processed into yarns with physical and chemical properties such as easy to dye, very absorbent, good air permeability, handle that ensures comfort to wear (Akankwasa et al., 2014, Garze-Bown, 2021), generally creamywhite, white or yellowish-white, moderately strong, affected by strong acids, microorganisms, and insects (Islam, 2013). These cotton yarns inherent with such properties are used or blended with other yarn types to produce fabrics for different applications.

Weave design: Three weave patterns as shown in Figure 4.15 were constructed using the Sedit software compatible with the Rapier Sample loom from CCI / SL7900 which uses the Dobby shedding motion. Still utilising the same weave patterns, a one-yarn picking pattern using a retro-reflective (RR) yarn, results in a fabric with one yarn type in the weft yarns.

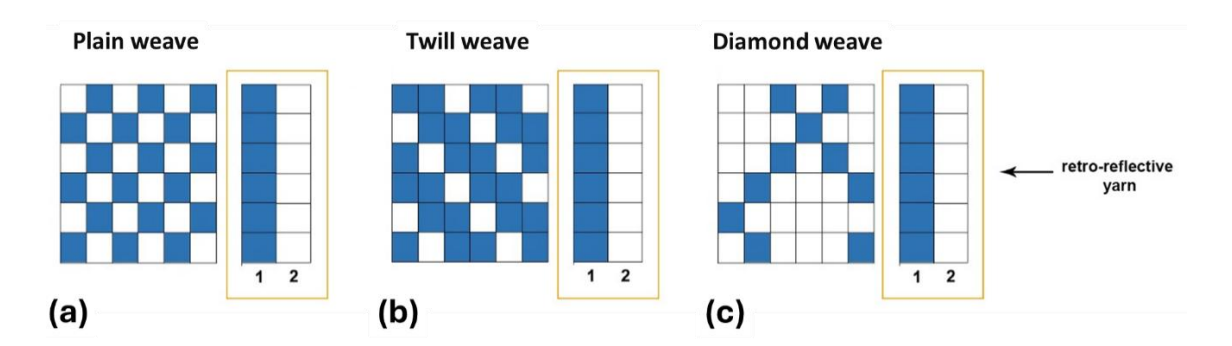


Figure 4.15. Plan for weave design, (a) plain weave (RF1), (b) twill weave (RF2), and (c) diamond weave (RF3), for one yarn picking pattern.

Note: RF means reflective fabric

Woven fabric samples: Three (3) woven samples were produced using the yarns on the Rapier Sample loom from CCI / SL7900 which uses the Dobby shedding motion. Table 4.4 provides the specifications of the woven fabrics. The appearance of the fabrics is shown in Figure 4.16 as captured under a microscope.

Table 4.4. Specification of the woven fabrics

Fabrics	Composition	Weave	Fabric setting	
			Ends/inch	Picks/inch
RF1	Reflective thread (50% polyester /	Plain	77	38
RF2	50% reflective material)	S-twill	77	38
RF3	100% Cotton	Diamond	77	38

4.3.2 Experimental and Characterisation

The structure morphology of the fabrics was observed under an optical microscope (Leica M165 C) at a magnification of 500 µm and 1 mm. The fabric weight and thickness were measured by using an electronic balance (BX300, Shimadzu Corp.) and a digital thickness gauge with a fixed pressure of 4 g/cm² respectively. Five specimens of each of the three fabric samples were measured for their weight and thickness following the testing method in ASTM D3776 and ASTM D1777-96 respectively. The average values of these five specimens were calculated and recorded accordingly. The low-stress mechanical properties of the fabrics were evaluated by using the Kawabata Evaluation System of Fabric (KES-F) testing instruments (Kato Giken Co., Ltd. Japan), i.e., tensile and shear tester (KES-FB1), pure bending tester (KES-FB2), compression tester (KES-FB3) and surface tester (KES-FB4). The testing of the fabrics was done by measuring and cutting them into standard dimensions of 20 x 20 cm. They were then conditioned under standard atmospheric air and humidity conditions. The air permeability of the fabrics was measured by using an air permeability tester (KES F8 AP1; Kato Giken Co., Ltd. Japan), to record the resistance R in kPa•s/m in accordance with ASTM D737-04. The air permeability test was repeated five times for each fabric, with their average values calculated and recorded.

The thermal conductivity was evaluated by using the KES FB7 Thermo Labo Tester (Kato Giken Co., Ltd. Japan) with the dry contact method. Testing was repeated five times for each fabric, with their average values calculated and recorded. The primary hand value (PHV) and total hand value (THV) of the three samples were measured in accordance with the Kawabata Evaluation System for Fabrics (KES FB). The mechanical

stress properties of the fabrics were calculated to obtain tactile comfort from the total hand value (Kawabata and Niwa, 1975).

4.3.3 Results and Discussion

This section provides the test results of the woven fabric samples.

Reflective effects

The woven samples produced with retro-reflective yarns were examined in daylight and dark room conditions. Images were taken from a distance of 1.5 meters using a digital camera to identify the retro-reflectivity of the woven samples, which are shown in Figure 4.16. results revealed that, the reflective effects are high on a diamond weave structure (Figure 4.16(b) B-3), followed by plain and twill weave structures shown in Figure 4.16(b) B-1 and Figure 4.16(b) B-2 respectively. Such high reflective effects are attributed to the long floats which exposed large surfaces of the reflective yarns (for diamond weave).

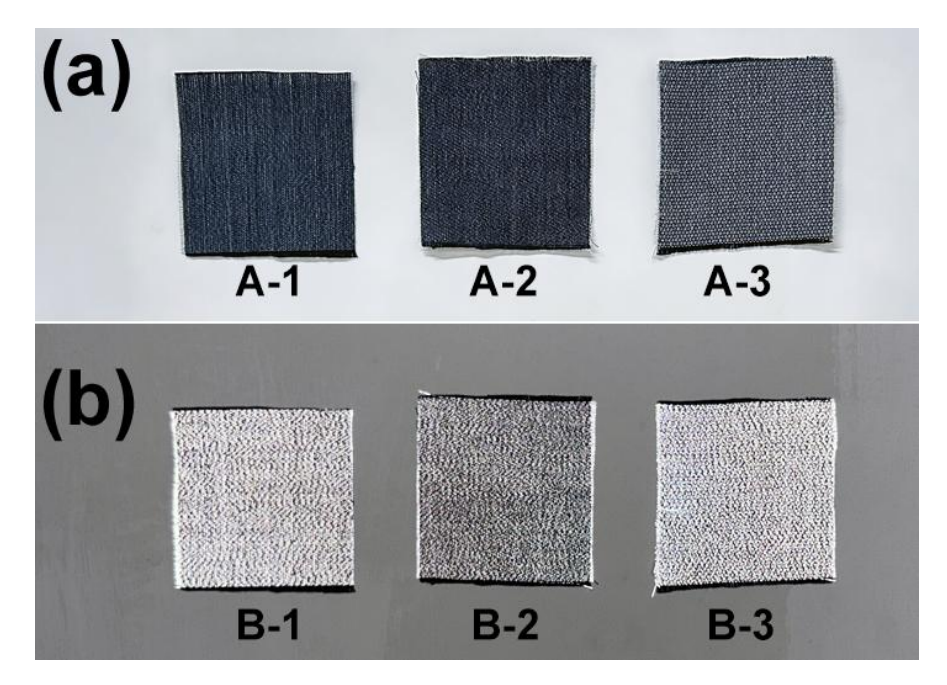


Figure 4.16. (a) Original appearance of the woven textiles with plain weave (A-1), twill weave (A-2), and diamond weave (A-3); (b) reflective effects of woven textiles with plain weave (B-1), twill weave (B-2), and diamond weave (B-3)

Structure morphology

The surface structure of the fabric samples was observed under a magnification scale of 1 mm (Figure 4.17). The images in Figure 3 show that the RR yarns are wrapped

with small glass beads that have the retro-reflective ability to bounce light back in the same path without scattering. Subsequently, the images show the weave structure and yarn arrangement that are used to form the fabric samples. The microscopic images further show more of the weft yarns in the fabric for diamond woven structures followed by plain and twill woven structures.

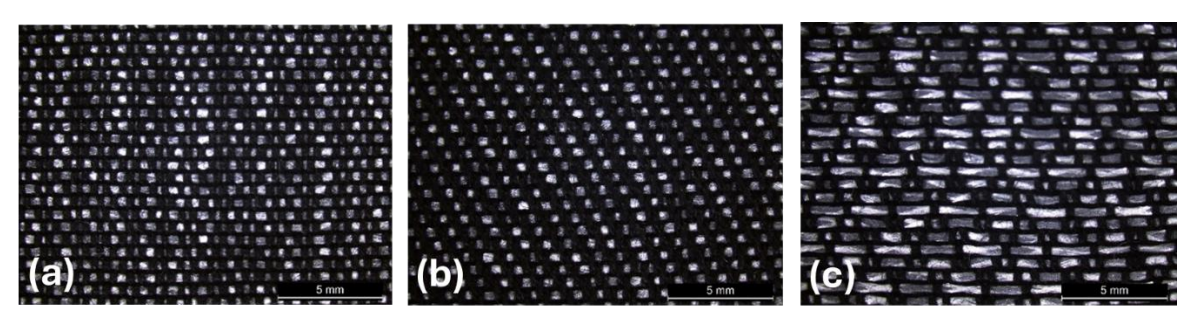


Figure 4.17. Microscopic images of the structural appearance of woven fabric samples (a) RF1 - plain weave, (b) RF2 - twill weave, (c) RF3 - diamond weave.

Fabric weight and thickness

The results in Table 4.5 indicate that RF1 is the heaviest as compared to RF2 with the lowest weight. This weight difference is due to the type and thickness or count of yarns used to produce the fabrics. RR yarns with a count of 22.348 in the weft influence the eventual weight of fabrics. With the same fabric setting parameters, the weave structures further influence the fabric weight and thickness. The results show that RF3 with a diamond weave was thicker than the other fabric samples at a pressure load of 4 g/cm². This is confirmed by Asayesh et al. (2018) that the weave structure of a woven fabric affects the fabric thickness at different levels of induced pressure.

Table 4.5. Fabric weight and thickness of the woven fabrics

Fabrics	Composition	Weave	Fabric weight (GSM)	Thickness* (mm)
RF1	Reflective thread (50% polyester / 50% reflective	Plain	238.45	0.50
RF2	material) 100% Cotton	S-twill	224.50	0.58
RF3		Diamond	225.55	0.70

Note. *Fabric thickness with 4 g/cm² of exerted pressure

Low-stress mechanical property

Bending property

The bending properties demonstrate the ability of a fabric to bend or its stiffness and recovery from bending. It is largely influenced by factors like the thickness and density of the yarn used in the construction of the fabric (Süle, 2012) and the friction between the fibers or yarns in the structure of the fabric (Yadav et al., 2006). The bending properties of the three woven fabric samples were determined by measuring the bending rigidity (B) and bending moment (2HB). B measures the amount of stiffness or ability of the fabric to resist bending with fabric handling. Higher B values indicate the ability of the fabric to resist bending. In Figure 4.18(a), RF1 has high B values hence the ability to resist bending in both warp-wise and weft-wise directions as compared to RF3 which has the lowest B value. Furthermore, the arithmetic mean showed that RF1 has the highest B values of 1.594 gf.cm²/cm, hence the ability to resist bending as compared to the others. It is interesting that these fabrics have inherently different weave structures and types of yarn in their construction even though they are all woven with cotton in the warp. This property according to Avinc et al. (2010) is attributed to the relationship between the inter-yarn and inter-fiber forces in the fabric structure.

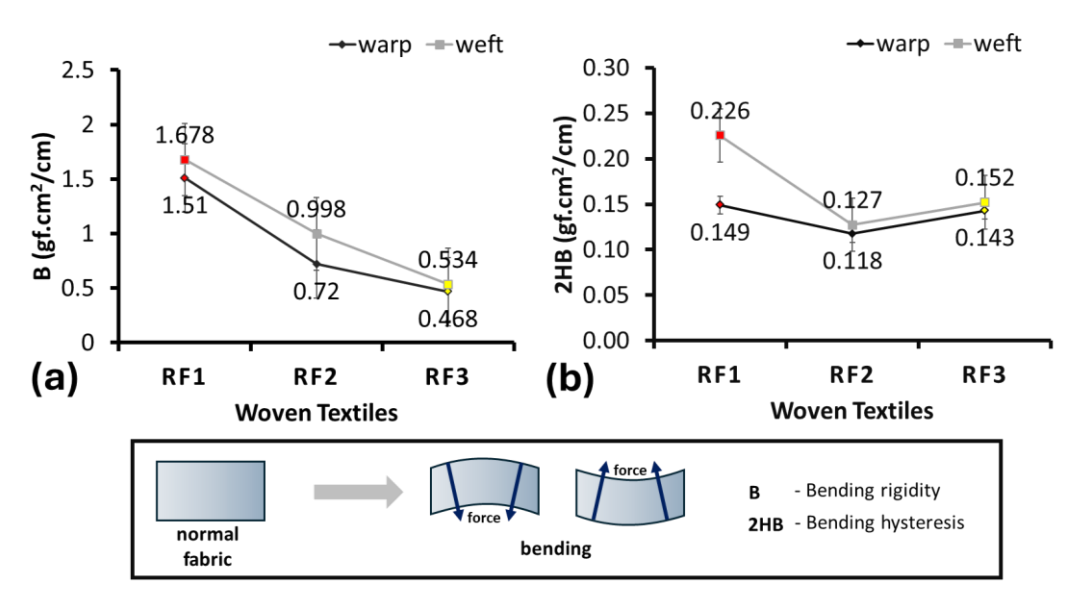


Figure 4.18. (a) Bending rigidity and (b) bending hysteresis of the fabric samples

With 2HB, it measures the recovery ability of fabric after bending. Lower 2HB values denote good recovery ability. The results in Figure 4.18(b) show that RF2 has the lowest 2HB values in both the warp-wise and weft-wise directions, hence better recovery ability after bending as compared to RF1 and RF3 (highest 2HB value). Subsequently, the

arithmetic mean of the 2HB values indicates that RF2 has the lowest 2HB values of 0.123 gf.cm²/cm, as compared to RF1 (highest 2HB value). This implies that overall, RF2 with a twill weave structure has good recovery ability after being subjected to bending, as compared to RF1 with a plain weave structure which has poor recovery ability. The practical implications illustrate that the use of only retro-reflective yarns in the weft gives the fabric samples the ability to resist bending at handling and relatively poor recovery when eventually bent.

Compression properties

The compression properties are determined by measuring the compressional linearity (LC), compressional energy (WC), and compressional resilience (RC) of fabrics. Additionally, the thickness of the fabric samples is measured at exerted pressures of 0.5 gf/cm² and 50 gf/cm² for T_o and T_m respectively. Figures 4.19(a), 4.19(b) and 4.19(c) are the various values that show the compression properties of the fabric samples. The LC indicates the feel of the fabric; hence a higher LC value denotes a hard feel after compression. The WC exemplifies the fluffy feeling of a fabric where a higher WC value means higher compressibility. Figure 4.19(a) shows that RF3 has the highest LC and WC value, meaning it has the hardest feel among all the other fabrics. Their hard feel might be attributed to the diamond weave structure. Additionally, the diamond weave structures have a fluffy feel, so they require a higher compression as compared to fabrics constructed of plain and twill weave structures.

The RC defines the ability of a fabric to recover back to its original shape after compression. As such, higher RC values denote good recoverability of fabric after the applied compression force is removed. RF3 have higher RC values as shown in Figure 4.19(b), hence they have a good recovery ability after compression. This implies that fabrics made of diamond weave structures may require high levels of compression but can easily revert to their original shape afterward. Furthermore, Figure 4.19(c) shows that, the thickness of the fabric samples with different compression pressures. At pressure To, RF3 is the thickest which might be attributed to the fabric structure i.e., floats in the diamond weave structure. Similar results can be observed when the fabrics are subjected to high pressure at Tm. This affirms the findings in Sirkova (2012) that the thickness of the fabric is dependent on the weave structure along with long floats and the yarn parameters.

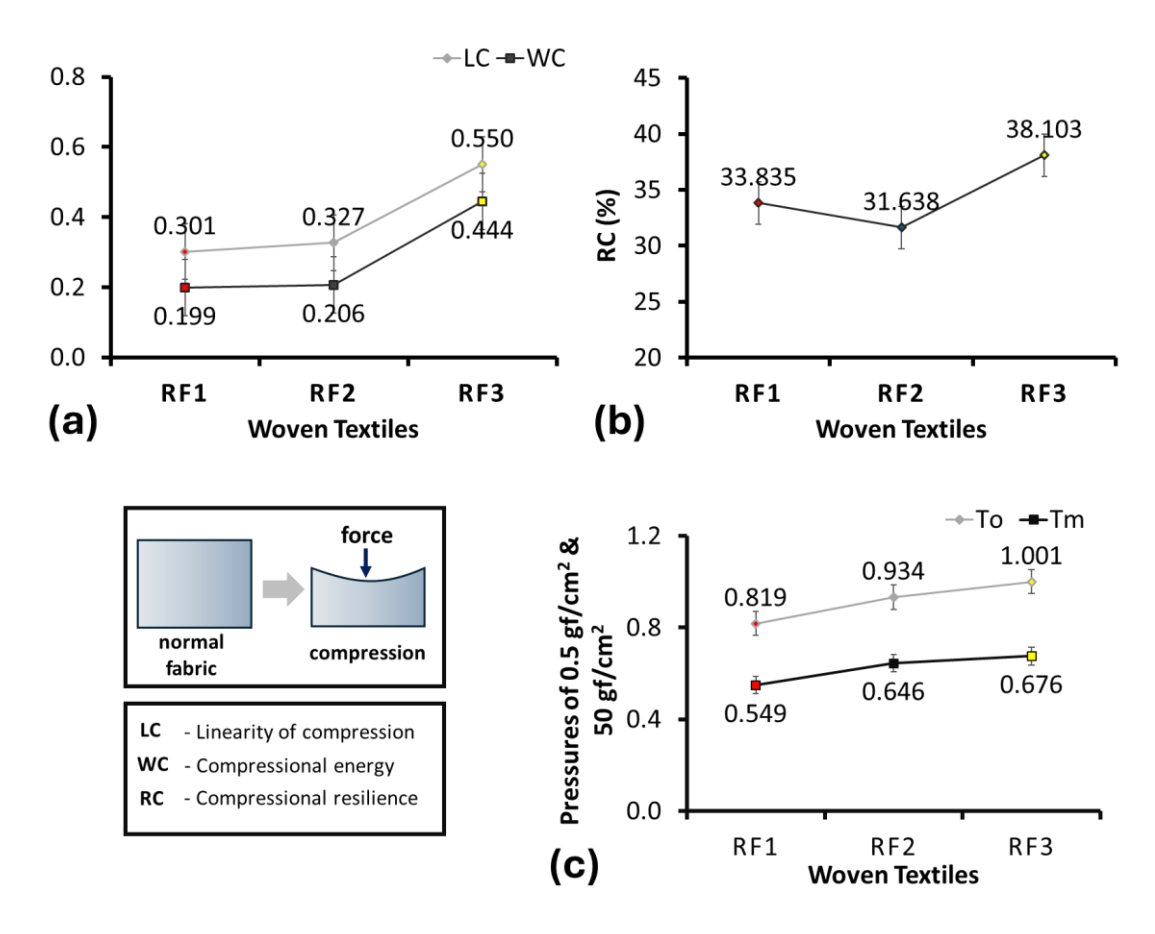


Figure 4.19. (a) Compressional linearity and compressional energy of the fabric samples, (b) compressional resilience of the fabric samples and (c) thickness values of the fabric samples at pressures $0.5 \text{ gf/cm}^2(T_o)$ and $50 \text{ gf/cm}^2(T_m)$

Surface properties

The surface properties of the fabric samples were determined by measuring the mean value of the coefficient of friction (MIU), mean deviation of MIU (MMD), and fabric surface roughness (SMD) as shown in Figures 4.20(a), 4.20(b) and 4.20(c) respectively. In terms of the MIU values (Figure 4.20(a)) in the warp-wise direction, RF1 has a higher value, so the sample has a higher frictional force and hence less tendency to slip. In the weft-wise direction, RF2 has the highest MIU value as compared to the other fabrics. The subsequent arithmetic mean MIU values show that RF1 (with a plain weave structure) has the highest MIU values followed by RF2 and RF3 with twill and diamond weave structures respectively. Hence, they can resist movement when rubbed between the fingers due to their good frictional force. To determine the roughness of the surface of a fabric, higher MMD values indicate higher surface roughness. As shown in Figure 4.20(b), RF3 has the highest MMD values in both warp-wise and weft-wise directions. The overall arithmetic mean MMD values suggest that RF3 has the highest MMD values, hence high surface

roughness. This may be attributed to the weave construction i.e., the diamond weave structure in the samples where the RR yarns on the surface of the fabric are exposed. Additionally, these RR yarns with embedded glass beads might contribute to the roughness of the fabric surface.

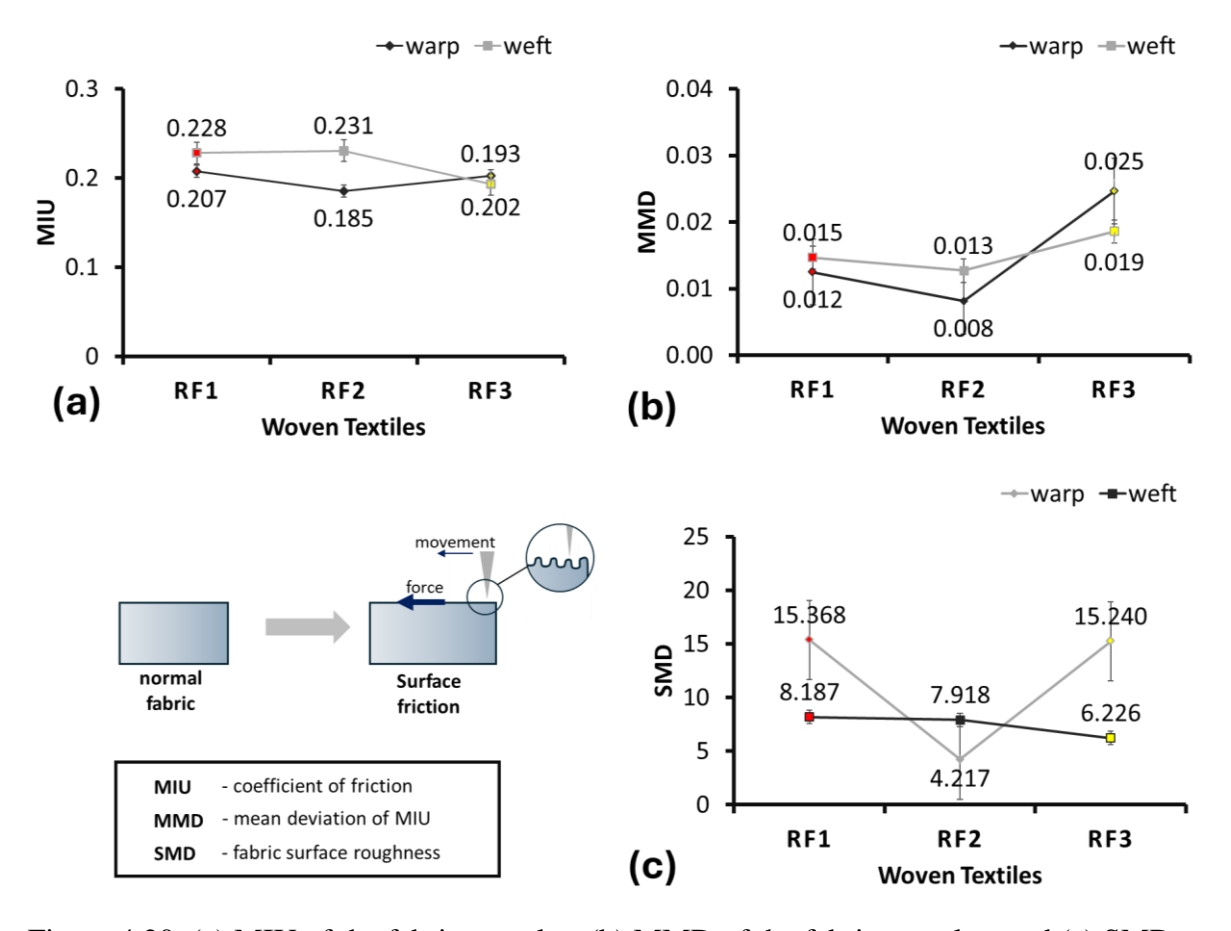


Figure 4.20. (a) MIU of the fabric samples, (b) MMD of the fabric samples, and (c) SMD of the fabric samples

The SMD values that are shown in Figure 4.20(c) reflect the evenness of the surface of the samples. With similar ranges of SMD values, RF1 and RF3 have the highest SMD values which indicate the unevenness of their surface in the warp-wise direction. RF1 has the highest SMD values as compared to the other fabric samples in the weft-wise direction. The overall arithmetic mean SMD values reveal that RF1 has the highest SMD value, which implies that its surface is very uneven. This might be attributed to its plain weave structure hence creating surface imperfection where the surface structure of the RR yarn with the glass beads may have been a contributing factor. As such, the next highest SMD mean values belong to RF3 with a diamond weave structure and different yarn composition in the weft. The structure of these fabrics further shows the yarn surfaces that may have been attributed to the unevenness.

Shearing properties

The shearing properties influence the hand behaviour, pliability, stiffness, and drapability of the samples in all directions (Hari, 2012, Kan and Lam, 2013). The shear rigidity (G) and shear hysteresis (2HG) values indicate the ability of the fabric to recover after shear deformation. This shear behaviour according to Hari (2012) contributes to the fabric's appearance and performance. Figures 4.21(a) and 4.21(b) show the G and 2HG values respectively for the fabric samples. The shear rigidity (G) indicates the sliding of the fibers against each other which influences the ability of the fabric to resist shear stress. Therefore, lower G values mean the ability of a fabric to shear is increased, hence a good drapability and better handle. The results for Figure 4.21(a) show that RF3 has the lowest G values in both the warp-wise and weft-wise directions. This implies that RF3 has a good drape ability since the fibers can easily slide against each other. Subsequently, the arithmetic mean values of G show that RF3 (0.501 gf/cm.°) with a diamond weave structure have the lowest G values which means the fabrics have better drape ability as compared to RF1 (1.594 gf/cm.°) and RF2 (0.859 gf/cm.°) with a plain and twill weaves which have poor drapability. This further implies that the weave structure in a fabric limits the ability of the fibers to slide against each other during shear deformation.

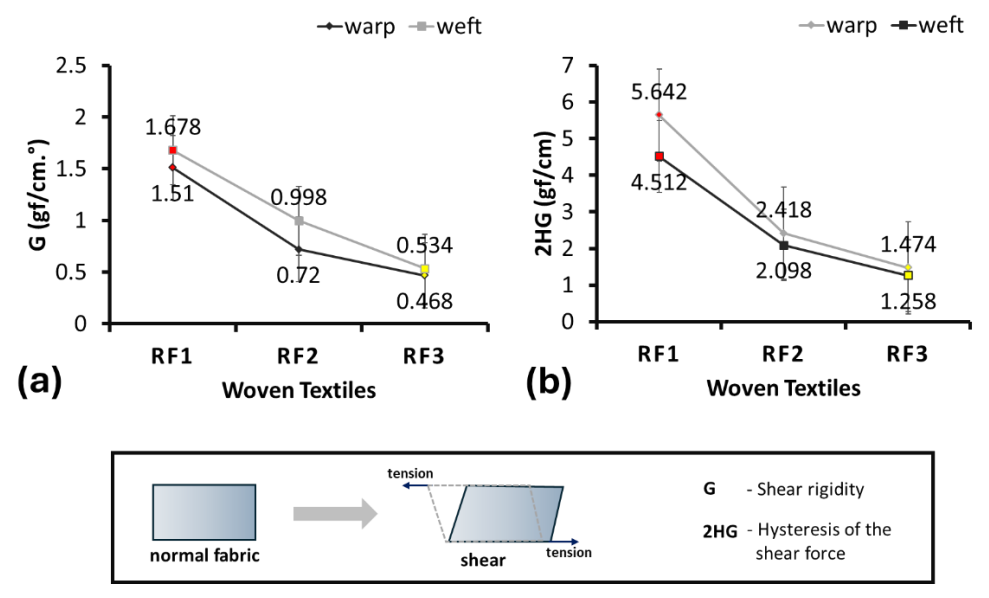


Figure 4.21. (a) Shear rigidity of the fabric samples and (b) shear hysteresis of the fabric samples

The 2HG shows the ability of a fabric to recover effectively after applying shear stress onto the fabric at an angle of 0.5°. A lower 2HG value means that the fabric has good recoverability while a higher 2HG value means poor recoverability. In Figure 4.21(b), RF1

has the highest 2HG value and RF3 has the lowest 2HG value in both the warp-wise and weft-wise directions. Hence, RF1 with a plain weave structure has poor recoverability. Subsequently, the arithmetic mean 2HG values show that RF1 (5.077 g/cm) has higher shear hysteresis as compared to RF3 (1.366 g/cm) with lower 2HG values. This means that RF1 with a plain weave structure is stiffer with poor recoverability after shearing as compared to RF3 which has good recoverability after shearing.

Tensile properties

The stretchability or extensibility of fabrics after tensile testing was measured by examining tensile resilience (RT), tensile energy (WT), tensile linearity (LT), and extensibility (EMT). As shown in Table 4.6, RF1 has the highest LT, WT, and EMT values in the warp direction and RF3 has higher RT values in the warp-wise direction. The arithmetic mean values show that RF1 has the highest LT values which means that they are more robust and harder than the other fabrics. Subsequently, RF1 which has the highest WT value (9.77 gf.cm/cm²) can easily stretch and withstand external stress during extension as compared to the other fabrics. RF2 has the highest RT value (57.191%) and hence has good recoverability after being subjected to tensile stress. RF3 has good extensibility or elongation since it has the highest EMT value (4.639%).

Table 4.6. Tensile properties of samples

Samples	Direction	Tensile pro			
		LT	LT WT		EMT
			(gf.cm/cm ²)	%	(%)
RF1	warp	0.9182*	16.24*	33.822	7.056*
	weft	0.931^{*}	3.3	73.45	1.42
RF2	warp	0.7788	13.75	37.236	7.046
	weft	0.926	3.63	77.146^*	1.568
RF3	warp	0.6894	8.87	43.554*	5.144
	weft	0.8184	5.25*	62.748	2.566^{*}

^(*) denotes higher values in warp-wise and weft-wise directions.

Air permeability

The air permeability of fabric measures the rate of airflow as it passes through the inherent structure or weave (Mishra et al., 2019, Saville, 1999). It is an imperative property influenced by factors such as the openness or pore size, density, and thickness of the fabric that influence the thermal comfort and transport of moisture or water vapour of a fabric

(Mishra et al., 2019, Roy Choudhury et al., 2011). The results from Figure 4.22 show that RF3 has the lowest R values as compared to RF1 with the highest R-value. This shows that RF3 with low R (kPa·s/m) values are permeable to air or more breathable than other fabrics. Even though these fabrics were made with the same fabric settings, their differential R values could be influenced by the weave structure and the type(s) of yarn used for the weft. Evidently, RF1 with a plain structure has a small pore size or small openings as compared to RF3 with the diamond weave. This may be attributed to the weft yarn float or interlacing of the yarns in the fabric, where the diamond weave yarn floats are visible in comparison to the twill and plain weave structures. This shows that the air permeability of fabric is affected by the fabric or design structure, that is, the yarn twist (Ogulata, 2006, Zupin et al., 2012, Angelova, 2012).

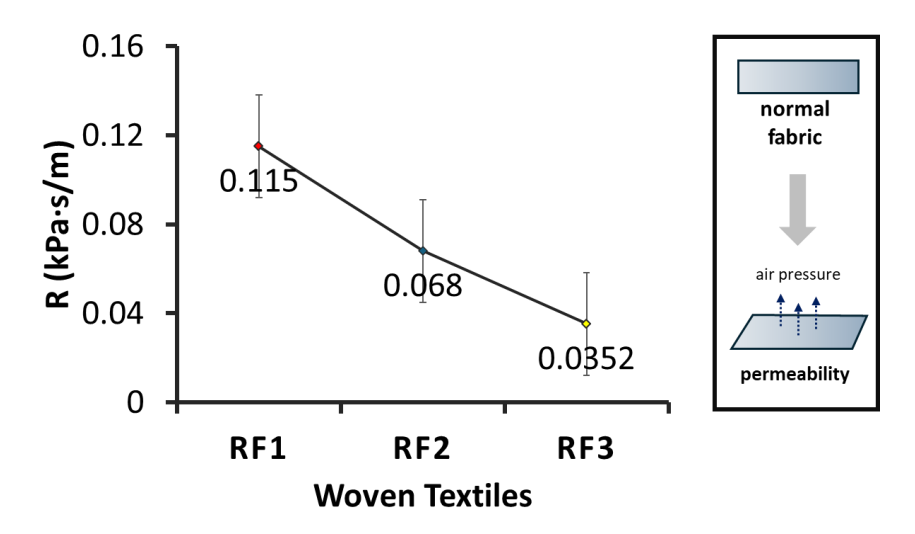


Figure 4.22. Air permeability of the fabric samples

Thermal conductivity

Thermal conductivity is an important fabric property that determines heat loss and transfers heat from the body to the environment (Siddiqui and Sun, 2018). Thermal conductivity directly influences wear comfort by maintaining a normal body temperature (Starr et al., 2015). Therefore, thermal conductivity was measured to obtain the necessary k values of the fabric samples. In Figure 4.23, RF1 has the highest k value which implies this sample with a plain weave structure but different yarn composition can readily transfer heat from the human body to the outside environment hence maintaining wear comfort. It is interesting to note that, following the plain woven fabrics in thermal conductivity value are RF2 with twill woven fabrics with the second highest k values as compared to RF3 with a diamond weave structure. This implies that plain woven fabrics have higher thermal

conductivity followed by twill and diamond woven fabrics. This supports the findings of Musa et al. (2021) in that the thermal conductivity of any fabric is influenced by the structure of the fabric.

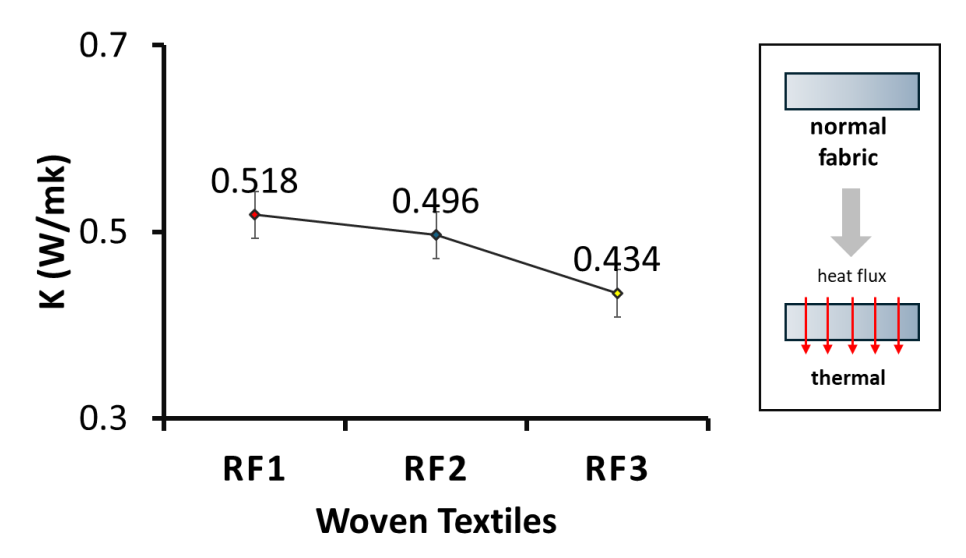


Figure 4.23. Thermal conductivity of the fabric samples

Total hand value

The three fabric samples were evaluated for the primary hand and total hand values by using the Kawabata system: koshi, shari, fukurami, hari and numeri as shown in Table 4.7. The samples were evaluated for both men's dress shirts (winter and summer) and thinner dresses for women (winter and summer). For example, the calculated primary hand value shows that RF1 has the highest shari (crispness) and highest koshi (stiffness) value in men's dress shirts as compared to the other fabrics. This is attributed to the high bending and shearing properties that influence the stiffness of any given fabric (Sun and Stylios, 2006). Subsequently, the total hand values for the fabrics showed that they are suitable for men's winter dress shirts and women's thin dresses. When evaluated for summer wear, that is, both men's dress shirts and women's thin dresses, the poor THV showed negative and positive values respectively. This implies that the fabrics are not suitable for both men's dress shirts and women's thin dresses in the summer.

In calculating the overall THV of the three fabrics by averaging their respective THVs, RF1 and RF2 showed good overall total hand value (THV) with average values of 3.0275 and 3.2 respectively.

Table 4.7. Primary and total hand values of samples

Properties	Primary hand value		
-	RF1	RF2	RF3
Men's dress shirt (winter)			
Koshi	7.55	6.45	5.83
Shari	3.46	2.68	2.87
Fukurami	12.08	12.33	13.63
Hari	6.74	5.62	4.71
Total hand value (THV)	7.01	6.95	7.60
Men's dress shirt (summer)			
Koshi	7.55	6.45	5.83
Shari	3.46	2.68	2.87
Fukurami	12.08	12.33	13.63
Hari	6.74	5.62	4.71
Total hand value (THV)	-0.49	-0.40	-0.78
Women's thin dress fabric (winter)			
Koshi	6.54	6.42	6.42
Numeri	6.83	8.22	6.85
Fukurami	9.08	10.18	9.38
Total hand value (THV)	4.39	5.48	4.52
Women's thin dress fabric (summer)			
Koshi	6.54	6.42	6.42
Numeri	6.83	8.22	6.85
Fukurami	9.08	10.18	9.38
Total hand value (THV)	1.20	0.77	0.75
Vashi (stiffeess) Name of (small through)	01 ' /		Enland

Koshi (stiffness), Numeri (smoothness), Shari (crispness), Fukurami (fullness and softness), Hari (anti-drape stiffness).

Hand value (HV); 1 - weak to 10 - strong

Total hand value (THV); 1 – poor to 5 – excellent

4.3.4 Summary

In this study, retro-reflective woven fabrics are produced to evaluate their reflective effects, mechanical and functional performances for thermal comfort and breathability. This is imperative due to the utilization of these woven fabrics for clothing which will come in contact with the body, hence understanding other properties is needed. Results from the visual evaluation show the reflective properties of plain and diamond weave structures are higher than that of the 2/2 twill weave. This may be attributed to the exposure of the black warp yarns on the surface of the fabric. The results for the three fabric samples indicate that they have good breathability and thermal comfort with all of the samples having an R (kPa·s/m) value less than 0.15 and 0.53 W/mk respectively. These coupled

with the good low-stress mechanical properties reveal their suitability for men's dress shirts and women's thin dresses in the winter. Overall, RF1 and RF2 showed good total hand value (THV) with average values of 3.0275 and 3.2 respectively. To conclude, the produced retro-reflective woven fabrics have good mechanical and functional performances and are suitable for design treatments on their surfaces.

4.4 Retro-reflective textiles treated with laser engraving

In this section, the three woven fabrics (RF1, RF2, and RF3) produced from the dobby loom were treated with laser to create design patterns on their surfaces. The use of laser treatment i.e. laser engraving most especially CO₂ lasers, provides creative opportunities to produce patterns directly on a fabric structure without further pollution to the environment (Dascalu et al., 2000a) as compared to other textile treatment methods. The eventual engraved fabric samples were investigated or evaluated for their surface morphology, Scanning Electron Microscope (SEM) images colour appearance, and visual appearance.

4.4.1 Methodology

Materials: Three different weave-structured (plain, twill, and diamond) fabric blends as explained in Section 4.3, were produced on a Dobby Rapier Sample Loom (CCI/SL7900) with a speed of 25 rpm and a weft density of 38 ends per inch. Two different yarn types were used; a 150D/2 silver-coloured reflective thread from Dongguan Cheng Wei Reflective Material Co., Ltd in China (which constitutes the weft) and a 40/2s 100% black cotton yarn (used for the warp). The specifications of the woven fabrics are shown in Table 4.8 with FB1 having plain weave, FB2 having twill weave and FB3 having diamond weave structures.

Table 4.8. Specification of fabrics

Fabric	Composition	Weave	Yarn colour
RF1	10001 10/2 7	plain	
RF2	- 100% 40/2s Cotton yarn (warp yarns) 150D/2 Reflective thread (weft yarns)	twill	black (warp) silver (weft)
RF3		diamond	(320)

Technique: The surface treatments on the samples were carried out in both warp and weft directions using a CO₂ laser, Flexi-e V2 from the manufacturer Jeanologia from Spain. The wavelength of the pointer was 670nm, pulse energy of <10mW, and beam diameter focused at ~2.0 mm. The eMark[®] software was used to interconnect the laser system to produce patterns on a surface. These patterns are first designed on Adobe Photoshop[®] 2022 and exported in jpeg format into the eMark[®] interface for the necessary laser parameters settings in resolutions (dpi) and pixel time (μs).

4.4.2 Laser treatments on the samples

The woven fabric blends were treated with varying laser parameters where the pixel time (μ s) was set from 110, 120, 130, 140, 150, and 160, with the resolutions (dpi) set from 30, 40, 50, 60, and 70. The engraving of the samples was carried out in both warpwise and weft-wise directions. Results from Figure 4.24 show the effects after laser engraving parameters were set on the different weave structures. The level of damage or fiber disintegration was evident in 70 dpi from 130 μ s to 160 μ s (for both yarn directions). The effectiveness or performance of the retro-reflective yarns in the fabric structure is destroyed with an increase in both resolutions (dpi) and pixel time (μ s).

Based on the appearance of the laser parameters as shown in Figure 4.24, the experiment process will utilise two parameters (30 dpi/120 μ s and 40 dpi/120 μ s) to understand the appearance of the design patterns when engraved on the surfaces of the three fabrics.

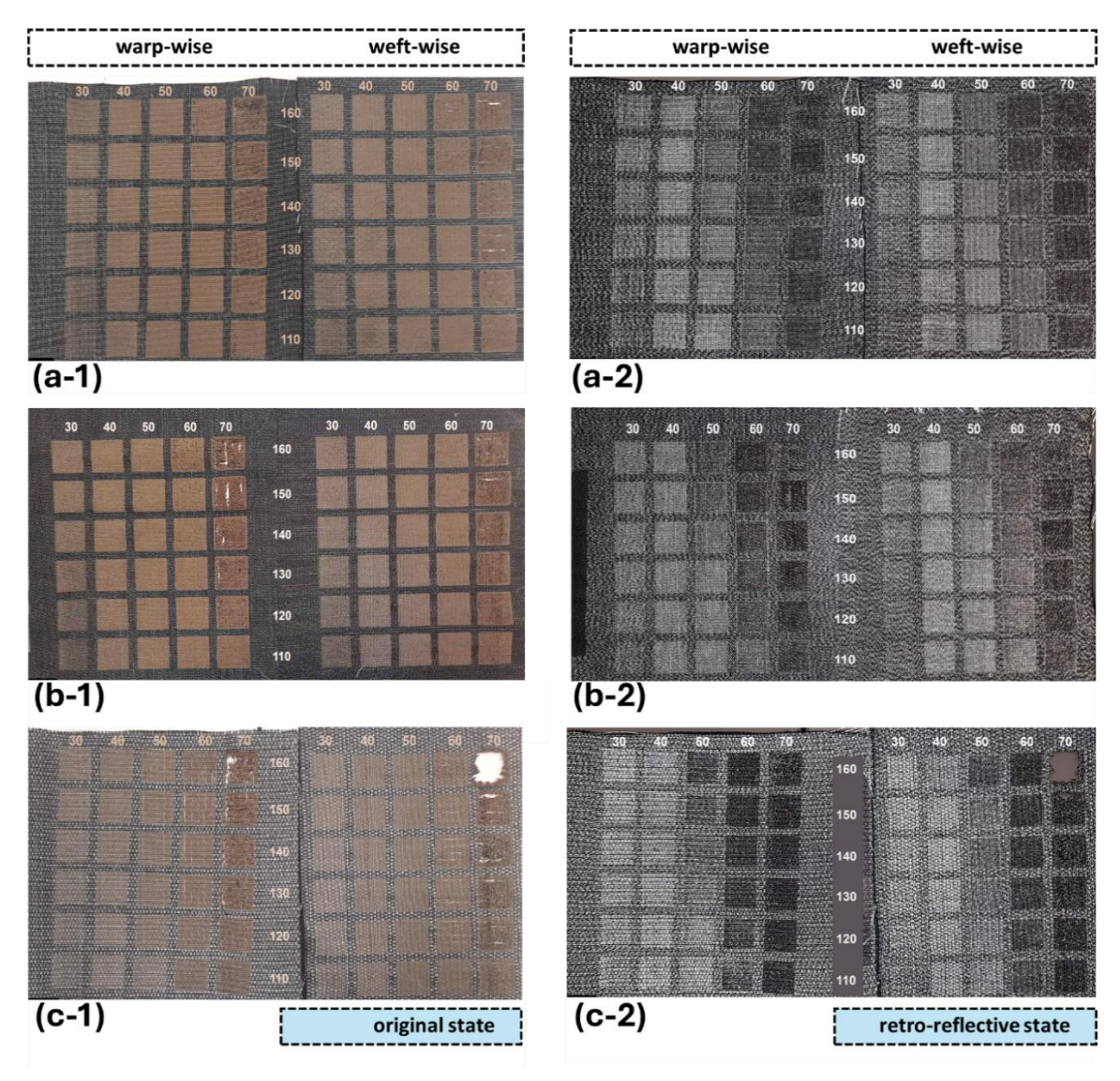


Figure 4.24. Original appearance of (a-1) plain woven fabric (b-1) twill woven fabric and (c-1) diamond woven fabric; Retro-reflective effects or appearance of the laser parameters on (a-2) plain woven fabric (b-2) twill woven fabric and (c-2) diamond woven fabric.

4.4.3 Experimental and Characterisation

The weight and thickness (of the original and laser engraved fabrics) were measured by using an electronic balance (BX300, Shimadzu Corp.) and a digital thickness gauge with a fixed pressure of 4 g/cm² respectively. Five specimens of each of the three fabric samples were measured for their weight and thickness in accordance with the testing method in ASTM D3776 and ASTM D1777-96 respectively. The average values of these five specimens were calculated and recorded accordingly. The structural morphology of the laser-engraved fabrics was observed under different magnification scales (200 µm and 500 µm) using an Optical Microscope (Leica M165 C). Additionally, the surface

morphology of the laser engraved fabrics was observed and analysed using the "Hitachi" Model TM-3000 Tabletop Scanning Electron Microscope. The colour characteristics of the samples both original and laser engraved was determined in CIE Lab values of L*, a*, b*, and C* using the Macbeth Color-Eye 7000a spectrophotometer through the reflectance mode, with D65 illuminant and 10° standard observer.

4.4.4 Results and Discussion

This section provides the test results of the woven fabric samples.

Visual appearance

Results (Figure 4.25(a-1) - 4.25(c-1)) captured for the visual appearance or pattern visibility of the engraved fabrics show that at 30 dpi-110 µs laser parameter, the patterns were more visible in the weft-wise direction for LA-RF1 and LA-RF2 with plain and twill weave structures respectively, a situation which is largely attributed to the yellowish colour observed in the weft-wise directions. Visibility of patterns was however difficult in the LA-RF3 with diamond weave in both yarn directions. With a higher laser parameter of 40 dpi-120 µs, pattern visibility was visible in LA-RF1 and LA-RF2 with plain and twill weave structures respectively for both yarn directions (Figure 4.25(a-2) - 4.25(c-2)). Visibility and clarity of patterns were however difficult in the diamond weave structure in both yarn directions. Overall, details like sharpness, visibility, and clarity of the design pattern or images were evident in the warp-wise directions for LA-RF1 and LA-RF2 with plain and twill weaves respectively.

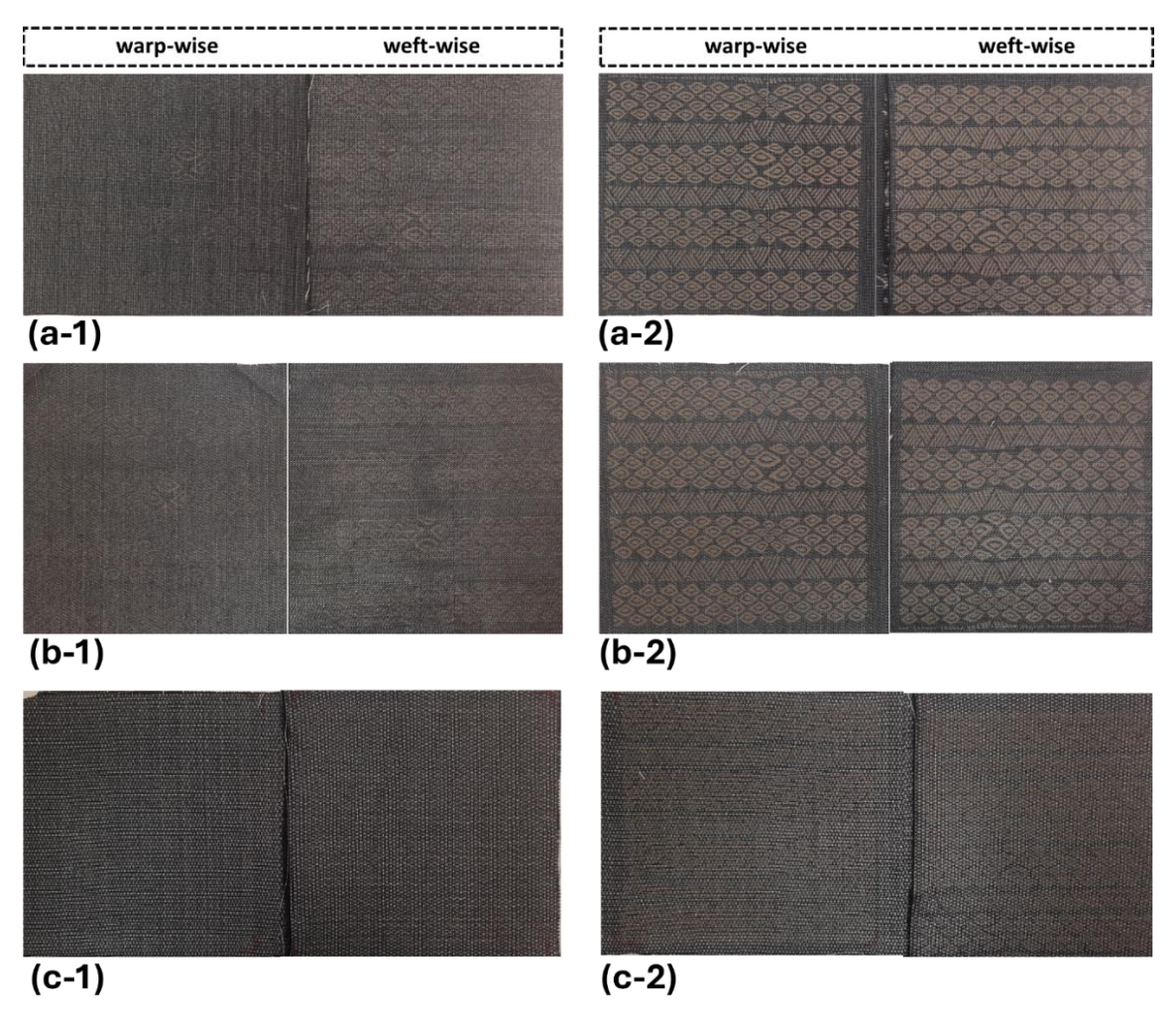


Figure 4.25. The appearance of (a-1) LA-RF1 (with plain weave), (b-1) LA-RF2 (with twill weave) and (c-1) LA-RF3 (with diamond weave) engraved with 30 dpi-110 μs parameters; appearance of (a-2) LA-RF3 (with plain weave), (b-2) LA-RF2 (with twill weave) and (c-2) LA-RF3 (with diamond weave) engraved with 40 dpi-120 μs parameters.

Fabric weight and thickness

The thickness and weight values in millimetre (mm) and grams per square metre (GSM) respectively, of the laser engraved and original fabrics are shown in Table 4.9. Results show that the thickness and weight of the laser-engraved fabrics were reduced as compared to the original fabrics. This confirms that an increase in resolution from 30 dpi to 40 dpi, engraves portions of the fiber surfaces hence a reduction in the fabric thickness. With such inherent feature of laser engraving, the eventual weight of the fabric is also reduced (Yuan et al., 2013b).

Table 4.9. Properties of the original and treated or engraved fabrics

Fabric	Pixel time (μs)	Fabric thickness* (mm)			Weight (GSM)		
		Original	30 dpi	40 dpi	Original	30 dpi	40 dpi
LA-RF1		0.50	0.49	0.46	238.45	220.54	219.77
LA-RF2	120	0.58	0.55	0.54	224.50	220.75	219.36
LA-RF3	-	0.70	0.69	0.65	225.55	218.49	217.02

Note. *Fabric thickness with 4 g/cm² of exerted pressure

Structure morphology

At a magnification scale of 200 μ m and 500 μ m, the optical microscope was used to observe the surface structure of the reflective threads and the laser-engraved portions of the fabrics. Figure 4.26(a) shows that the reflective thread is in two parts, the reflective core inherent with glass beads and a silver-coloured polyester thread wrapped around it. In Figure 4.26(b), the laser beam engraving burns out the structural fiber of the cotton yarn which in fact gives off the yellowish colour shade.



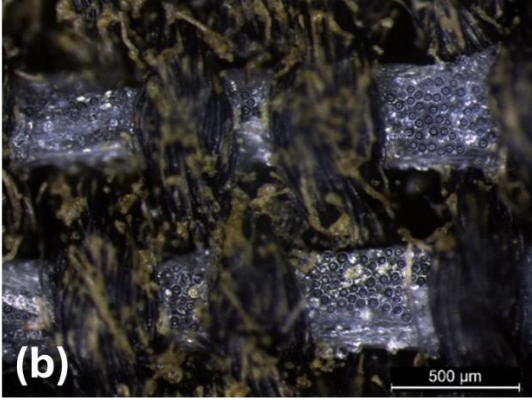


Figure 4.26. (a) Structure of the reflective thread captured under a magnification scale of 200 μ m, (b) burning effect of the laser engraving on the woven structure under a magnification scale of 500 μ m

Subsequently, at a magnification of $500 \, \mu m$, the optical microscope was used to observe the surface structure of the laser-engraved portions of the fabrics. The laser beam engraving burns out the structural fiber of the cotton yarn which in fact gives off the yellowish colour shade. As such, the action of the laser beam burns on the cotton threads more without any substantial burns on the reflective core with the glass beads components

for an increase in parameters from 30 dpi/120 μ s to 40 dpi/120 μ s as shown in Figure 4.27(a) - 4.27(c) and Figure 4.27(d) - 4.27(f) respectively.

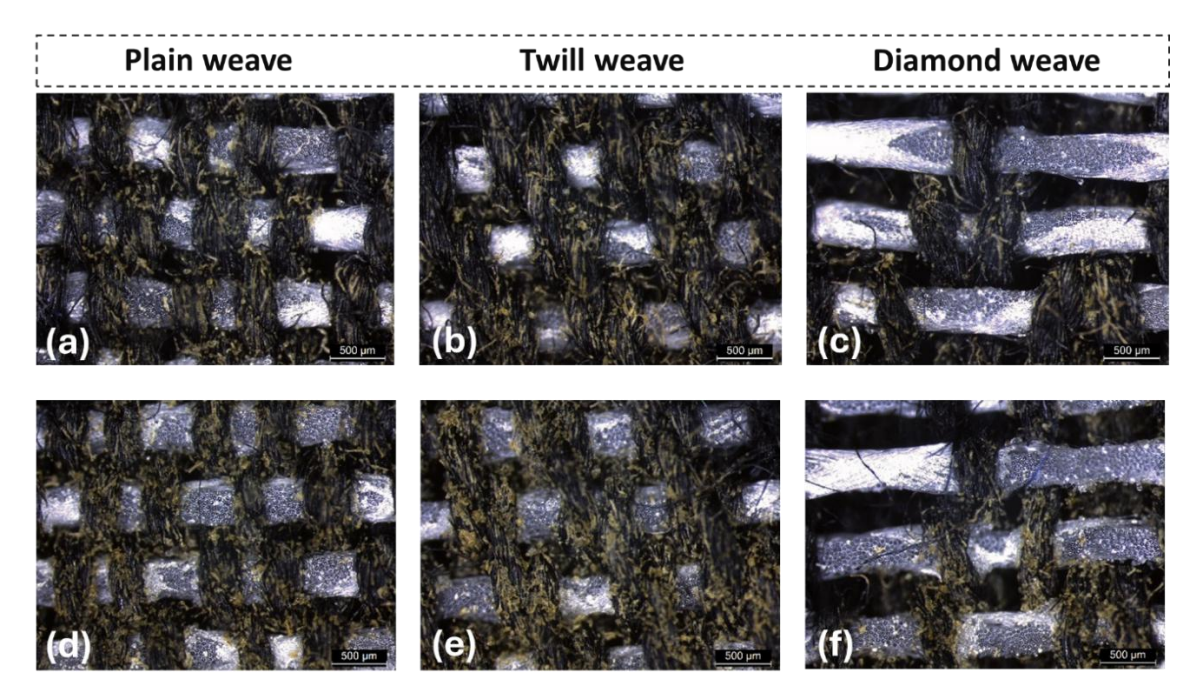


Figure 4.27. Microscopic images of laser-treated fabrics under 500 μ m magnification, (a) – (c) engraved with 30 dpi/120 μ s and (d) – (f) engraved with 40 dpi/120 μ s.

Scanning electron microscope (SEM)

The surface morphology of the fabric samples was observed and analysed using SEM. Figure 4.28(a) - 4.28(f) shows the images after the fabrics were treated with different laser parameters. The SEM images showed a significant change on the surface of the fabrics at different laser engraving parameters i.e., $30 \, \text{dpi/120} \, \mu \text{s}$ and $40 \, \text{dpi/120} \, \mu \text{s}$. Figure 4.28(a) - 4.28(c) shows the effects and changes on the fibre structure under laser treatment $30 \, \text{dpi/120} \, \mu \text{s}$. It is observed from the images that, at lower resolution and pixel time, the low laser power density affected a few fiber structures in the fabric. At such low laser power, the glass beads were not affected or degraded to influence their performance abilities. With an increase in resolution and pixel time at $40 \, \text{dpi/120} \, \mu \text{s}$, more fibers were burnt off as shown in Figure 4.28(d) - 4.28(f). This high laser power engraved and degraded more fibers along its structure resulting in a sponge-like appearance. The latter according Ferrero et al. (2002) to is due to the increase or swelling of the fiber structures caused by the gaseous products during engraving.

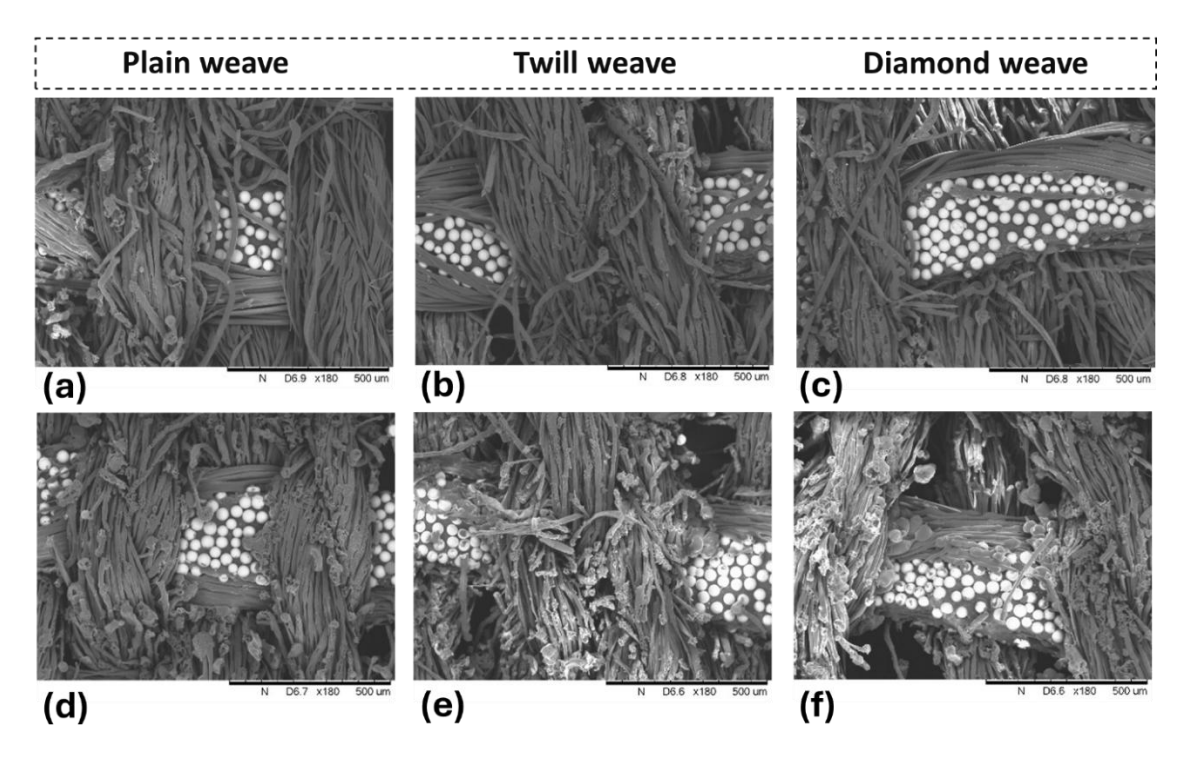


Figure 4.28. SEM images of the laser-treated fabrics under x180 magnification, (a) - (c) engraved with 30 dpi/120 μ s and (d) - (f) engraved with 40 dpi/120 μ s.

It was further observed under higher magnification that, the polyester structure wrapped around the glass bead structure was melted, with the polymer deposited on the surface of some glass bead structures as shown in Figure 4.29. This phenomenon may affect the performance of the glass beads to retro-reflect lights when the fabrics are further subjected to engraving under high laser power density.

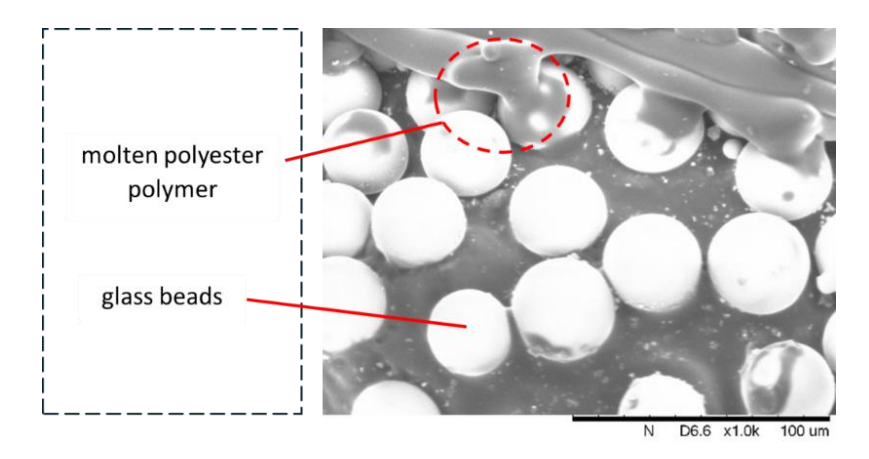


Figure 4.29. SEM images showing molten polyester on the surface of the glass beads at 40 dpi/120 µs laser engraving under x180 magnification,

Colour appearance

The CIE $L^*a^*b^*$ measurement was conducted to determine the colour shade of the laser-treated fabric samples from the untreated as shown in Table 4.10. The lightness is determined using the L^* values, with higher values denoting the lightness of the shade of the fabric samples. It is observed that there is a significant increase in L^* values of the treated fabric samples as the resolution and pixel time increased from 30 dpi/120 µs to 40 dpi/120 µs. The shade of the fabrics was lighter in LA-RF3 (with diamond weave) followed by LA-RF2 (with plain weave) and LA-RF2 (with twill weave) for both laser parameters. Additionally, an increase in resolution and pixel time to 40 dpi/120 µs resulted in high laser power density that removed more fibres from the surface of the fabric structure hence influencing the pale shade of the fabric samples. The use of the RR threads in the fabric structure may have also influenced the higher L^* values in LA-RF3 either untreated or treated with both laser parameters. The inherent diamond weave structure with floats of the RR threads with glass beads reflects all the incidence light hence making the colour of such fabric lighter. The redness and greenness of the untreated and laser-treated fabric samples were measured using the a^* values. With the increase in laser parameters i.e., pixel time and resolution, the a* values for LA-RF1 and LA-RF2 increased with positive a^* values hence the shade of the fabric sample became redder than the untreated. LA-RF3 however produced reducing a^* values from the untreated that had more green shade to a lighter green shade as the resolution and pixel time increased from 30 dpi/120 μ s to 40 dpi/120 μ s. This implies that an increase in laser power density reduces the a^* values for LA-RF3 (diamond weave with long floats).

Table 4.10. Colour appearance of the untreated and laser-treated fabric samples

Fabric	Weave	Description	Laser	CIE L* a* b* values		values
	structure		parameters	L*	a*	b *
LA-RF1	Plain	Untreated		30.882	0.060	-0.882
		Treated	30dpi - 120μs	33.034	0.170	-0.095
			40dpi - 120μs	33.199	0.223	0.680
LA-RF2	Twill	Untreated		30.453	0.087	-0.825
		Treated	30dpi - 120μs	30.360	0.205	-0.044
			40dpi - 120μs	31.717	0.352	1.506
LA-RF3	Diamond	Untreated	-	40.361	-0.112	-0.928
		Treated	30dpi - 120μs	41.663	-0.081	-0.557
			40dpi - 120μs	42.190	-0.046	0.118

Note: LA-RF denotes laser-engraved retro-reflective fabrics

The *b** values were produced after testing to measure the yellowness and blueness of the laser-treated fabric samples. Here, the higher the *b** values are positive, the samples become yellowish as compared to a more bluish colour when *b** values are negative. Results revealed that at 30 dpi/120 μs the low laser power reduced the bluish colour of the untreated fabric samples, where fabric 1C was more bluish than LA-RF1 and LA-RF2. With an increase in laser parameter to 40 dpi/120 μs, the high laser power density was removed and burnt off more fibre structures. This changed the bluish colour appearance of the untreated fabric samples to a more yellowish colour with fabric LA-RF2 > LA-RF1 > LA-RF3. The weave structure in LA-RF2 exposed more of the cotton yarn followed by LA-RF1 and with less exposure in LA-RF3 with diamond weave. An increased laser power density resulted in the engraving of the exposed cotton yarns in the fabric samples which influenced the yellowish colour in LA-RF2. Aside from this, the effect of thermal oxidation from the laser engraving process also influenced the yellow colour shade in the fabric samples.

4.4.5 Summary

The visual evaluation of the laser-engraved fabrics allows for the estimation of changes in colour and microscopic morphology. Experimental results show variations in surface colour, pattern visibility, and sharpness after changes in laser parameters i.e. an increase in pixel time and resolution may lead to differences in appearance from slight to deep burns. This may further influence the stability or strength of the fabric structure. With the difference in fabric structure used for the experiments, morphology observation shows laser beam burns on the cotton yarns of the fabrics with less impact on the reflective core of the reflective threads with changes in laser parameters. For example, at 30 dpi-110 µs laser parameter, pattern visibility is marginally evident in the weft-wise direction as compared to the warp-wise directions. This may be attributed to the yellowish colour change of the fabric surface in that yarn direction. Similar results were evident in the 40 dpi-120 µs parameter even though pattern sharpness on the surface was good since the laser engraves along its yarn length. In conclusion, the weave pattern, yarn direction, and laser parameter can influence the colour change on the fabric's surface which may affect the pattern visibility, sharpness, and the retro-reflective property of the inherent yarn used during weaving. Overall, laser engraving with a 40 dpi-120 µs parameter produced a visibility pattern design on LA-RF1 and LA-RF2.

4.5 General summary

This chapter details the experimental results from retro-reflective fabrics produced via jacquard and dobby weaving looms for design and basic weave structures respectively. The best results from the experiments are used to produce the final prototypes in the study. The jacquard woven fabric RF 3 with ¼ satin, move 2 and ½ twill, has an overall good total hand value (THV) with an average values of 2.605. Retro-reflective woven fabrics such as RF1 (plain weave) and RF2 (twill weave) produced with the dobby weaving loom both have good properties. Even though RF1 with an average total hand value (THV) of 3.0275 than RF2 with THV of 3.2, the retro-reflective properties of RF1 were higher than RF2. Based on this, RF1 was selected with design treatments of 40 dpi-120 µs parameter on their surfaces. Overall, details like sharpness, visibility, and clarity of the design pattern or images were evident for LA-RF1 with plain weaves.

CHAPTER 5: Development and Integration of materials and systems

5.1 Introduction

In this chapter, the design and development of the interactive unit or system and braided electronic-yarn are described. Herein, the success of the interactive unit to produce the necessary safety output of sound, vibration and lights was achieved. The production of the needed lighting effects is achieved by the effective integration and encapsulation of the LEDs to the stainless-steel conductive threads to form braided electronic-yarn. Subsequent washing tests show the stability and durability of the braided electronic yarns produced using a simple encapsulation process. The successful results from the development of interactive unit and braided electronic-yarn are integrated effectively into the jacquard woven fabric and dobby woven fabric with laser-engraving design patterns. This integration aided in forming smart interactive clothing for pedestrian safety. Key test like the range of detection of this clothing was conducted in a laboratory setting, which shows a 25 m range of detection.

5.2 Design and development of the interactive system³

In this section, an interactive system is developed to effectively produce safety features using developed e-yarns and retro-reflective fabrics to interact and improve the visibility of pedestrians. E-yarns which are critical components are used to produce sufficient illumination (red light-intensity effects). Subsequently, an interactive system was developed using a microcontroller, a vibration motor, and a light detector sensor. These components were collectively coordinated via a written code that produced the desired three outputs; sound, vibration, and lights (via the LEDs) for advanced communication with the approaching vehicle and interactive ability to the wearer or pedestrian on the road a night time.

³ Parts of this chapter was approved for a *Patent* and published in a paper with details. Jiang, S.X., **Seidu, R. K.** Jing, L. 一种带有互动装置的夜间行人安全服, *China Patent*, 202322678021.6, 2024/03/22.

Seidu, R. K., Jiang, S.X. (2024) Design and development of Functional Electronic-yarn. *MRS Bulletin*, https://doi.org/10.1557/s43577-024-00736-3

5.2.1 Methodology

The experimental work adopted a methodological approach where activities aided in achieving the set goals. Figure 5.1 clearly illustrates 3-step activities undertaken to effectively integrate and coordinate combined materials. The first step is the design of an interactive system entails using appropriate sensors that are coordinated by a written code. Subsequently, the design of e-yarns that are developed using LEDs systematically arranged on stainless steel conductive yarns. The assembled e-yarn is needed to produce sufficient illumination for improved visibility and communication with the approaching vehicle. After the successful completion of e-yarn and the design of an interactive system, they are ultimately combined and integrated into a sample clothing for testing the system. This is to provide insights into the workability or usability of the assembled system for effective interaction with the wearer.

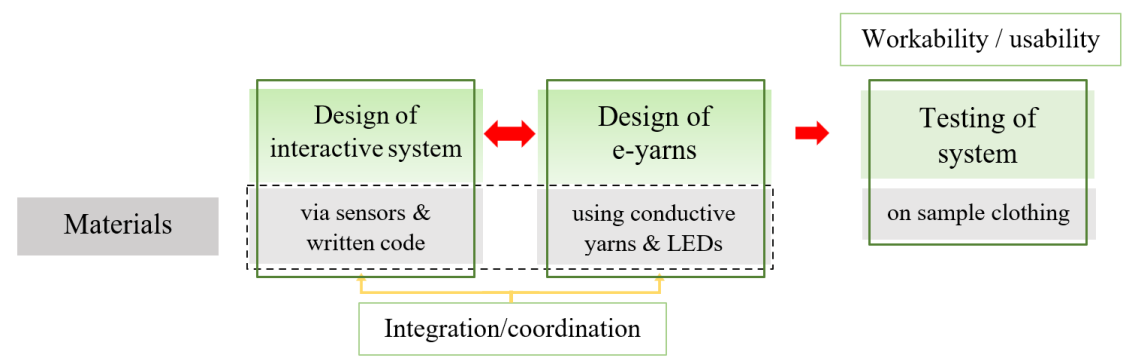


Figure 5.1. Methodological approach used in the experimental work.

5.2.2 Design Concept

In this interactive system, the design principle (Figure 5.2) details that, when a light falls on the surface of a light detector sensor, it triggers the illumination of the light-emitting diodes (LEDs), vibration motor and sound. Alternatively, without the presence of light, the presiding actions by the components will not be triggered to effectively interact with the pedestrian. This coordination of the sensor to trigger the needed outcomes is controlled by a printed circuit board (PCB) via written code.

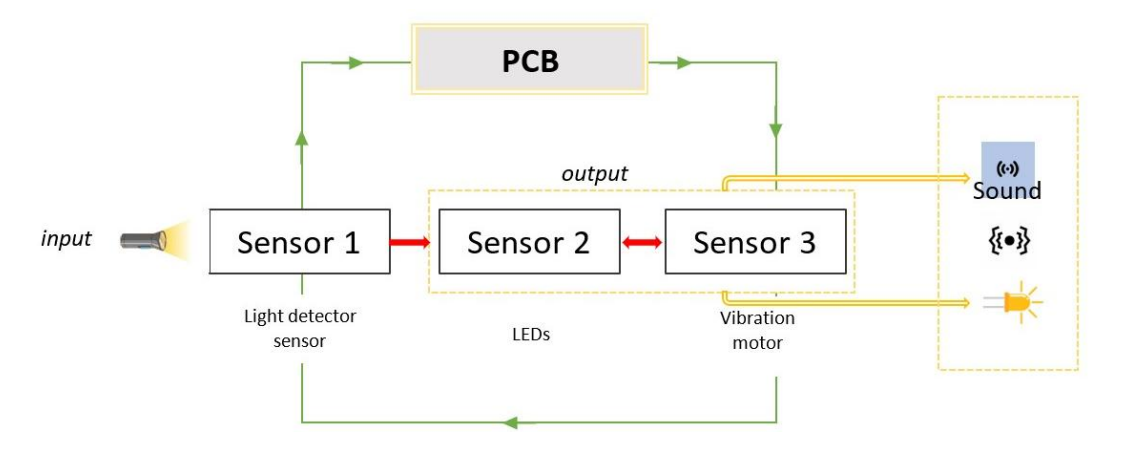


Figure 5.2. Design principle of the electronic interactive system

In this experiment, an open-sourced system (Micro:bit V2) as shown in Figure 5.3, a 3V sensor shield, and sensor modules such as a light detector sensor and vibration motor (Table 5.1) were purchased from Shenzhen KEYES DIY Robot Co. Ltd, China. A MakeCode programming software (editor) for Micro:bit was used to generate the needed codes to aid in the effective coordination and performance of the electronic interactive system. The Micro:bit system comes with several in-built components like programmable buttons, temperature and light sensors, an accelerometer, a compass and an LED display, coupled with several external materials (Cederqvist, 2022). Programming for the microcontroller (Micro:bit) is accomplished via the MakeCode editor using block or language-based text codes either in Python or JavaScript (Teiermayer, 2019, Cederqvist, 2022).

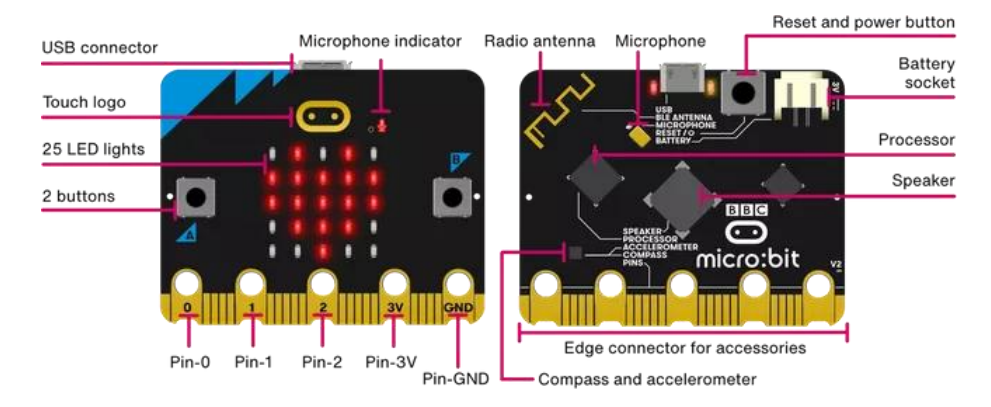


Figure 5.3. Open-sourced system (Micro:bit V2) by BBC in UK. (a) features of the micro:bit (Source: https://microbit.org/get-started/user-guide/overview/)

Table 5.1. Parameters of the electronic components used for the interactive unit.

Product	Parameters	Image
Micro:bit V2 main board	 Wireless BLE Bluetooth 5.0 Dedicated I2C bus On board touch sensor, LED indicator, MEMS microphone, speaker 128KB RAM and 512KB Flash 200mA current available 3V power supply port 	
TEMT6000 Light Sensor Module	Analog output signalDC 3V of working voltage	CONTRACTOR OF THE PROPERTY OF
Vibration motor module	DC 5V of operating voltage35mA operating current	
Transistor 2N3904 model	 NPN transistor type Maximum of 5V, 50V and 40V for emitter-base, collector-base and collector-emitter voltages 300 MHz maximum frequency 	B B C
Lithium Polymer Li-Po li ion rechargeable cell	 Lithium battery with thickness (8.0mm), width (20mm) and height (35mm) 3.7V~4.2V Working temperature of -10°~50° Capacity of 500mAh 	20mm 8.0mm
Lithium Polymer Li-Po li ion rechargeable cell	 Lithium battery with thickness (6.0mm), width (20mm) and height (30mm) 3.7V~4.2V Working temperature of -10°~50° Capacity of 300mAh 	- Q. 602030 + 3.70 30400 190 20mm

5.2.1.1 Design of the interactive controlling unit or system

The e-yarn formed (by encapsulating the LEDs with the conductive yarns) and the sensory devices coordinated via the written code, are assembled, and integrated onto a sample t-shirt. This prototyping on the t-shirt was to assess the workability and effective coordination of the components to produce the needed interactive actions i.e. lights, sound and vibration. During sample testing (Figure 5.4), the e-yarns consisting of sixteen 0603 LEDs were connected to the output terminal from the PCB. However, the supplied 3V power connected to the PCB could not light up the e-yarn. This may be attributed to the use of 3V to power the PCB and related sensory devices, hence less supply power to light up the diodes in the e-yarn. This confirms the results as indicated earlier (see Figure 5.4) that there is a voltage drop when more diodes are contained in an e-yarn.

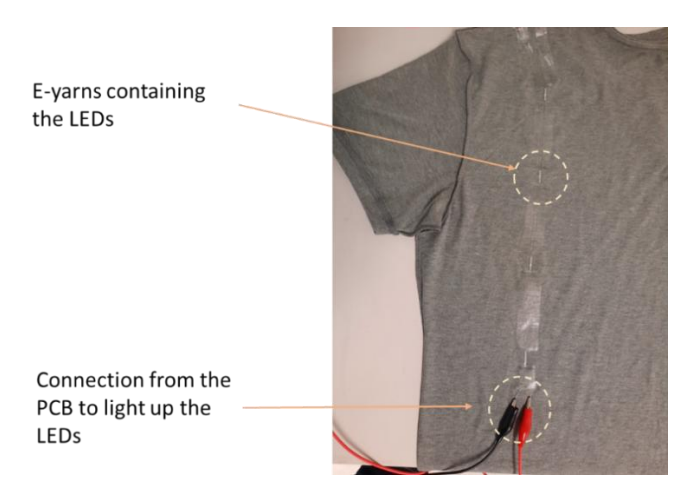


Figure 5.4. Testing procedure to light up the LEDs using the power supplied from the PCB.

To overcome such a challenge, it was imperative to separate the source of power for the microcontroller and the diodes in the e-yarn. With such a large number of sixteen diodes in the e-yarn, a large power load is required to produce the needed lights. A transistor composed of an emitter, base and controller pins were employed to control, separate, and supply a new current load to the LEDs (e-yarn). Wendt and Cook (2018) revealed that a transistor aids in isolating a new current load from another or separating an electrical signal which is effectively controlled by an output. This implies that signals from the micro-controller can be multiplied or relayed, switching a separate load used for controlling another function. With such functional ability, the transistor 2N3904 model was used to collect output from the micro-controller, and a new current load was attached to supply power to the e-yarn. A signal from the micro-controller results in a closed switch on the transistor hence current is supplied to power the e-yarns. Alternatively, when no

signal is supplied from the micro-controller, the transistor is in an open switch. Here, the connection of a battery is used to power only the micro-controller with the related sensory devices whereas the transistor unit (which acts to break out the powering unit from the microcontroller) is connected to battery unit. This approach is designed so that a separate power source which is used to control the e-yarns. This design makes it possible for further modification in using any type of battery to power up the e-yarns. With a written code downloaded onto the micro-controller, it detects the presence of light from the light detector sensor, causing the action of the vibration motor and lighting effects of the diodes embedded in the e-yarns.

The eventual micro-controller coupled with their accessories was housed in a 3D printed case using resin material. This casing carefully secured all components in-place as shown in Figures 5.5(b) and 5.5(c). The microbit micro-controller (Figure 5.5(a)) was used to build the interactive controller unit which comprises a transistor, wires and connectors, battery, and charger module, all housed in the rectangular 3D model casing (Figure 5.5(b)). Herein, connectors are designed to fit with it corresponding connector on the sewed garment. The charger module makes it possible to effectively recharge the battery when the power is low. Furthermore, openings in both casings at the top is designed to ensure easy exit of heat (if any). In Figure 5.5(b), a 3.7 Lithium Polymer Li-Po battery with a capacity of 500mAh rechargeable battery was connected to the micro-conrtoller to provide separate power for the braided e-yarns in the outfit. Herein, an NPN transistor is used to separate or break the power hence a new battery is used to power the red lighting effects of the braided e-yarns. Additionally, a 3.7 Lithium Polymer Li-Po battery with a capacity of 300mAh was used to build the controller switch unit (Figure 5.5(c)). This is used to supply power to the interactive controller unit. When the switch is off, the interactive controller unit is not active for effective functioning. This 300mAh rechargeable battery only supplies power to the micro-controller.

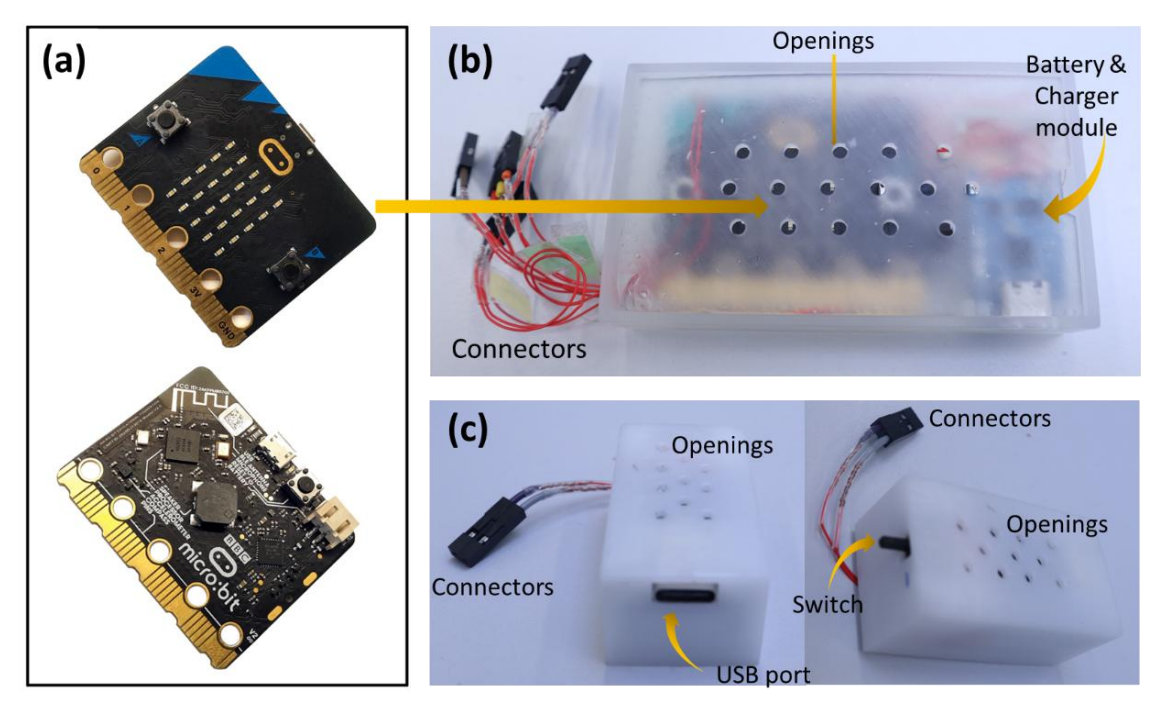


Figure 5.5. (a) Modelling case housing the interactive unit and (b) case housing the micro-controller with its related components. (c) controller switch unit (case housing the battery for easy supply of power to the micro-controller).

5.2.3 Preliminary procedure for the design of e-yarns

The e-yarns are created using stainless steel conductive yarns arranged in parallel to carefully house the LEDs. The following activities detail evaluating the direct current consumed by the LEDs arranged on the SS conductive yarns and the encapsulation process to protect and secure the joint between the yarn and the diodes.

Materials

In this experimental work, stainless steel conductive yarns of different thickness types were purchased from Fujian QL Metal Fiber Co. Ltd, and light-emitting diodes (LEDs) with warm white and red colour-producing light was purchased from Shenzhen Dejurenhe Industrial Technology Co. Ltd respectively. Test methods such as appearance using an optical microscope, electrical resistance using a digital multimeter, and laundering ability of the stainless-steel conductive yarns were conducted. The optical microscope was used to observe the surface morphology of the stainless-steel conductive yarns of different thicknesses as shown in Figure 5.6. Even though all these yarns are 3-ply, evident from Figure 5.6 shows that 91*3 thread with THK of 0.36mm has many hairy structures on its surfaces as compared to the others with smooth surfaces. Additionally, the number of individual and single yarns contributed to the bulk nature or thickness of

the stainless-steel conductive yarns. As such, Figure 5.6(d) with 1000 single yarn strands when plied in three (3) produced a heavy thread with high thickness and weight.

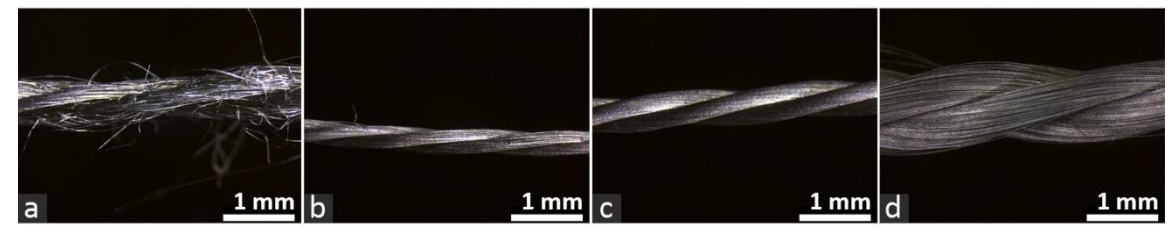


Figure 5.6. Stainless Steel conductive yarns. (a) 91*3 thread with THK of 0.36mm (b) 100*3 thread with THK of 0.25mm, (c) 275*3 thread with THK of 0.42mm, and (d) 1000*3 thread with THK of 0.65mm. (THK means thickness)

Subsequently, the optical microscope was used to capture the images of the LED obtained for the experiment. Figure 5.7 identifies the two different diodes (producing red light). It is evident from Figure 5.7 that, the relative size of the diode captured in Figure 5.7(a) is smaller than the diode in Figure 5.7(b). Additionally, the design structure and solder pads of the diodes in Figure 5.7(a) are relatively different from the diode in Figure 5.7(b), even though they all have two opposite terminals (negative and positive). The structure of the solder pads in Figure 5.7(a) provides different options for attaching or embedding it onto a conductive yarn as compared to diodes in Figure 5.7(b).

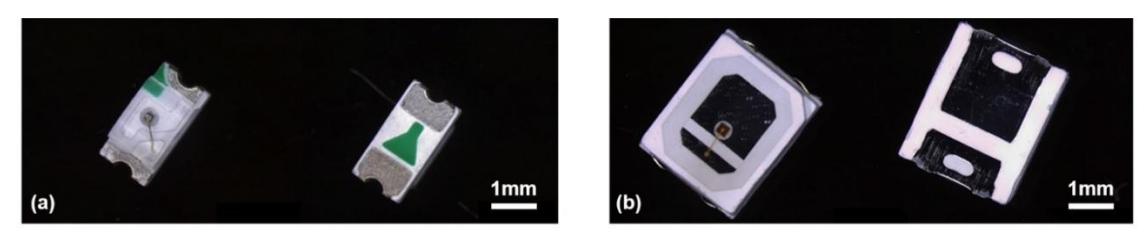


Figure 5.7. Two LEDs were used in the experiments. (a) front and back image of 0603 diodes (red), (b) front and back image of 2835 diodes (red)

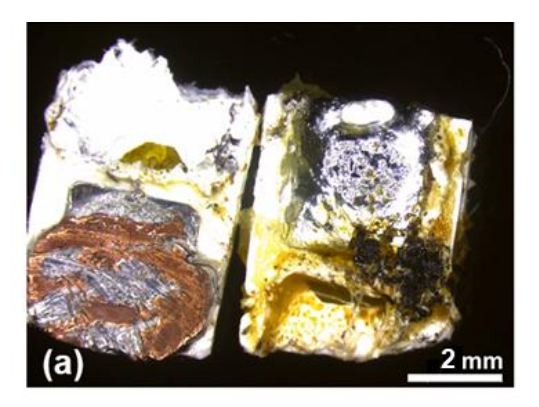
The electrical resistance of the four different stainless steel conductive yarns was measured along a 5cm length. The resistance in ohms (Ω) was repeated on 10 samples for each yarn type (of 5cm) and the average was calculated. Evident from Table 5.2 is the resistance recorded for each yarn type. Results showed that Yarn D (with a large yarn diameter and individual fibers) has the lowest resistance whereas Yarn A has the highest resistance across the length. Averagely such low resistance shows a potential high current flow in the yarn. Due to the hairy structures on the surface of Yarn A, the individual resistance value for the yarn length of 5cm varied considerably as compared to a fairly constant resistance value for Yarn B, C, and D for 10 repeat measurements.

Table 5.2. Resistance measurement of stainless-steel conductive yarns

Yarn types	Components	Resistance (Ω)
Yarn A	91*3	2.88
Yarn B	100*3	1.34
Yarn C	275*3	0.58
Yarn D	1000*3	0.31

Encapsulation procedures

An appropriate encapsulation method is imperative to secure and insulate the stainless-steel conductive threads to the LEDs. This aims to prevent any short circuit when power is supplied. To understand the effective approach, two (2) procedures were adopted; soldering the conductive threads to the solder pads of the LEDs and securing the conductive threads to the solder pads of the LEDs using a heat-shrinkable tube (HST) (Figure 5.8). As shown in Figure 5.8(a), the soldering process was used to solder the conductive threads to the solder part of the LEDs, however, due to the nature of the stainless-steel conductive threads, the soldering process damaged the solder pads of the LEDs. Such difficulty is attributed to the oxide layer on the surface of the stainless steel. In Figure 5.8(b), a heat-shrinkable tube secured the stainless-steel conductive threads to the solder pads of the LEDs. This process was not time-consuming and firmly held the LEDs to the threads. With the success of this approach, it is possible to arrange the LEDs with the same terminal either positive or negative facing one side connected to stainlesssteel conductive threads. This exposes the ends of the conductive threads which when in contact, could disturb the flow of power. To address this situation, different materials i.e. TPU film and heat-shrinkable tube are used to insulate the conductive threads.



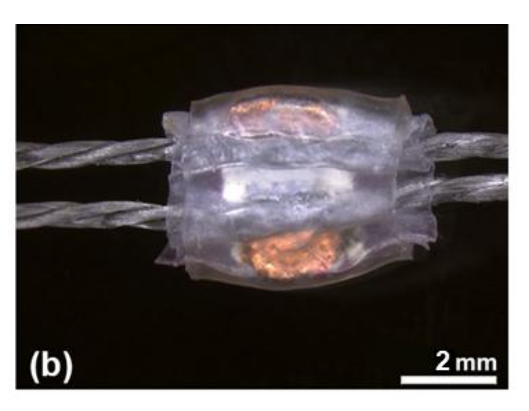


Figure 5.8. (a) Appearance of the solder pads of the LEDs after using the soldering process (b) appearance after using a heat-shrinkable tube to encapsulate the LEDs to the stainless-steel conductive threads.

Table 5.3 illustrates the three (3) different design approaches adopted to insulate the stainless-steel conductive threads. Herein, one layer of thermoplastic polyurethane (TPU) film is used to insulate one side of the SS-CT (for Design 1) whereas two layers of TPU film are used to insulate both sides of the SS-CTs (for Design 2). The use of TPU material is imperative due to its poor electrical conductivity (Manap et al., 2021, Maganty et al., 2016) hence could act as a good insulator. Based on such property, the material was used to insulate the conductive yarns and prevent disruption in the transfer of current to power the various LEDs embedded in the braided e-yarns. It was observed that using one layer of the TPU film did not effectively insulate the conductive threads hence when it was braided, the LEDs did not light up when supplied with power. However, when the layers of the film were doubled, it provided the necessary insulation even after braiding for effective lighting effects. In an alternative approach, a heat-shrinkable tube is used to insulate one side of the SS-CT (for Design 3). Heat-shrinkable tubes are materials made from polymers that can be expanded or shrunk when heated at high temperatures but maintain the exact shape at lower temperatures (Dinsmoor, 1963, Tsutsumi et al., 2013, Kong and Xiao, 2017). These materials can be used for varying applications to insulate material parts. When braiding is applied, the heat shrinkable tube can prevent contact of the two conductive threads which could affect the lighting effects of the LEDs in the braided e-yarns. As such, Design 3 was identified as an ideal approach for further adoption and testing.

Table 5.3. Different approaches were adopted to insulate the stainless-steel conductive threads.

Sample	Encapsulation approach	Results	
Design 1	One layer of TPU film is used to insulate one side of the SS-CT. SS conductive threads (SS-CT) encapsulated LED with HST TPU film		No lighting effects are produced when the positive and negative terminals are connected to the battery. It was time-consuming to cut and attach the TPU film to insulate one side of the SS-CTs.
Design 2	Two layers of TPU film are used to insulate both sides of the SS-CTs. encapsulated LED with HST TPU film		Lighting effects are produced when the positive and negative terminals are connected to the battery. It was time-consuming to cut and attach the TPU film to insulate both sides of the SS-CTs.
Design 3	A heat-shrinkable tube is used to insulate one side of the SS-CT. SS conductive threads (SS-CT) encapsulated LED with HST Heat shrinkable tube		Lighting effects are produced when the positive and negative terminals are connected to the battery. A shorter time was used to cut, attach, and insulate one side of the SS-CTs.

Note: TPU means Thermoplastic Polyurethane; SS-CT means stainless-steel conductive threads and HST means heat-shrinkable tube

5.2.4 Evaluating direct current voltage (V_{DC})

[i] 2835 LEDs

To understand the voltage consumed by the two different LEDs, they were attached or connected to the four SS conductive yarn types with the help of Scotch® magic tape. Here, the solder pads of the LEDs were placed on two parallel similar yarn types to form the positive and negative terminals. The direct current voltage (V_{DC}) consumed by 1, 3, and 5 LED lights embedded in series were tested using the power supplied by the control unit. Figure 5.9(a-l) shows the responsive action (on/off) of the connected diodes to different SS conductive yarn types. It is evident from Figure 5.8(a,e,i) that, the diodes embedded in Yarn A (91*3) did not produce any light effect when supplied with power. Similar observations were recorded for Yarn C (275*3) and Yarn D (1000*3) with 5 diodes even though when the number of diodes was reduced to 1 and 3, the supplied power was able to light up the diodes.

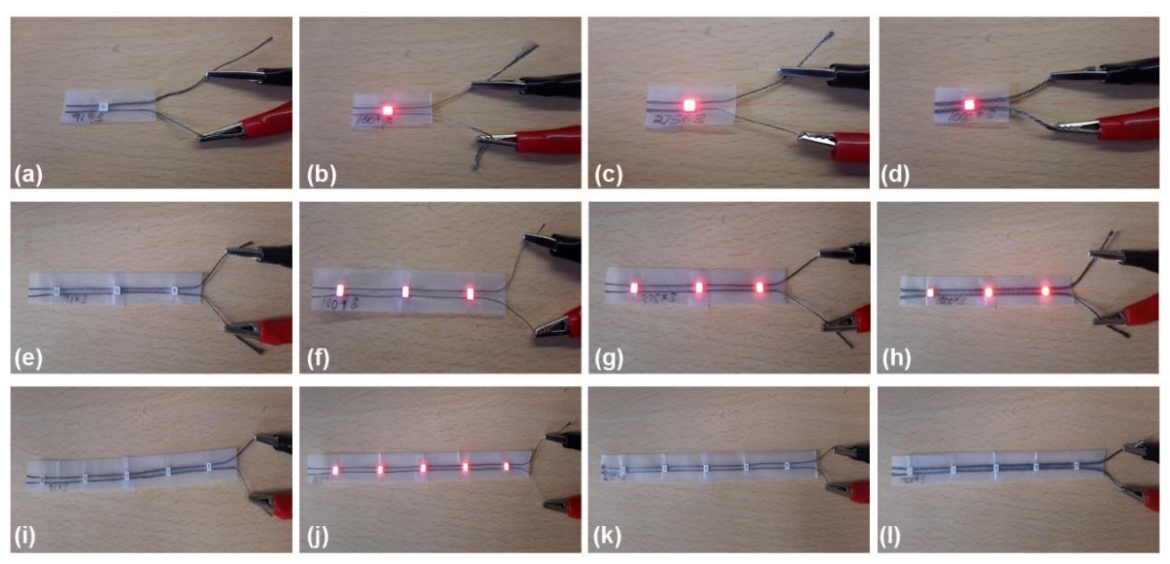


Figure 5.9. Appearance of responsive action (lights turned on/off) of the 2835 LEDs (red) embedded in different yarn types. (a,e,i) – yarn A with 1, 3, and 5 diodes, (b,f,j) – yarn B with 1, 3, and 5 diodes, (c,g,k) – yarn C with 1, 3, and 5 diodes, and (d,h,l) – yarn D with 1, 3 and 5 diodes.

Affirming results in Figure 5.9, a digital multimeter was used to measure the V_{DC} with power supplied from the control unit, overall results indicate that there is a voltage drop when the number of diodes increased. Figure 5.10(a,b) indicates the V_{DC} of the different yarn types when embedded with 1, 3, and 5 LEDs. With an original V_{DC} of 2.947V from the control unit, it is evident that the voltage (0.25V) passing through Yarn A was insufficient to light up 1, 3, and 5 LEDs when embedded. As explained, the hairy nature of the yarn structure and the high resistance (2.88 Ω) recorded for Yarn A may have

been attributed to the drop in voltage necessary to light up the LEDs. Similar results were observed for Yarn C and Yarn D when the LEDs were increased to 5. A voltage of less than 0.5 was insufficient to light up the 5 diodes embedded in the yarns. Subsequently, even though the voltage dropped for Yarn B, the average voltage of more than 1.75V was sufficient to light up the diodes when increased from 1 to 5.

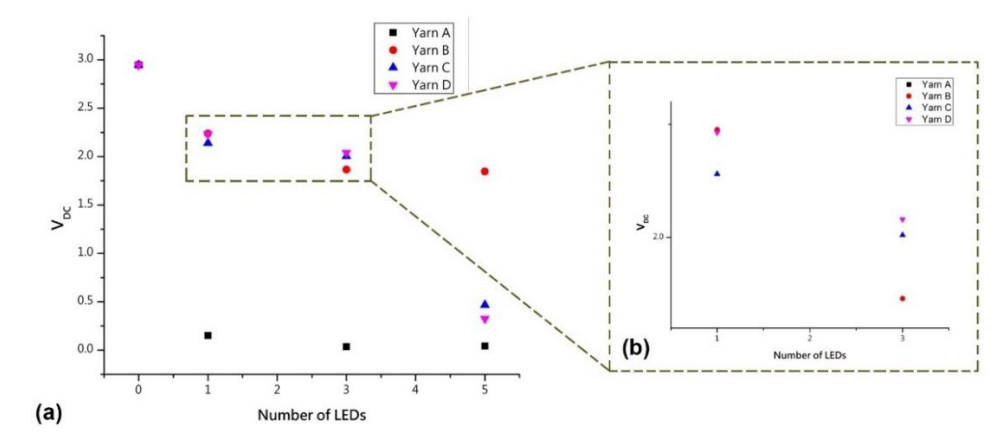


Figure 5.10. Effect of the number of 2835 LED lights embedded in different yarn types on the direct current voltage (V_{DC}). (a) V_{DC} against the number of LEDs, (b) magnified diagram of V_{DC} against the number of LEDs showing values for all yarn types embedded with 1, 3, and 5 diodes above 1.5V. Measurements were taken using a digital multimeter.

[ii] 0603 LEDs

With regards to testing the voltage when 0603 LEDs (see Figure 5.11(a-i)) are embedded in the four different SS conductive yarns. It is evident from Figure 5.11(a,e,i) that, diodes embedded in Yarn A did not light up when supplied with power. Similarly, in Figure 5.11(l), no lighting effects were produced when 5 LEDs were embedded in Yarn D. With regards to the latter when the number of diodes was reduced to 3 and 1, the power passing through the yarn was able to power them or light up the diodes. In all cases, for Yarn B (Figure 5.11(b,f,j)) and Yarn C (Figure 5.11(c,g,k)), the power for the control unit caused the number of diodes (1, 3, and 5) to light up.

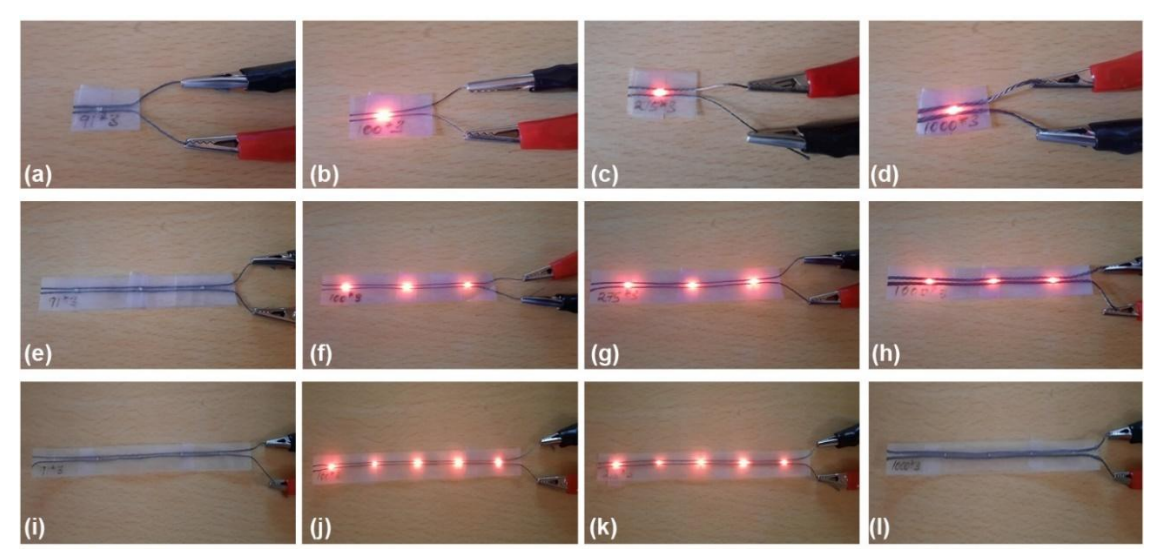


Figure 5.11. Appearance of responsive action (lights turned on/off) of the 0603 LED lights (red) embedded in different yarn types. (a,e,i) – yarn A with 1, 3, and 5 diodes, (b,f,j) – yarn B with 1, 3, and 5 diodes, (c,g,k) – yarn C with 1, 3, and 5 diodes, and (d,h,l) – yarn D with 1, 3 and 5 diodes.

Results captured in Figure 5.12 (a,b) further confirm the observations in Figure 5.11(a-i). Overall results indicate that there is a voltage drop when the number of diodes increases. With an original V_{DC} of 2.947V from the control unit, the power dropped below 0.5V when connected to Yarn A embedded with 1, 3, and 5 diodes. This indicates that due to the hairy nature of the yarn structure and the high resistance (2.88 Ω) recorded for Yarn A, it is unable to allow the flow of current to light up the diodes. Subsequently, for Yarn D, the V_{DC} dropped considerably below 0.5V when 5 diodes were embedded in series. Alternatively, Figure 5.12 confirmed that the V_{DC} for Yarn B and C was above 2.59V even with an increase in diode numbers.

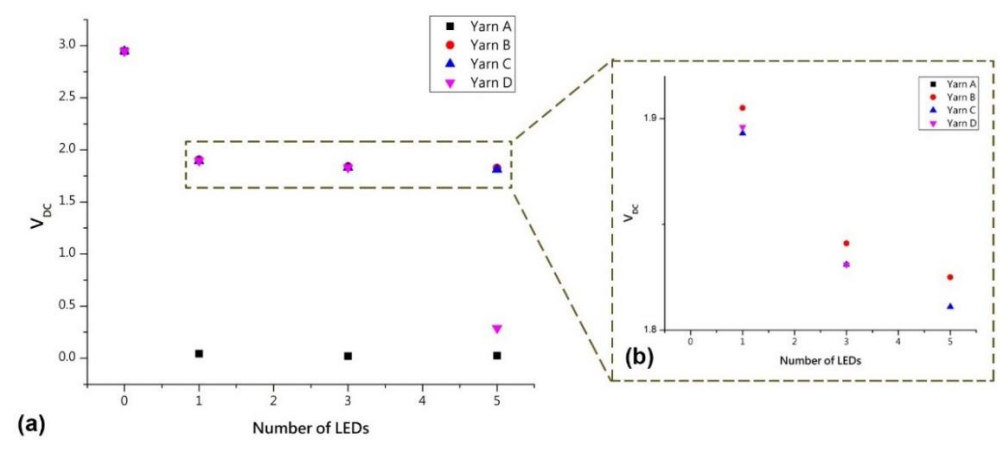


Figure 5.12. Effect of the number of 0603 LED lights embedded in different yarn types on the direct current voltage (V_{DC}). (a) V_{DC} against the number of LEDs, (b) magnified diagram of V_{DC} against the number of LEDs showing values for all yarn types embedded with 1, 3, and 5 diodes above 1.8V. Measurements were taken using a digital multimeter.

5.2.5 Summary

Herein, red 2835 and 0603 LEDs, and 100*3 stainless-steel conductive threads were employed and experimented with two approaches to embed the diodes into the threads. Results revealed that the design of 0603 LEDs made it easier to encapsulate in 0.25mm SS conductive yarns and the even distribution of power to the embedded LEDs. Alternatively, three (3) design methods were explored to insulate the stainless-steel conductive threads to prevent any short circuits. Further analysis from the direct current voltage test, showed that an increase in the number of LEDs embedded in conductive yarns results in a reduction in voltage supplied from the micro-controller to the LEDs. These results provided insight to separate the supplier power to the microcontroller and the LEDs (e-yarns). As such, a transistor was employed to separate and supply a new set of power to the LEDs. This power separation component using a transistor was considered in the design of the interactive system or unit. A research concept of achieving three outputs; sound, lights, and vibration, was realised via a written code and the interactive system.

In conclusion, the 0603 LED was selected due to its size and ease of attaching the conductive thread to the solder pads. Furthermore, 100*3 stainless-steel conductive threads and insulation method (design 3) were selected for further experimentation and testing to ensure the durability and robustness of the e-yarns.

5.3 Design and development of functional electronic yarn

This section describes the fabrication and characterization of a simple approach to develop low-cost electronic yarns (e-yarns) by embedding light emitting diodes (LEDs) in series onto two stainless steel (SS) threads, which are then braided and woven into e-textiles. The use of advanced materials and technology for interactive purposes and to provide necessary feedback and information has been on the rise. These advanced products have a wide range of uses, from providing aesthetics to having a more functional application. To help achieve functional performance, electronic components are now being integrated into textile materials. These electronic textiles or so-called e-textiles comprise the integration of electronic systems and components into the structure of textile materials for effective control and advanced functions (Service, 2003, Zheng et al., 2021). Appropriate microcontrollers, sensors, and powering devices are integrated into textile structures to sense environmental changes and provide real-time monitoring. Zeng et al. (2014) attributed the effectiveness of these e-textiles to their wear comfort, flexibility,

efficiency, and high sensitivity. Other functions include the capability for wireless communication as well as the gathering and monitoring of sensitive information (Marculescu et al., 2003). Unfortunately, the wearability and wear comfort of some modern e-textiles is affected by the use of very limited rigid electronic materials. However, in recent years, there have been studies that focus on the fabrication of flexible e-textiles to address the shortcomings of rigid materials, which use a large number of stretchable and highly conductive electronic yarns (e-yarns). E-yarns are fabricated by incorporating electronic components with conductive threads that can be integrated into the textile structure for various functional applications (Rathnayake and Dias, 2015). Most importantly, studies have integrated vibration, motion, and accelerometer sensors to produce e-yarns to detect falls or near falls, and monitor vibration in the index finger and palm to classify gait alterations respectively (Rahemtulla et al., 2023, Rahemtulla et al., 2021, Lugoda et al., 2022). Other notable e-yarns are the development of light-emitting diode (LED) e-yarns which are embedded into clothing for applications in health care, art, fashion, entertainment, and road safety (to make pedestrians visible) (Seidu and Jiang, 2023).

LED e-yarns are usually fabricated by embedding LEDs into conductive yarns to produce light when supplied with an external source of power. Hardy et al. (2022) used an automated manufacturing process of embedding LEDs onto copper wires, Satharasinghe et al. (2018) embedded photodiodes onto copper wires, while Satharasinghe et al. (2019) embedded LEDs and photodiodes onto copper wires to monitor heart rate. LED e-yarns have also been used for entertainment purposes. Hardy et al. (2018) embroidered e-yarns onto the surface of a stretchable fabric with zig-zag stitches for a costume garment. Here, the e-yarns attached pose no discomfort to the wearer but provide the needed illumination for the dancer. More recent studies have adopted a manual approach to integrating LEDs into conductive threads for woven fabrics. For example, Simegnaw et al. (2023) embedded surface-mounted devices (SMDs) on conductive yarns by using a reflow soldering machine, and used crimp beads to bond the LEDs to the conductive yarns (Simegnaw et al., 2022b). These studies have explored the integration of LEDs onto copper wires, silver yarn, and stainless-steel (SS) threads through automated or manual processes.

To further contribute to the growing volume of work on e-yarns and increase their range of applications, this study proposes e-yarns that can be woven into fabric for clothing that enhances the visibility of pedestrians. The World Health Organization (2018) reported pedestrian accidents as among the leading causes of global deaths on the road. The large

number of pedestrian accidents has been largely due to their lack of visibility and conspicuity, and the ability of drivers on the road to see them at night, which places pedestrians in a vulnerable position (Tyrrell et al., 2016). To help improve the visibility of pedestrians and the ability of drivers to identify pedestrians, one approach is to integrate lighting effects on the clothing of pedestrians. Herein, this experimental work develops low-cost e-yarns by embedding LEDs in series onto two SS threads, which are then braided and woven into e-textiles. A different approach to fabricating e-yarns with LEDs is proposed. The issues of breakages at the connection joint (between the LED and the crimp beads) (Simegnaw et al., 2022b) and breakage of copper wires after washing (Satharasinghe et al., 2018) would be limited in our proposed approach. The stainless-steel threads are used in the fabrication process due to their heat resistance, exceptional durability, and conductivity.

The resultant e-textiles have lighting effects when connected to a power source and can be used for interactive clothing for visibility at night. The braided e-yarns and e-textiles are also subjected to 20 washing cycles to evaluate their wash durability, workability, and reliability. In this section, braided electronic yarns and electronic textiles are fabricated using stainless steel conductive threads and LEDs as illustrated in a four-step production process (Figure 5.13). The eventual braided e-yarns are integrated into the structure of the woven fabric during weaving. Herein, two heat-shrinkable tubes are used in the encapsulation process to produce two samples of braided electronic yarns and electronic textiles.

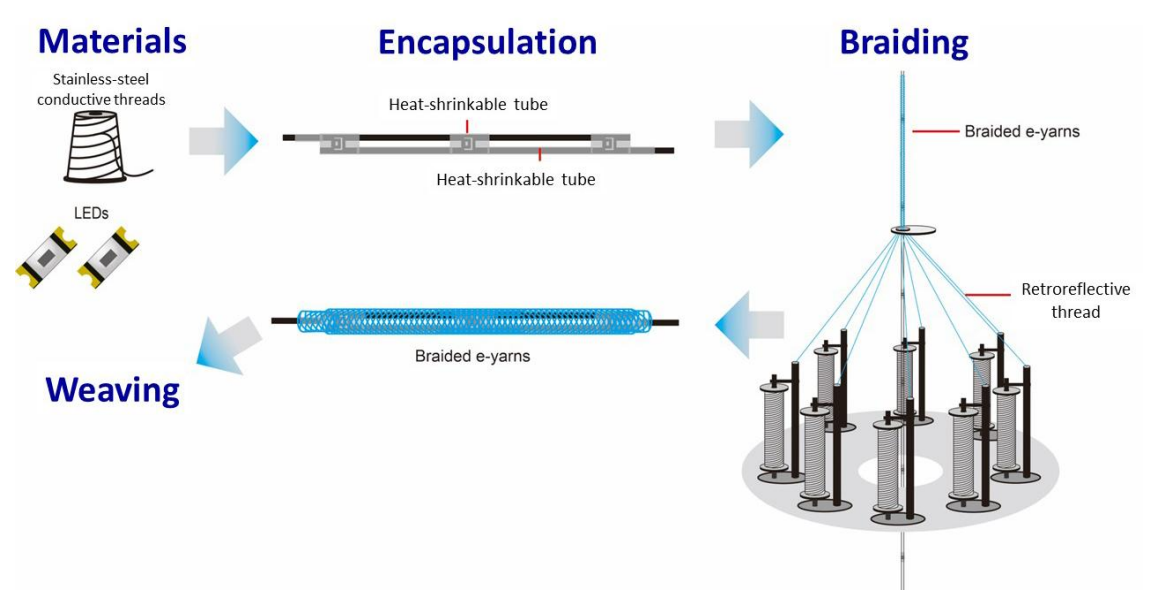


Figure 5.13. Four steps of the production procedure (materials, encapsulation, braiding, and weaving)

5.3.1 Methodology

Materials: In the experimental work, different materials are used for the design and production of e-yarns that are integrated into a retro-reflective (RR) woven fabric; see Figures 12(a)-12(d). 150D/2 retro-reflective (RR) threads with thicknesses of 0.12 mm and 22.348 NE were purchased from Dongguan Cheng Wei RR yarns Material Co., Ltd, China. Miniature LEDs (SMD 0603) with two solderable metallic parts (positive and negative terminals) were purchased from Shenzhen Lianxinrui Technology Co. Ltd, China. This type of LED produces a red colour when connected to a battery source. Furthermore, 3ply SS conductive threads or yarns were purchased from Fujian QL Metal Fiber Co. Ltd, China. According to the manufacturer, these yarns are highly conductive and flexible and have unique properties including resistance to high temperatures (350°-800°C) and alkaline and acid, with a diameter of 0.33 mm strength of 5.63 kgf, weight/m of 0.27 gram, so they can easily be used for woven or knitted products. Scotch® brand transparent adhesive tape (AT) (from the 3M Company, USA) was used to secure the conductive threads or yarns to the two terminals of the LEDs. A Ø0.6 mm transparent heat shrinkable tube (HST) (type: S-902-600), 600V, and 105°C for voltage and temperature ratings respectively, was purchased from Shenzhen CXCW Electronic Co. Ltd, China.

Additionally, a Ø1.5 mm white and a Ø2.0 mm transparent HST were purchased from Welfare Electronic Component Ltd, Hong Kong SAR, China. The HSTs were used to insulate certain parts of the conductive yarns and secure the SS conductive yarns to the two solderable terminal parts of the SMD 0603 LEDs. These materials (Figure 5.14) were combined to produce two samples of e-yarns named Sample 1 (encapsulated with Ø1.5 mm HST) and Sample 2 (encapsulated with Ø0.6 mm HST). The FLUKE 107 CAT III 600 V Digital Multimeter and the LX-101 Lux Meter were purchased from Welfare Electronic Component Ltd, Hong Kong SAR, China.

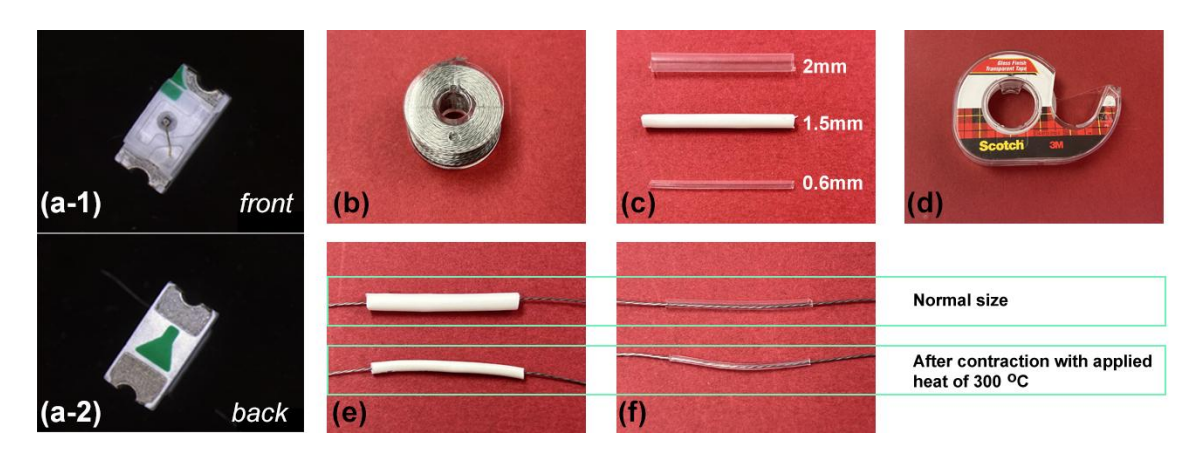


Figure 5.13. (a-1) Front of SMD 0603 LED and (a-2) Back of SMD 0603 LED, (b) stainless steel conductive yarns, (c) different types of HSTs, (d) scotch[®] transparent tape, (e) Ø1.5 mm HST before and after shrinkage, and (f) Ø0.6 mm HST before and after shrinkage.

5.3.1.1 Encapsulation procedures

As mentioned earlier, encapsulation was conducted to secure the SS conductive yarns to the two solderable terminal parts of the SMD 0603 LEDs and insulate certain parts of the conductive yarns during the fabrication of the e-yarns. Here, two experimental approaches that use either conductive adhesive paste or AT together with the HST were explored to understand the feasibility and workability of the encapsulation design plan. This new design plan is different from the previously assembled e-yarns (Figure 5.14) which made it difficult to weave into the structure of the fabric due to the ease of the conductive yarns touching each other. This limited the flow of energy from the battery to power the LEDs arranged. Also, the previous design placed all the powering terminals of the conductive yarns at one side, a situation which limited the distribution of even electrical power to the LEDs arranged.

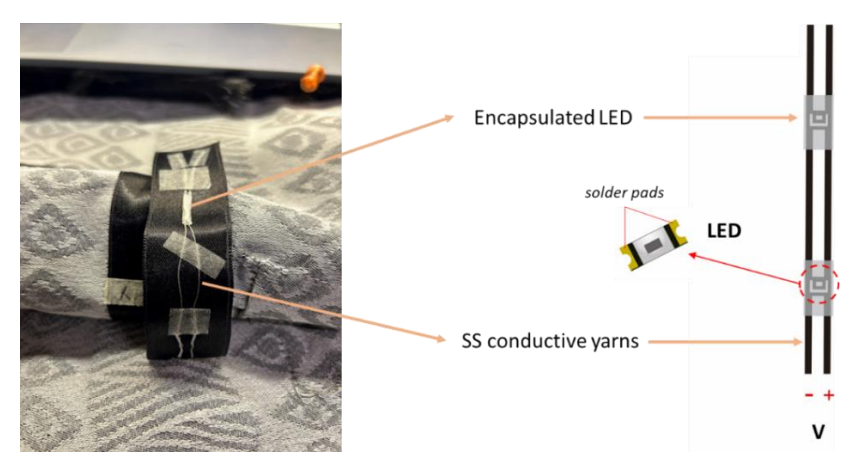


Figure 5.14. Initial design of the e-yarns without insulting the stainless-steel conductive threads.

Encapsulation design one (using conductive adhesive paste and HST): Figures 5.15(a) to 5.15(d) show the schematic of the cross-sectional view of the embedding of the LED onto the SS conductive yarn and the encapsulation procedure. First, the SMD 0603 LED is placed face down on the sticker base of the adhesive tape, exposing its solder pads upwards. A small quantity of conductive adhesive is applied to the solder pads with the two conductive yarns (in parallel) held under tension and placed onto the conductive adhesive. The properties of the conductive yarns mean that the conductive adhesive has to dry for some time (approximately 30 min to 1 hour). Upon drying, the conductive yarns are held to the diodes. Adhesive tape is subsequently used to attach the side of one of the parallel yarns close to the diode for insulation purposes so that upon encapsulation, the surface of the two parallel yarns does not come into contact. Otherwise, this could affect the electric current flow that passes through the two yarns that are acting as positive and negative points to power the LEDs.

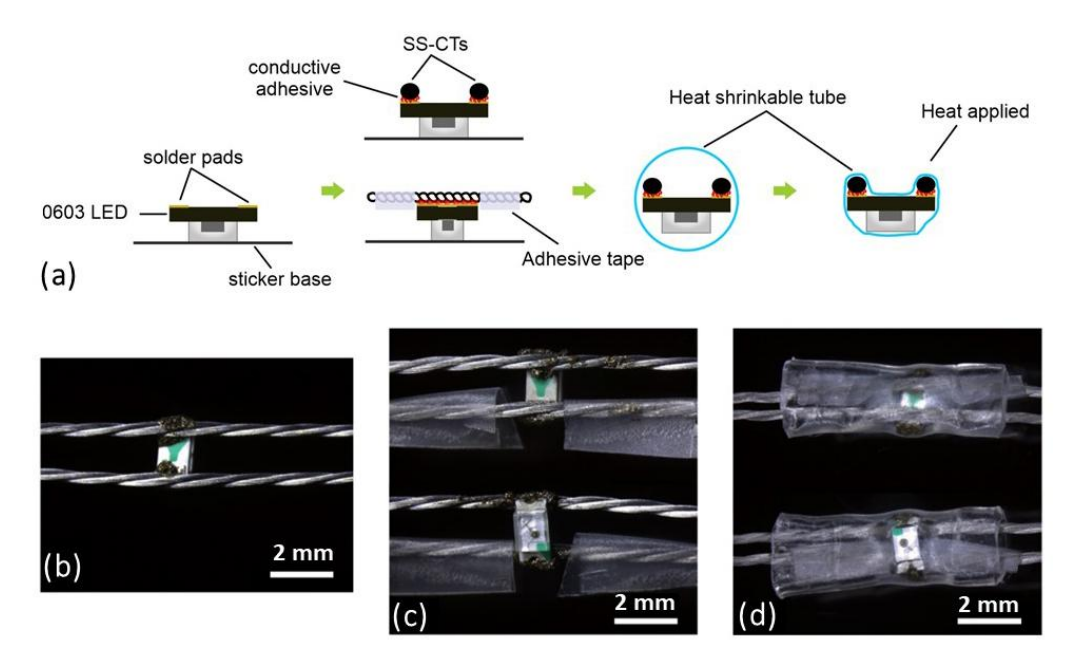


Figure 5.15. Design one fabrication process of e-yarn. (a) schematic of the cross-sectional view of embedding SMD 0603 LEDs on stainless-steel (SS) conductive yarns and encapsulating with HST, (b) attaching two parallel yarns to the solder pads using conductive adhesive, (c) placing AT on one side of the parallel yarn to prevent short-circuiting when the surface of the yarns come into contact, and (d) encapsulating the light-emitting diode (LED) to the yarns with a heat-shrinkable tube (HST).

A transparent polymer HST with a diameter of Ø2.0 mm is cut and passed through the parallel yarns to the diode area. The diode and conductive thread are held together firmly in the heat-shrinkable tube (HST) after heat is applied with a hot air gun which shrinks the HST. The shrinkage of the HST reduces its inner diameter to firmly hold the diode and

conductive yarn in place and encapsulate the joint. The ends of the HST are pressed together to ensure that the conductive yarns are still in parallel. This approach is time-consuming due to the length of time required for the drying of the conductive adhesive.

Encapsulation design two (using AT and HST): A schematic of the cross-sectional view of the embedding of the LED onto the conductive yarns and encapsulation with the transparent HST as shown in Figure 5.16(a). The SMD 0603 LED (Figure 5.16(b)) is placed on its side onto AT (Figure 5.15(c)), where its solder pads face the right and left sides. Two conductive yarns are placed in contact with the solder pads (Figure 5.16(d)) which act as the positive and negative terminals to power the LEDs. Another piece of AT is placed on top to secure the contact between the conductive yarns and the solder pads of the LEDs as shown in Figure 3(e). A \varnothing 2.0 mm transparent polymer HST is then cut and passed through the parallel yarns to encapsulate the yarn-diode area (Figure 5.16(f)). The joined diode and conductive yarns are held firmly in the HST after heat is applied and the HST shrinks.

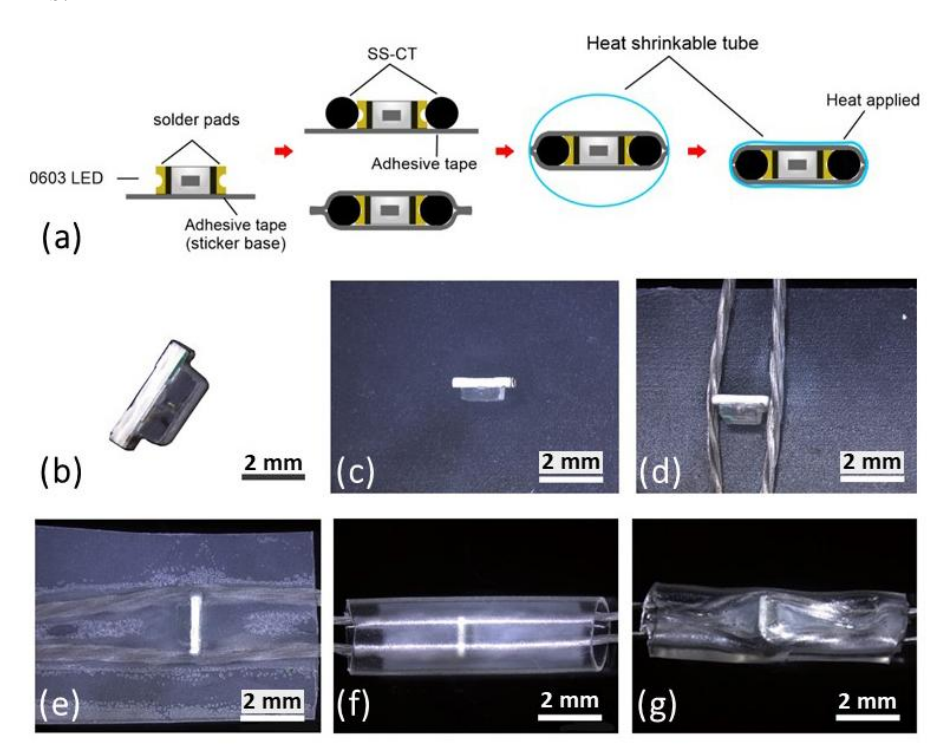


Figure 5.16. Design two fabrication processes of e-yarn. (a) schematic of cross-sectional view of embedding SMD 0603 LEDs on stainless-steel (SS) conductive yarns and encapsulating with heat-shrinkable tube (HST), (b) cross-sectional view of SMD 0603 light-emitting diode (LED), (c) placing side of LED on AT, (d) placing two SS conductive threads on both sides of LED, (e) concealing using adhesive tape (AT) to ensure yarns come into contact with LED, (f) placing HST over the concealed region, and (g) encapsulating the LED with the threads in an HST.

The shrinkage of the HST reduces its inner diameter which holds and encapsulates the joint firmly in place (Figure 5.16(g)). The ends of the HST are then pressed together to ensure that the conductive threads are still in parallel. This approach is fast and not time-consuming, and effectively secures the critical components together. Hence, this design is adopted and used to fabricate the e-yarns in this study.

5.3.1.2 E-yarn development

After confirming the ease and effectiveness of encapsulation design two which uses AT and HST to encapsulate the SS conductive threads (SS-CTs) to the LED on its two solder pads, the next stage involved the fabrication of the e-yarns with several LEDs embedded on a single strand of the yarns. Here, Scotch® brand transparent adhesive tape was used to first secure two SS-CTs to the solder pads (positive and negative) of a series of LEDs as shown in Figures 5.17(a) and 5.17(d). This leaves a trail of SS-CTs as the positive terminal and the other as the negative terminal. Secondly, Ø1.5 mm and Ø0.6 mm HSTs are separately used to encapsulate or insulate one part of the exposed long SS-CT. This insulation is done to prevent contact with the conductive surface of the thread which prevents current flow and hence no light will be emitted from the LEDs. The use of the Ø1.5 mm and Ø0.6 mm HSTs produces Samples 1 and 2, respectively. In Sample 1 as shown in Figures 5.17(a) to 5.17(c), after using the Ø1.5 mm HST to insulate one side of the threads, a hot air gun is used at a set temperature of 300°C to shrink the HST and firmly secure the components together. The ends of the HST are carefully pressed together and shaped as shown in Figure 5.17(g). For Sample 2, a Ø0.6 mm HST was used to insulate one side of the threads, and a heat source was applied at a set temperature of 300°C to shrink the HST to firmly secure the components together. Another Ø0.6 mm HST was used to insulate the ends of the SS-CT; see Figures 5.17(e) and 5.17(h). Afterward, the formed e-yarn was tested to ensure its workability and then braided. The braiding machine used is shown in Figure 5.17(i) which uses eight (8) bobbins (wound with RR threads) to braid around the e-yarn inserted in the middle.

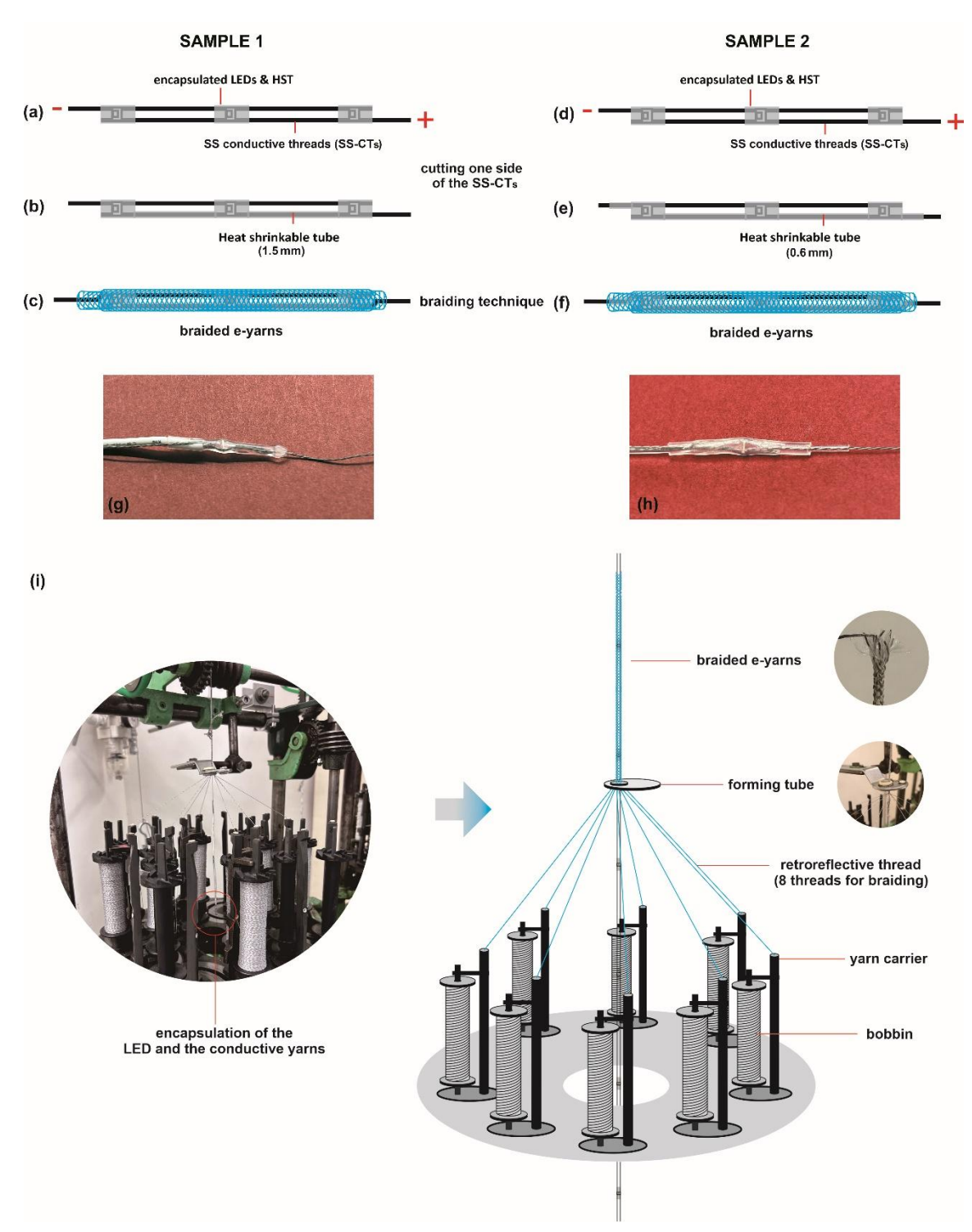


Figure 5.17. (a-c) E-yarn development process with Ø1.5 mm heat-shrinkable tube (HST), (d-f) e-yarn development process with Ø0.6 mm heat-shrinkable tube (HST), (g-h) shape of the ends of the encapsulated light-emitting diodes (LEDs) for Samples 1 and 2 respectively, (i) insertion and braiding technique of the e-yarns. Eight core RR threads are used to braid around two conductive threads with light-emitting diodes (LEDs) in series.

5.3.1.3 Braided e-yarns embedded in woven fabric

The braided e-yarns with a length of about 24.13 cm long were integrated into a woven fabric. A Rapier Sample loom (CCI/SL7900) with a dobby shedding motion was used to produce an e-textile with a 1/1 plain weave structure (Figure 5.18). Two textile samples i.e., one made with Sample 1 braided e-yarns and the other made with Sample 2 braided e-yarns, were produced with the yarns and loom parameters as shown in Table 5.4.

Table 5.4. Specification of the woven e-textiles
--

Electronic Textile	Size of HST used to cover the yarn	Yarn	composition	Weave structure	Loom Setting
		Warp	Weft		
Sample 1	Ø1.5 mm	40/2s Cotton	Retro- reflective yarn	Plain	Weft den./inch (40 picks/inch)
Sample 2	Ø0.6 mm	yarn	8-core braided e-yarn with 3 embedded LEDs		Loom speed (25 rpm)

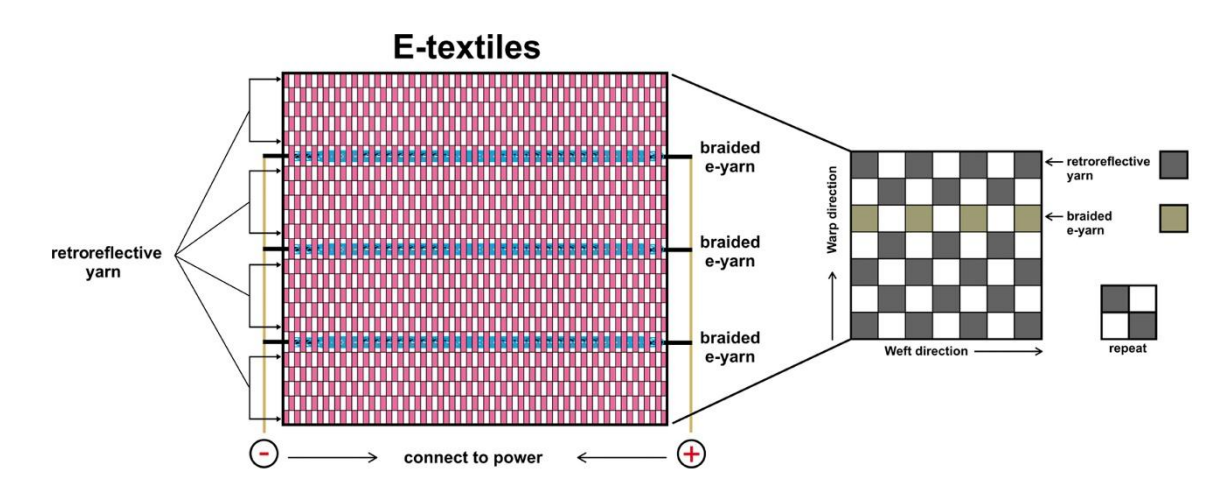


Figure 5.18. Design plan to produce the e-textiles on a loom

5.3.2 Characterisation

Structure morphology: The structure of the fabric samples was observed under an optical microscope (Leica M165 C) at a magnification of 5 mm. Additionally, the microscope was used to analyse or measure the dimensions of the encapsulated yarn, braided e-yarn, and insertion of the braided e-yarn into the fabric.

Tensile Strength: The tensile strength of Sample 1 and Sample 2 which comprises both eyarns and the braided e-yarns were measured using an Instron 5566 Universal Testing Machine. The test method used to measure the tensile strength of the samples was in accordance with ISO 2062:2009. Herein, the clamping distance or gauge length was set at 100 mm. Five samples were tested for each of Sample 1 and Sample 2 and the average results were calculated and recorded.

Fabric weight and thickness: An electronic balance (BX300, Shimadzu Corp.) and digital thickness gauge were used to measure the weight and thickness of the fabric samples produced with the insertion of the braided e-yarn into certain areas of the fabric. The woven fabrics measure 3 x 9.5 in. with two braided e-yarns (which contain six embedded LEDs).

Shear properties: The tensile and shear tester (KES-FB1) of the Kawabata Evaluation System of Fabric (KES-F) was used to evaluate the shearing properties of the e-textiles made from Samples 1 and 2. Here, each e-textile sample contains two braided e-yarns inserted one inch apart. The shearing test was conducted in only the weft direction under standard testing conditions of a relative humidity of $65 \pm 2\%$ for 24 h and temperature of $21^{\circ}\text{C} \pm 1^{\circ}\text{C}$ (atmospheric air).

Effects of power on heat distribution: Infrared (IR) images were taken to ensure heat distribution or dissipation when a 3V battery was used to supply the power. Here, the etextiles that measure 7.62 x 24.13 cm were placed on the wrist of a human arm for a 30-second exposure to IR radiation (for image capturing). A subject was recruited to wear the sample fabric for the images to be captured. The blue-to-white colour bar represents the lowest to the highest temperature in Figure 5.19. This measurement is done to investigate if the supplied power will result in heat distribution in the SS conductive threads which could affect the eventual wear comfort of the user.

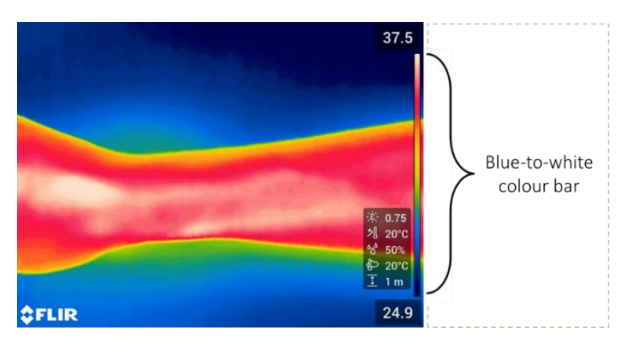


Figure 5.19. Temperature colour indicators for captured infrared (IR) images

Effects on lighting values: This is an experimental approach to investigate the effects of the AT, HST, and braided yarn structure on the light-emitting values produced by the SMD

0630 LEDs embedded in the SS conductive yarns. Here, the study adopts an experimental set-up of measuring the light intensity using a Lux meter placed one inch above the sample as shown in Figure 5.20.

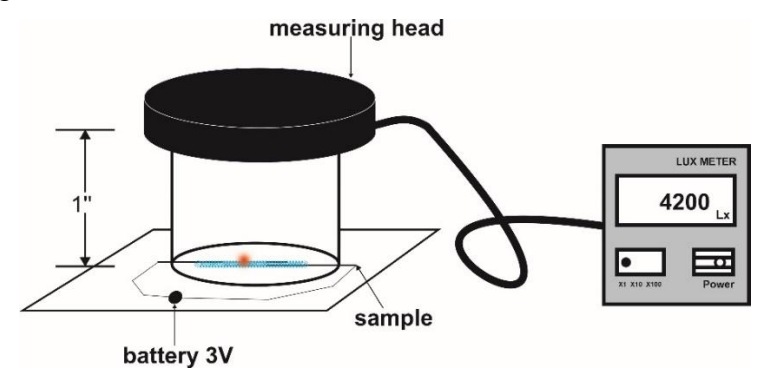


Figure 5.20. Experimental set-up to measure the light intensity values with lux meter

Washing testing: The braided e-yarns and sample fabrics were washed in a standard domestic washing machine in accordance with AATCC 135 and AATCC Monograph M6, Standardization of Home Laundry Test Conditions (66 ± 1 g of detergent, temperature of 20° C and fabric load of 1800 g), which influence methods for studies by (Lee et al., 2019). Here, four samples each from Samples 1 and 2 in the fabric and braided e-yarn forms attached to a white-cotton t-shirt (Figure 5.21) were used to test for durability, workability, and reliability, when subjected to 5, 10, 15, and 20 washing and drying cycles. Four samples were tested for each of Sample 1 and Sample 2 and the average results were calculated and recorded.

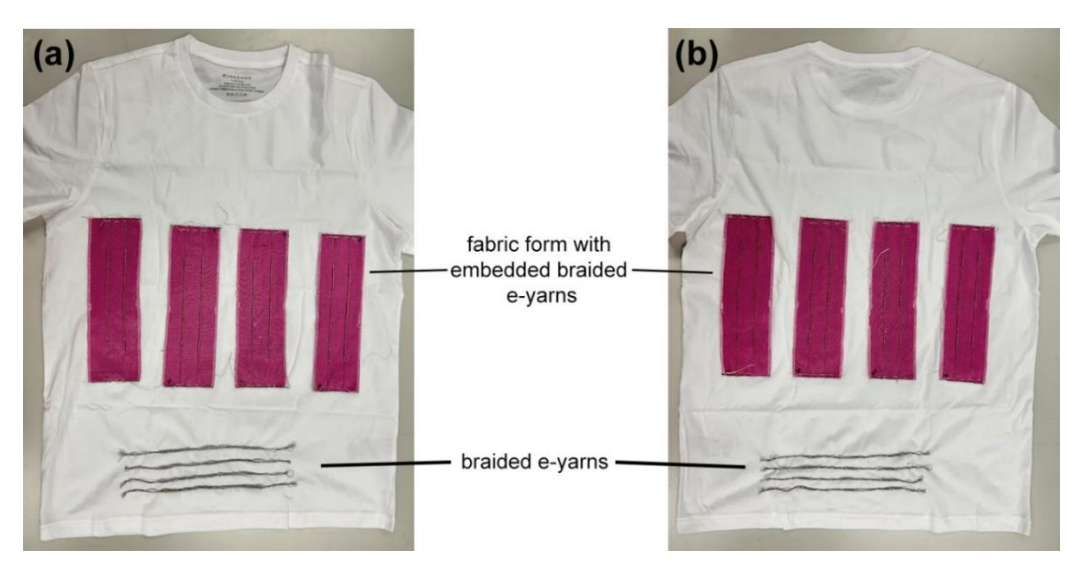


Figure 5.21. (a) Front view of a white t-shirt with Sample 1 in both fabric and braided e-yarn forms and, (b) back view of a white t-shirt with Sample 2 in both fabric and braided e-yarn forms

5.3.3 Results and Discussion

5.3.3.1 Structure morphology

A magnification scale of 5 mm was used to measure the dimensions of the encapsulated and braided e-yarns and the insertion of the braided e-yarn in the fabric (Figure 5.22). The images in Figures 5.22(a) and 5.22(b) show the amount of space occupied by the inserted braided e-yarns with the \emptyset 1.5 mm and \emptyset 0.6 mm HSTs for Samples 1 and 2 respectively. Here, the insertion areas are raised from the normal fabric structure. It is thus not surprising that the relative thickness of the insulated and braided areas with the \emptyset 1.5 mm HST is larger than the areas with a \emptyset 0.6 mm HST (Figures 5.22(c) and 5.22(d)). This issue could eventually affect the stiffness or flexibility of the fabric samples and hence the wear comfort of the sample.

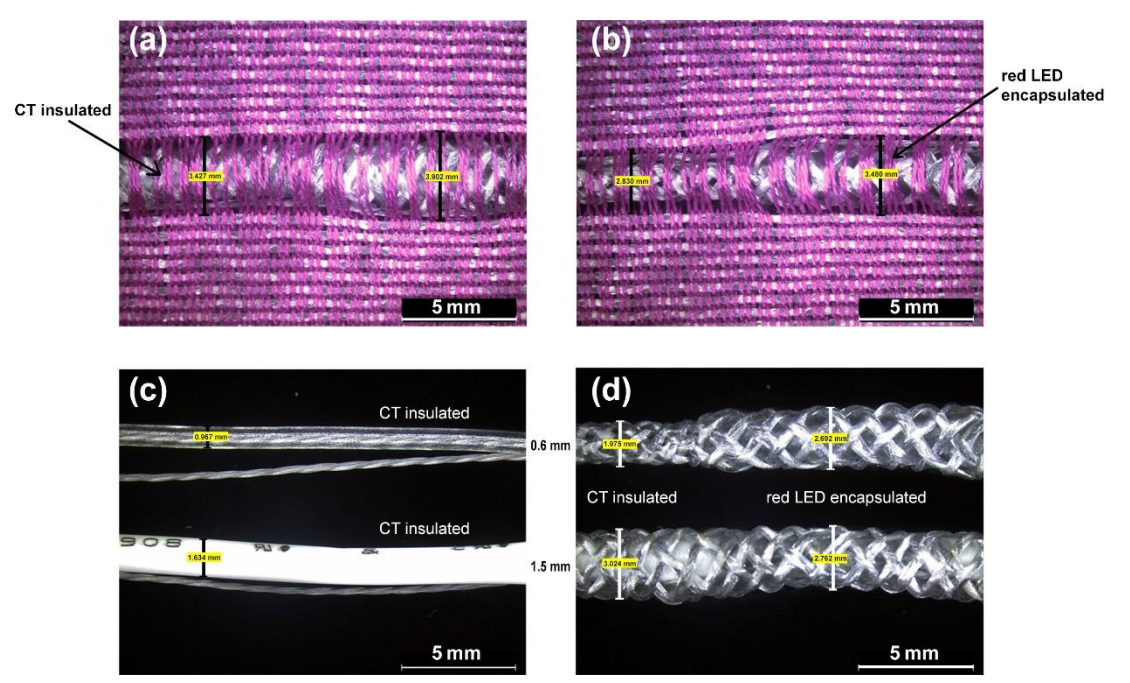


Figure 5.22. Surface morphology of: (a) sample 1 with $\emptyset 1.5$ mm HST, (b) Sample 2 with $\emptyset 0.6$ mm HST, (c) thickness of the insulated conductive thread with $\emptyset 0.6$ mm HST (top) and $\emptyset 1.5$ mm HST (bottom), and (d) thickness of braided e-yarns at CT insulated regions with $\emptyset 0.6$ mm HST (top) and $\emptyset 1.5$ mm HST (bottom) (Note: CT denotes conductive thread)

5.3.3.2 Tensile strength

The mechanical property i.e. the tensile strength of the e-yarns and braided e-yarns was investigated as reported in Figure 5.23. Results from Figure 5.23(a) show that, the breaking extension of the fabricated e-yarns for Sample 2 (5.72 mm) was less than that of Sample 1 (7.98 mm), which required a lesser breaking load. It was observed that, breaks

for both Sample 1 and Sample 2 occurred at the joints (where the SS-CT was encapsulated with the LEDs) as shown in Figures 5.23(c-1 and c-2) and 5.23(d-1 and d-2d) respectively. Herein, the encapsulated part of the SS-CT was however extended or stretched without breaking. This could be attributed to the extension property of these heat-shrinkable tubes (Ø1.5 mm and Ø0.6 mm). further results indicated that the braiding of 8-core retroreflective threads around the fabricated e-yarns influenced the tensile strength. As shown in Figure 4(a), the breaking extension and breaking load for both Sample 1 and Sample 2 increased. It is further confirmed that Sample 1 (made with Ø1.5 mm HST) has the highest tenacity as compared to Sample 2 (made with Ø0.6 mm HST).

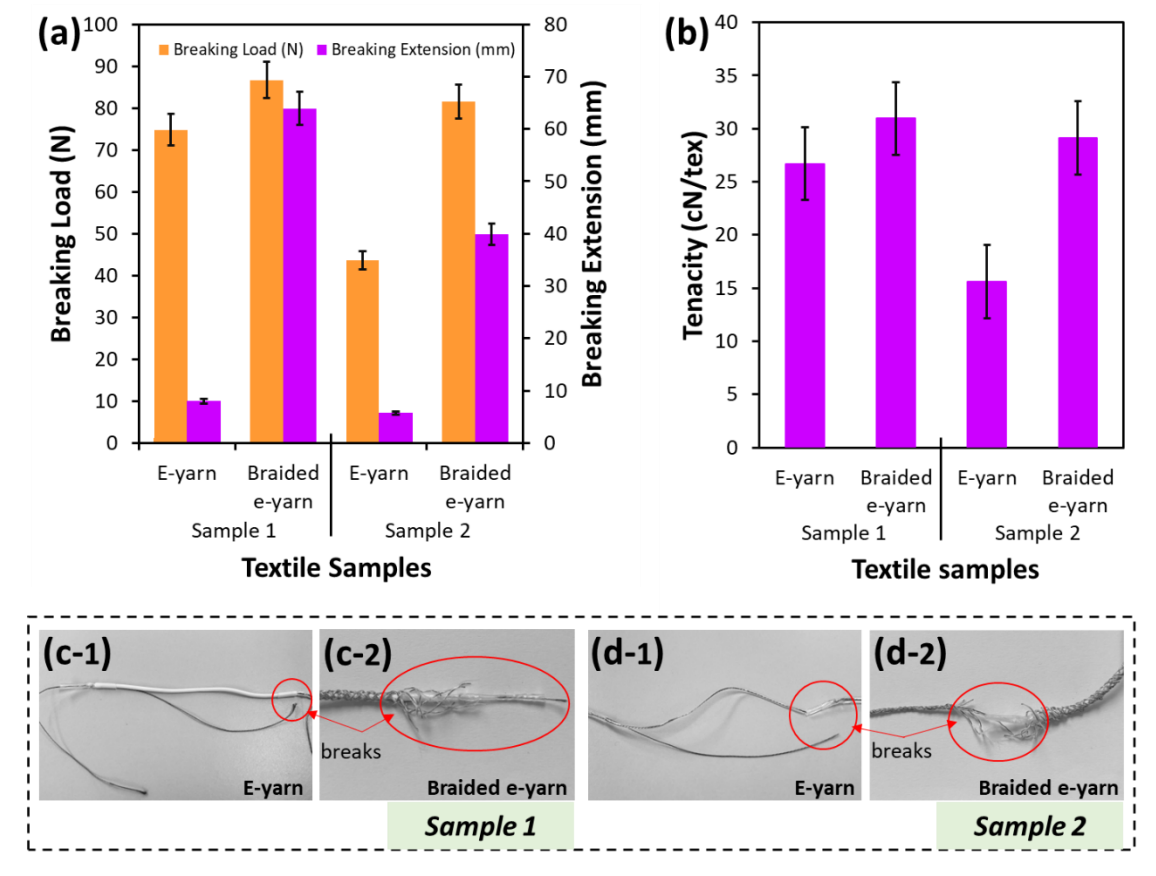


Figure 5.23. Tensile strength of e-yarns and braided for Samples 1 and 2. (a) breaking load and breaking extension for samples 1 and 2, (b) tenacity for samples 1 and 2, (c-1 and c-2) nature of the fabricated e-yarn and braided e-yarn after tensile strength test for sample 1 and (d-1 and d-2) nature of the fabricated e-yarn and braided e-yarn after tensile strength test for Sample 2.

5.3.3.3 Fabric weight and thickness

The final weight of the fabric samples varies, as shown in Figure 5. The weight of Sample 1 is higher (335 GSM) compared to Sample 2 (313 GSM). Even though the number of embedded LEDs, fabric dimensions, and structure are the same, the use of a \emptyset 1.5 mm

HST in Sample 1 could have attributed to the higher weight hence making the fabric heavier. On the other hand, the relative thickness of the encapsulated yarn with the use of a Ø1.5 mm HST is higher than that of Sample 2 encapsulated with a Ø0.6 mm HST. The thickness of the different encapsulated areas is very visible on the fabrics.

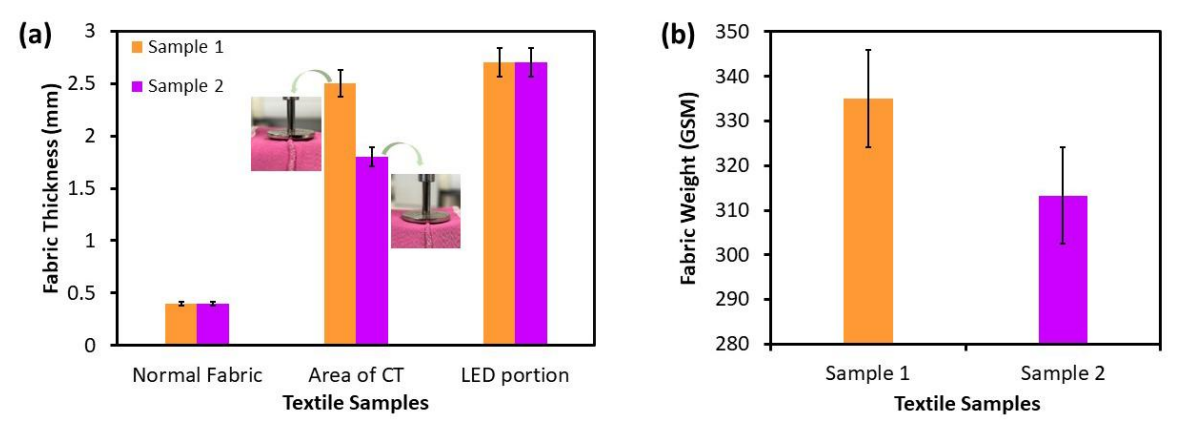


Figure 5.24. (a) Thickness of fabric samples, (b) weight of fabric samples. (Note: Area of CT means the area where the HST is used to cover the side of the SS-CT, and the LEDs portion means the encapsulated region that joins the LED to two SS conductive threads for positive and negative terminals)

5.3.3.4 Shear properties

The friction and contact pressure between yarns (Cho et al., 2022), and the sliding or moving of the yarns in the fabric structure against each other, influences the shear rigidity (G). When a shear tension of 10 gf/cm is applied to the samples, lower G means less resistance to shearing (the shear ability of the fabric) or higher G means higher resistance to shearing. Alternatively, lower hysteresis of the shear force at 2HG and hysteresis of the shear force at 5° (2HG5) mean good recoverability and poor recoverability for higher values, respectively. The results in Figure 5.25 show that the e-textiles made with the insertion of Sample 2 braided e-yarns (as the weft) have a lower G which suggests the ease of the shear ability of the yarns in the structure. However, due to their higher 2HG and 2HG5 values, the e-textiles have poor recoverability after shearing. This is relatively different from e-textiles made with the insertion of Sample 1 braided e-yarns. The sample exhibited a slightly higher G but relatively lower 2HG and 2HG5, which points to good recoverability after shearing.

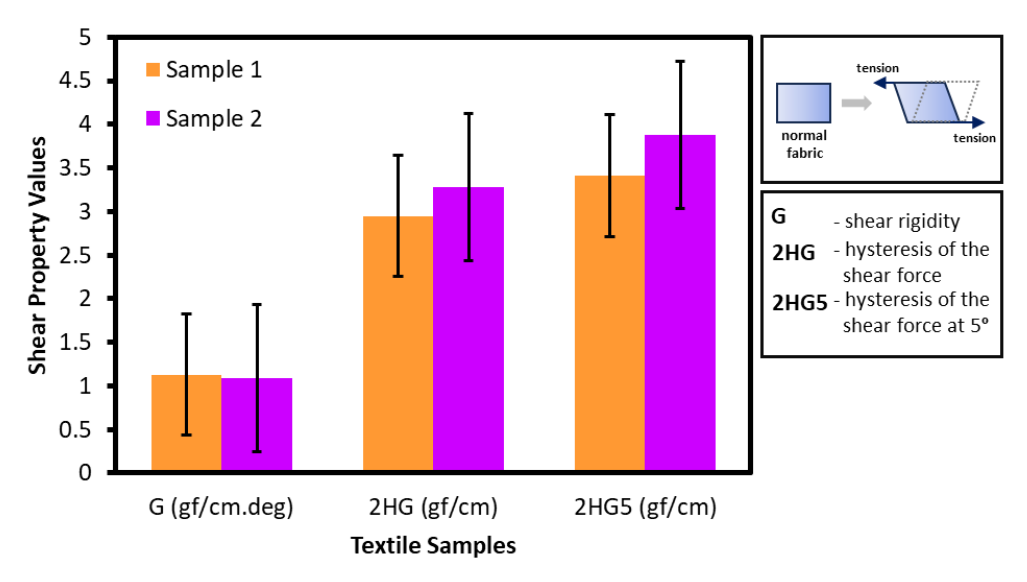


Figure 5.25. Shearing property values of e-textiles in the weft direction. (Note: G means shear rigidity, 2HG means hysteresis of the shear force and 2HG5 means hysteresis of the shear force at 5°)

5.3.3.5 Effects of power on heat distribution

The power supplied to the fabric samples was a 3V battery to light up the series of LEDs arranged in the braided e-yarns. Herein, the stainless-steel conductive threads (SS-CTs) allowed the flow of current from the 3V battery to power the LEDs, hence an IR thermographic image was taken to confirm the heat dissipation of the CTs and the LEDs when emitting light. Temperature is at normal levels when there is no supply of battery power to the braided e-yarns in the electronic textiles for samples 1 and 2. Furthermore, with the supply of power, the heat distribution and dissipation of the SS-CTs are too insignificant to affect the wear comfort of the e-textiles (Figure 5.26). Results from the IR thermographic images (using the hot spot mode measurement) show an increase in heat produced from the LEDs after 5 mins, i.e., 31.8°C to 32.3°C for Sample 1 (Figure 5.26(a-2)) and 5.26(b-2)) and 32.3°C to 32.5°C for Sample 2 (Figure 5.26(c-2) and 5.26(d-2)). These temperatures which range from 30.2 °C to 32.5 °C, are within a comfortable level that will not affect the wearer. This implies that the temperature of the LEDs when exposed to a thermal camera for 5 minutes increased under room temperature. These results are consistent with the findings in Simegnaw et al. (2022a), which shows the appropriateness of the developed braided e-yarns for e-textiles for wearables without affecting the wear comfort.

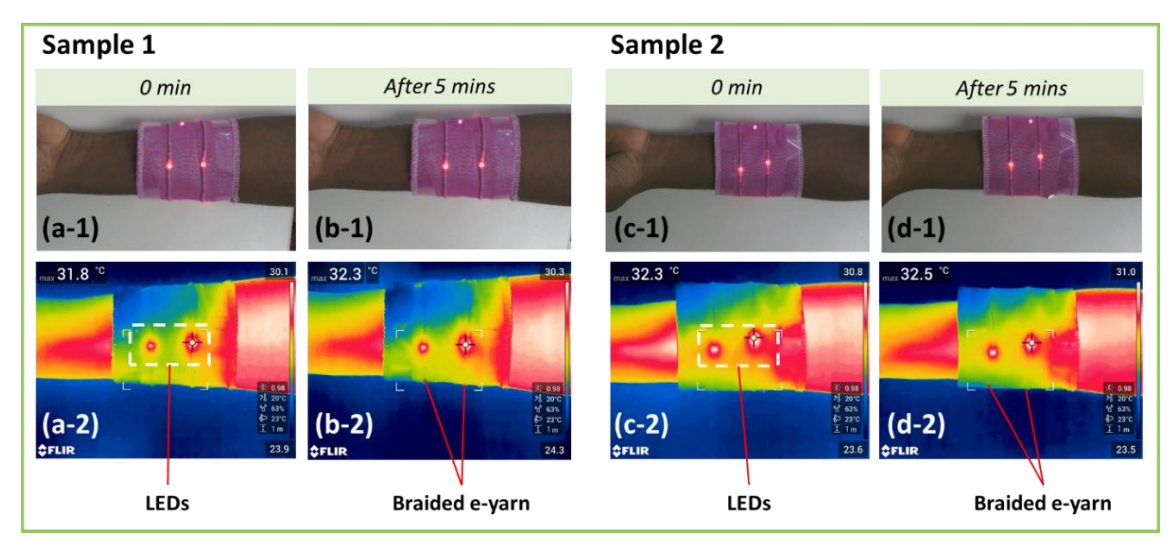


Figure 5.26. (a-1) and (b-1) Sample 1 electronic textiles powered with the use of a 3 V battery. (a-2) IR images of Sample 1 electronic textiles at 0 min and (b-2) IR images of sample 1 electronic textiles after 5 mins; (c-1) and (d-1) sample 2 electronic textiles powered with the use of a 3 V battery. (c-2) IR images of Sample 2 electronic textiles at 0 min and (d-2) IR images of Sample 2 electronic textiles after 5 mins.

5.3.3.6 Effects of encapsulation on light values

The light intensity produced by an LED is relatively different after materials are wrapped around its surface. Here, the experimental approach uses a digital Lux meter, where the lux values are measured to understand the effects of attaching the transparent adhesive tape (AT), heat shrinkable tube (HST), and braided yarn on the surface of an LED. The findings show a drop in light intensity of the final braided e-yarn after encapsulating with AT, HST, and yarns wrapped around the LED; see Figure 5.27. This shows that the use of the 8-core braided RR threads influences or blocks some of the light rays produced by the LEDs. Further results show a reduced light intensity when the braided e-yarns are woven into the fabric. This confirms that the composite fibre sheath affects the amount of light scattered (Satharasinghe et al., 2018). Additionally, findings show a 40% difference in the amount of light scattered when the e-yarns are braided with 8-core retroreflective and 46.15% when woven into the fabric. However, this decline did not eventually affect the visibility of the red lights produced by the LEDs. This is because a larger amount of the produced light is scattered through the voids of the braided sheath on the e-yarns.

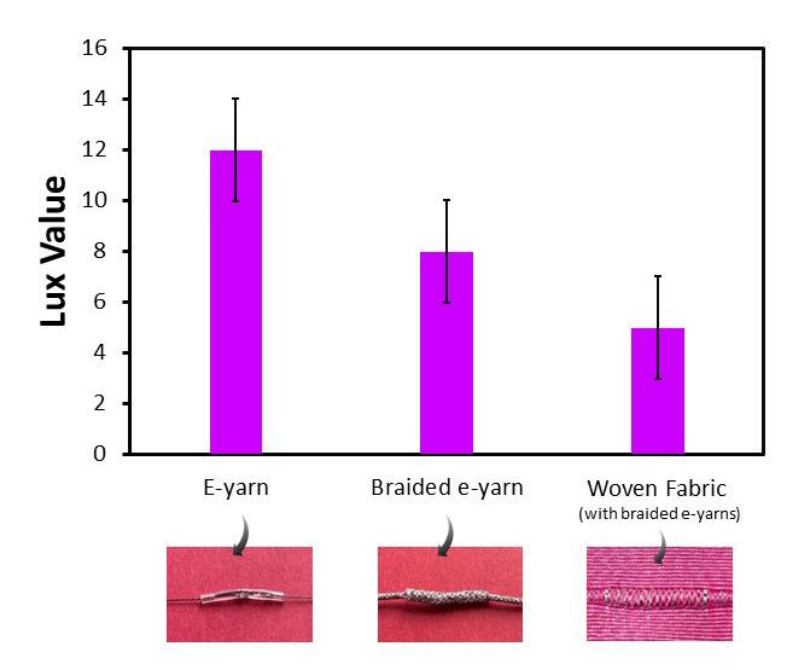


Figure 5.27. Effects of encapsulation on the light intensity values of the LEDs

Wash durability test

The samples in the braided e-yarn and fabric forms were then subjected to high mechanical agitation through a wash-and-tumble-dry process based on several cycles to investigate their durability and workability (Figure 5.28). The LEDs embedded in the braided e-yarns were still fully functional even after 20 cycles of washing and drying which demonstrates the durability of the braided e-yarns. However, the mechanical stress and agitation caused the detachment of the ends of the encapsulated area of the Set 1 braided e-yarns (Figure 5.29(a)). This issue could be attributed to the design and shaping of the ends but does not affect the final functionality of the yarns. The results from the washing test for the fabric form revealed that one of the LEDs is not functional after 10 to 20 washing and drying cycles for Sample 1 and after 20 washing and drying cycles for Sample 2 braided e-yarns. Further analysis revealed the instability of the LEDs which could be attributed to the manufacturing process (Figures 5.29(b) and 5.29(c)). Yarn breakage could have disrupted the supply of power to the LEDs but this is not the case. The breakage of the joined parts was revealed in Satharasinghe et al. (2018), who concluded that copper wire breakage in the manufactured e-yarns affects the supply of power and the non-functioning of the photodiodes. However, the non-functioning LEDs in this study might be the insufficient contact of the solder pads with the SS-CTs that act as the positive and negative terminals. This further prevents the power from circulating through the SS-CTs to light up the LEDs.

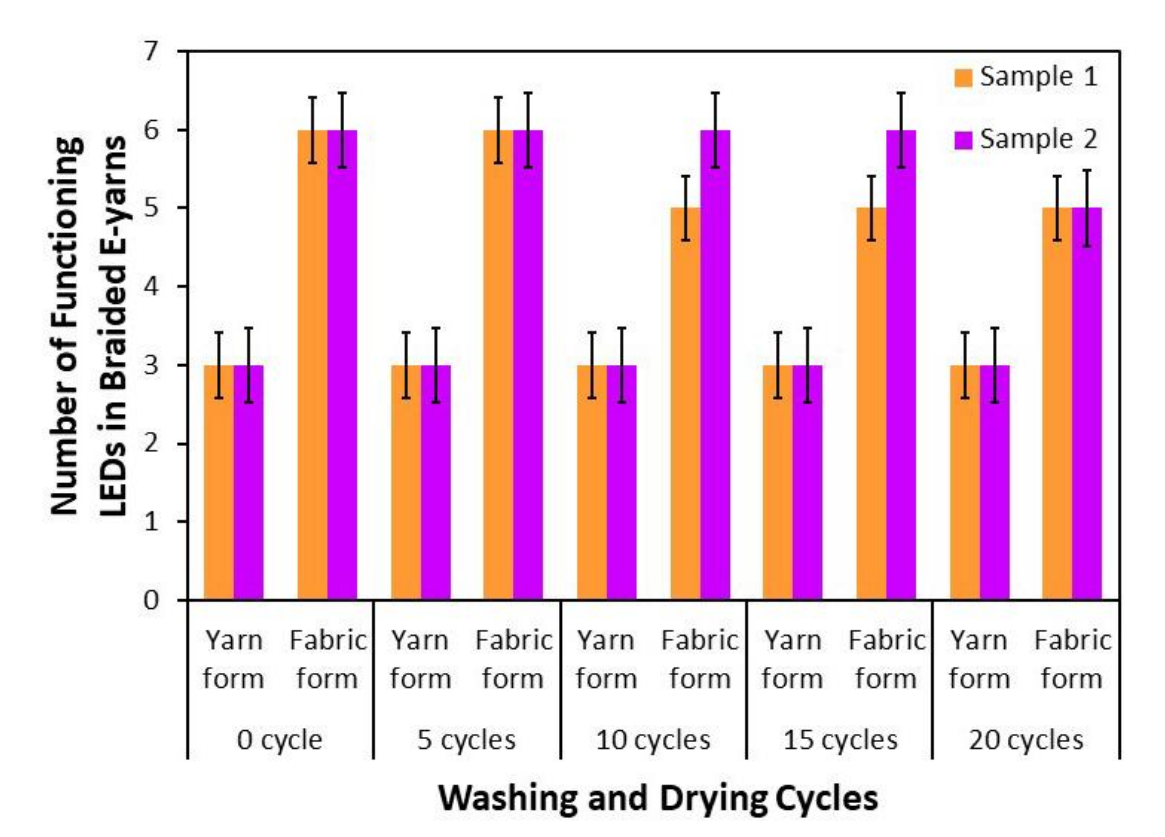


Figure 5.28. Washing durability results of braided e-yarns: various washing and drying cycles.

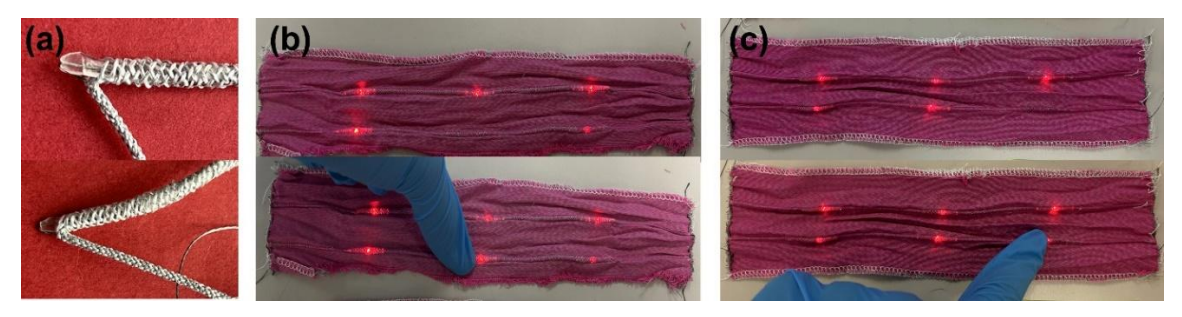


Figure 5.29. (a) Detachment of braid at end of the encapsulated area of sample 1 braided e-yarns, (b) non-functioning LED in Sample 1 braided e-yarns, and (c) non-functioning LED in sample 2 braided e-yarns

5.3.4 Proof of concept

A set of braided e-yarns was first tested to ensure their workability before insertion as weft yarn into fabric. Their short length meant that they had to be inserted by hand through the shed created and further tested before and after beat-up to ensure their workability. This was done to ensure that the reed movement to pack the braided e-yarns does not affect their functionality or damage them in the process. This procedure was employed during the insertion of all of the braided e-yarns after every inch in the textile structure. The rest of the plain weave was woven with RR yarns because the surface was

both flat and raised. Figure 5.30(a,e) and Figure 5.30(b,c,f,g) show the actual images of the braided e-yarns and e-textiles embedded with three and six LEDs respectively. The results show the ability of the braided e-yarns and e-textiles to emit light (when using a 3 V battery) even under bending stress done manually. However, the e-textiles produced by inserting Sample 1 braided e-yarns are not consistently flexible (Figure 5.30(d)) as compared to the much more flexible e-textiles inserted with Sample 2 braided e-yarns (Figure 5.30(h)).

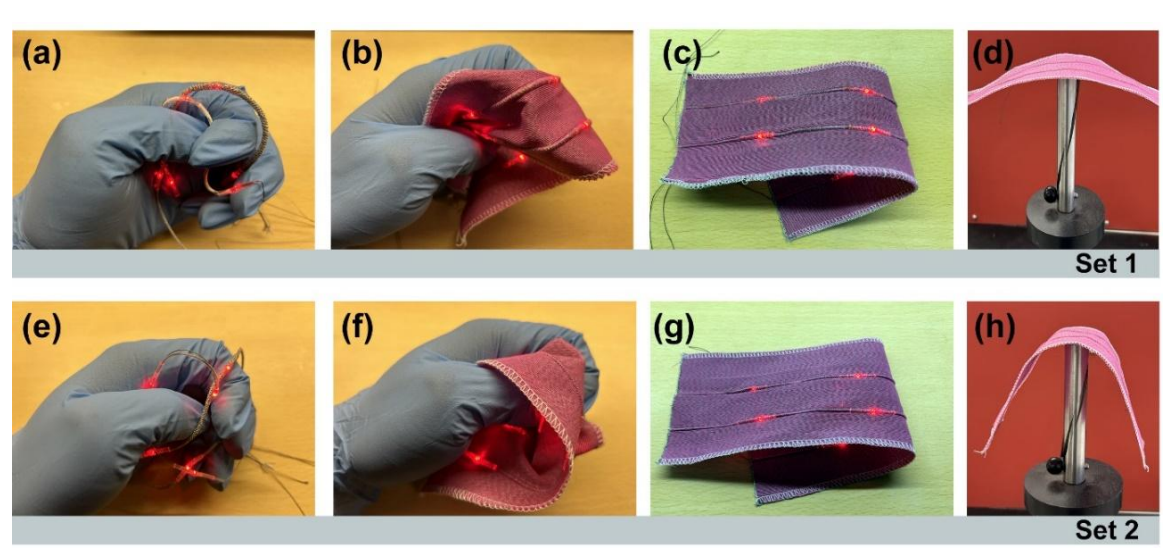


Figure 5.30. (a) Braided e-yarns with 1.6 mm HST, used for (b) and (c) woven e-textiles, (d) flexible nature of the e-textiles; (e) braided e-yarns with 0.5 mm HST, used for (f) and (g) woven e-textiles, (h) flexible nature of the e-textiles.

Illustration of the proof of concept here plus the ability of the braided e-yarns and resultant woven fabrics to withstand mechanical agitation from washing and drying cycles shows their potential for wearables. In fact, the work in this section paves the way for the potential use of the concept in the production of safety clothing to enhance the visibility of pedestrians when connected to sensors and a control unit.

5.3.5 Summary

The fabrication of a low-cost e-yarn with LEDs embedded in SS-CTs and the resultant woven e-textiles have potential applications for clothing that enhance the safety of pedestrians. Herein, LEDs are embedded in series in two SS-CTs, encapsulated with HSTs with different diameters to secure the LEDs to the SS-CTs, and insulating one side of the SS-CTs. A hot air gun is used to supply the appropriate heat to shrink the HST. Braiding is then used to wrap 8 core RR threads on the constructed e-yarn. The findings reveal the flexibility of Sample 2 braided e-yarns and e-textiles which use a \emptyset 0.6 mm HST.

The IR images show that the heat distribution and dissipation of the SS-CTs are not significant enough to affect the wear comfort of the e-textile. Furthermore, the e-yarns easily shear in the e-textiles with sectional weft insertion when using Sample 2 braided e-yarns. On average, Samples 1 and 2 braided e-yarns and e-textiles have approximately the same amount of total resistance. Similarly, the washing test shows the robustness of the braided e-yarns even after 20 washing and drying cycles. However, one of the LEDs is non-functional after 10 to 20 washing and drying cycles of Sample 1 braided e-yarns and after 20 washing and drying cycles of Sample 2 braided e-yarns. This issue could be attributed to the attachment and securing method of the LEDs to the SS-CTs. It is further confirmed that Sample 1 (made with Ø1.5 mm HST) has the highest tenacity as compared to Sample 2 (made with Ø0.6 mm HST). To conclude, Sample 2 braided e-yarns and electronic textiles have less fabric weight and are more flexible which retains the characteristics of the woven fabric as compared to Sample 1.

Finally, a proof of concept illustrates the effectiveness of the e-textiles with the braided e-yarns to produce the necessary red lighting effects for pedestrian safety purposes. The success of this experiment calls on further research work to enhance the durability and flexibility of braided e-yarns and e-textiles to provide better wear effects to users. Additionally, future research studies can integrate effective energy harvesting devices, for example, yarn-based supercapacitors, to e-yarns in a textile material. This design structure can effectively supply an appropriate amount of energy or power needed to power the LEDs embedded in e-yarns. This would contribute to a much lower weight of the external batteries when attached to the textile to supply power which would reduce negative impacts on the wear comfort.

5.4 Smart interactive clothing for pedestrian safety

This section describes the integration of the developed system in section 5.2 to the retro-reflective fabrics described in Chapter 4 to form smart interactive-based clothing prototypes. Herein, the effectiveness of the clothing was investigated, and results were presented.

Light-emitting diodes (LEDs) are light-producing sources that are dependent on electroluminescent and semiconductor materials (Demerdash and Mostafa, 2018). LEDs are semiconductor devices that according to Banerjee and Chattopadhyay (2018) emit lights (either white or from red to blue-violet) when there is a flow of electric current. They

are further regarded as "electrically efficient light sources" as opined by Lanoue et al. (2019), where the wavelength of the produced light influences its efficiency. For example, blue and red wavelengths are regarded as more efficient than that of orange or green. The use of LEDs has played a vital role in fabricating products like shoe lights, arm bands, and headlamps amongst others for varying applications. Aside from its use in rescue operations, individuals have also applied them during running or hiking most especially at night time. The use of LEDs at night is critical to producing sufficient illumination for effective recognition by an approaching vehicle. Such applications have influenced researchers to advance the use of LEDs with other technologies for smart clothing.

These developments are for relevant purposes like ensuring safety, communication, entertainment, and aesthetic effects in the environment. Research studies have been conducted to satisfy any of the above-mentioned purposes. Notably, Cheng et al. (2009) developed an intelligent clothing that produces lights. This approach utilises optical fibres where the ends are connected to LEDs for sufficient illumination. The eventual output is identified as promising protective clothing for users. In a study by Kim et al. (2017), an interactive smart fashion with visible light communication ability was designed (Figure 5.31(a)). A stepwise strategy was adopted to develop the smart fashion with a modular zipper slider and strapped cuffs that housed the LEDs. This modular system was designed for easy detachment and attached to the clothing by the users. With an enabling Bluetooth platform of the visual-MIMO (multiple-input multiple-output), users can communicate emotionally by changing the colour patterns of the LEDs. In a more design aesthetic approach, Demerdash and Mostafa (2018), Syed Muhammad and Ahmed Dawood (2020), and Kwasa et al. (2022) reported on the creation of an illuminative smart fashion for women. Figure 5.31(b) illustrates the design produced by Demerdash and Mostafa (2018). This design concept employed LEDs arranged in varying patterns on a constructed garment to improve its aesthetic value or appeal.

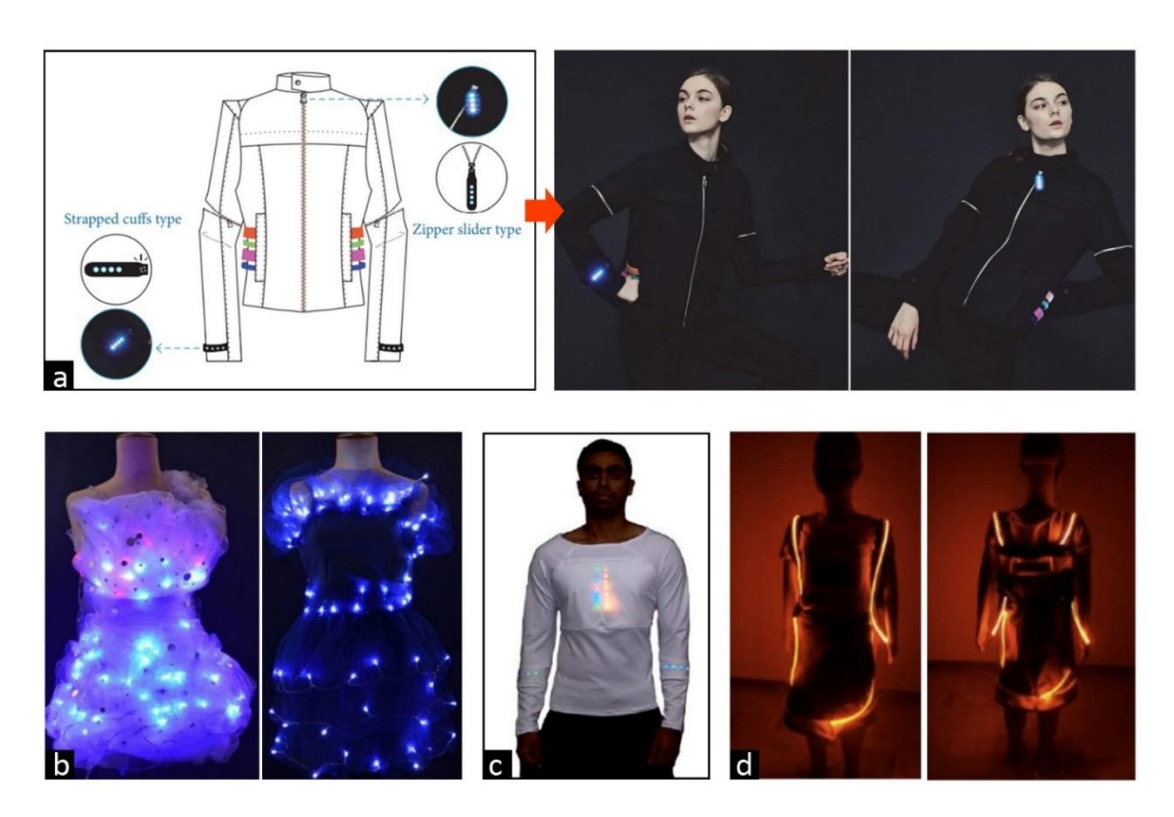


Figure 5.31. Application of light-emitting materials for safety and aesthetic clothing. (a) interactive smart fashion with visible light communication ability (Kim et al., 2017), (b) illuminative smart fashion for women (Demerdash and Mostafa, 2018), (c) design concept of LED clothing for cyclists (Wei et al., 2015), and (d) transformable warning clothing for children (Studzińska et al., 2022)

Towards a more safety protection application, Wei et al. (2015) designed and integrated LEDs into clothing to improve the visibility of bicyclists at night time (Figure 5.31(c)). In this study, the proof of design concept revealed the direct integration of a battery holder and arranged LEDs fitted at the chest, back, and sleeve region of the clothing. This approach acknowledges the non-washability and bulky nature of the fitted parts. In a recent study by Studzińska et al. (2022), they reported the design of transformable warning clothing to improve visibility and ensure the safety of children during night traffic (Figure 5.31(d)). In this approach, side-emitting polymer optical fibers (SEPOF), fluorescent materials, and 3M reflective tapes were used in developing the warning clothing. SEPOF was connected to light light-producing source with SMD LEDs where the focused lights are transmitted along the fibers arranged on the clothing. These assemblies are not sewn but placed on the clothing, hence promoting easy removal. Results revealed the improved visibility of the clothing in a darkroom setting.

The study acknowledges the gains and approaches adopted by other researchers for the integration of LEDs in clothing for different applications. This experimental work details a different approach in using LEDs and microcontrollers for effective smart interactive clothing to improve the safety of pedestrians on the road at night-time. As early on mentioned, the LEDs are connected to other sensors with a microcontroller that produces sound, lights, and vibrating effects which have not been explored by other studies. The smart interactive system developed for clothing will benefit the pedestrians most esp. blind and deaf individuals who use the road at night time. This will aim to alert them of an approaching vehicle. Herein, braided e-yarns were developed with green and red SMD 0603 LEDs to produce effective lighting effects to alert the drivers. These lighting colours were chosen due to their improved visibility and increased conspicuity (Fakhrmoosavi et al., 2021). The application of green and red lighting effects is imperative due to their wavelength situated between 585 nm to 620 nm within the visible light spectrum. These colour amber are visible to users on the road from a very far distance.

5.4.1 Methodology

Materials: In the experimental work, a 12 V LED projector lens (with 8000 lumens and 6000K white light) for automotive headlight was purchased from Kindle Industry Limited, Shenzhen, China. This product together with its related accessories such as a switch, rechargeable battery, and wires, were used to build simulated car headlights for testing of the interactive clothing. Other materials such as Litz wires, were purchased from BXL2001, OSCO Ltd., Milton Keynes, UK with a 254µm outer diameter. This commercially available wire includes seven copper wires which are enamelled and covered in nylon. These wires were used to effectively connect the terminals of the braided e-yarns and the various sensor components like the light detector sensor and vibration motor. Subsequently, 3-ply SS conductive yarns (purchased from Fujian QL Metal Fiber Co. Ltd, China), SMD 0603 green light-emitting diode (purchased from RS Component Ltd, UK) and SMD 0603 red light-emitting diode (purchased from Shenzhen Lianxinrui Technology Co. Ltd, China), were used to develop a braided e-yarns which can separately produce red and green lighting effects. They were used together with the developed interactive controlling unit or system to produce the prototypes for the smart interactivebased clothing for pedestrian safety.

5.4.1.1 Initial prototype

In this sample making, jacquard woven retro-reflective fabrics with African patterns were utilized in producing the garment. These fabrics were produced from

Experiment I carefully captured under Chapter 4. Here, results revealed that the fabric samples (RF1, RF2, and RF3) are retro-reflective, and have good thermal conductivity, tensile strength, and air permeability. Subsequently, the THV results proved the suitability of all fabrics for both summer and winter men's and women's wear as compared to the suitability of fabric samples RF2 and RF3 for only women's summer wear. Other materials used include 100*3 SS conductive yarns, fabric stiffer, snap fasteners, and sensory devices. A schematic diagram or prototype plan was illustrated (Figure 5.32) to show the various arrangements of the components (RR woven fabrics and sensory devices). In the structural arrangement, two light detector sensors were placed on the front bodice and back bodice, a vibration motor was placed at the shoulder region, the controlling interactive system or unit was positioned at the upper part of the back bodice, and a battery package was positioned at the lower left side.

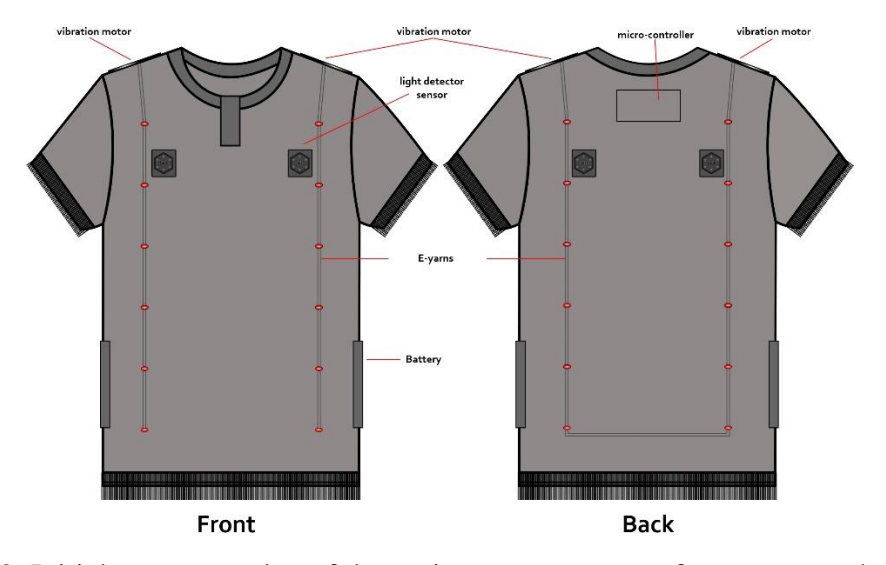


Figure 5.32. Initial prototype plan of the various components of a garment to be constructed using jacquard retro-reflective woven fabrics.

Different parts i.e. fabric pattern cutting, light detector sensing casing, vibration motor casing, and interactive control unit were constructed separately before being joined together. The 100*3 SS conductive yarn aided in creating the appropriate circuitry on the constructed garment to connect the various sensory devices and the interactive control unit. As earlier indicated, retro-reflective woven fabrics from Experiment I used African design patterns and jacquard weaving technology was utilised in producing clothing that houses various sensory devices, interactive units, and e-yarns. Figure 6.20a shows the front and back appearance of the assembled clothing with the attached components. It is evident that the casing of the various sensory devices formed part of the clothing design. As such,

Figures 5.33(c), 5.33(d), 5.33(e), and 5.33(f) illustrate the positioning of the light detector sensor casing (on the front bodice), vibration motor casing (placed on the shoulder line), pocket to house the controlling unit (placed at the upper side of the back bodice) and pocket for housing the battery pack (placed at the side) respectively. To report on the reflective effects of the assembled clothing, an experimental qualitative approach of capturing the effects from a 1.5m distance using a digital camera. This was captured in a darkroom condition at the laboratory, where the design patterns are slightly visible on the clothing with a reflective ability (Figure 5.33(b)).



Figure 5.33. Assembled components on the jacquard retro-reflective woven fabrics. (a) the appearance of the assembled components on the front and back bodice, (b) reflective effects in the darkroom setting taken by a digital camera, (c) and (d) positioning of the light detector sensor and vibration motor, (e) positioning of the controlling unit at the upper side of the back bodice, (f) pocket for housing the batter pack to power the microcontroller.

Alternatively, to test the effectiveness and workability of the assembled components for the research concept, a hand-held touch was directed to the light detector sensor on the front bodice in a darkroom condition. At light detection, the micro-controller (micro: bit) triggers the production of lighting effects from the red LEDs (Figure 5.34(c)) arranged vertically on the clothing (both back and front bodice) followed immediately by the action of the vibration motor and, production of sound from the micro-controller. These additional safety features are aimed at improving the conspicuity of and alerting the pedestrian. Subsequently, the production of the lighting effects draws the attention of the

approaching vehicle to the presence of a pedestrian on the road. This first success of the research concept expands the possibilities of advancing smart interactive systems for pedestrian safety.

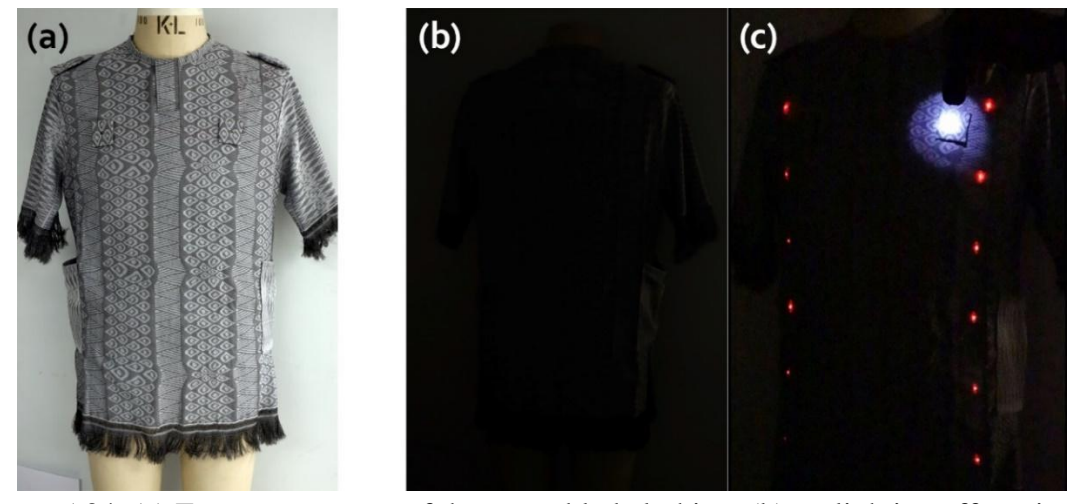


Figure 5.34. (a) Front appearance of the assembled clothing, (b) no lighting effects in the darkroom setting taken by a digital camera, (c) lighting effects of the red LEDs when light is detected in the darkroom conditions at the laboratory taken by a digital camera.

5.4.2 Characterisation

Terminal voltage change: This is an experimental set-up approach to investigate the change in discharge voltage when the batteries are used to power the various components in the smart clothing. Herein, a FLUKE 107 CAT III 600 V Digital Multimeter was used to measure the voltage change at an interval of every 15 mins. This test provides a significant understanding of the length of time these batteries can run for the effective functioning of the smart interactive clothing.

Effects of vibration patterns: This is an experimental set-up approach to investigate the vibration patterns of the vibration motor using three different patterns set with a time pause of 100ms, 300ms, and 500ms. As shown in Figure 5.35(a), the vibration is measured from the vibration motor placed on top of the accelerometer which is connected to the computer for data logging. Additionally, in Figure 5.35(b), a retro-reflective textile material is placed in between the vibration motor and the accelerometer to investigate any change in vibration patterns recorded.

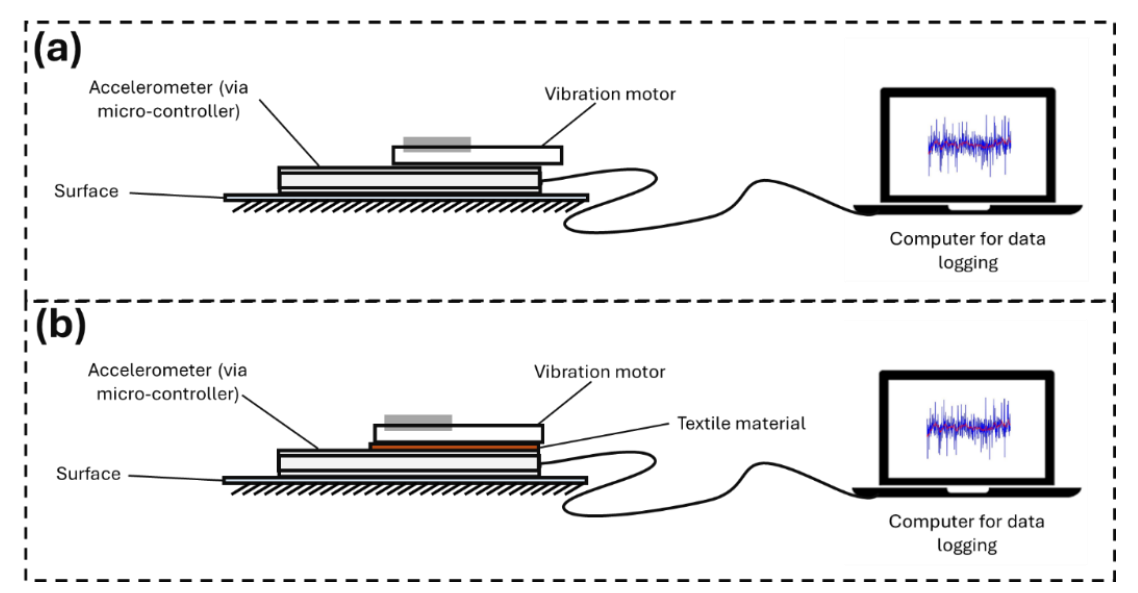


Figure 5.35. Experimental set-up to measure the vibration patterns of the vibration motor. (a) no retro-reflective textile material is placed in between the vibration motor and the accelerometer. (b) retro-reflective textile material is placed in between the vibration motor and the accelerometer

Effects of sound patterns: In this experiment, the sound levels are measured and recorded on the computer from the micro-controller. Herein, three different sound patterns are investigated from the list of play tones in the Music section of the MakeCode for the micro-controller. The data is logged onto the micro-controller, which is transferred and analysed on the computer.

Range of detection: In this experimental set-up, using a developed simulated car with 8000 lumens headlights (Figure 5.36), the light detector sensor on the interactive clothing was tested to detect and measure the light values from a range of distances. In this experimental setting, the range of detection was conducted at 5 meters, 10 meters, 15 meters, 20 meters, and 25 meters (Figure 5.37). As such, the simulated car headlights were positioned at various range points to investigate if the light detector sensor from the smart interactive clothing could detect the lights produced by the headlights. With the presence of lights coupled with its detection, the light detector sensor transmits a signal to the microcontroller to activate the vibration motor and the LEDs in the braided e-yarns. The microcontroller is connected to the computer to record readings for further visualization.

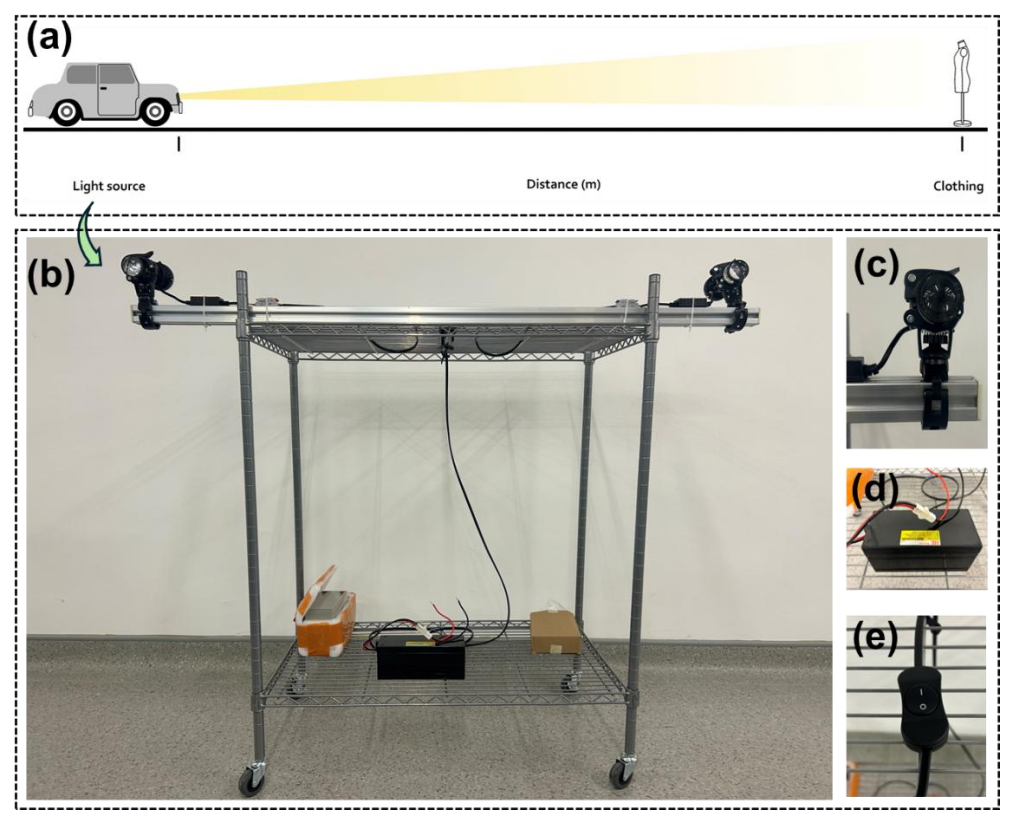


Figure 5.36. Experimental set-up to test the range of detection of the smart interactive clothing. (a) image of the laboratory experimental set-up (b) image of the developed simulated car headlights (c) 12V LED projector lens with 8000 lumens and 6000K white light for automotive headlight (d) image of the rechargeable battery (e) image of the switch button to turn on/off the headlight.

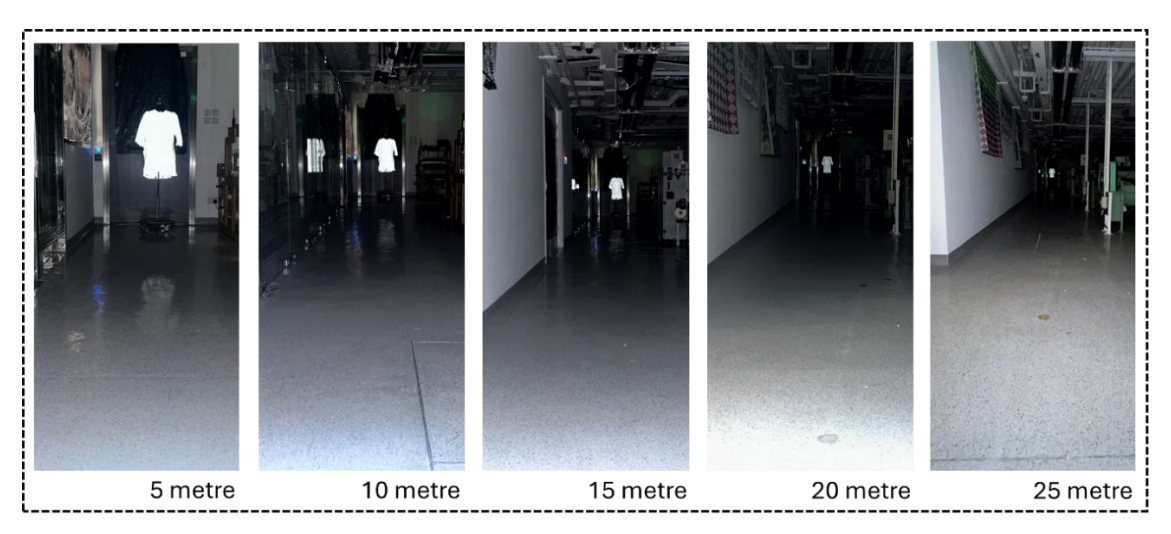


Figure 5.37. Laboratory set-up for the range of detection test (Note: the laboratory settings and the power of the battery could influence the lights produced and detected)

5.4.3 Evaluation

This section reports on the results from the vibration patterns, sound patterns, range of detection, and the battery performance to power the braided e-yarns, the vibration motor, and the interactive unit.

Effects of vibration patterns

The intensity and delay time of the vibration patterns are effective in alerting the pedestrian about an approaching vehicle. Herein, three delay times (100ms, 300ms, and 500ms) were investigated to understand the vibration patterns (Figure 5.38). In Figure 5.38(a-1), the vibration patterns are very intense with less delay time of 100ms. This implies that the pause time or delay is shorter hence the vibration pattern is somewhat continuous. With a much longer delay time of 300ms and 500ms (Figure 5.38(b-1)(c-1)), the vibration patterns are significantly different. These vibration patterns mimic its functionality when in contact with the human skin. To understand if the insertion of a fabric could influence the vibration patterns, a further test was conducted. In Figure 5.38, it can be observed that the acceleration of the vibration patterns for all three delay times has reduced when in contact with the retro-reflective clothing. However, the vibration patterns remained similar to previous results. This implies that, when a fabric comes into contact with the vibration motor and the human skin, the acceleration felt by the human being would be slightly reduced even though the vibration patterns remained similar to previous results.

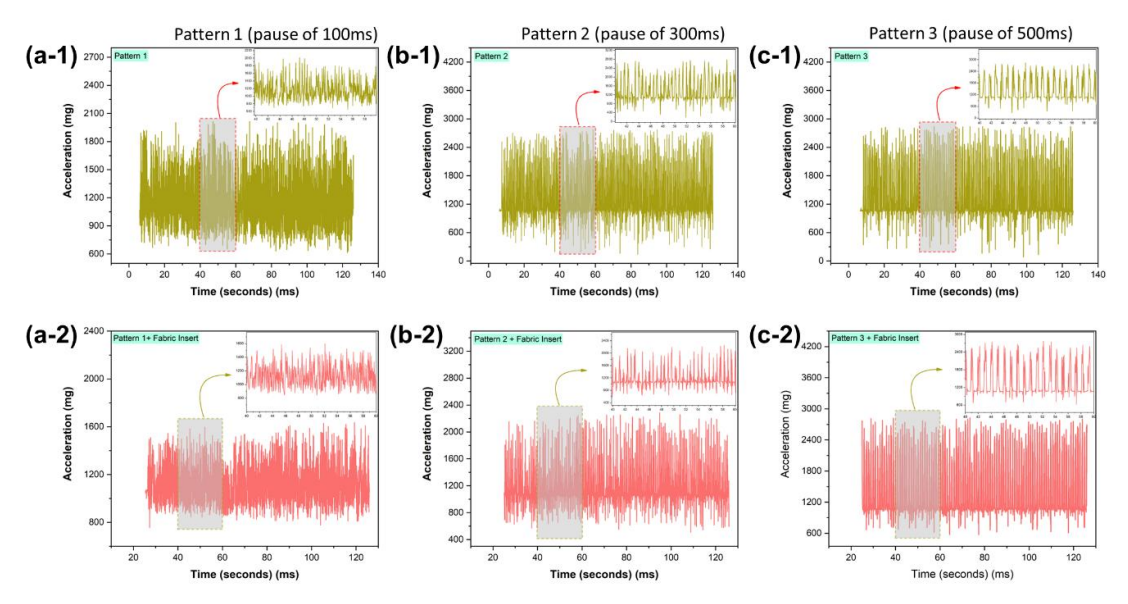


Figure 5.38. (a) No retro-reflective textile material is placed in between the vibration motor and the accelerometer (b) retro-reflective textile material is placed in between the vibration motor and the accelerometer.

Effects of sound patterns

The effect of sound patterns plays a critical role in alerting the wearer to be aware of the approaching vehicle on the road. This is confirmed in a previous study by Belenguer et al. (2022) on the use of sound levels to effectively alert pedestrians on the road. Hence, a simple measurement of three sound patterns from the microcontroller was conducted to understand their sound levels as shown in Figure 5.39. It was evident that Ringtone Low B, Middle B, and High B have a sound level of 157Hz, 153Hz, and 161Hz respectively as shown in Figures 5.39(a), 5.39(b), and 5.39(c). This implies that Ringtone High B has a higher sound effects (as confirmed in Figure 5.39(d)), hence can be heard more and clearly, a situation needed in alerting the wearer on the road.

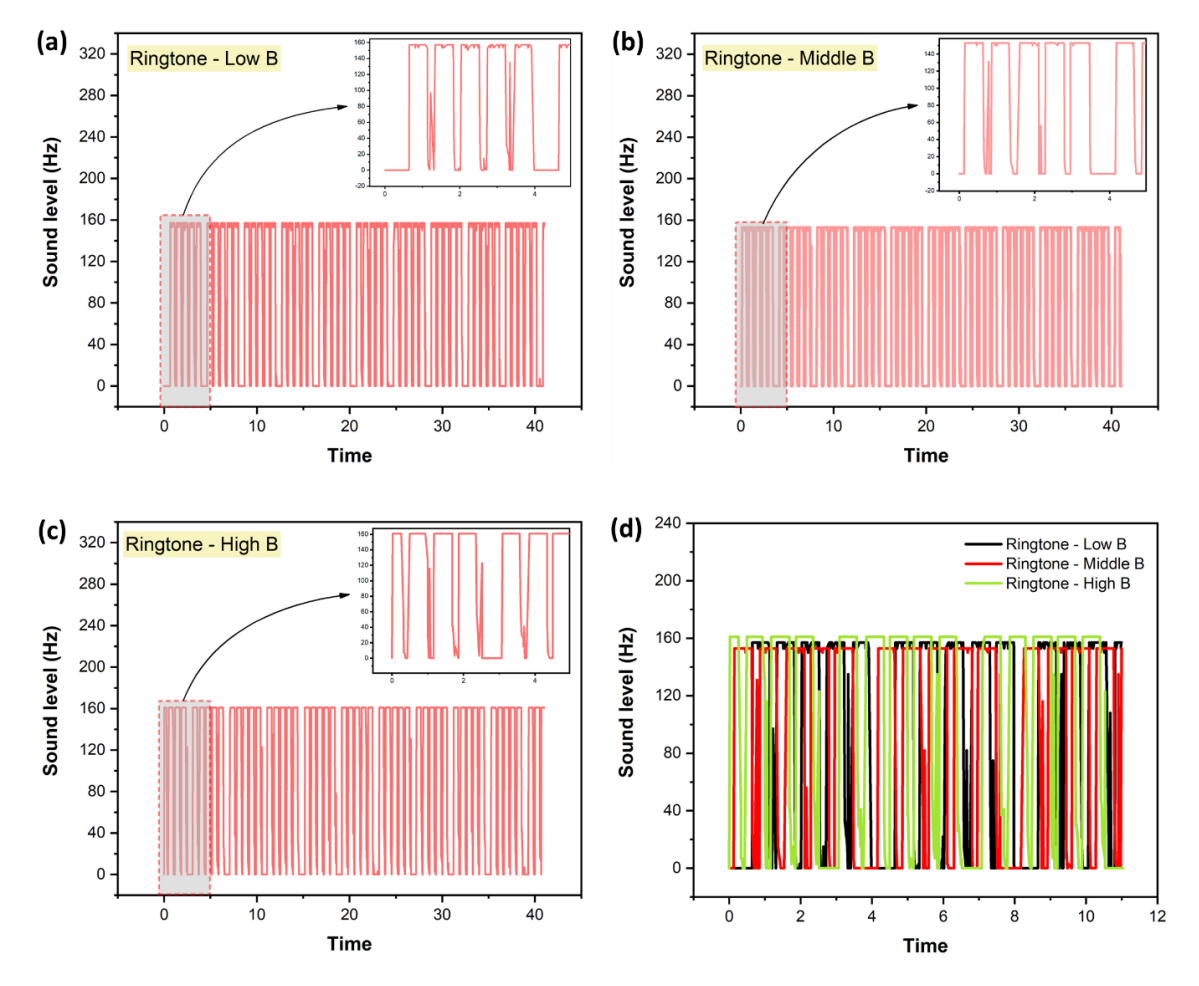


Figure 5.39. Sound levels (Hz) of (a) ringtone - low b. (b) ringtone - middle b. (c) ringtone - high b. and (d) sound levels of all ringtones from the micro-controller.

Range of detection

The ability of the interactive system accompanied by the light detector sensors to detect the appropriate light levels is important for effective recognition by the driver and response to the pedestrian. To understand the range of detection of this system, an experimental set-up was conducted at the laboratory using a built simulated car headlight (Figure 5.40(a)). It was evident from the results in Figure 5.40(b) to 5.40(f) that, the light levels recorded reduced as the distance between the light and the interactive clothing was afar. Furthermore, at a distance of 25 metre, the lights from the headlights were still detected by the light detector sensor on the interactive clothing with an average light level of 10.35 (average of the first 100 values).

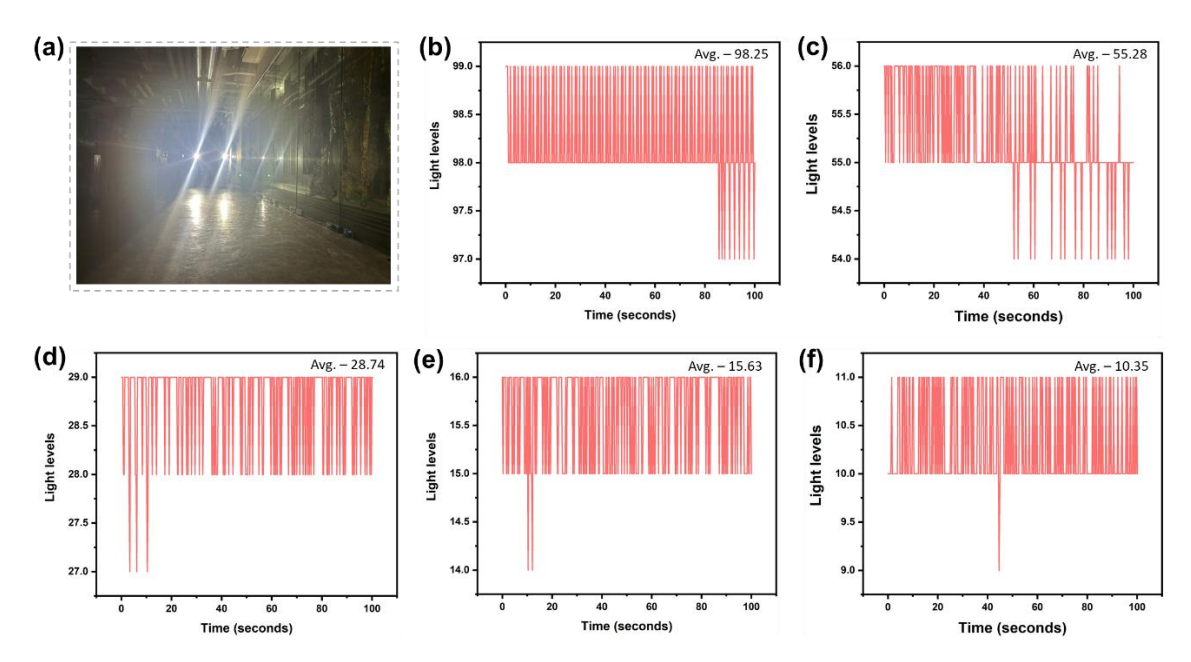


Figure 5.40. The range of detection of the presence of lights from (a) simulated car headlight; under (b) 5 metre, (c) 10 metre (d) 15 metre, (e) 20 metre and (f) 25 metre.

5.5 Prototypes

Herein, two smart interactive clothing were designed; one shirt sleeve garment and one long sleeve garment, with design inspirations drawn from the African design patterns most specifically from the Sirigu wall paintings of Ghana. These are figurative and geometric designs patterns created on the walls of indigenous mud houses with significant symbolic meanings and have been well described in studies (Wemegah, 2013, Woets, 2014, Asante and Opoku–Asare, 2011, Asmah and Okpattah, 2013). Herein, the description of the two smart interactive clothing is provided below.

5.5.1 Smart interactive clothing one

In this work, a sleeve men's shirt was designed as shown in the technical sketch (Figure 5.41(a)). This illustrates the positioning of the various braided e-yarns, the battery,

micro controller, and the sensors. Herein, the vibration motors are placed at the shoulder region, the light detector sensors are placed at the front and back side of the shirt, the battery unit to power the micro-controller is located at the left side of the bottom pocket, the micro-controller located at the upper part of the shirt, and the braided e-yarns are arranged in a vertical manner on both sides. A total of eight (8) braided e-yarns containing sixty-six (66) green 0603 SMD LEDs were designed to fit the structure of the shirt.

Based on this design plan, the sleeve men's shirt was created using a plain-woven retro-reflective fabric which was surface embellished with design patterns from the Sirigu murals from Ghana. Results from the laser engraving experiments in Chapter 4.4 revealed that RF1 (plain weave) was selected with design treatments of 40dpi-120µs parameter on their surfaces. Details like sharpness, visibility, and clarity of the design pattern or images were evident for LA-RF1 with plain weaves. The Wanzagsi motif and Zaalinga motif were selected as design patterns from the Sirigu wall paintings to embellish the surface of the fabric via laser engraving technique. These engravings were placed at the front and back sides of the shirt as shown in Figure 5.41(d). The triggering sensor (which communicates the necessary inputs for the micro-controller) i.e. the light detector sensor (Figure 5.41(b)) was carefully covered with fabric and placed at the front and back sides of the shirt (Figure 5.41(d)). The position of the sensors exposes them to receive the needed amount of lights from the approaching vehicle and communicate same to the micro-controller via written code. A slot (Figure 5.41(c)) was created to house the various braided e-yarns in the shirt, a design approach for easy removal and placement. A pocket to house the micro-controller unit (positioned at the upper part) and a side pocket for the battery to power the microcontroller unit is shown in Figure 5.41(e) and Figure 5.41(e) respectively.

Subsequently, flexible Litz wires were incorporated into the shirt to connect or link the braided e-yarns (for positive and negative terminals), light detector sensors, and vibration motors. Litz wires which are described extensively by Blanc et al. (2023) and Born et al. (2022) are relatively flexible with insulations that can form different shapes, withstand some mechanical loads (Stormont et al., 2023), and reduce eddy current losses based on frequency-dependent effects (Panchal et al., 2021). Due to the flexible nature of the Litz wires, they were carefully embedded or incorporated into the weave structure to carry power supplied from the various battery units.

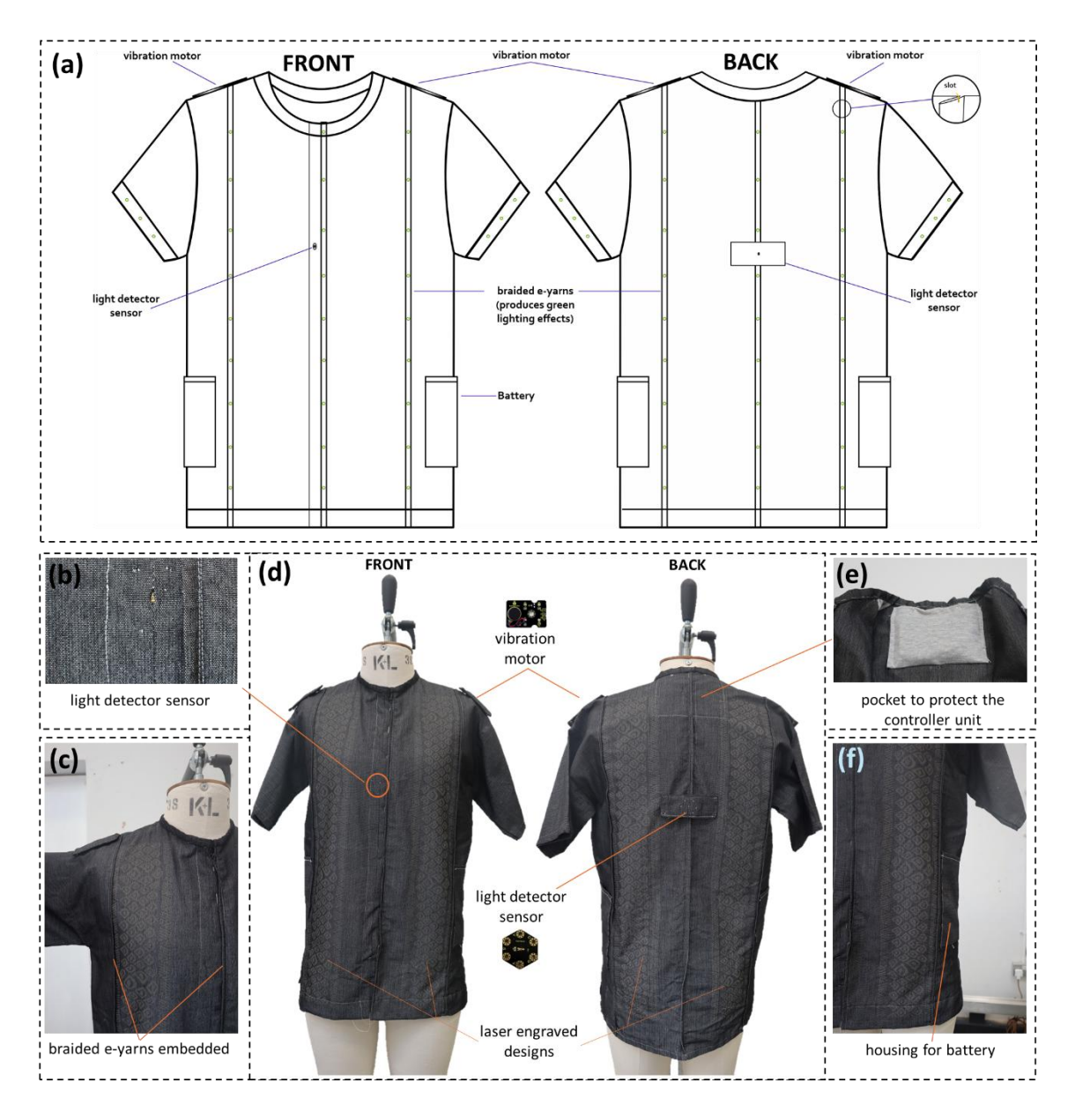


Figure 5.41. (a) Technical drawing of the sleeve men's shirt showing the positions of the various components. (b) light detector sensor. (c) location of the braided e-yarns. (d) appearance of the smart interactive clothing showing the front and backside. (e) location of the pocket for the micro-controller unit and (f) location of the pocket for the battery unit to power the micro-controller unit.

5.5.1.1 Evaluation

An experimental qualitative approach of capturing retro-reflective effects from a 1.5m distance using a digital camera was conducted on the assembled clothing. This was captured in a darkroom condition at the laboratory, where the design patterns are visible on the clothing with a reflective ability (Figure 5.42(b)). Herein, when the light source was directed at the smart interactive clothing, the light detector sensor received light signals

which were then transferred to the micro-controller to affect the necessary safety features of producing sound, driving the vibration motors, and causing the green lighting effects of the braided e-yarns embedded in the clothing (Figure 5.42(c)). These functional features as stated earlier will benefit pedestrians most especially, the blind and deaf individuals who use the road at night time. This will aim to alert them of an approaching vehicle.



Figure 5.42. (a) Appearance of the assembled clothing with no lighting effects in the darkroom setting. (b) retro-reflective effects in the darkroom setting. (c) lighting effects of the green LEDs when light is detected in the darkroom conditions at the laboratory.

Subsequently, a terminal voltage change of the 300mAh and 500mAh 3.7 Lithium Polymer Li-Po rechargeable battery was conducted using a FLUKE 107 CAT III 600 V Digital Multimeter. This was conducted to test and understand the length of time these batteries could function before being discharged. Findings revealed that the voltage of the battery changes slowly from ~4.175V to ~3.4V, after which the battery changes were faster (Figure 5.43). it must be noted that, around a battery discharge of ~2.8V and below, the battery was not significantly sufficient to power the electronic components in the clothing. Specifically, at battery discharge of ~2.676V at 600 mins (10 hours), the power in Battery A was not sufficient to switch on the lighting effects of the green braided e-yarns in the clothing. Similarly, at battery discharge of ~2.757V at 300 mins (5 hours) for Battery B, the voltage was not sufficient to power the micro-controller hence no sound and vibration patterns were produced. Since the micro-controller could not function due to low voltage supply, there was no coordination for the functioning ability of the lighting effects from

the braided e-yarns. As such, once the voltage supplied from Battery B with a 300mAh capacity is low, the interactive unit can not function.

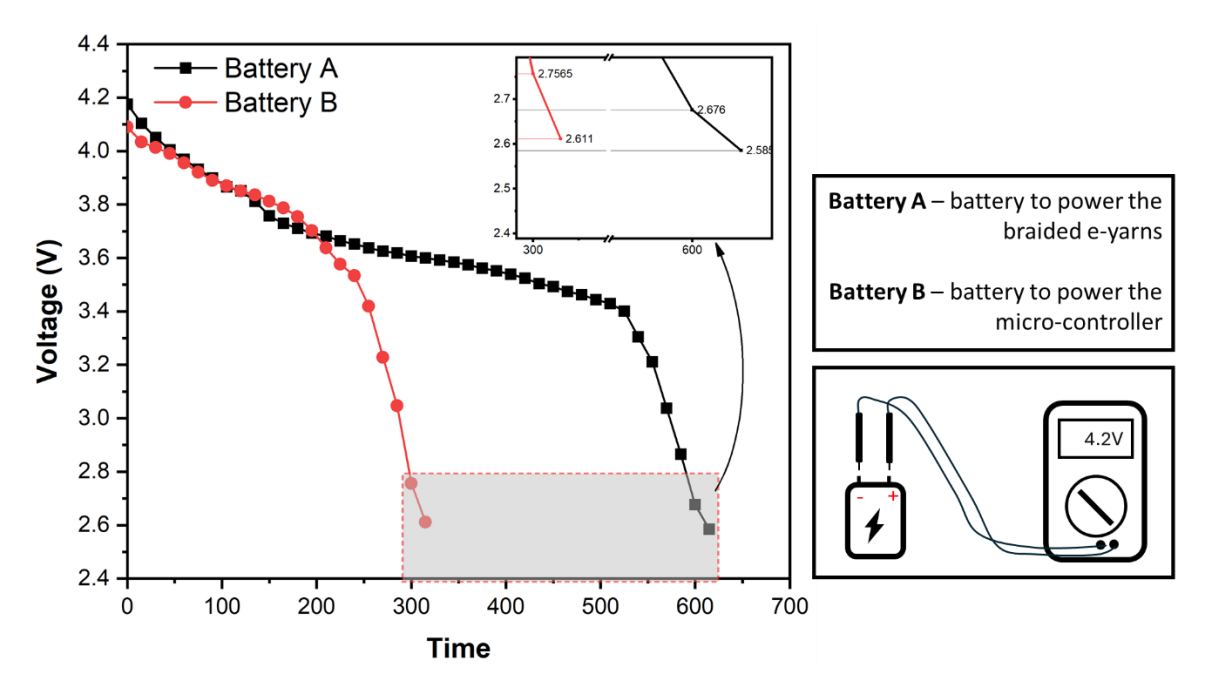


Figure 5.43. Terminal voltage change of battery A (500mAh) and battery B (300mAh) when charged and discharged.

5.5.2 Smart interactive clothing two

In this work, a long-sleeve men's outfit was designed as shown in the technical sketch (Figure 5.43(a)). This illustrates the positioning of the various braided e-yarns, the battery, microcontroller, and the sensors. Herein, just like the design approach for the short-sleeve men's shirt, the vibration motors are placed at the shoulder region, the light detector sensors are placed at the front and back side of the outfit, the battery unit to power the micro-controller is located at the left side of the bottom pocket, the micro-controller located at the upper part of the outfit, and the braided e-yarns are arranged vertically on both sides. A total of twelve (12) braided e-yarns containing seventy-two (72) red 0603 SMD LEDs were designed to fit the structure of the shirt.

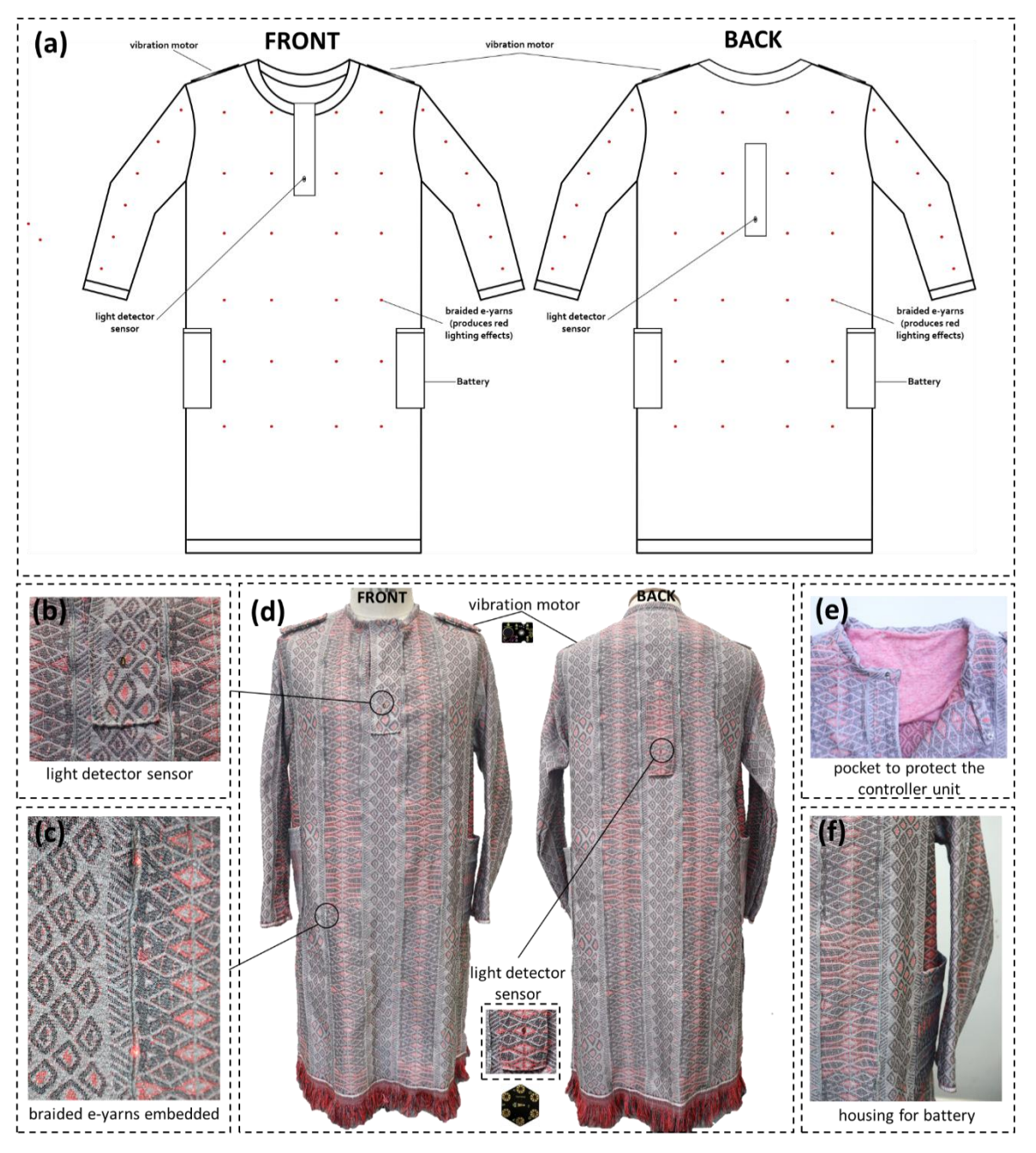


Figure 5.43. (a) Technical drawing of the sleeve men's shirt showing the positions of the various components. (b) light detector sensor. (c) location of the braided e-yarns. (d) appearance of the smart interactive clothing showing the front and backside. (e) location of the pocket for the micro-controller unit and (f) location of the pocket for the battery unit to power the micro-controller unit.

Based on the design plan, eight (8) braided e-yarns were inserted into the woven structure using the Jacquard weaving loom. After every insertion, the workability of the braided e-yarns was tested before weaving continuous. This activity is necessary to ensure that the beat-up action by the reed does not impact greatly the braided e-yarns. Results from the jacquard woven fabrics with African design patterns in Chapter 4.2 revealed that the jacquard woven fabric RF 3 with ¼ satin, move 2, and ½ twill, has an overall good

total hand value (THV) with an average value of 2.605. Using the same weave parameter, a new woven fabric was produced to have three (3) colours. The *Ligipela* motif, *Wanzagsi* motif and *Zaalinga* motif were selected as design patterns from the Sirigu wall paintings to produce the retro-reflective woven fabric via jacquard weaving technology. The positioning of the light detector sensors, braided e-yarns, vibration motor, pockets to house the micro-controller unit, and battery unit for powering the micro-controller unit are illustrated in Figure 5.43(a) - Figure 5.43(f). In this long-sleeve men's outfit, Litz wires were also used to connect the various braided e-yarns and sensory components. As stated early on, the flexible nature of the Litz wires made it possible to incorporate wires into the weave structure, to carry power supplied from the various battery units.

5.5.2.1 Evaluation

Similarly, as was described for the short sleeve men's shirt, an experimental qualitative approach was adopted to capture the retro-reflective effects of the assembled clothing in a darkroom setting from a 1.5m distance using a digital camera (Figure 5.44(a)). The retro-reflective effects of the long-sleeve men's outfit are presented in Figure 5.44(b), showing its functionality when lights fall on it. Subsequently, the functionality of the smart interactive clothing i.e. lighting effects, sound, and vibration are carefully coordinated when a light source falls on the light detector sensor. Figure 5.44(c) shows the green lighting effects of the outfit when a light source falls on the sensory unit. This feature provides further safety to alert the driver in the approaching vehicle of the presence of the pedestrian on the road. Other features like sound and vibration aim at benefiting pedestrians most especially, the blind and deaf individuals who use the road at night time hence alerting them of an approaching vehicle.



Figure 5.44. (a) Appearance of the assembled clothing with no lighting effects in the darkroom setting. (b) retro-reflective effects in the darkroom setting. (c) lighting effects of the red LEDs when light is detected in the darkroom conditions at the laboratory.

A terminal voltage change of the 300mAh and 500mAh 3.7 Lithium Polymer Li-Po rechargeable battery was conducted using a FLUKE 107 CAT III 600 V Digital Multimeter. In Figure 5.45, it can be observed that both Battery A and Battery B were at full charge of ~4.1735V and ~4.1215V respectively. A battery discharge from Battery A to power the braided e-yarns and Battery B to power the micro-controller, all experienced a decline in voltage. There was however a sharp decline in voltage after 3.4V. Subsequently, at a discharge time of 350 mins (5.8 hours) and voltage of 2.8035 for Battery A (capacity of 500mAh), the twelve (12) braided e-yarns containing seventy-two (72) red 0603 SMD LEDs could not produce the needed red lighting effects. This implies that the sufficiency of 2.8035V was limited to power all the braided e-yarns at 350 mins. Alternatively, at the same discharge time of 350 mins and voltage of 2.6915 for Battery B (capacity of 300mAh), the power was not sufficient to power up the micro-controller to produce sound and the vibration motor to generate the necessary vibration patterns. This implies that, at a discharge voltage of ~2.8V, the power is not sufficient to power the micro-controller and the braided e-yarns. But it is imperative to note that, both rechargeable batteries discharge their respective voltage at 350mins (5.8 hours) during the continuous testing procedure.

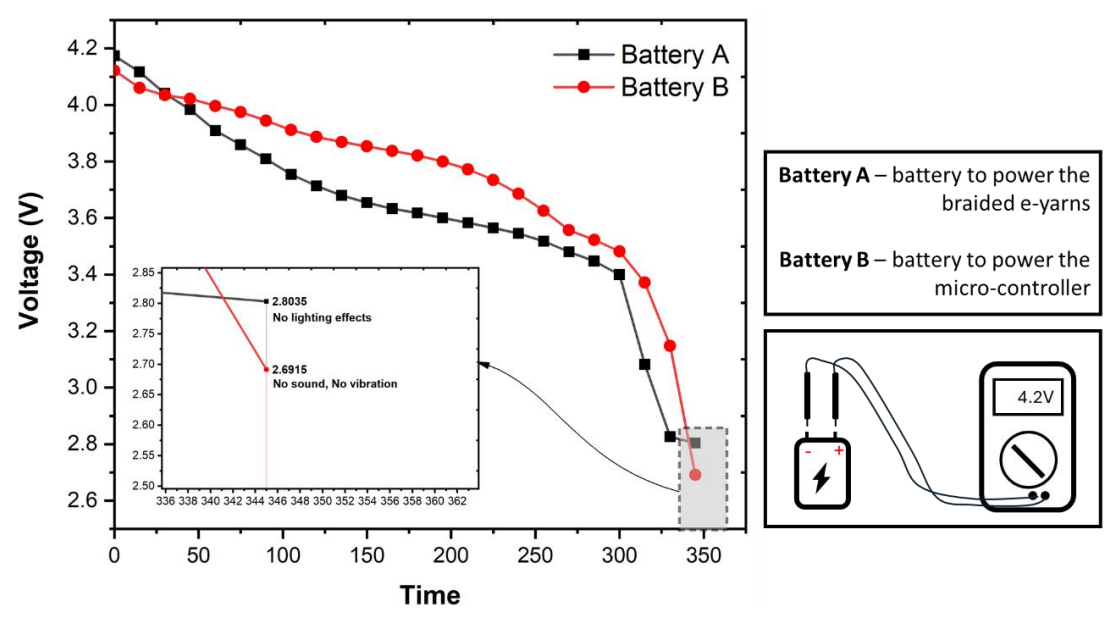


Figure 5.45. Terminal voltage change of battery A (500mAh) and battery B (300mAh) when charged and discharged.

5.6 Performance of the prototype smart interactive retro-reflective clothing

The design and development of the smart interactive RR clothing provide the first prototype for improving the safety of pedestrians most especially the deaf and blind using a combined approach of design and technology. Herein, the rechargeable battery provides approximately 6 hours of constant power supply for the micro-controller. The latter is well coordinated with other components such as the braided e-yarns to provide the needed green and red lighting effects due to their high wavelength and suitability for traffic safety. Additionally, a sound level of 161 Hz by the micro-controller and regular vibration patterns of 100 ms are produced for the smart clothing for effective alert of pedestrians. Finally, the smart clothing is effective in detecting light levels from a 25-metre distance with an average light level of 10.35 (average of the first 100 values) recorded by the micro-controller. Figure 5.46 illustrates a summary of the related performance of the developed smart interactive retro-reflective clothing to improve the safety of pedestrians at night.

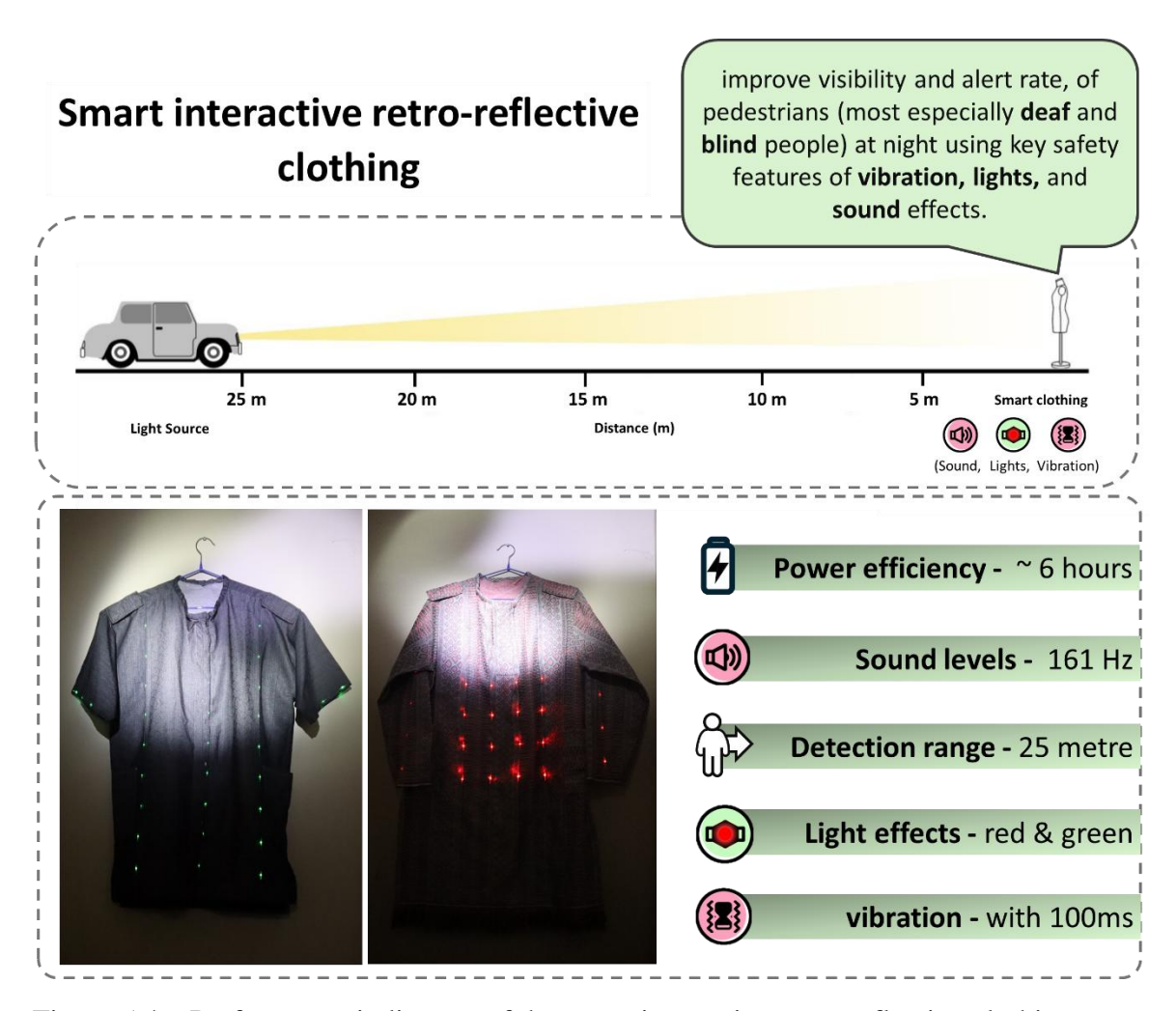


Figure 5.46. Performance indicators of the smart interactive retro-reflective clothing

5.7 Summary

In this section, red and green 0603 light emitting diodes (LEDs) are embedded and encapsulated in two stainless steel conductive yarns to produce braided e-yarns which are incorporated in the design of two smart interactive clothing. Herein, fabrics especially, RF1 (plain weave) with design treatments of 40dpi-120µs parameter on their surfaces and jacquard woven fabric RF 3 with ¼ satin, move 2 and ½ twill (with an overall good total hand value (THV) with average values of 2.605) were selected for the design of a short sleeve and long sleeve men's outfit respectively. The design patterns in these outfits were inspired by the Sirigu wall paintings of Ghana. Results revealed that a delay time of 100ms showed a very intense vibration pattern for effective alert response, ringtone High B exhibited higher sound effects of 161Hz, and the ability of the smart clothing to effectively detect lights from a 25-metre distance under dark test conditions at the laboratory. Subsequently, smart clothing two has rechargeable batteries (500mAh and 300mAh) that discharge their respective voltage at 350mins (5.8 hours). Smart clothing one (1) however

has varying results with a battery discharge of ~2.676V at 600 mins (10 hours) for Battery A and ~2.757V at 300 mins (5 hours) for Battery B. It must be noted at these battery discharge voltages, there was insufficient power for the lighting effects of the braided e-yarns, for the micro-controller to produce sound and drive the vibration motors in the clothing. Overall, the battery discharge for both smart clothing could last over ~5 hours of constant usage by pedestrians on the road at night-time to improve the conspicuity and alertness of pedestrians.

CHAPTER 6: Conclusions and Suggestions for future research

The concluding remarks of the experimental works conducted, and findings are presented in the study "A smart interactive retro-reflective clothing for pedestrian safety at night-time". The experimental work presented the development of retro-reflective textiles made using jacquard and dobby looms, the creation of braided electronic yarns (embedded with LEDs) to produce the necessary lighting effects, the design and development of the controller switch unit and interactive controller unit. These key components were integrated to develop the smart interactive retro-reflective clothing which has safety features like vibration, sound, and lighting effects, aside from its inherent ability to retro-reflect lights. It is also critical to note that, the design elements used in this project were sourced from the Sirigu wall paintings of Ghana which are historically produced by the women in the Sirigu communities with significant symbolic connotations. The SIRC design model aided in comprehensively designing, developing, and validating the results for the creation of two working prototype clothing. The main conclusions, limitations, and suggestions for future research are discussed.

6.1 Conclusions

The study's goal of developing a smart interactive retro-reflective clothing for pedestrian safety at night-time influenced the structuring of four key research objectives, where a comprehensive literature review was conducted to provide an in-depth overview of the related solutions presented by key researchers to improve pedestrian safety i.e., visibility and recognition, for reduced accidents at night time. The key solutions like the application of retro-reflective materials as strips on the various moving parts of the human body on the clothing known as biomotion configurations, were widely investigated by research studies. Results showed that full biomotion configurations on the clothing provide a good silhouette of the human body at night hence enhancing the visibility and recognition of the pedestrian. Even though this approach has some significant benefits, studies revealed that the nature and design of these clothing were uncomfortable and unattractive to wear. Other findings illustrated the use of LEDs as a primary component integrated into the clothing and operated manually to further improve the visibility of the pedestrians. These core findings from previous studies provided foundational knowledge for the study to develop smart interactive clothing that adopts LEDs to build braided electronic yarns (for the necessary lighting effects) and retro-reflective threads to create woven textiles.

Additionally, relevant design models were reviewed which influenced the creation of a unique model for the study.

The practice-based methodology as discussed in the literature highlights the generation of new knowledge which is obtained when undertaking an original investigation in the field of practice. These creative outcomes contribute to knowledge, where experimental procedures are conducted to directly answer research questions and objectives of the study. This research method carefully addresses the core problems initially identified for an effective solution. As such, a novel SIRC design model for smart interactive retro-reflective clothing was proposed with three (3) distinct parts; concept, exploration and evaluation, and application. Inherent in these core stages are identifying and designing an action plan (concept), development material, electronic yarns, and the interactive system (exploration and evaluation) and the development of prototypes (application) after combining key components. Herein, the Sirigu wall paintings of Ghana played a critical role in design inspiration for design patterns that are used in the study. These design patterns are of significant importance and have symbolic significance which embodies the history and heritage of the people in the community. The integration of these traditional and indigenous design patterns reflects a deep narrative and belonging, where these symbolic patterns are showcased through textile design. This further projects these design patterns through its use for the creation of the study's prototypes, hence adding aesthetic values to the smart interactive clothing. By combining the unique properties of retro-reflective materials, sensory devices, and design elements, the current study provides an approach where design and technology can be harnessed effectively for the creation of smart interactive retro-reflective clothing aimed at improving the visibility and recognition of the pedestrian.

In this study, three (3) key experiments are conducted guided by the SIRC design model to ensure the successful creation of the smart interactive retro-reflective clothing. The first experiment details the creation of three retro-reflective textiles produced with African design patterns on a jacquard loom. Results showed that with different weave combinations, some woven textiles exhibited unique properties for use as a base material for smart clothing. For example, fabric RF 3 with ¼ satin, move 2, and ½ twill, has an overall good total hand value (THV) with an average value of 2.605. Premise on this, the same weave combination was used for the making of the final prototypes with three colour schemes. For the second experiment, different retro-reflective textiles with basic weave

structures (plain, twill, and diamond) were created on a dobby loom. These woven textiles would further form the basic material for surface embellishments. It was revealed that the low-stress mechanical properties of the woven textiles influenced their total hand value (THV) which is a unique property for their use in the creation of smart clothing. For example, the eventual THV of RF2 was higher than RF1, even though the unique retroreflective property of RF1 was higher than RF2. Employing the laser engraving technique, design patterns were experimented on the surfaces of the woven textiles using different parameters. Results showed that higher pixel time (µs) and resolutions (dpi) negatively affected the performance of the retro-reflective yarns in the woven textiles hence its ability to retro-reflect lights back to its source of origin is destroyed. Based on this, the study adopted 40 dpi-120 µs as a working parameter to embellish the surface of the woven textiles. This parameter did not affect the retro-reflective nature of the textiles but ensured the clarity of the design patterns on the textiles. In the last experiment conducted, braided electronic yarns were effectively designed and developed as carefully depicted in Chapter 5. This experiment utilised heat-shrinkable tubes, stainless steel threads, and 0603 lightemitting diodes (LEDs) as core materials to develop the braided e-yarns. Herein, the braiding technique aided in effectively securing the various components of the electronic yarns together for effective integration in the woven textiles. The design approach for the development of the braided e-yarns showed a robust structure that still worked (producing the necessary lighting effects) even after twenty (20) mechanical washing and drying cycles. Aside from the braided e-yarns, Chapter 5 further details the design and development of the interactive unit which comprised of a micro-controller, rechargeable battery, transistor, and sensors (vibration motor and light detector). This interactive unit was equipped with a transistor to ensure power separation i.e. a battery unit to power the micro-controller and another to power the braided e-yarns. The interactive unit was the main controlling unit that coordinated the working of the braided e-yarns, the vibration motor, the light detector sensor, and the sound. With the trigger being a light source falling on the light detector sensor integrated into the woven textiles, the interactive unit influences the working of the vibration motor and the production of sound and lighting effects. Findings showed that ringtone High B (161Hz sound levels) and 100ms of delay time for the vibration patterns, were effective in producing the needed sound and vibration respectively, to alert the pedestrian. Further results revealed the ability of the smart clothing to detect light from a 25-metre distance with average light levels of 10.35. Overall, two (2) working smart interactive retro-reflective clothing with design patterns from Sirigu wall paintings of Ghana, were created with two distinct lighting effects, red and green. Results from the current research provide the first proposed prototype that opens a commercial application for the use of smart interactive clothing to enhance the safety of pedestrians on the road at night. This will significantly help pedestrians most especially the elderly and disabled (deaf and blind) pedestrians for improved visibility, alert levels, and recognition on the road.

6.2 Suggestions for Future Research

Based on the findings of the current study coupled with the related findings from the comprehensive literature review, suggestions for future research are provided herein to guide researchers and relevant stakeholders in this critical area.

- a) *Durability and Performance:* The study suggests research direction towards understanding the effects of extreme conditions like sunlight, wear abrasion, rain, mechanical washing, and drying could affect the retro-reflective abilities of woven textiles produced using retro-reflective threads. Studies that subject these woven retro-reflective textiles to such conditions would further provide insights into the robustness, durability, and performance of these textiles hence providing a better understanding of the ideal period for replacing them. These critical data would aid pedestrians have a clear understanding of how certain extreme conditions could affect the performance and durability of their woven retro-reflective clothing. Aside from this, future studies on the performance of the smart interactive clothing when subjected to rain conditions i.e., would water droplets from rain affect the workability of the smart interactive clothing?
- b) Design innovation: Wear comfort and style or design of the retro-reflective textiles and the eventual smart clothing could influence their use by road users. This is because a previous study conducted by Aldred and Woodcock (2015) in England revealed discomfort and cycling less influence the use of safety devices and clothing by road users. This was largely linked to the nature or design of the safety clothing which affected their use by pedestrians. Premise on this, future studies should consider wearing comfort and design innovation to develop aesthetically pleasing and functional smart clothing that would otherwise not lead to discomfort of the pedestrians. Alternatively, combining different yarn types coupled with

retro-reflective threads for the development of woven textiles would further provide comprehensive insights into the functionality and properties of these textiles which promote wear comfort. These experiments provide an opportunity for growth and innovation in the research field.

- c) Perception and Behaviour: The ultimate usability of smart clothing to enhance and improve the safety of pedestrians on the road is premised on behaviours and perceptions which are influenced by certain factors. Future studies should be conducted to understand how factors, such as education, cultural and social influences, and policy campaigns can directly influence pedestrian's behaviour and perceptions, which would then contribute to promoting effective measures that would increase interest and desire to use this type of smart safety clothing. Both qualitative and quantitative approaches could be applied to adopt the needed responses from pedestrians to test how critical variables mentioned early on could influence the use of these smart clothing.
- d) *Technology advancement:* The use of modern technology and methods such as sensors, can provide the appropriate wearables for the development of smart interactive clothing. Such integration into woven textiles could provide effective solutions aimed at improving the recognition and visibility of road users These safety features could be vital for workers or pedestrians who are in industrial workplaces or face severe weather conditions, respectively. Future studies should further advance the use of sensory devices integrated into clothing to enhance the safety of road users. It is imperative that there are still more technological approaches to explore, design, and develop for pedestrian safety.

6.3 Limitations of the study

The current research significantly provides the first working prototypes of smart interactive retro-reflective clothing to improve the recognition of and visibility of pedestrians on the road. Even though different experimental works were conducted, however, there are certain limitations acknowledged in the research. Firstly, due to the unavailability of an appropriate instrument to test the retro-reflectivity of woven textiles, a qualitative approach was developed in this research to report the retro-reflective nature

of woven textiles. Subsequently, only a few yarn types i.e., polyester and cotton yarns coupled with retro-reflective threads were utilised for the creation of the woven textiles to complete the objectives set out in the research. The study only focused on these materials where their related properties were provided. Lastly, the working prototypes developed in this research provided insights into the ability of smart clothing to enhance the safety of pedestrians. These prototypes are at their conceptual stages hence critical research is needed to advance their migration into commercial production for effective use of flexible sensory devices. Critical issues like the effects of mechanical washing and drying, rain, and wear abrasion on the robustness of the flexible sensors and the woven textiles would provide great insights into the full realisation of comfortable smart interactive clothing for pedestrian use at night-time.

References

- 3m. 2014. 3MTM ScotchliteTM Reflective Material Visibility Solutions [Online]. 3M. Available: https://multimedia.3m.com/mws/media/765694O/3m-visibility-solutions-brochure.pdf?&fn=3M%20Slite%20Brochure.pdf [Accessed October 17 2021].
- 3m Safety. 2021. What is retroreflectivity & why is it important? [Online]. 3M. Available: https://www.3m.com.au/3M/en_AU/road-safety-au/resources/road-transportation-safety-center-blog/full-story/~/road-signs-retroreflectivity/?storyid=43090124-0448-4c58-9e7d-930892c42b18 [Accessed October 3 2021].
- Abdel-Aty, M. & Abdelwahab, H. 2004. Modeling rear-end collisions including the role of driver's visibility and light truck vehicles using a nested logit structure. *Accident Analysis & Prevention*, 36, 447-456.
- Abdel-Aty, M. & Keller, J. 2005. Exploring the overall and specific crash severity levels at signalized intersections. *Accident Analysis & Prevention*, 37, 417-425.
- Ackaah, W. & Adonteng, D. O. 2011. Analysis of fatal road traffic crashes in Ghana. *International Journal of Injury Control and Safety Promotion*, 18, 21-27.
- Ahsan, M., Teay, S. H., Sayem, A. S. M. & Albarbar, A. 2022. Smart Clothing Framework for Health Monitoring Applications. *Signals*, 3, 113-145.
- Akankwasa, N., Jun, W., Yuze, Z. & Mushtaq, M. 2014. Properties of cotton/T-400 and 100% cotton plain knitted fabric made from ring spun yarn: Eigenschaften von Baumwolle/T-400 und 100% Baumwolle glattgestrickten Fasern aus Ringspinngarn. *Materialwissenschaft und Werkstofftechnik*, 45, 1039-1044.
- Åkerstedt, T. & Kecklund, G. 2001. Age, gender and early morning highway accidents. *Journal of sleep research*, 10, 105-110.
- Al-Ghamdi, A. S. 2002. Using logistic regression to estimate the influence of accident factors on accident severity. *Accident Analysis & Prevention*, 34, 729-741.
- Aldred, J. 2016. Anti-paparazzi scarf has become a popular celebrity fashion accessory that's rendered completely useless by turning off the flash [Online]. DIYPhotography. Available: https://www.diyphotography.net/anti-paparazzi-scarf-become-popular-celebrity-fashion-accessory-thats-rendered-completely-useless-turning-off-flash/ [Accessed April 13 2022].
- Aldred, R. & Woodcock, J. 2015. Reframing safety: An analysis of perceptions of cycle safety clothing. *Transport Policy*, 42, 103-112.
- Andre, J. & Owens, D. A. 2001. The twilight envelope: a user-centered approach to describing roadway illumination at night. *Human factors*, 43, 620-630.
- Angelova, R. A. 2012. Air permeability of woven structures: Influence of the mesostructure. *Proceedings of the 4th International Course*.
- Areo, M. O. & Kalilu, R. O. R. 2013. Origin of and visual semiotics in Yoruba textile adire. *Arts and Design Studies*, 12, 22-34.
- Arfken, G. B., Griffing, D. F., Kelly, D. C. & Priest, J. 1984. chapter 39 REFLECTION, REFRACTION, AND GEOMETRIC OPTICS. *In:* ARFKEN, G. B., GRIFFING, D. F., KELLY, D. C. & PRIEST, J. (eds.) *University Physics*. Academic Press.
- Arslan, P., Ferreira, A. M. & Akpınarlı, H. F. (eds.) 2020. *Cultural Heritage*, *Collaborative Practices and Sustainable Fabric Design: Ottoman Sultans' Life Stories on Jacquard Design*, Cham: Springer International Publishing.
- Asante, E. A. & Opoku–Asare, N. A. 2011. Cultural identity in the murals of Sirigu women and their role in art education and social sustainability. *International Journal of Education Through Art*, 7, 187-202.

- Asayesh, A., Mirgoli, F. & Gholamhosseini, A. 2018. An investigation into the effect of fabric structure on the compressional properties of woven fabrics. *The Journal of The Textile Institute*, 109, 32-38.
- Asibey, M. O., Agyeman, K. O. & Yeboah, V. 2017. The impact of cultural values on the development of the cultural industry: Case of the Kente textile industry in adanwomase of the Kwabre East District, Ghana. *Journal of Human Values*, 23, 200-217.
- Asmah, A. E., Frimpong, C. & Okpattah, V. 2013. Sirigu symbols: Traditional communicative images for fashion designed prints. *International Journal of Innovative Research and Development*, 2, 193-202.
- Asmah, A. E. & Okpattah, V. 2013. Sirigu Symbols: A Metaphoric Element for Batik Prints. *Arts and Design Studies* 12, 49-57.
- Atalie, D., Gideon, R. K., Ferede, A., Tesinova, P. & Lenfeldova, I. 2021. Tactile comfort and low-stress mechanical properties of half-bleached knitted fabrics made from cotton yarns with different parameters. *Journal of Natural Fibers*, 18, 1699-1711.
- Avinc, O., Wilding, M., Gong, H. & Farrington, D. 2010. Effects of softeners and laundering on the handle of knitted PLA filament fabrics. *Fibers and polymers*, 11, 924-931.
- Babic, D. Impact of Heavy Vehicle Visibility on Traffic Safety. The International Scientific Conference-ZIRP, 2014.
- Babić, D., Babić, D., Fiolić, M. & Ferko, M. 2021. Factors affecting pedestrian conspicuity at night: Analysis based on driver eye tracking. *Safety Science*, 139, 105257.
- Baek, S.-H., Jeon, D. S., Tong, X. & Kim, M. H. 2018. Simultaneous acquisition of polarimetric SVBRDF and normals. *ACM Trans. Graph.*, 37, 268:1-268:15.
- Balk, S. A., Carpenter, T. L., Brooks, J. O., Rubinstein, J. S. & Tyrrell, R. A. 2005. The conspicuity of pedestrians at night: How much biological motion is enough? *Journal of Vision*, 5, 19-19.
- Balk, S. A., Tyrrell, R. A., Brooks, J. O. & Carpenter, T. L. 2008. Highlighting Human Form and Motion Information Enhances the Conspicuity of Pedestrians at Night. *Perception*, 37, 1276-1284.
- Banerjee, D. & Chattopadhyay, K. K. 2018. Chapter 5 Hybrid Inorganic Organic Perovskites: A Low-Cost-Efficient Optoelectronic Material. *In:* THOMAS, S. & THANKAPPAN, A. (eds.) *Perovskite Photovoltaics*. Academic Press.
- Begum, M. S. & Milašius, R. 2022. Factors of Weave Estimation and the Effect of Weave Structure on Fabric Properties: A Review. *Fibers*, 10, 74.
- Belenguer, F. M., Martínez-Millana, A., Ramón, F. S. C. & Mocholí-Salcedo, A. 2022. The Effectiveness of Alert Sounds for Electric Vehicles Based on Pedestrians' Perception. *IEEE Transactions on Intelligent Transportation Systems*, 23, 2956-2965.
- Berces, A. 2010. Improving Worker Safety through Better Visibility. *Journal of the Australasian College of Road Safety*, 21, 28-31.
- Berces, A. Improving road safety by increased truck visibility. Proceedings of the Australasian road safety research, policing and education conference, 2011.
- Bible, R. C. & Johnson, N. 2002. Retroreflective material specifications and on-road sign performance. *Transportation research record*, 1801, 61-72.
- Black, A. A., Bui, V., Henry, E., Ho, K., Pham, D., Tran, T. & Wood, J. M. 2021. Using retro-reflective cloth to enhance drivers' judgment of pedestrian walking direction at night-time. *Journal of safety research*, 77, 196-201.

- Black, A. A., Duff, R., Hutchinson, M., Ng, I., Phillips, K., Rose, K., Ussher, A. & Wood, J. M. 2020. Effects of night-time bicycling visibility aids on vehicle passing distance. *Accident Analysis & Prevention*, 144.
- Blanc, F. S. L., Born, H. C., Drexler, D., Reising, S., Münster, A. Z., Platte, V., Kampker, A. & Dorn, B. Comparative Conductor Design Study of Processing and Insulation Characteristics for Continuous Hairpin Stators Using Profiled High Frequency Litz Wires. 2023 13th International Electric Drives Production Conference (EDPC), 29-30 Nov. 2023 2023. 1-12.
- Bland, C. C. 1964. Method for production of glass beads by dispersion of molten glass. Google Patents.
- Born, H. C., Oehler, F., Platte, V., Kampker, A., Heimes, H., Dorn, B., Brans, F., Drexler, D., Blanc, F. S. L. & Reising, S. Manufacturing Process and Design Requirements of Litz Wire with Focus on Efficiency Improvement of Traction Motors. 2022 12th International Electric Drives Production Conference (EDPC), 29-30 Nov. 2022 2022. 1-7.
- Borzendowski, S. a. W., Sewall, A. a. S., Fekety, D. K. & Tyrrell, R. A. 2014. Effects of an Educational Intervention on Athletes' Attitudes Toward Wearing Conspicuity-Enhancing Garments at Night. *Proceedings of the Human Factors and Ergonomics Society Annual Meeting*, 58, 2141-2145.
- Braddock, M., Lapidus, G., Cromley, E., Cromley, R., Burke, G. & Banco, L. 1994. Using a geographic information system to understand child pedestrian injury. *American Journal of Public Health*, 84, 1158-1161.
- Candy, L. 2006. Practice based research: A guide. Sydney, Australia: University of Techology.
- Castellani, B., Gambelli, A. M., Nicolini, A. & Rossi, F. 2020. Optic-energy and visual comfort analysis of retro-reflective building plasters. *Building and Environment*, 174, 106781.
- Cederqvist, A. M. 2022. Designing and coding with BBC micro:bit to solve a real-world task a challenging movement between contexts. *Education and Information Technologies*, 27, 5917-5951.
- Chang, F.-R., Huang, H.-L., Schwebel, D. C., Chan, A. H. & Hu, G.-Q. 2020. Global road traffic injury statistics: Challenges, mechanisms and solutions. *Chinese journal of traumatology*, 23, 216-218.
- Che-Him, N., Roslan, R., Rusiman, M. S., Khalid, K., Kamardan, M. G., Arobi, F. A. & Mohamad, N. Factors Affecting Road Traffic Accident in Batu Pahat, Johor, Malaysia. Journal of Physics: Conference Series, 2018. IOP Publishing, 012033.
- Chegg. 2021. *Retroreflection* [Online]. Chegg Inc. Available: https://www.chegg.com/learn/physics/introduction-to-physics/retroreflection [Accessed October 3 2021].
- Cheng, K. W. E., Kwok, K. W., Kwok, Y. L., Chan, K. W., Cheung, N. C., Ho, Y. K. & Kwok, K. F. LED lighting development for intelligent clothing. 2009 3rd International Conference on Power Electronics Systems and Applications (PESA), 20-22 May 2009 2009. 1-4.
- Cho, A. H., Kim, T. Y. & Park, B. H. 2017. Circular intersection accident models of day and nighttime by gender. *International Journal of Highway Engineering*, 19, 143-151.
- Cho, H. & Song, H. 2021. The effect of backside elements on the light emission of a plastic optical fiber assembly. *Textile Research Journal*, 91, 2682-2691.
- Cho, H. S., Yoon, H. J., Lee, B. H., Woo, J. C., Choi, H. Y., Shim, E. & Youk, J. H. 2022. Evaluation of Touch and Durability of Cotton Knit Fabrics Treated with Reactive Urethane-Silicone Softener. *Polymers*, 14, 1873.

- Chong, S.-L., Chiang, L.-W., Allen Jr, J. C., Fleegler, E. W. & Lee, L. K. 2018. Epidemiology of Pedestrian–Motor vehicle fatalities and injuries, 2006–2015. *American journal of preventive medicine*, 55, 98-105.
- Christie, S., Lyons, R. A., Dunstan, F. D. & Jones, S. J. 2003. Are mobile speed cameras effective? A controlled before and after study. *Injury Prevention*, 9, 302-306.
- Damsere-Derry, J., Ebel, B. E., Mock, C. N., Afukaar, F. & Donkor, P. 2010.

 Pedestrians' injury patterns in Ghana. *Accident Analysis & Prevention*, 42, 1080-1088.
- Dascalu, T., Acosta-Ortiz, S. E., Ortiz-Morales, M. & Compean, I. 2000a. Removal of the indigo color by laser beam—denim interaction. *Optics and lasers in engineering*, 34, 179-189.
- Dascalu, T., E Acosta-Ortiz, S., Ortiz-Morales, M. & Compean, I. 2000b. Removal of the indigo color by laser beam—denim interaction. *Optics and Lasers in Engineering*, 34, 179-189.
- Demerdash, E. & Mostafa, D. 2018. Aesthetics of Light-Emitting Diode (LED) in Illuminating Women Smart Fashion Design. *International Design Journal*, 8, 53-62.
- Dennison, A. 2022. *Reflectives* [Online]. Avery Dennison Corporation. Available: https://reflectives.averydennison.com/en/home/products/retroreflective-sheeting/temporary-traffic-control-sheeting.html [Accessed April 12, 2022].
- Dimaggio, C. & Durkin, M. 2002. Child pedestrian injury in an urban setting descriptive epidemiology. *Academic emergency medicine*, 9, 54-62.
- Dinakar, S., Suway, J., Muttart, J. & Edewaard, D. 2021. Systematic Degradation of Retroreflective Materials for Testing and Research. *SAE Technical Paper*, 01-08.
- Dinsmoor, J. A. 1963. SHRINKABLE INSULATING TUBING. *Journal of the Experimental Analysis of Behavior*, 6, 170-170.
- Dunne, B. 2015. *Adidas Introduces Dazzling 'Xeno' Technology* [Online]. Sole Collector. Available: https://solecollector.com/news/2015/02/adidas-xeno-pack-zx-flux-superstar-metro-attitude [Accessed October 24 2021].
- Essel, O. Q. 2019. Dress Fashion Politics of Ghanaian Presidential Inauguration Ceremonies from 1960 to 2017. *Fashion and Textiles Review*, 1, 35-55.
- Evans, B. 2017. *African Patterns* [Online]. Contemporary African Art. Available: https://www.contemporary-african-art.com/african-patterns.html [Accessed].
- Evans, L. 1991. *Traffic safety and the driver*, Van Nostrand Reinhold: New York, Science Serving Society.
- Evans, L. 2004. Traffic Safety; Science Serving Society. Bloomfield Hills, MI, 179.
- Everest, J. 1992. *The involvement of alcohol in fatal accidents to adult pedestrians*, Crowthorne, Bershire, Her Majesty Stationary Office.
- Fakhrmoosavi, F., Saedi, R., Jazlan, F., Zockaie, A., Ghamami, M., Gates, T. J. & Savolainen, P. T. 2021. Effectiveness of Green Warning Lights with Different Flashing Patterns for Winter Maintenance Operations. *Transportation Research Record*, 2675, 1505-1521.
- Fekety, D. K., Edewaard, D. E., Stafford Sewall, A. A. & Tyrrell, R. A. 2016.

 Electroluminescent Materials Can Further Enhance the Nighttime Conspicuity of Pedestrians Wearing Retroreflective Materials. *Human Factors*, 58, 976-985.
- Ferguson, S. A., Preusser, D. F., Lund, A. K., Zador, P. L. & Ulmer, R. G. 1995. Daylight saving time and motor vehicle crashes: the reduction in pedestrian and vehicle occupant fatalities. *American Journal of Public Health*, 85, 92-95.
- Ferraro, O. E., Orsi, C., Popa, I., Montomoli, C. & Morandi, A. 2020. Avoiding bicycle collisions: Experience on safety bike behavior among Italian bicycle users,

- individual and conspicuity characteristics. *Journal of Transportation Safety & Security*, 12, 653-670.
- Ferrero, F., Testore, F., Tonin, C. & Innocenti, R. 2002. Surface degradation of linen textiles induced by laser treatment: comparison with electron beam and heat source. *Autex Res. J.* 2, 109-114.
- Filtness, A. J., Reyner, L. A. & Horne, J. A. 2012. Driver sleepiness—Comparisons between young and older men during a monotonous afternoon simulated drive. *Biological Psychology*, 89, 580-583.
- Flagger Force. 2017. *The Technology Behind Retro-reflectivity* [Online]. United States: Flagger Force. Available: https://flaggerforce.com/blog/technology-behind-retroreflectivity/ [Accessed November 12, 2021].
- Flaxman, S. R., Bourne, R. R., Resnikoff, S., Ackland, P., Braithwaite, T., Cicinelli, M. V., Das, A., Jonas, J. B., Keeffe, J. & Kempen, J. H. 2017. Global causes of blindness and distance vision impairment 1990–2020: a systematic review and meta-analysis. *The Lancet Global Health*, 5, e1221-e1234.
- Fleming, B. 2012. New automotive electronics technologies [automotive electronics]. *IEEE Vehicular Technology Magazine*, 7, 4-12.
- Fontaine, H. & Gourlet, Y. 1997. Fatal pedestrian accidents in France: A typological analysis. *Accident Analysis & Prevention*, 29, 303-312.
- Foreman, J., Xie, J., Keel, S., Ang, G. S., Lee, P. Y., Bourne, R., Crowston, J. G., Taylor, H. R. & Dirani, M. 2018. Prevalence and causes of unilateral vision impairment and unilateral blindness in Australia: the National Eye Health Survey. *JAMA ophthalmology*, 136, 240-248.
- Fylan, F., Bentley, L. A., Brough, D., King, M., Black, A. A., King, N. & Wood, J. M. 2021. Designing cycling and running garments to increase conspicuity. International Journal of Fashion Design, Technology and Education, 14, 263-271
- Fylan, F., King, M., Brough, D., Black, A. A., King, N., Bentley, L. A. & Wood, J. M. 2020a. Increasing conspicuity on night-time roads: perspectives from cyclists and runners. *Transportation research part F: traffic psychology and behaviour*, 68, 161-170.
- Fylan, F., King, M., Brough, D., Black, A. A., King, N., Bentley, L. A. & Wood, J. M. 2020b. Increasing conspicuity on night-time roads: Perspectives from cyclists and runners. *Transportation Research Part F:Traffic Psychology and Behaviour*, 68, 161-170.
- Gangakhedkar, N. S. 2010. 10 Colour measurement methods for textiles. *In:* GULRAJANI, M. L. (ed.) *Colour Measurement.* Woodhead Publishing.
- Garze-Bown, C. 2021. *Knitting with Cotton Yarn: Properties, Uses and More* [Online]. Knitfarious. Available: https://knitfarious.com/knitting-with-cotton-yarn-properties-uses-more/ [Accessed October 28 2021].
- Geurts, K., Thomas, I. & Wets, G. 2005. Understanding spatial concentrations of road accidents using frequent item sets. *Accident Analysis & Prevention*, 37, 787-799.
- Globenewswire. 2022. High Visibility Clothing Market Size [2022-2028] To Reach USD 2033 Million at a CAGR of 6.1% by Vantage Market Research [Online]. GlobeNewswire Available: https://www.globenewswire.com/en/news-release/2022/08/09/2495216/0/en/High-Visibility-Clothing-Market-Size-2022-2028-To-Reach-USD-2033-Million-at-a-CAGR-of-6-1-Industry-Trends-Share-And-Growth-Analysis-Vantage-Market-Research.html [Accessed August 30, 2023].
- Glombikova, V., Komarkova, P., Vik, M., Adamcova, J., Nemcokova, R., Vikova, M. & Havelka, A. 2021. Approach to performance rating of retroreflective textile

- material considering production technology and reflector size. *Autex Research Journal*, 1-12.
- Goodall, N. J. 2016. Can you program ethics into a self-driving car? *IEEE Spectrum*, 53, 28-58.
- Grand View Research 2019. Retro-Reflective Materials Market Size, Industry Report, 2019-2025. San Francisco, United States.
- Green, M. 2021. Why Pedestrians (And Bicyclists) Die. And What To Do About It [Online]. Marc Green, Phd. Available: https://www.visualexpert.com/Resources/WhyPedsdie.html [Accessed].
- Green, P., Kubacki, M., Olson, P. & Sivak, M. 1979. Accidents and the nighttime conspicuity of trucks.
- Greenspon, J. E. 2003. Acoustics, Linear. *In:* MEYERS, R. A. (ed.) *Encyclopedia of Physical Science and Technology (Third Edition)*. New York: Academic Press.
- Gustavsson, L., Nguyen, T., Sathre, R. & Tettey, U. Y. A. 2021. Climate effects of forestry and substitution of concrete buildings and fossil energy. *Renewable and Sustainable Energy Reviews*, 136, 110435.
- Haque, M. M., Chin, H. C. & Huang, H. 2009. Modeling fault among motorcyclists involved in crashes. *Accident Analysis & Prevention*, 41, 327-335.
- Hardy, D. A., Anastasopoulos, I., Nashed, M.-N., Oliveira, C., Hughes-Riley, T., Komolafe, A., Tudor, J., Torah, R., Beeby, S. & Dias, T. 2022. Automated insertion of package dies onto wire and into a textile yarn sheath. *Microsystem Technologies*, 28, 1409-1421.
- Hardy, D. A., Moneta, A., Sakalyte, V., Connolly, L., Shahidi, A. & Hughes-Riley, T. 2018. Engineering a Costume for Performance Using Illuminated LED-Yarns. *Fibers*, 6, 35.
- Hari, P. K. 2012. 1 Types and properties of fibres and yarns used in weaving. *In:* GANDHI, K. L. (ed.) *Woven Textiles*. Woodhead Publishing.
- Hashempour, R., Tahmasebi, A., Veysi, M., Amini, M. & Tavakoli, N. 2019. Cost analysis of accidents according to demographic factors in Iran. *Iranian journal of public health*, 48, 1346.
- Highviz. 2022. *Antiflame reflective* [Online]. Available: www.highviz.cn/products_detail/productId=65.html [Accessed April 12, 2022].
- Hogrefe, H. & Neumann, R. 1997. Adaptive light pattern-a new way to improve light quality. *SAE transactions*, 1117-1124.
- Holmes, B. 1997. Europe raises the standards of performance for high visibility clothing. *Technical Textiles International*, 6, 18-21.
- Holubowycz, O. T. 1995. Age, sex, and blood alcohol concentration of killed and injured pedestrians. *Accident Analysis & Prevention*, 27, 417-422.
- Hooke, A., Knox, J. & Portas, D. 1996. *Cost benefit analysis of traffic light & speed cameras*, Home Office, Police Research Group London, UK.
- Hosseinian, S. M., Najafi Moghaddam Gilani, V., Mirbaha, B. & Abdi Kordani, A. 2021. Statistical analysis for study of the effect of dark clothing color of female pedestrians on the severity of accident using machine learning methods. *Mathematical Problems in Engineering*, 2021.
- Høye, A. K., Johansson, O. & Hesjevoll, I. S. 2020. Safety equipment use and crash involvement among cyclists—Behavioral adaptation, precaution or learning? *Transportation research part F: traffic psychology and behaviour, 72*, 117-132.
- Hu, W. & Cicchino, J. B. 2018. An examination of the increases in pedestrian motor-vehicle crash fatalities during 2009–2016. *Journal of safety research*, 67, 37-44.

- Huang, H., Chin, H. C. & Haque, M. M. 2008. Severity of driver injury and vehicle damage in traffic crashes at intersections: A Bayesian hierarchical analysis. *Accident Analysis & Prevention*, 40, 45-54.
- Hughes–Ifsta, T. Emergency Vehicle Visibility and Conspicuity Study FA-323/August 2009U. S. Fire Administration.
- Iizuka, T., Kawamorita, T., Takenaka, C., Tsuji, H., Kanai, H., Hirai, T., Suzuki, H., Handa, T. & Ishikawa, H. 2021. High Visibility Conditions in a Sunset Environment. *Applied Sciences*, 11, 7229.
- Iizuka, T., Kawamorita, T., Tsuji, H., Kanai, H., Hirai, T., Suzuki, H., Handa, T. & Ishikawa, H. 2022. High visibility colored fabrics for normal trichromats and individuals with color vision defects in a sunset-simulated environment. *PLOS ONE*, 17, e0274824.
- Inoue, T., Shimo, T., Ichinose, M., Takase, K. & Nagahama, T. 2017. Improvement of urban thermal environment by wavelength-selective retro-reflective film. *Energy Procedia*, 122, 967-972.
- Insightslice. 2021. Retro-reflective Materials Global Sales are Expected to Witness Healthy Growth to Reach US\$ 29.5 billion by 2031 [Online]. InsightSLICE. Available: https://www.globenewswire.com/en/news-release/2021/06/28/2254105/0/en/Retro-reflective-Materials-Global-Sales-are-Expected-to-Witness-Healthy-Growth-to-Reach-US-29-5-billion-by-2031.html [Accessed September 14 2021 2021].
- Islam, S. 2013. *Physical Properties and Chemical Properties* [Online]. Textile Craft. Available: https://textile-craft.blogspot.com/2013/12/cotton-fibre-physical-properties-and.html [Accessed October 28 2021].
- Islam, S. & Hossain, A. B. 2015. Comparative analysis of injury severity resulting from pedestrian—motor vehicle and bicycle-motor vehicle crashes on roadways in Alabama. *Transportation research record*, 2514, 79-87.
- Jahani, S. & Jacob, Z. 2015. Breakthroughs in photonics 2014: relaxed total internal reflection. *IEEE Photonics Journal*, 7, 1-5.
- James, J. L. & Kim, K. E. 1996. Restraint use by children involved in crashes in Hawaii, 1986–1991. *Transportation research record*, 1560, 8-12.
- Jcroman. 2015. *Ndebele House Painting-South Africa* [Online]. Juliocesarroman. Available: https://juliocesarroman.com/ndebele-house-painting-south-africa/ [Accessed].
- Jones, A. P. & Jørgensen, S. H. 2003. The use of multilevel models for the prediction of road accident outcomes. *Accident Analysis & Prevention*, 35, 59-69.
- Julien, A. & Carré, J.-R. 2002. Cheminements piétonniers et exposition au risque. *Recherche - Transports - Sécurité*, 76, 173-189.
- Kan, C.-W. 2014. CO2 laser treatment as a clean process for treating denim fabric. *Journal of Cleaner Production*, 66, 624-631.
- Kan, C.-W. & Lam, Y.-L. 2013. Low stress mechanical properties of plasma-treated cotton fabric subjected to zinc oxide-anti-microbial treatment. *Materials*, 6, 314-333.
- Kang, M. & Lee, S. 2017. Visibility evaluation of various retroreflective fabric types and LED position on safety life jacket. *Journal of the Korean Society of Clothing and Textiles*, 41, 352-361.
- Kawabata, S. 2005. The standardization and analysis of hand evaluation. *Effect of mechanical and physical properties on fabric hand*. Elsevier.
- Kawabata, S. & Niwa, M. Analysis of Hand Evaluation of Wool Fabrics for Men's Suits using Data of a Thousand Samples and Computation. Proceedings of the 5th International Wool Textile Research Conference, 1975 Aachen 413-424.

- Kent, K. 1971. West African Cloth, Denver, Colorado, Denver Museum of Natural History.
- Kerbow, K. 2020. What is Hi Vis Clothing and Why is it Critical for Safety? [Online]. Lakeland Inc. Available: https://blog.lakeland.com/blog/what-is-hi-vis-clothing-and-why-is-it-critical-for-safety [Accessed February 27 2022].
- Kharenkova, D. 2018. *Jednota protikladů (Unity of Opposites)*. Technicka Univerzita Liberci.
- Kim, D.-G., Lee, Y., Washington, S. & Choi, K. 2007. Modeling crash outcome probabilities at rural intersections: Application of hierarchical binomial logistic models. *Accident Analysis & Prevention*, 39, 125-134.
- Kim, H., Tan, J. & Toomey, A. 2019. User experience and interactive textiles: A textile designer's perspective. *International Journal of Design Management and Professional Practice*, 13, 1-10.
- Kim, J.-E., Kim, Y.-H., Oh, J.-H. & Kim, K.-D. 2017. Interactive Smart Fashion Using User-Oriented Visible Light Communication:<i> The Case of Modular Strapped Cuffs and Zipper Slider Types</i> Wireless Communications and Mobile Computing, 2017, 5203053.
- Kim, J.-K., Ulfarsson, G. F., Shankar, V. N. & Mannering, F. L. 2010. A note on modeling pedestrian-injury severity in motor-vehicle crashes with the mixed logit model. *Accident Analysis & Prevention*, 42, 1751-1758.
- Kim, K., Brunner, I. M. & Yamashita, E. 2008. Modeling fault among accident— Involved pedestrians and motorists in Hawaii. *Accident Analysis & Prevention*, 40, 2043-2049.
- Kim, K., Kim, S. & Yamashita, E. 2000. Alcohol-impaired motorcycle crashes in Hawaii, 1986 to 1995: An analysis. *Transportation research record*, 1734, 77-85.
- Kim, M. & Song, C. S. 2021. Understanding Police Officers' Usage of High-Visibility Safety Apparel: The Role of Safety Ethics and Professional Appearance. *Safety*, 7, 15.
- Kimani, N. 2018. *Abomey Applique: Remnants of a Fallen Kingdom, Made In Benin* [Online]. The Designers Studio. Available: https://tdsblog.com/abomey-applique/ [Accessed].
- Kimlin, J. A., Black, A. A. & Wood, J. M. 2017. Nighttime driving in older adults: effects of glare and association with mesopic visual function. *Investigative ophthalmology & visual science*, 58, 2796-2803.
- Ko, E. & Lee, H. 2003. Effect of dyeing by immature persimmon juice on the hand of fabrics. *Journal of the Korean Society of Clothing and Textiles*, 27, 883-891.
- Kong, D. & Xiao, X. 2017. Rigid High Temperature Heat-Shrinkable Polyimide Tubes with Functionality as Reducer Couplings. *Scientific Reports*, 7, 44936.
- Kong, L. B., Lekawa, M., Navarro, R. A., Mcgrath, J., Cohen, M., Margulies, D. R. & Hiatt, J. R. 1996. Pedestrian-motor vehicle trauma: an analysis of injury profiles by age. *Journal of the American College of Surgeons*, 182, 17-23.
- Kubota, T., Lee, H. S., Trihamdani, A. R., Phuong, T. T. T., Tanaka, T. & Matsuo, K. 2017. Impacts of land use changes from the Hanoi Master Plan 2030 on urban heat islands: Part 1. Cooling effects of proposed green strategies. *Sustainable cities and society*, 32, 295-317.
- Kwan, I. & Mapstone, J. 2004. Visibility aids for pedestrians and cyclists: a systematic review of randomised controlled trials. *Accident Analysis & Prevention*, 36, 305-312.
- Kwan, I. & Mapstone, J. 2006. Interventions for increasing pedestrian and cyclist visibility for the prevention of death and injuries. *Cochrane Database of Systematic Reviews*.

- Kwasa, I. F. a. E., Haroun, S., Nasif, S. M. A., Al, D. & Attiya, M. I. 2022. Enrichment of the Aesthetics of the Art of Modeling on the Dress by using Lighting in the Costom Design. *Journal of Arts & Applied Sciences (JAAS)*, 9, 1-31.
- Lahrmann, H., Madsen, T. K. O., Olesen, A. V., Madsen, J. C. O. & Hels, T. 2018. The effect of a yellow bicycle jacket on cyclist accidents. *Safety science*, 108, 209-217.
- Laing, R., Niven, B., Bevin, N., Matthews, M. & Wilson, C. 2006. High visibility, UVR protection and passive cooling integrated in workplace clothing. *Journal of Occupational Health and Safety, Australia and New Zealand*, 22, 567.
- Lan, T. T., Kanitpong, K., Tomiyama, K., Kawamura, A. & Nakatsuji, T. 2019. Effectiveness of retro-reflective tape at the rear of heavy trucks to increase visibility and reduce rear-end collisions. *IATSS Research*, 43, 176-184.
- Langham, M. & Moberly, N. 2003. Pedestrian conspicuity research: a review. *Ergonomics*, 46, 345-363.
- Lanoue, J., Leonardos, E. D. & Grodzinski, B. 2019. 4.68 Artificial Lighting Technologies for Agricultural Production. *In:* MOO-YOUNG, M. (ed.) *Comprehensive Biotechnology (Third Edition)*. Oxford: Pergamon.
- Lascala, E. A., Gerber, D. & Gruenewald, P. J. 2000. Demographic and environmental correlates of pedestrian injury collisions: a spatial analysis. *Accident Analysis & Prevention*, 32, 651-658.
- Lee, C. & Abdel-Aty, M. 2005. Comprehensive analysis of vehicle—pedestrian crashes at intersections in Florida. *Accident Analysis & Prevention*, 37, 775-786.
- Lee, J. C., Liu, W., Lo, C. & Chen, C. C. Laundering Reliability of Electrically Conductive Fabrics for E-Textile Applications. 2019 IEEE 69th Electronic Components and Technology Conference (ECTC), 28-31 May 2019 2019. 1826-1832.
- Lee, Y. M. & Sheppard, E. 2018. The effect of lighting conditions and use of headlights on drivers' perception and appraisal of approaching vehicles at junctions. *Ergonomics*, 61, 444-455.
- Leibowitz, H. W., Owens, D. A. & Tyrrell, R. A. 1998. The assured clear distance ahead rule: Implications for nighttime traffic safety and the law. *Accident Analysis & Prevention*, 30, 93-99.
- Lenguerrand, E., Martin, J. L. & Laumon, B. 2006. Modelling the hierarchical structure of road crash data—Application to severity analysis. *Accident Analysis & Prevention*, 38, 43-53.
- Lin, M.-R., Chang, S.-H., Pai, L. & Keyl, P. M. 2003. A longitudinal study of risk factors for motorcycle crashes among junior college students in Taiwan. *Accident Analysis & Prevention*, 35, 243-252.
- Lloyd, J. 2008. A brief history of retroreflective sign face sheet materials. The principles of retroreflection [Online]. Available: http://www.rema.org.uk/pub/pdf/history-retroreflective-materials.pdf [Accessed 2022].
- Lugoda, P., Hayes, S. C., Hughes-Riley, T., Turner, A., Martins, M. V., Cook, A., Raval, K., Oliveira, C., Breedon, P. & Dias, T. 2022. Classifying Gait Alterations Using an Instrumented Smart Sock and Deep Learning. *IEEE Sensors Journal*, 22, 23232-23242.
- Maganty, S., Roma, M. P. C., Meschter, S. J., Starkey, D., Gomez, M., Edwards, D. G., Ekin, A., Elsken, K. & Cho, J. 2016. Enhanced mechanical properties of polyurethane composite coatings through nanosilica addition. *Progress in Organic Coatings*, 90, 243-251.
- Mäkinen, H. 2008. 17 Firefighters' protective clothing. *In:* HORROCKS, A. R. & PRICE, D. (eds.) *Advances in Fire Retardant Materials*. Woodhead Publishing.

- Manap, A., Mahalingam, S., Vaithylingam, R. & Abdullah, H. 2021. Mechanical, thermal and morphological properties of thermoplastic polyurethane composite reinforced by multi-walled carbon nanotube and titanium dioxide hybrid fillers. *Polymer Bulletin*, 78, 5815-5832.
- Manassero, G. & Dalmasso, M. T. 1998. Adaptive headlamp: a contribution for design and development of motorway light. *SAE transactions*, 37-42.
- Marculescu, D., Marculescu, R., Zamora, N. H., Stanley-Marbell, P., Khosla, P. K., Park, S., Jayaraman, S., Jung, S., Lauterbach, C., Weber, W., Kirstein, T., Cottet, D., Grzyb, J., Troster, G., Jones, M., Martin, T. & Nakad, Z. 2003. Electronic textiles: A platform for pervasive computing. *Proceedings of the IEEE*, 91, 1995-2018.
- Martin, M., Wong, N. & Ichinose, M. Impact of retro-reflective glass façades on the surface temperature of street pavements in business areas of Singapore and Tokyo. IOP Conference Series: Earth and Environmental Science, 2019. IOP Publishing, 012020.
- Martínez-Borreguero, G., Pérez-Rodríguez, Á. L., Suero-López, M. I. & Naranjo-Correa, F. L. 2018. A didactic reformulation of the laws of refraction of light. *Revista Brasileira de Ensino de Física*, 40.
- Mary, A. 2021. *What is Retro-Reflection?* [Online]. Torrance, CA American Permalight, Inc. Available: https://www.americanpermalight.shop/general/what-is-retro-reflection/ [Accessed October 10 2021].
- Mathur, K. 2018. Advancements in Pattern Coloration for Jacquard Woven Tapestry Fabrics. *Journal of Textile and Apparel, Technology and Management,* 10.
- Maycock, G. 1996. Sleepiness and driving: the experience of UK car drivers. *Journal of sleep research*, 5, 229-231.
- Mercier, C. R., Shelley, M. C., Rimkus, J. B. & Mercier, J. M. 1997. Age and gender as predictors of injury severity in head-on highway vehicular collisions. *Transportation Research Record*, 1581, 37-46.
- Mian, J. & Caird, J. K. 2018. The effects of speed and orientation on recognition judgments of retro-reflectively clothed pedestrians at night. *Transportation research part F: traffic psychology and behaviour*, 56, 185-199.
- Mishra, R., Militky, J. & Venkataraman, M. 2019. 7 Nanoporous materials. *In:* MISHRA, R. & MILITKY, J. (eds.) *Nanotechnology in Textiles*. Woodhead Publishing.
- Moberly, N. J. & Langham, M. P. 2002. Pedestrian conspicuity at night: failure to observe a biological motion advantage in a high-clutter environment. *Applied Cognitive Psychology*, 16, 477-485.
- Morgan, C. 2001. The effectiveness of retroreflective tape on heavy trailers.
- Mortimer, R. G. 1988. A further evaluation of the Motorcycle Rider Course. *Journal of Safety Research*, 19, 187-196.
- Mosberger, R., Andreasson, H. & Lilienthal, A. J. 2014. A Customized Vision System for Tracking Humans Wearing Reflective Safety Clothing from Industrial Vehicles and Machinery. *Sensors*, 14, 17952-17980.
- Movahhed, M. B., Ayoubinejad, J., Asl, F. N. & Feizbahr, M. 2020. The effect of rain on pedestrians crossing speed. *Computational Research Progress in Applied Science & Engineering (CRPASE)*, 6.
- Mphela, T., Mokoka, T. & Dithole, K. 2021. Pedestrian Motor Vehicle Accidents and Fatalities in Botswana-An Epidemiological Study. *Frontiers in Sustainable Cities*, 3.

- Mukhopadyhay, A., Dash, A. & Kothari, V. 2002. Thickness and compressional characteristics of air-jet textured yarn woven fabrics. *International Journal of Clothing Science and Technology*, 14, 88-99.
- Musa, A. B. H., Malengier, B., Vasile, S. & Langenhove, L. V. Determination of comfort indices of fabrics using fabric touch tester (FTT). AIP Conference Proceedings, 2021 Shah Alam, Malaysia. AIP Publishing LLC, 020005.
- Mussone, L., Ferrari, A. & Oneta, M. 1999. An analysis of urban collisions using an artificial intelligence model. *Accident Analysis & Prevention*, 31, 705-718.
- Nourbakhsh, S., Ebrahimi, I. & Valipour, P. 2011. Laser treatment of the wool fabric for felting shrinkage control. *Fibers and Polymers*, 12, 521-527.
- Nualdaisri, P. 2022. Creative textile: the interactive art installation from Thai silk. *Humanities, Arts and Social Sciences Studies*, 22, 112-121.
- Obeng, D. A., Owusu, V. & Tuffour, Y. A. 2021. Degradation of retro-reflectivity of thermoplastic pavement markings on trunk roads in Ghana. *Transportation Engineering*, 5, 100082.
- Ogulata, R. T. 2006. Air permeability of woven fabrics. *Journal of Textile and Apparel, Technology and management,* 5, 1-10.
- Olson, P. L., Halstead-Nussloch, R. & Sivak, M. 1981. The Effect of Improvements in Motorcycle/Motorcyclist Conspicuity on Driver Behavior. *Human Factors*, 23, 237-248.
- Önlü, N. & Halaçeli, H. 2012a. Visual effects of stainless steel and retro-reflective yarns on woven fabrics. *Research Journal of Textile and Apparel*, 16, 82-95.
- Önlü, N. & Halaçeli, H. 2012b. Visual Effects of Stainless Steel and Retro-Reflective Yarns on Woven Fabrics. *Research Journal of Textile and Apparel*.
- Önlü, N. & Yaşar, N. 2011. Visual textures combined with metallic, retro-reflective and stainless steel yarns in semi-transparent fabrics. *Research Journal of Textile and Apparel*.
- Ortiz-Morales, M. N., Poterasu, M., Acosta-Ortiz, S. E., Compean, I. & Hernandez-Alvarado, M. R. 2003. A comparison between characteristics of various laser-based denim fading processes. *Optics and Lasers in Engineering*, 39, 15-24.
- Oshacademy Occupational Safety and Health Training. 2022. *Personal Flotation Devices* [Online]. United States: OSHAcademy Occupational Safety and Health Training,. Available: https://www.oshatrain.org/courses/mods/895m3.html [Accessed April 12, 2022].
- Öström, M. & Eriksson, A. 2001. Pedestrian fatalities and alcohol. *Accident Analysis & Prevention*, 33, 173-180.
- Owens, D. A. 2003. Twilight vision and road safety: Seeing more than we notice but less than we think. *Visual perception: The influence of H. W. Leibowitz*. Washington, DC, US: American Psychological Association.
- Owens, D. A., Antonoff, R. J. & Francis, E. L. 1994. Biological motion and nighttime pedestrian conspicuity. *Human Factors*, 36, 718-732.
- Owens, D. A. & Brooks, J. C. 1995. Drivers' vision, age, and gender as factors in twilight road fatalities. University of Michigan, Ann Arbor, Transportation Research Institute.
- Owens, D. A. & Sivak, M. 1996. Differentiation of visibility and alcohol as contributors to twilight road fatalities. *Human Factors*, 38, 680-689.
- Owens, D. A. & Tyrrell, R. A. 1999. Effects of luminance, blur, and age on nighttime visual guidance: A test of the selective degradation hypothesis. *Journal of Experimental Psychology: Applied*, 5, 115.
- Owens, D. A., Wood, J. M. & Owens, J. M. 2007. Effects of age and illumination on night driving: a road test. *Human Factors*, 49, 1115-1131.

- Oxley, J., O'hern, S. & Jamaludin, A. 2018. An observational study of restraint and helmet wearing behaviour in Malaysia. *Transportation research part F: traffic psychology and behaviour*, 56, 176-184.
- Özgüney, A. T., Taşkin, C., Özçelik, G., Ünal, P. G. & Özerdem, A. 2009. Handle properties of the woven fabrics made of compact yarns. *Textile and Apparel*, 19, 108-113.
- Pai, C.-W. & Saleh, W. 2007. Exploring motorcyclist injury severity resulting from various crash configurations at T-junctions in the United Kingdom—An application of the ordered probit models. *Traffic Injury Prevention*, 8, 62-68.
- Panchal, J., Lehikoinen, A. & Rasilo, P. 2021. Efficient finite element modelling of litz wires in toroidal inductors. *IET Power Electronics*, 14, 2610-2619.
- Park, M.-W. & Brilakis, I. 2012. Construction worker detection in video frames for initializing vision trackers. *Automation in Construction*, 28, 15-25.
- Park, S. 2019. An evaluation of the suitability of fluorescent fabrics and retroreflective materials for road traffic warning clothing in compliance with international standards. *Fashion and Textiles*, 6, 1-15.
- Parkin, J., Wardman, M. & Page, M. 2007. Models of perceived cycling risk and route acceptability. *Accident Analysis & Prevention*, 39, 364-371.
- Pościk, A. 2013. Determining Ultraviolet Degradation of High-Visibility Warning Clothing With Photochromic Indicators. *International Journal of Occupational Safety and Ergonomics*, 19, 79-86.
- Pościk, A., Szkudlarek, J. & Owczarek, G. 2019. Photometric properties of retroreflective materials in dependence on their structure and angle of illumination. *Fibres & Textiles in Eastern Europe*.
- Pour-Rouholamin, M. & Zhou, H. 2016. Investigating the risk factors associated with pedestrian injury severity in Illinois. *Journal of Safety Research*, 57, 9-17.
- Prati, G. 2018. The effect of an italian nationwide mandatory visibility aids law for cyclists. *Journal of Transport & Health*, 9, 212-216.
- Ptak, M. 2019. Method to assess and enhance vulnerable road user safety during impact loading. *Applied Sciences*, 9, 1000.
- Quddus, M. A., Noland, R. B. & Chin, H. C. 2002. An analysis of motorcycle injury and vehicle damage severity using ordered probit models. *Journal of Safety research*, 33, 445-462.
- Radwan, E., Abdel-Aty, M. A., Yan, X. & Harb, R. C. 2006. Light Truck Vehicle Contribution to Rear-End Collisions.
- Rahemtulla, Z., Hughes-Riley, T. & Dias, T. 2021. Vibration-Sensing Electronic Yarns for the Monitoring of Hand Transmitted Vibrations. *Sensors*, 21, 2780.
- Rahemtulla, Z., Turner, A., Oliveira, C., Kaner, J., Dias, T. & Hughes-Riley, T. 2023. The Design and Engineering of a Fall and Near-Fall Detection Electronic Textile. *Materials*, 16, 1920.
- Rahman, T., Nagano, K. & Togawa, J. 2019. Study on building surface and indoor temperature reducing effect of the natural meso-porous material to moderate the indoor thermal environment. *Energy and Buildings*, 191, 59-71.
- Rathnayake, A. & Dias, T. 2015. Yarns with embedded electronics. *Adjunct Proceedings* of the 2015 ACM International Joint Conference on Pervasive and Ubiquitous Computing and Proceedings of the 2015 ACM International Symposium on Wearable Computers. Osaka, Japan: Association for Computing Machinery.
- Research and Markets. 2021. *Global Retro Reflective Materials Market 2021-2026* [Online]. Available:
 - https://www.researchandmarkets.com/reports/5354576/global-retro-reflective-materials-market-2021-

- <u>2026?utm_source=GNOM&utm_medium=PressRelease&utm_code=gfkpv5&utm_campaign=1574078+-</u>
- +Opportunities+and+Growth+in+the+Global+Retro+Reflective+Materials+Mark et+to+2026%3a+Public+and+Worker+Safety+Regulations+Driving+Growth&ut m_exec=cari18prd [Accessed September 14, 2021].
- Rose, A. 2013. Ndebele. Available from: http://lightcolorsound.blogspot.com/2013/12/ndebele.html.
- Roy Choudhury, A. K., Majumdar, P. K. & Datta, C. 2011. 1 Factors affecting comfort: human physiology and the role of clothing. *In:* SONG, G. (ed.) *Improving Comfort in Clothing*. Woodhead Publishing.
- Rua Seguridad. 2020. *Reflective Glass Beads* [Online]. Quezon City: Philippines. Available: https://www.ruacorp.com/things-you-should-know-about-reflective-glass-beads/ [Accessed October 16 2021].
- Samuel, O. O. 2015. Increasing motorcycle conspicuity-design and assessment of intervention to enhance rider safety (book review). *Ergonomics*, 59, 735-735.
- Sandhu, N. K. 2012. Leaching of metals and metalloids from highway marking glass beads and the potential environmental impact. PhD Dissertation, New Jersey Institute of Technology.
- Satharasinghe, A., Hughes-Riley, T. & Dias, T. 2018. Photodiodes embedded within electronic textiles. *Scientific Reports*, 8, 16205.
- Satharasinghe, A., Hughes-Riley, T. & Dias, T. 2A2_0564_ Photodiode and Led Embedded Textiles for Wearable Healthcare Applications. Proceedings of the 19th World Textile Conference-Autex 2019, 2019.
- Saville, B. P. 1999. 8 Comfort. *In:* SAVILLE, B. P. (ed.) *Physical Testing of Textiles*. Woodhead Publishing.
- Savolainen, P. & Mannering, F. 2007a. Effectiveness of motorcycle training and motorcyclists' risk-taking behavior. *Transportation research record*, 2031, 52-58.
- Savolainen, P. & Mannering, F. 2007b. Probabilistic models of motorcyclists' injury severities in single-and multi-vehicle crashes. *Accident Analysis & Prevention*, 39, 955-963.
- Sayer, J. R. & Buonarosa, M. L. 2008. The roles of garment design and scene complexity in the daytime conspicuity of high-visibility safety apparel. *Journal of Safety Research*, 39, 281-286.
- Sayer, J. R. & Mefford, M. L. 2004. High visibility safety apparel and nighttime conspicuity of pedestrians in work zones. *Journal of Safety Research*, 35, 537-546.
- Seidu, R. K. & Jiang, S. 2023. Performance Quality of Braided e-Yarns for Pedestrian Interactive Textiles. *Engineering Proceedings*, 52, 4.
- Service, R. F. 2003. Electronic Textiles Charge Ahead. Science, 301, 909-911.
- Shah, S. a. R. & Ahmad, N. 2019. Road infrastructure analysis with reference to traffic stream characteristics and accidents: An application of benchmarking based safety analysis and sustainable decision-making. *Applied Sciences*, 9, 2320.
- Shankar, V. & Mannering, F. 1996. An exploratory multinomial logit analysis of single-vehicle motorcycle accident severity. *Journal of Safety Research*, 27, 183-194.
- Shinar, D. 1984. Actual versus estimated night-time pedestrian visibility. *Ergonomics*, 27, 863-871.
- Shinar, D. 1985. The Effects of Expectancy, Clothing Reflectance, and Detection Criterion on Nighttime Pedestrian Visibility. *Human Factors*, 27, 327-333.
- Siddiqui, M. O. R. & Sun, D. 2018. Development of experimental setup for measuring the thermal conductivity of textiles. *Clothing and Textiles Research Journal*, 36, 215-230.

- Siddiqui, N. A., Chu, X. & Guttenplan, M. 2006. Crossing locations, light conditions, and pedestrian injury severity. *Transportation research record*, 1982, 141-149.
- Simegnaw, A. A., Malengier, B., Getnet, M. & Van Langenhove, L. 2023. Connecting surface-mounted electronic elements with amber strand metal-clad conductive fibers by reflow soldering. *Textile Research Journal*, 93, 4068-4079.
- Simegnaw, A. A., Malengier, B., Tadesse, M. G., Rotich, G. & Van Langenhove, L. 2022a. Study the Electrical Properties of Surface Mount Device Integrated Silver Coated Vectran Yarn. *Materials*, 15, 272.
- Simegnaw, A. A., Malengier, B., Tadesse, M. G. & Van Langenhove, L. 2022b. Development of Stainless Steel Yarn with Embedded Surface Mounted Light Emitting Diodes. *Materials*, 15, 2892.
- Sirkova, B. K. 2012. Description of fabric thickness and roughness on the basis of fabric structure parameters. *AUTEX Research Journal*, 12, 40-43.
- Skains, R. L. 2018. Creative Practice as Research: Discourse on Methodology. *Media Practice and Education*, 19, 82-97.
- Stapleton, T. & Koo, H. S. 2017. Bicyclist biomotion visibility aids: a 3D eye-tracking analysis. *International Journal of Clothing Science and Technology*, 29, 262-269.
- Starr, C. L., Cao, H., Peksoz, S. & Branson, D. H. 2015. Thermal effects of design and materials on quadgard[™] body armor systems. *Clothing and Textiles Research Journal*, 33, 51-63.
- Štěpánková, M., Wiener, J. & Dembický, J. 2010. Impact of laser thermal stress on cotton fabric. *Fibres & Textiles in Eastern Europe*, 18, 80.
- Stone, M. & Broughton, J. 2003. Getting off your bike: cycling accidents in Great Britain in 1990–1999. *Accident Analysis & Prevention*, 35, 549-556.
- Stormont, R. S., Davies, G. R., Ross, P. J., Lurie, D. J. & Broche, L. M. 2023. A flexible 8.5 MHz litz wire receive array for field-cycling imaging. *Physics in Medicine & Biology*, 68, 055016.
- Studzińska, A., Frydrych, I. & Łężak, K. 2022. Transformable Warning Clothing for Children with Active Light Sources. *Autex Research Journal*, 22, 234-242.
- Süle, G. 2012. Investigation of bending and drape properties of woven fabrics and the effects of fabric constructional parameters and warp tension on these properties. *Textile Research Journal*, 82, 810-819.
- Sullivan, J. & Flannagan, M. 2001. Characteristics of pedestrian risk in darkness (Report No. UMTRI-2001-33). *Ann Arbor: The University of Michigan Transportation Research Institute*.
- Sullivan, J. M., Adachi, G., Mefford, M. L. & Flannagan, M. J. 2004. High-beam headlamp usage on unlighted rural roadways. *Lighting Research & Technology*, 36, 59-65.
- Sullivan, J. M. & Flannagan, M. J. 2002. The role of ambient light level in fatal crashes: inferences from daylight saving time transitions. *Accident Analysis & Prevention*, 34, 487-498.
- Sullivan, J. M. & Flannagan, M. J. 2012. Heavy trucks, conspicuity treatment, and the decline of collision risk in darkness. *Journal of safety research*, 43, 157-161.
- Sun, D. & Stylios, G. 2006. Investigation of the effect of continuous finishing on the mechanical properties and the handle of wool fabrics. *Fibers and Polymers*, 7, 245-249.
- Syed Muhammad, S. & Ahmed Dawood, S. 2020. New Visions to Design Women's Clothing using light-emitting Materials as an inspiration source. *Journal of Arts & Applied Sciences (JAAS)*, 7, 41-60.
- Taek, J., Maleck, T. L. & Taylor, W. C. 1999. Pavement making material evaluation study in Michigan. *Institute of Transportation Engineers. ITE Journal*, 69, 44.

- Teiermayer, A. 2019. Improving students' skills in physics and computer science using BBC Micro: bit. *Physics Education*, 54.
- Tosi, J. D., Poó, F. M., Ledesma, R. D. & Firsenko, E. 2021. Safety of child passengers who ride to school on a motorcycle: an observational study in two Argentine cities. *IATSS research*, 45, 176-181.
- Tsuji, T., Hattori, H., Watanabe, M. & Nagaoka, N. 2002. Development of night-vision system. *IEEE Transactions on Intelligent Transportation Systems*, 3, 203-209.
- Tsutsumi, Y., Ohashi, M. & Miyoshi, Y. 2013. Temperature-sensitive mechanical LPFG using contractive force of heat-shrinkable tube. *Optical Fiber Technology*, 19, 55-59.
- Turner, P. A. & Georggi, N. 2001. Analysis of alcohol-related motorcycle crashes in Florida and recommended countermeasures. *Transportation research record*, 1779, 189-196.
- Tyrrell, R. A. & Patton, C. W. 1998. The Effectiveness of Educating Pedestrians about their own Nighttime Visibility. *Proceedings of the Human Factors and Ergonomics Society Annual Meeting*, 42, 1205-1209.
- Tyrrell, R. A., Patton, C. W. & Brooks, J. O. 2004a. Educational interventions successfully reduce pedestrians' overestimates of their own nighttime visibility. *Human Factors*, 46, 170-182.
- Tyrrell, R. A., Wood, J. M. & Carberry, T. P. 2004b. On-road measures of pedestrians' estimates of their own nighttime conspicuity. *Journal of Safety Research*, 35, 483-490.
- Tyrrell, R. A., Wood, J. M., Carberry, T. P., Faulks, T. & Jones, K. 2003. On-road measures of the visibility of pedestrians at night. *Journal of Vision*, 3, 549-549.
- Tyrrell, R. A., Wood, J. M., Chaparro, A., Carberry, T. P., Chu, B.-S. & Marszalek, R. P. 2009. Seeing pedestrians at night: Visual clutter does not mask biological motion. *Accident Analysis & Prevention*, 41, 506-512.
- Tyrrell, R. A., Wood, J. M., Owens, D. A., Whetsel Borzendowski, S. & Stafford Sewall, A. 2016. The conspicuity of pedestrians at night: A review. *Clinical and experimental optometry*, 99, 425-434.
- Ulfarsson, G. F., Kim, S. & Booth, K. M. 2010. Analyzing fault in pedestrian–motor vehicle crashes in North Carolina. *Accident Analysis & Prevention*, 42, 1805-1813.
- Uttley, J. & Fotios, S. 2017. The effect of ambient light condition on road traffic collisions involving pedestrians on pedestrian crossings. *Accident Analysis & Prevention*, 108, 189-200.
- Valentin, V., Mannering, F. L., Abraham, D. M. & Dunston, P. S. 2010. Evaluation of the visibility of workers' safety garments during nighttime highway-maintenance operations. *Journal of transportation engineering*, 136, 584-591.
- Vandenberg, J. L., Billingsley, B. G., Reule, J. L. & Fox, F. J. 2002. Continuous process for making high performance retroreflective fabric. Google Patents.
- Vijayan, A., Islam, S., Jones, M., Padhye, R. & Arnold, L. 2016. Degradation of fluorescent high-visibility colors used in safety garments for the Australian railway industry. *Journal of safety research*, 56, 1-7.
- Virginia Department of Transportation 2016. Pavement Marking Certification Study Guide 2016.
- Walker, I., Garrard, I. & Jowitt, F. 2014. The influence of a bicycle commuter's appearance on drivers' overtaking proximities: An on-road test of bicyclist stereotypes, high-visibility clothing and safety aids in the United Kingdom. *Accident Analysis & Prevention*, 64, 69-77.

- Wang, C., Zhu, Y. & Guo, X. 2019. Thermally responsive coating on building heating and cooling energy efficiency and indoor comfort improvement. *Applied Energy*, 253, 113506.
- Wang, J., Liu, S., Meng, X., Gao, W. & Yuan, J. 2021. Application of retro-reflective materials in urban buildings: A comprehensive review. *Energy and Buildings*, 247, 111137.
- Wang, Q. 2018. *Designing smart garments for rehabilitation*. PhD Thesis, Technische Universiteit Eindhoven.
- Wang, Y., Mauree, D., Sun, Q., Lin, H., Scartezzini, J. & Wennersten, R. 2020. A review of approaches to low-carbon transition of high-rise residential buildings in China. *Renewable and Sustainable Energy Reviews*, 131, 109990.
- Webster, J., Holland, E. J., Sleivert, G., Laing, R. M. & Niven, B. E. 2005. A light-weight cooling vest enhances performance of athletes in the heat. *Ergonomics*, 48, 821-837.
- Wei, B., Mei, K. & Sulaiman, J. LED Illuminated Cloth for bicyclists. International Textile and Apparel Association Annual Conference Proceedings, 2015. Iowa State University Digital Press, 1-2.
- Wemegah, R. 2013. Murals In Sirigu Culture: Philosophical and Cultural Importance. *International Journal of Arts and Commerce*, 2, 101-111.
- Wendt, Z. & Cook, J. 2018. *Microcontroller Power Switching With Transistors* [Online]. EEWorld Online. Available: https://www.eeworldonline.com/microcontroller-power-switching-with-transistors/ [Accessed November 29, 2022].
- Whetsel Borzendowski, S. A., Stafford Sewall, A. A., Rosopa, P. J. & Tyrrell, R. A. 2015. Drivers' judgments of the effect of headlight glare on their ability to see pedestrians at night. *Journal of Safety Research*, 53, 31-37.
- Whetsel, S. A., Stafford, A. A., Rosopa, P. J. & Tyrrell, R. A. 2012. The Accuracy of Drivers' Judgments of the Effects of Headlight Glare on Pedestrian Recognition at Night. *Proceedings of the Human Factors and Ergonomics Society Annual Meeting*, 56, 2241-2245.
- Whittaker, J. 1996. An investigation into the effects of British Summer Time on road traffic accident casualties in Cheshire. *Emergency Medicine Journal*, 13, 189-192.
- Woets, R. 2014. "This is What Makes Sirigu Unique" Authenticating Canvas and Wall Paintings in (Inter)national Circuits of Value and Meaning. *African Arts*, 47, 10-25
- Wood, J. & Chaparro, A. 2011. Night driving: How low illumination affects driving and the challenges of simulation.
- Wood, J., Chaparro, A., Carberry, T. & Chu, B. S. 2010a. Effect of simulated visual impairment on nighttime driving performance. *Optometry and vision science*, 87, 379-386.
- Wood, J. M. 2020. Nighttime driving: visual, lighting and visibility challenges. *Ophthalmic and physiological optics*, 40, 187-201.
- Wood, J. M., Chiu, C.-N., Kim, G. H., Le, J., Lee, H. J., Nguyen, T. & Black, A. A. 2021. Refractive blur affects judgement of pedestrian walking direction at night. *Ophthalmic and physiological optics*, 41, 582-590.
- Wood, J. M., Lacherez, P. F., Marszalek, R. P. & King, M. J. 2009. Drivers' and cyclists' experiences of sharing the road: Incidents, attitudes and perceptions of visibility. *Accident Analysis & Prevention*, 41, 772-776.
- Wood, J. M., Marszalek, R., Carberry, T., Lacherez, P. & Collins, M. J. 2015. Effects of Different Levels of Refractive Blur on Nighttime Pedestrian Visibility. *Investigative Ophthalmology & Visual Science*, 56, 4480-4485.

- Wood, J. M., Tyrrell, R. A. & Carberry, T. P. 2005. Limitations in drivers' ability to recognize pedestrians at night. *Human factors*, 47, 644-653.
- Wood, J. M., Tyrrell, R. A., Lacherez, P. & Black, A. A. 2017. Night-time pedestrian conspicuity: effects of clothing on drivers' eye movements. *Ophthalmic and Physiological Optics*, 37, 184-190.
- Wood, J. M., Tyrrell, R. A., Marszalek, R., Lacherez, P. & Carberry, T. 2013. Bicyclists overestimate their own night-time conspicuity and underestimate the benefits of retroreflective markers on the moveable joints. *Accident Analysis & Prevention*, 55, 48-53.
- Wood, J. M., Tyrrell, R. A., Marszalek, R., Lacherez, P., Carberry, T., Chu, B. S. & King, M. J. 2010b. Cyclist Visibility at Night: Perceptions of Visibility Do Not Necessarily Match Reality. *Journal of the Australasian College of Road Safety*, 21, 56-60.
- Wood, J. M., Tyrrell, R. A., Marszalek, R., Lacherez, P., Chaparro, A. & Britt, T. W. 2011. Using biological motion to enhance the conspicuity of roadway workers. *Accident Analysis & Prevention*, 43, 1036-1041.
- World Health Organization. 2013. *Make walking safe: A brief overview of pedestrian safety around the world* [Online]. Geneva, Switzerland: World Health Organization. Available: https://www.who.int/publications/i/item/make-walking-safe-a-brief-overview-of-pedestrian-safety-around-the-world [Accessed].
- World Health Organization. 2018. *Global status report on road safety 2018: Summary* [Online]. Geneva: World Health Organization. Available: https://www.who.int/violence_injury_prevention/road_safety_status/2018/en/ [Accessed January 18 2022].
- Wyse. 2020. Reflective materials more popular in casual wear and fashionable tide brand clothing [Online]. Shenzhen: WYSE. Available:

 https://wysecn.com/article/reflective-materials-more-popular-in-casual-wear-and-fashionable-tide-brand-clothing-i00004i1.html [Accessed April 13 2022].
- Yadav, A., Prasad, V., Kathe, A., Raj, S., Yadav, D., Sundaramoorthy, C. & Vigneshwaran, N. 2006. Functional finishing in cotton fabrics using zinc oxide nanoparticles. *Bulletin of materials Science*, 29, 641-645.
- Yuan, G., Chen, Z. & Luzzi, D. 2018. Application of Laser Technology in Fashion Industry. *In:* CHOW, P.-S., CHIU, C.-H., C. Y. YIP, A. & K. Y. TANG, A. (eds.) *Contemporary Case Studies on Fashion Production, Marketing and Operations.* Singapore: Springer Singapore.
- Yuan, G., Jiang, S., Newton, E. & Au, W. 2013a. Application of laser engraving for sustainable fashion design. *Research Journal of Textile and Apparel*, 17, 21-27.
- Yuan, G., Jiang, S., Newton, E., Fan, J. & Au, W. 2012a. Embellishment of fashion design via laser engraving. *Research Journal of Textile and Apparel*, 16, 106-111.
- Yuan, G. X., Jiang, S. X., Newton, E. & Au, W. M. 2013b. Application of Laser Engraving for Sustainable Fashion Design. *Research Journal of Textile and Apparel*, 17, 21-27.
- Yuan, G. X., Jiang, S. X., Newton, E., Fan, J. T. & Au, W. M. 2012b. Application of laser treatment for fashion design. *Journal of the Textile Institute*, 103, 48-54.
- Yuan, J. 2018. Application of Glass Beads in Building Exterior Wall Surface Materials. *Advances in Glass Science and Technology*, 173.
- Yuan, W. 2000. The effectiveness of the 'ride-bright' legislation for motorcycles in Singapore. *Accident Analysis & Prevention*, 32, 559-563.

- Zajac, S. & Ivan, J. N. 2003. Factors influencing injury severity of motor vehicle—crossing pedestrian crashes in rural Connecticut. *Accident Analysis & Prevention*, 35, 369-379.
- Zeng, W., Shu, L., Li, Q., Chen, S., Wang, F. & Tao, X.-M. 2014. Fiber-Based Wearable Electronics: A Review of Materials, Fabrication, Devices, and Applications. *Advanced Materials*, 26, 5310-5336.
- Zhang, G., Yau, K. K. W. & Zhang, X. 2014. Analyzing fault and severity in pedestrian—motor vehicle accidents in China. *Accident Analysis & Prevention*, 73, 141-150.
- Zheng, Z., Jur, J. & Cheng, W. 2021. Smart materials and devices for electronic textiles. *MRS Bulletin*, 46, 488-490.
- Zhou, X., Carmeliet, J., Sulzer, M. & Derome, D. 2020. Energy-efficient mitigation measures for improving indoor thermal comfort during heat waves. *Applied Energy*, 278, 115620.
- Zimmerman, J., Forlizzi, J. & Evenson, S. Research through design as a method for interaction design research in HCI. Proceedings of the SIGCHI conference on Human factors in computing systems, 2007. 493-502.
- Zupin, Ž., Hladnik, A. & Dimitrovski, K. 2012. Prediction of one-layer woven fabrics air permeability using porosity parameters. *Textile Research Journal*, 82, 117-128.